



HAL
open science

Structural elucidation of secondary metabolites from Hypoxylon fragiforme, using high resolution mass spectrometry and gas-phase ion-molecule reactions

Ljubica Svilar

► **To cite this version:**

Ljubica Svilar. Structural elucidation of secondary metabolites from Hypoxylon fragiforme, using high resolution mass spectrometry and gas-phase ion-molecule reactions. Biochemistry [q-bio.BM]. Université Pierre et Marie Curie - Paris VI, 2012. English. NNT : 2012PAO66468 . tel-00836214

HAL Id: tel-00836214

<https://theses.hal.science/tel-00836214>

Submitted on 20 Jun 2013

HAL is a multi-disciplinary open access archive for the deposit and dissemination of scientific research documents, whether they are published or not. The documents may come from teaching and research institutions in France or abroad, or from public or private research centers.

L'archive ouverte pluridisciplinaire **HAL**, est destinée au dépôt et à la diffusion de documents scientifiques de niveau recherche, publiés ou non, émanant des établissements d'enseignement et de recherche français ou étrangers, des laboratoires publics ou privés.

THESE DE DOCTORAT DE
L'UNIVERSITE PIERRE ET MARIE CURIE
et UNIVERSITE DE NIS

Spécialité Systems Bioorganique / Spectrochimie
Ecole doctorale de Chimie Moleculaire (ED 406)

Présenté par

Ljubica SVILAR
Pour obtenir le grade de
DOCTEUR de l'UNIVERSITÉ PIERRE ET MARIE CURIE

**Structural elucidation of secondary metabolites from
Hypoxylon fragiforme, using high resolution mass
spectrometry and gas-phase ion-molecule reactions**

soutenue le 11 Octobre 2012

devant le jury composé de :

Directeurs de thèse

M. Jean-Claude TABET

Mme. Vesna STANKOV-JOVANOVIC

Rapporteurs :

M. David RONDEAU

Mme. Estelle PARIS

Examineurs:

Mme. Gordana STOJANOVIC

M. Christophe JUNOT

M. Louis FENSTERBANK

Title: Structural elucidation of secondary metabolites from *Hypoxylon fragiforme*, using high resolution mass spectrometry and gas-phase ion-molecule reactions

SUMMARY

Fungi produce a wide variety of biologically active compounds/metabolites that could be used for medicinal and pharmaceutical purposes. Mitorubrines, members of the family of azaphilones, constitute a particularly interesting set of structurally diverse secondary metabolites, exhibiting a wide range of biological activities (*e.g.* antimicrobial, antibacterial, antimalarial). This work describes the development of several mass spectrometry-based approaches to solve the natural structural diversity and complexity of azaphilones extracted from *Hypoxylon fragiforme* fungus.

The first part of this manuscript is dedicated to the development and validation of an analytical methodology involving liquid chromatography coupled to high resolution mass spectrometry for the efficient and accurate detection of trace-level azaphilones in complex fungal extracts. Further collision-induced dissociation and hydrogen/deuterium exchange experiments were performed to fully elucidate and characterize the azaphilones and their nitrogenized analogues from *Hypoxylon fragiforme*.

The second part is devoted to the application of these different analytical strategies to the in-depth characterization of a novel family of secondary metabolites derived from azaphilones, the mitorubramines.

Lastly, these different secondary metabolites were further purified to confirm their chemical structures by NMR spectroscopy.

Keywords: Azaphilone; mitorubramines; *Hypoxylon fragiforme*; LC-ESI-MS; LTQ-Orbitrap; MSⁿ; triple quadrupole; gas-phase H/D exchange.

Titre : Elucidation de la structure des métabolites secondaires d'*Hypoxylon fragiforme* par spectrométrie de masse haute résolution et réactions ions-molécules en phase gazeuse

RESUME

Les champignons produisent une grande variété de composés/métabolites biologiquement actifs qui peuvent être utilisés à des fins médicinales et pharmaceutiques. Les mitorubrines, membres de la famille des azaphilones, constituent un ensemble particulièrement intéressant de métabolites secondaires, présentant une grande étendue d'activités biologiques (e.g. antimicrobienne, antibactérienne, antipaludique). Ce travail présente le développement de plusieurs approches de spectrométrie de masse permettant de résoudre la diversité structurelle naturelle et la complexité des azaphilones extraits des champignons *Hypoxylon fragiforme*.

La première partie de ce manuscrit est dédiée au développement et à la validation d'une méthodologie analytique impliquant la chromatographie liquide couplée à la spectrométrie de masse haute résolution pour la détection efficace et précise de traces d'azaphilones dans des extraits fongiques complexes. En outre, des expériences de spectrométrie de masse en mode tandem (par dissociation induite par collision, CID) et d'échange hydrogène/deutérium ont été effectuées pour élucider et caractériser les azaphilones et leurs analogues azotés chez *Hypoxylon fragiforme*.

La deuxième partie est consacrée à l'application de ces différentes stratégies analytiques pour la caractérisation approfondie d'une nouvelle famille de métabolites secondaires dérivés des azaphilones, les mitorubramines.

Enfin, ces différents métabolites secondaires ont été purifiés pour confirmer leur structure chimique par spectroscopie RMN.

Mots-clés : Azaphilone; mitorubramines; *Hypoxylon fragiforme*; LC-ESI-MS; LTQ-Orbitrap; MSⁿ; triple quadripole; échanges H/D en phase gazeuse.

To the Universe

Acknowledgments

First and foremost I thank my mentors Prof. Dr. Jean-Claude Tabet and Dr. Vesna Stankov-Jovanovic for their guidance and support of my work in their laboratories in France and Serbia. I took advantage of the occasion they gave me to work under their supervision, to learn a great amount during this time. I enjoyed the stimulating and pleasant atmosphere in their research groups in France and Serbia.

I thank to French Government for its financial support during my sojourn in France and for all benefits I had with that scholarship.

I wish to express my great gratitude to Dr. Estelle Paris and Prof. Dr. David Rondeau for accepting to judge this work as referees. I would also like to thank Prof. Dr. Gordana Stojanovic, Dr. Christophe Junot and Dr. Louis Fensterbank for their participation as the exam committee.

I wish to thank all the people with whom I have worked and contributed to the development of this work. Great thanks to Danis Lesage for long discussions on the gas-phase reactions and for its support, availability and ingenious suggestions. I want to thank to Heloise Dossmann for having achieved the theoretical calculations. Her participation was one of the essentials for clarification of misunderstandings we have met during this work. I am particularly grateful to Hristo Nedev giving me many answers on many questions concerning orbitrap mass spectrometer, as well as for the help for making preparative HPLC working properly. I want to thank him for having been always available to answer my questions. Furthermore, I want to thank him for being a real friend during these years spent in UPMC, for making a lot of jokes, for teaching me French language and for reminding me every day on my fatherland.

I thank the NMR team of the Institut Parisienne de Chimie Moleculaire for the measurement of NMR spectra. I wish to acknowledge the contribution of Elsa Caytan in offering valuable interpretation and carrying out of important NMR spectra.

Thanks to my workmates from Jussieu: Adrian, Bessem, Farid, Xiaohua, Viet, Baiyi, Vera, Chafia, Ludo. They were real friends; I will never forget their support and jokes and lunches at Chinese restaurants! Thanks to my workmate from Serbia, Marija Ilic for good times spent in the lab and for the great team works we did together.

Thanks to Jérôme for supporting my bad moments, but thanks even more for passing a positive moments with me. Thanks to my sisters for being always there for encouraging me. I want to thank to Natali as well for being as a sister to me during this four years spent in France, and for listening all of my doubts and excitements.

The most I want to thank to my Master Mind group, Branka, Ivana, Miso for making me a better person from day to day.

I am finally indebted to my mom who gave all her best for my education.

Table of content

SUMMARY	3
RESUME	4
Acknowledgments	9
Table of content.....	11
List of Figures.....	15
List of Tables	19
List of abbreviations	21
Preface	25
General part	29
1. Natural products	29
1.1 Fungi and its significance	29
1.2 The Xylariaceae family	30
1.3 General and ecological aspect of Xylariaceae.....	32
1.3.1 Taxonomy of Xylariaceae	33
1.3.2 Chemical diversity of Xylariaceae and its use in taxonomy.....	34
1.3.3 What about Hypoxylon?.....	38
2. Fungal metabolites and secondary metabolism.....	42
2.1 Biological activities of metabolites from Xylariaceae fungi.....	42
2.1.1 Concentricolide.....	43
2.1.2 Cytochalasins.....	43
2.1.3 Bynaphtyl	44
2.1.4 Azaphilones	45
2.2 Fungal secondary metabolism.....	51
2.2.1 Expression and regulation of secondary metabolites.....	51
2.2.2 Functions and roles of defence secondary metabolites.....	52
2.2.3 Roles of secondary metabolites from Xylariaceae.....	53
2.3 Azaphilones, fungal secondary metabolites	53
2.3.1 Biosynthesis of azaphilones.....	55
2.3.2 Chemical synthesis of azaphilones	58
2.3.3 Reaction with quaternary ammonium.....	59

3. Analytical methods for investigation of fungi	62
3.1 Sample preparation and extraction.....	63
3.1.1 Sonication or ultrasound extraction.....	63
3.1.2 Liquid-Solid Extraction.....	64
3.1.3 Solid Phase Extraction.....	64
3.2 High Performance Liquid Chromatography separation.....	65
3.2.1 Reverse-phase liquid chromatography.....	67
3.2.2 Hydrophilic interaction liquid chromatography.....	68
3.2.3 Preparative HPLC.....	68
3.3 Spectroscopic methods.....	70
3.3.1 Spectroscopy Methods.....	70
3.3.2 UV spectroscopy.....	70
3.3.3 Nuclear magnetic resonance spectroscopy in structure elucidation of fungal secondary metabolites.....	71
3.3.4 Mass spectrometry.....	72
4. Mass spectrometry	73
4.1 Ionization techniques.....	75
4.1.1 Gas Phase Ionization – Electron Ionization.....	75
4.1.2 Atmospheric Pressure Ionization.....	80
4.1.3 The case of Electrospray ionization.....	80
4.1.4 In-Source CID.....	84
4.1.5 ESI-MS for analysis of azaphilones.....	84
4.2 Mass analysers.....	86
4.2.1 High resolution mass spectrometry - Orbitrap mass spectrometer.....	86
4.2.2 LTQ-Orbitrap, a hybrid mass spectrometer with high resolving power.....	87
4.2.3 Triple quadrupole.....	92
4.3 Collision induced dissociation (CID) and collision activated reaction (CAR).....	94
4.3.1 Ion-molecule reactions in the gas phase.....	95
4.3.2 Ion-dipole complexes.....	95
4.3.3 Gas phase H/D exchange.....	96
4.4 LC-MS interfacing.....	100
Experimental part	105
1. Solvents and chemicals	106
2. Sample preparation	106
2.1 Solid Phase Extraction.....	106
3. Synthesis of vinillogous pyrodones	108
4. Liquid Chromatography	109

4.1	Analytical High Performance Liquid Chromatography (HPLC)	109
4.2	Preparative High Performance Liquid Chromatography	110
5.	Mass Spectrometry	111
5.1	Optimization of electrospray ionization conditions	111
5.2	High resolution tandem mass spectrometry	113
5.3	Gas phase H/D exchange and TQ parameters	114
5.4	Density functional theory (DFT).....	116
6.	NMR spectroscopy	117
Results and discussion		119
1.	<i>Hypoxylon fragiforme</i> chemical composition.....	120
1.2	Separation of mitorubrin azaphilones by reverse phase liquid chromatography	121
1.3	Isolation of <i>Hypoxylon fragiforme</i> constituents by preparative HPLC	125
2.	Synthesis of mitorubramine	127
3.	NMR spectroscopy results of isolated azaphilones.....	128
4.	Techniques used in MS investigation of mitorubrin azaphilones and polar compounds	
	130	
4.1	High resolution mass spectrometry and accurate mass measurements	131
4.2	Optimization of desorption ionization conditions for detection of nitrogenized mitorubrin analogues	
	136	
4.3	Collision induced dissociation	139
4.3.1	Behavior of protonated mitorubrins and mitorubramines under resonant CID conditions	140
4.3.2	Sequential MS ³ experiments of bicyclical product ions	143
4.3.2.1	Differences in behaviour of mitorubrins and mitorubramines	143
4.3.2.2	Main product ions	143
4.3.2.3	Formation of diagnostic product ions	146
4.4	Gas-phase H/D exchange for structural elucidation.....	150
4.4.1	Gas-phase H/D exchange of protonated mitorubrins and mitorubramines in collision cell ...	151
4.4.2	Theoretical calculations and a model system	154
4.4.3	Explanation of gas-phase H/D exchange of mitorubrins and mitorubramines	156
Conclusion		161
References		165
Annex 1 – NMR spectra.....		175

Annex 2 - High-resolution mass spectrometry and hydrogen/deuterium exchange study of mitorubrin azaphilones and nitrogenized analogues	183
Annex 3 - Distinctive gas-phase fragmentation pathway of the mitorubramines, novel secondary metabolites from Hypoxylon fragiforme	192

List of Figures

Figure 1: Phylogenetic tree and taxonomy of Fungi	31
Figure 2: Example of the vertical section of a) stroma, b) anamorph and c) ascospore of some <i>Hypoxylon</i> , Xylariaceae	32
Figure 3: Different <i>Hypoxylon</i> species containing orselinic acid and azaphilone esters	40
Figure 4: Examples of compounds with present functions that influence biological activities	42
Figure 5: Structure of concentrolide	43
Figure 6: Structures of Cytochalasin A.....	44
Figure 7: Structure of bynaphtyl	45
Figure 8: Structures of a) mitorubrin, b) sassafrin, c) multiformin, d) daldinin and e) rubiginosin.....	46
Figure 9: Structure of rutilin A	47
Figure 10: Structures of kasanosins A and B	48
Figure 11: Common structure for all azaphilones	54
Figure 12: Proposed biosynthetic pathway for formation of azaphilone bicyclic core.....	56
Figure 13: Proposed biosynthetic pathway of cytochalasins.....	57
Figure 14: First synthesis of azaphilones proposed by Whilley.....	58
Figure 15: Proposed retro-synthetic pathway for chloroazaphilones	59
Figure 16 Proposed biosynthetic pathway for the formation of vinylogous γ -pyrydones.	60
Figure 17: Schematic presentation of solid phase extraction for sample purification	64
Figure 18: Schematic presentation of an HPLC system	66
Figure 19: Reverse phase column.....	67
Figure 20: Schematic presentation of elution of compounds from the reverse phase	68
Figure 21: Potential energy curve crossing for polyatomic molecules and ions	76
Figure 22: EI spectrum of mitorubrin.	77

Figure 23: Proposed fragmentation mechanism of molecular ion from mitorubrin under EI conditions	79
Figure 24 Influence of the electric charge on the orientation of small water jet; the origins of electrospray	81
Figure 25: Schematic presentation of electrospray ionization process	82
Figure 26: Schematic presentation of the ion emission in the gas phase during the ionization / desorption according to ES theory of Dole	83
Figure 27: Schematic presentation of the ion emission in the gas phase during the ionization / desorption according to ES theory of Iribarne and Thomson	83
Figure 28: Nominal mass spectra from direct infusion of fungal extract into electrospray mass spectrometry	86
Figure 29: Orbitrap mass detector	87
Figure 30: Schematic presentation of LTQ-Orbitrap XL hybrid mass spectrometer	88
Figure 31: Schematic presentation of linear ion trap	88
Figure 32: MS/MS experiments based on analysis using two spatially separate mass analysers	92
Figure 33: Schematic presentation of TQ with potential gradient	93
Figure 34 Electrostatic interaction between the dipole and cation	95
Figure 35 General mechanism of an H/D exchange process between a RXH^+ ion and YD_x	98
Figure 36 Step by step presentation for the sample preparation	108
Figure 37 Elution conditions used for crude extract analysis	109
Figure 38 LC gradient for preparative isolation of azaphilones	110
Figure 39 Structure of <i>iso</i> -propanyl orsellinate, model system used for theoretical studies	116
Figure 40 TIC chromatogram of <i>Hypoxylon fragiforme</i> methanol extract after purification by SPE, obtained in isocratic elution mode	121
Figure 41 Section of the HPLC-UV chromatograms (210 nm) of MeOH extracts from stromata of <i>Hypoxylon fragiforme</i>	122
Figure 42 TIC of crude methanol extract of <i>Hypoxylon fragiforme</i> obtained by gradient elution	124

Figure 43 DAD chromatogram of <i>Hypoxylon fragiforme</i> extract	125
Figure 44 3D DAD chromatogram of <i>Hypoxylon fragiforme</i> , showing the UV spectra of constituents and their abundance in the extract	126
Figure 45 Nomenclature of mitorubrin for explanation of NMR spectra.....	129
Figure 46 Mass spectrum of assumed mitorubraminol	133
Figure 47 Mass spectrum of assumed mitorubramini acid	133
Figure 48 Mass spectrum of assumed mitorubramine and mitorubraminol acetate.....	134
Figure 49 Mass spectrum of mitorubrinol	134
Figure 50 Mass spectrum of mitorubrinic acid	134
Figure 51 Mass spectrum of mitorubrinol acetate	134
Figure 52 Mass spectrum of mitorubrin.....	135
Figure 53 Dependence of normalized intensities of mitorubrins and polar components at different capillary voltage conditions.....	137
Figure 54 Ion abundance dependence upon the tube lens potential difference.....	138
Figure 55 Variation of the intensity ratio of mitorubramines and mitorubrins with the tube lens potential difference	139
Figure 56 CID spectra of mitorubrins and mitorubramines.....	140
Figure 57 Proposed mechanism of fragmentation of protonated mitorubrins and mitorubramines during the CID of normalized collision energy of 15 %.....	141
Figure 58 Sequential CID spectra of product ions from protonated mitorubrinol and mitorubraminol; (normalized collision energy, 22%).....	145
Figure 59 Proposed mechanism for the water loss from bicyclic product ion from mitorubraminol	146
Figure 60 Proposed mechanism for the losses of keten and metoxy radical from the bicyclic product ion from mitorubraminol	148
Figure 61 Proposed mechanism of losses of formic acid and carbon dioxide from bicyclic product ion from mitorubraminol.....	149

Figure 62 CAR spectra of gas-phase exchange of mitorubins ($X_O = 1_O, 2_O, 3_O, 4_O$) and mitorubramines ($X_N = 1_N, 2_N, 3_N, 4_N$); $E_{lab} = 3$ eV	152
Figure 63 Sites of mitorubins and mitorubramines where the H/D exchange is possible.....	152
Figure 64 Gas phase H/D exchanges from CAR spectra of fragment m/z 151 (M_{151}^+) and $[MH-(150)]^+$ ions from protonated mitorubins and nitrogenized derivatives	153
Figure 65 Structure of model system (MS) used for the theoretical explanation of gas-phase H/D exchange of mitorubins and mitorubramines	154
Figure 66 Transition states for the H/D exchanges between MSH^+ and ND_3	158
Figure 67 Structures of neutrals from m/z 151 and their PA.....	159

List of Tables

Table 1: Major genera of <i>Xylariaceae</i>	34
Table 2: Generic distribution of major metabolites in <i>Xylariaceae</i> in different genera of the family	37
Table 3: Biological activities of selected <i>Xylariaceae</i> species and compounds responsible for the activity	49
Table 4: Structures, monoisotopic masses and accurate masses of azaphilone adducts that can be formed in ESI and detected in orbitrap mass spectrometer during analysis of <i>Hypoxylon fragiforme</i>	90
Tableau 5 Parameters utilized for HPLC pumps and autosampler	109
Table 6 Parameters used for preparative separation of azaphilones from methanol fungal extract.....	110
Table 7 Utilized capillary voltages and tube lens offsets for optimization of ionization conditions and approach to the nitrogenized mitorubrin analogues	112
Table 8 Parameters used for HRMS and CID experiment.....	113
Table 9 Parameters used for H/D exchange experiments.....	115
Table 10 Secondary metabolites obtained in isolation by preparative HPLC, and quantities observed.....	126
Table 11 Results obtained from NMR analysis of isolates from preparative HPLC of <i>Hypoxylon fragiforme</i>	129
Table 12 Retention times, obtained azaphilones and nitrogenized analogues, <i>m/z</i> of their characteristic peaks and elemental composition by LC/HR-MS	132
Table 13 Displayed main product ions in CID spectra of selected product ions generated from the $[M+H]^+$ precursors	144
Table 14 Proton affinities for different reagent used in gas phase H/D exchange ion-molecule reactions.....	150

Table 15 Calculated proton affinities of different sites of mitorubrins (1 _O) and mitorubramines (1 _N).....	155
Table 16 Relative energies (in kcal/mol) of the ions, complexes and transitions structures involved in the H/D exchange process between MSH ⁺ and ND ₃	157
Table 17 Relative energies (in kcal/mol) of the ions, complexes and transitions structures involved in the gas-phase H/D exchange process between <i>m/z</i> 151 (M ₁₅₁ ⁺) and ND ₃ on three different sites.....	158

List of abbreviations

GC	<i>gas-chromatography</i>
(UV/Vis)	<i>ultra-violet/visible</i>
¹³ C NMR	<i>carbon nuclear magnetic resonance</i>
¹ H NMR	<i>proton nuclear magnetic resonance</i>
a.u.	<i>arbitrary units</i>
AP	<i>atmospheric pressure</i>
APCI	<i>atmospheric pressure chemical ionization</i>
API	<i>atmospheric pressure ionization</i>
APPI	<i>atmospheric pressure photo ionization</i>
BNT	<i>binaphthyl</i>
CAR	<i>collision activated reaction</i>
CI	<i>chemical ionization</i>
CID	<i>collision induced dissociation</i>
COSY	<i>homonuclear shift-correlation spectroscopy</i>
DAD	<i>Diode Array Detection</i>
DART	<i>direct analysis at real time</i>
DC	<i>direct current</i>
DFT	<i>density functional theory</i>
diESI-MS	<i>direct inlet electrospray ionization Mass Spectrometry</i>
EI	<i>electron ionization</i>
ELSD	<i>evaporative light scattering detector</i>
ESI	<i>electrospray</i>
ESI-MS	<i>electrospray mass spectrometry</i>
FT	<i>Fourier transformation</i>
FWHM	<i>full width half maximum</i>
H/D	<i>hydrogen/deuterium exchange</i>
HILIC	<i>hydrophilic interaction liquid chromatography</i>
HMBC	<i>heteronuclear multiple-bond correlation</i>
HMQC	<i>heteronuclear multiple quantum-coherence</i>
HOMO	<i>highest occupied molecular orbital</i>

HPLC	<i>high performance liquid chromatography</i>
HR/MS	<i>high resolution mass spectrometry</i>
i.d	<i>internal diameter</i>
ICR	<i>ion-cyclotron resonance</i>
Idp	<i>ion-dipol complex</i>
IMR	<i>Ion-molecule reaction</i>
In-Source CID	<i>“in-source” collision induced dissociation</i>
IT	<i>Ion trap</i>
LC	<i>liquid chromatography</i>
LC-MS	<i>liquid chromatography-mass spectrometry</i>
LC-NMR	<i>liquid chromatography-nuclear magnetic resonance spectroscopy</i>
LSE	<i>liquid-solid extraction</i>
LTQ	<i>linear trap quadrupole</i>
<i>m/z</i>	<i>mass -to-charge ratio</i>
MALDI	<i>matrix assisted laser desorption ionization</i>
MS	<i>mass spectrometry</i>
NMR	<i>nuclear magnetic resonance</i>
NOESY	<i>nuclear overhauser spectroscopy</i>
PA	<i>proton affinity</i>
Q-TOF	<i>quadrupole-time-of-flight</i>
RF	<i>radio-frequency</i>
RP	<i>reverse phase</i>
RP-LC	<i>Reverse-Phase Liquid Chromatography</i>
RRKM	<i>quasi-equilibrium theory</i>
SLD	<i>soft laser desorption</i>
SPE	<i>solid phase extraction</i>
SPME	<i>solid-phase micro-extraction</i>
TFA	<i>trifluoroacetic acid</i>
TIC	<i>total ion current</i>
TLC	<i>thin layer chromatography</i>
TOF-TOF	<i>time-of-flight - time-of-flight</i>

TQ	<i>triple-quadrupole</i>
TS	<i>transition state</i>
UPLC	<i>ultra-high performance liquid chromatography</i>
UV	<i>Ultra-violet</i>

Preface

Fungi have been used in medical purposes for a long time. They have evolved secondary metabolic pathways with the capacity to produce a various compounds displaying an impressive array of biological activity. The fact that these metabolites or their derivatives have pharmacological functions in the treatment of human diseases has been the cornerstone of new lead discovery for decades.

The chemical composition and bioactivities of many native fungi has not yet been studied in detail, though it has become a trend in the last two decades. Interestingly, fungi lack a protective outer layer, such as epidermis or bark, and are forced to rely only on their chemical defensive mechanisms to be able to survive in their environmental conditions. It is precisely these defensive chemicals that play a great role in many bioactivities. Many of such secondary metabolites have been determined in the sense of their chemical structure and bioactivities, but there is unlimited number metabolites still waiting to be explored.

Ascomyceteous fungi, Xylariaceae shows a rich spectrum of secondary metabolites too. Its particularity is that they also produce an interesting set of secondary metabolites, azaphilones. Azaphilones presents a structurally diverse class of fungal secondary metabolites (polyketide derivatives), namely pigments with pyrone-quinone structures containing a highly oxygenated bicyclic core and a chiral quaternary centre.* In the wide research of these compounds it was revealed that they show a wide spectrum of biological activities. It was also revealed that these secondary metabolites are often characteristic for the certain families, genus or species.†

Over the past decade, methods that offer both high accuracy and sensitivity for the measurement of highly complex mixtures of compounds have been established. Mass spectrometry has become a method of choice for identification of unknown compounds. Compared with the gas-chromatography (GC) technologies, liquid chromatography (LC) interfaced with mass spectrometry (MS) offers several distinct advantages. Whereas GC based approaches can only be used with volatile compounds or compounds, liquid chromatography-mass spectrometry (LC-MS) can be adapted to a wider array of molecules, including a range of secondary metabolites.‡ Since the interface of high performance liquid chromatography (HPLC)

* Natalia Osmanova • Wulf Schultze • Nahla Ayoub Azaphilones: a class of fungal metabolites with diverse biological activities *Phytochem Rev* (2010) 9:315–342

† Stadler M Importance of secondary metabolites in the Xylariaceae as parameters for assessment of their taxonomy, phylogeny, and functional biodiversity *Current Research in Environmental & Applied Mycology* Doi 10.5943/cream/1/2/1

‡ Alisdair R. Fernie, Richard N. Trethewey, Arno J. Krotzky and Lothar Willmitzer; Metabolite profiling: from diagnostics to systems biology. *NATURE REVIEWS, MOLECULAR CELL BIOLOGY*, VOLUME 5 | SEPTEMBER 2004

and MS, it has also become a useful technique for analyzing complex matrixes, such as soils, plants, fungi, microorganisms, diverse biological fluids, etc. Since invent of metabolomics and metabolite profiling, mass spectrometry has become one of the principal methods used in chemotaxonomy of plants, yeast, molds and fungi.

In the study of primary and secondary metabolites, two approaches are commonly used: metabolic fingerprinting and metabolic profiling. Metabolic fingerprinting means the analysis of metabolites with no consideration of condition optimization for molecules of interest, since all the detected metabolites are of interest, even their structural identification is not. Metabolic profiling means analysis of smaller number of already defined metabolites under the already defined conditions.* In the last twenty to thirty years a classification of Xylariaceae using metabolite profiling underwent expansion. Many different species were classified based on their secondary metabolite profiles and some new genera were also divided on several new ones.

Our contribution by this work primarily to the chemistry of natural compounds and furthermore to the mycochemistry and mycology is to give more information on the chemical structures of azaphilones from *Hypoxylon fragiforme*, a specie from family of Xylariaceae, and to reveal a new secondary metabolites from this fungi, by using mass spectrometry techniques, as they are frequently utilized in this domain. Beside the LC-MS, a high resolution mass spectrometry (HR/MS), collision induced dissociation (CID) and gas-phase ion-molecule reactions (IMR), such as hydrogen/deuterium (H/D) exchange have been utilized in elucidating the structure of known and newly discovered azaphilones.

* Fiehn O., Combining genomics, metabolome analysis and biochemical modeling to understand metabolic networks, *Comparative and Functional Genomics*, **2001**, 2:155-168

General part

1. Natural products

In the first chapter of the manuscript, concerning the chemical richness of fungal kingdom, we do a small overview about several species from this kingdom. This part gives a better insight into which position and role the azaphilones have, among the different families of natural chemical compounds existing in these samples. Such bibliography is useful in understanding the importance of such natural products for human race.

1.1 Fungi and its significance

Microorganisms such as yeasts, molds and mushrooms are classified as a kingdom of fungi separated from plants, animals, and bacteria. Major difference is that fungal cell walls contain chitin (polymer of N-acetylglucosamine), like arthropods, nematodes and insects,[1] while the cell walls of plants contain cellulose. These and other differences, such as living and reproduction style classify fungi and related organisms in a single group, *Eumycota*. [2]

Although widespread over the world, most fungi are inconspicuous because of its small size, and underground lifestyles. Often fungi are located on dead matter or live in symbiosis with plants, animals or other fungi. They play an important role in the decomposition of organic matter and are fundamental roles in nutrition cycling. [3, 4]

Fungi have been used in medical purposes for a long time. They shows a wide range of biological activities[5], due to the presence of active organic compounds produced during the metabolism for different purposes, such as secondary metabolites or other extrolites*, often produced for defense and protection against environmental danger. Frisvad gave a definition extrolites: "*Extrolite is an ecological term for outwards directed metabolites that potentially can play a role in the interaction between organisms.*" [6]

* According to the initial definition (Samson & Frisvad, 2004), the term "extrolites" includes secondary metabolites, but is not restricted to them (Extrolites is an ecological term for outwards directed metabolites that potentially can play a role in the interaction between organisms (Frisvad et al. 2004, 2007))

Since the dawn of medicine, compounds derived from animals, plants and microbes have been used as therapeutic agents. Prior to the 1800's, the active constituents of most medicines, which were generally plant-based, were unknown. Commercialization of the antibiotic penicillin in the 1940's was arguably the most significant milestone in drug discovery research, as it spurred enormous efforts in this field. As a result, about 40% of today's therapeutic agents are derived from biological sources. Fungi show a various biological activities such as antimicrobial, antiparasitic, antitumor[7], antifungal, antioxidant[8], antiviral, anti-HIV[9] etc. Indeed, a recent literature survey found that over 1500 fungal metabolites, characterized between 1993 and 2001 that have been found to exhibit antibiotic or antitumor activity.

1.2 The Xylariaceae family

On the basis of an estimated 1.5 million species,[10] the number of fungi in the world represents, after the insects and probably the bacteria, one of greatest but underutilized living resources. Only 5% of these have been formally classified, which is about 72,000 species.[11]

The fungus kingdom includes an enormous diversity of taxa with various ecologies, life style strategies and morphologies ranging from single-celled aquatic fungi to large mushrooms. During 18th and 19th century fungi have been classified according to their morphology (*e.g.*, characteristics such as spore color or microscopic features). Nowadays, DNA analysis and various instrumental analytical methods are included in the taxonomy. Phylogenetic studies[12] published in the last decade have helped the classification of fungal kingdom (**Figure 1**), which is divided into nine subkingdom, seven phyla, and ten subphyla. As a subkingdom of Fungi, Dikarya is divided on two phyla, Ascomycota and Basidiomycota. They include most of so called "higher fungi", but also many anamorphic species that have been classified as molds in earlier literature.

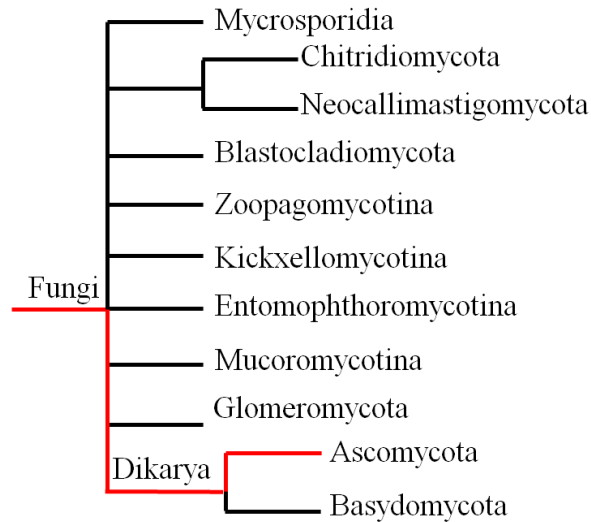


Figure 1: Phylogenetic tree and taxonomy of Fungi.[13]

The Xylariaceae (Xylariales, Ascomycotina) is a large family that belongs to the phyla Ascomycota and comprises around 40 genera.[11, 14] It has its representatives in the most countries of the world, and they exhibit its greatest diversity in the tropical regions.[15] As a result of comparative taxonomic studies, including biochemical, cultural and chemical approaches, there is now a reasonable understanding of species boundaries and intergeneric relationships within the family.

The Xylariaceae are a family of mostly small ascomyceteous fungi. It is one of the most commonly encountered groups of ascomycetes and is found throughout the temperate and tropical climate regions. They are typically found on wood, seeds, fruits, or plant leaves. Most of these decay woods and are plant pathogens.[15, 16]

In general, the fruiting body of Xylariaceae fungus is consisted of stroma (**Figure 2**), perithecia, asci*, ascospore† and anamorphs‡. Stroma is the connective tissue framework of an organ or other structure of fruiting body. Perithecia is a small flask-shaped fruiting body in some ascomycete fungi that encloses the asci (spore sacs), and that can be embedded in the conspicuous stroma at Xylariaceae.

* Asci - sexual spore-bearing cell; plural-ascus

† Ascospore - spore placed in an ascus, or product of an ascus

‡ Anamorphs - life stage of fungus when it produces sexual spores; There exist teleomorphs, sexual reproductive stage (fruiting body), and holomorphs, the whole fungus, with anamorph and teleomorph

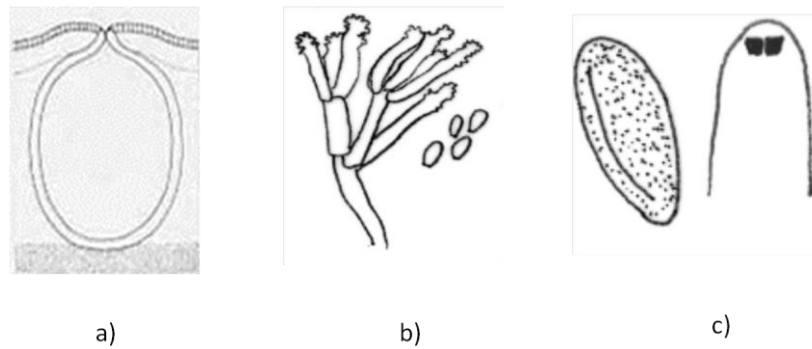


Figure 2: Example of the vertical section of a) stroma, b) anamorph and c) ascospore of some *Hypoxylon*, Xylariaceae [17]

The considerable variation in general stromatal morphology in certain species of genus *Xylaria* has in the past resulted in putting the same species in separate taxa. [18, 19] In developing a modern systematic arrangement within the family, teleomorphic features such as stromal form and color, type of ostiole*, structure of the asci, shape and dimensions of ascospores etc., have all proved to be useful taxonomic characters.[14] Examination of the anamorphs, when these are produced, has also provided a valuable source of taxonomic characters. In the absence of a realistic inventory of the Xylariaceous genera it is still not possible to accurately assess the number of existing species or to predict with confidence how many species might be expected.[20]

1.3 General and ecological aspect of Xylariaceae

Morphological and anatomical features of the stroma have been traditionally used in generic classification of the Xylariaceae. The ascospores† are designed to survive in the environment for a long time after discharge, and the germ slit allows a rapid germination under favorable conditions. Production of many species is not as dependent on the season as of the sexual stages, and may occur several times throughout the vegetation period under favorable conditions. [7]

Xylariaceae have long been considered to be wood-destroying or coprophilous saprobes, aside from a few facultative tree parasites. A frequent parasite of beech, are

* Ostiole - a small opening through which fungi release mature spore

among the few important xylariaceous plant parasites of the Northern Hemisphere.[21]

A great majority of Xylariaceae colonizes dead and decaying wood. Some species, including *Hypoxylon fragiforme* appear in the succession of wood-decomposing fungi quite early, with at least formation of their stromata. The mechanisms of wood biodegradation have been studied extensively in some temperate[22] and tropical Xylariaceae.[23, 24] Recently it was shown that wood-grown cultures of a fungus *Daldinia concentrica* degraded ¹⁴C-labelled synthetic lignin in wood and other organic substrates.[25]

The Xylariaceae have also received considerable attention because of their mutual relationships with plants. For example, it was found, and results were verified by molecular data the presence of 14 different species of Xylariaceae in orchids. The Xylariaceae were found in all organs of the plant, while the liverworts are predominantly colonised by “xylarialean” endophytes.[26]

1.3.1 Taxonomy of Xylariaceae

Many studies on the taxonomy of Xylariaceae have been done in the last two century. Among the first studies, work of Möller was published at the beginning of 19's century on neotropical Xylariaceae.[27] He included meticulous field observations, microscopic studies on their anamorphs and stromatal development of the species. Later, Miller provided several important papers on their taxonomy, including the first world monograph on *Hypoxylon*. [28] He divided 120 species and varieties into four main sections, based on the nature of the ostiole. In 1976, Whalley classified the genus *Hypoxylon* by so-called numerical taxonomy, where he used 55 characters (such as stromatal shape, diameter, texture, perithecial diameter, characteristics of ascospore etc.) for the statistical classification of each species studied. [29] Furthermore, utilizing the thin layer chromatography, he classified *Hypoxylon* relying on the presence or absence of stromatal pigments in different species. Stromatal pigments seemed to provide information for the separation of certain species which were sometimes confused. [20]

In early taxonomic studies of the Xylariaceae, investigators were often confused by the wide variation in morphological form exhibited by many of the taxa.[11] In the absence of a realistic inventory of the Xylariaceous genera it is still not possible to accurately assess the number of existing species. However, on the basis of the recent revisions of some species it is possible to provide some indication of likely numbers for Xylariaceous genera (**Table 1**).

Table 1: Major genera of Xylariaceae

Genus	Number of known species	Predicted number of species
<i>Anthostomella</i> Sacc.	50	~100
<i>Biscogniauxia</i> Kuntze	25	>40
<i>Camillea</i> Fr.	30	>40
<i>Daldinia</i> Ces. & De Not.	17	>20
<i>Hypoxylon</i> Bull	126	>200
<i>Rosellinia</i> De Not.	100	?
<i>Xylaria</i> Hill ex Schrank	100	>500

1.3.2 Chemical diversity of Xylariaceae and its use in taxonomy

Most of the genera of Xylariaceae are known to produce manifold stromatal pigments. These stromatal pigments colors 10% KOH solution, and this “control test” is today used before any other analysis or verification of the *Daldinia* and *Hypoxylon* genus.[14] This test is now employed as key feature in addition to morphological characters for segregation of species. The lack of coloration of KOH solution is also of taxonomical significance. For instance, *Nemania* and *Xylaria*, and many other Xylariaceae with *Geniculosporium*-like anamorphs do not produce the characteristic pigments of *Hypoxylon* and *Daldinia*.[30] It is also very important to mention that the concentration of coloring agents (and thus the intensity of pigments in KOH) can vary with the age and state of preservation.[31] Frequently, but not always, the color intensity of pigments in KOH is high in young and freshly collected specimens. This may indicate a role of these compounds in the means of protection of stromata

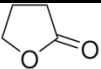
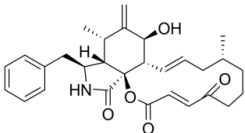
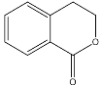
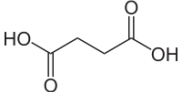
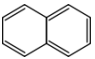
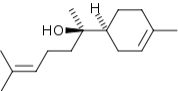
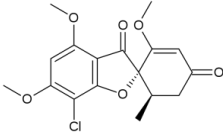
during maturation. On the other hand, over mature specimens, or those dried at high temperature, may yield low amounts of extractable compound.[32] For instance, the xylariaceous *Hypoxylon fragiforme* produces different compound classes in its ascigenous stromata than in the young immature stromata, and still other extrolites prevail in its mycelial cultures.[33] The colors of the subsurface granules and KOH-extractable stromatal pigments are indispensable for species recognition in *Daldinia* and *Hypoxylon/Annulohypoxylon*. The similar pigment colors may either be due to the presence of same or similar metabolites in groups of related species, or the result of different chemical compounds.[34] *Xylariaceae* in general are rich in such compounds. Whalley and Edwards[11] demonstrated that in cultures of *Xylariaceae*, the occurrence of secondary metabolites is of high taxonomic significance.[12]

The chemotaxonomy of genus *Daldinia* has not been revised by Whalley and Edwards, though they have mentioned the occurrence of secondary metabolites in this species.[11] Several years later chemotaxonomy of *Daldinia* was summarized, [35] comparing the results of secondary metabolite analysis and PCR fingerprinting techniques with classical taxonomy in a polyphasic approach. The occurrence of characteristic secondary metabolites in extracts derived from stromata and cultures of *Daldinia* spp. was investigated by analytical HPLC with ultra-violet/visible (UV/Vis) and mass detection. With obtained information on the structures of present secondary metabolites many of them have been confirmed. Thus, the production of secondary metabolites in *Xylariaceae* is consistent and reliable feature for development of their chemotaxonomy.

Unlike most ascomycete genera, *Xylariaceae* has received considerable attention over the two decades regarding the studies of their secondary metabolites. They are quite creative in the production of natural chemicals, hence their stromatal pigment colors usually results from the presence of a mixture of several metabolites.[32] Rosellinic acid and diketopiperazine were isolated from cultures of *Rosellinia necatrix*, as well as cytochalasin E. Engleromycin, an epoxide of cytochalasin D was later isolated from the xylariaceous taxon, *Engleromyces goetzii*. More recently *Hypoxylon fragiforme* was found to owe its orange to brick red stromal colour to mitorubrin and its derivatives

whilst *Xylaria polymorpha* produces a hydroxyphthalide derivative, xylaral, which develops a violet purple colour with aqueous ammonia. The major metabolites produced by the representatives of Xylariaceae can be grouped as **dihydroisocoumarins** and derivatives, **succinic acid** and derivatives, **butyrolactones**, **cytochalasins**, **sesquiterpene alcohols** (punctaporonins), **griseofulvin** and griseofulvin derivatives, **naphthalene** derivatives and long chain **fatty acids** as presented at **Table 2**. Generally the presence of these compounds can be closely related to systematic position.

Table 2: Generic distribution of major metabolites in Xylariaceae in different genera of the family Erreur ! Signet non défini.

Example of metabolites	1	2	3	4	5	6	7	8	9	10	11
Butyrolactones 							+				
Cytochalashins 							+			+	+
Dihydroisocoumarins 	+	+				+					
Succinic acid and derivatives 											+
Naphtalenes 			+	+							
Sesquiterpen alcohols 								+			
Griseofulvin and derivatives 											+

*1-Biscogniauxia, 2-Camillea, 3-Daldinia, 4-Entonaema, 5-Hypoxylon, 6-Kretzschmaria, 7- Nemanina, 8- Poronia, 9-Thamnomycetes, 10-Rosellinia, 11-Xylaria

The dihydroisocoumarins are widely distributed throughout the family but are probably more representative of *Hypoxylon*, *Biscogniauxia* and *Camillea*. Butyrolactones so far appear to be restricted to *Nemania serpens* whilst cytochalasins are more frequently encountered in species of genus *Xylaria* and *Rosellinia*.

Classification of Ju and Rogers[14] is much more different from the one of Miller[28] Ju and Rogers pay more attention to anamorphic characteristics and stromatal pigments, beside the usual teleomorphic characteristics that are usually utilized in the modern approach. Whalley and Whalley[20] showed in that the species of the genus *Hypoxylon* may be classified based on the secondary metabolites composition determined by the thin layer chromatography of the ethyl-acetate stromatal extracts. They were the first ones to show the importance of chromatographic methods in taxonomy of Xylariaceae family. Nowadays, a set of chromatographic methods like HPLC, GC, 2D nuclear magnetic resonance (NMR) and HR-MS are widely used, especially in the taxonomic purposes, where the milligrams of crude samples are necessary for complete elucidation and specie determination.[36]

1.3.3 What about *Hypoxylon*?

Hypoxylon is the largest genus of Hypoxyloideae (Xylariaceae), and is recently divided in two section, *Hypoxylon* which includes about 170 species (a number which may increase to 200 or more, once a complete survey of its manifold),[37] and *Annulata* (*Annulohypoxylon*), which includes about thirty species.[38] *Hypoxylon* is a cosmopolitan genus, but has its highest diversity in the tropics and subtropics.*

The genus *Hypoxylon* is delimited by four main characteristic:

1. *Nodulisporium* -like anamorphs - the primary criterion for recognizing a xylariaceous fungus as a member of Hypoxyloideae,
2. stromata unipartite,

*<http://mycology.sinica.edu.tw/Xylariaceae/generalInfo.asp?qrySectionName=Hypoxylon&qryPageID=1>

3. stromatal tissue below the perithecial layer solid and homogeneous,
4. stromata not upright, *i.e.*, with the height less than the length and the breadth.

Some other characteristics are useful in determination of *Hypoxylon*. Unfortunately, these properties do not universally belong to taxa of *Hypoxylon*, and therefore their usefulness in defining is limited.[34] These characters include the dehiscent perispore, the flat ascus apical ring, the germ slit on the convex side of the ascospore, the waxy stromatal tissue, and the KOH-extractable stromatal pigments. For example, there are more than thirty taxa of *Hypoxylon* in which the perispore is not easily dehiscent, and many taxa have nearly equilateral ascospores which make the position of the germ slit, whether it is on the convex or the flattened side, impossible to assess.

In today's classification of *Hypoxylon* and other genus of Xylariaceae, chemotaxonomy plays a great role. **Figure 3** presents several different *Hypoxylon* species whose classification was based on the secondary metabolite profiling. It may be noticed that only the small differences in color, coming from different pigment composition affects their classification.

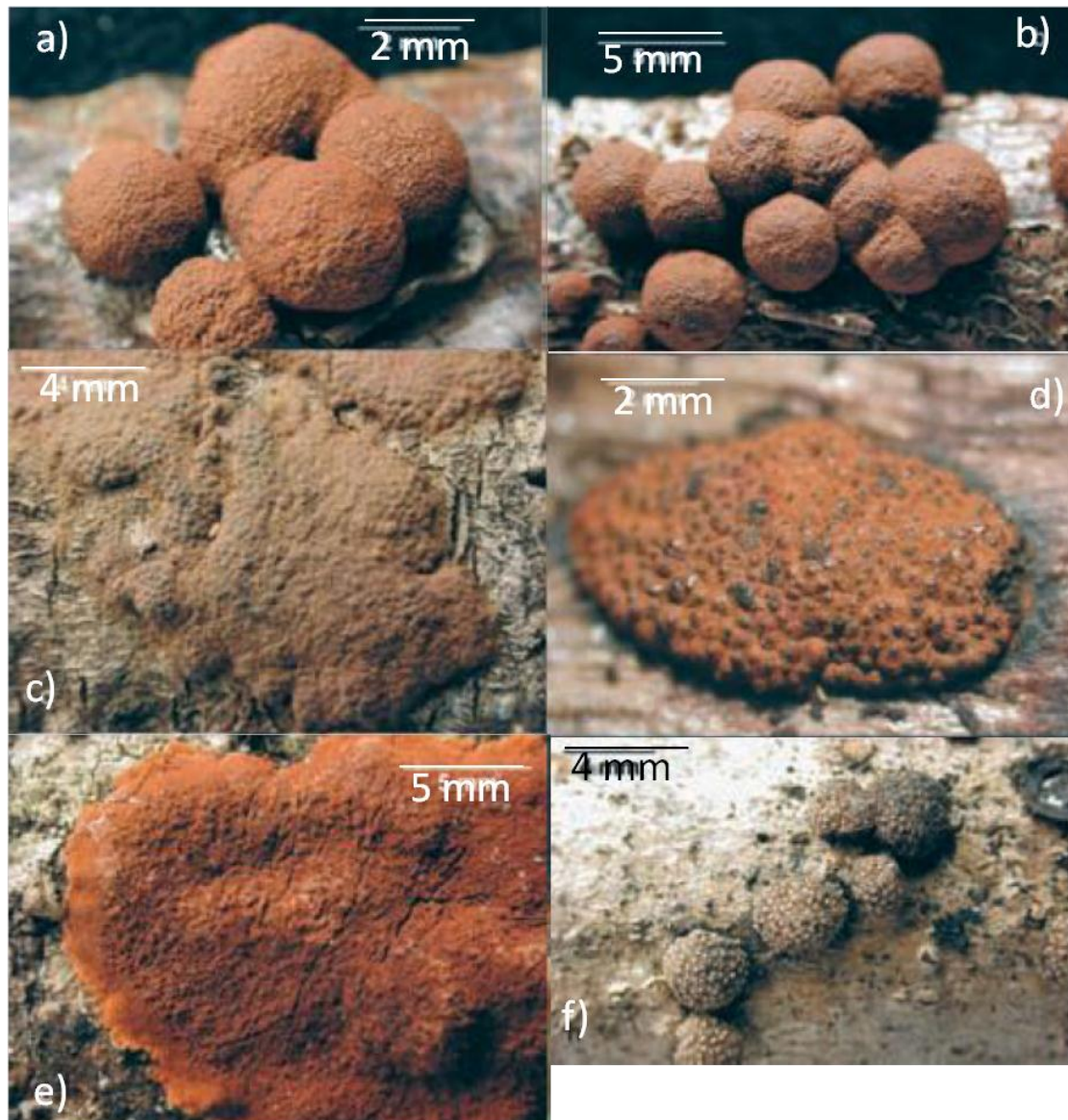


Figure 3: Different Hypoxylon species containing orselinic acid and azaphilone esters: a) *H. fragiforme* (containing mitorubrins), b) *H. howeanum* (containing mitorubrins), c) *H. rubiginosum* (containing mitorubrins and rubiginosins), d) *H. rutilum* (mitorubrins, rubiginosins, rutilins), e) *H. ticinense* (mitorubrins), f) *H. intermedium* (hypomiltin)[34]

Hypoxylon fragiforme[31] is a species belonging to the genus of Hypoxylon, and family of Xylariaceae. It is one of the most widespread ascomycetes. Perithecial stromata of *Hypoxylon fragiforme* are common on dead trunks and branches of beech, *Fagus sylvatica*, but are only occasionally found on other woody hosts. Colonization is not extensive so long as the water content of infected host tissue remains high, but if branches are cut from living trees and allowed to dry, the mycelium extends rapidly. Fruiting first occurs when conidial stromata develop at the surface of the bark covered with the pale brown hat of conidiophores. As the conidial stromata enlarge,

it becomes reddish brown, and converts into a perithecial stroma by the development of the numerous perithecia in the outer part, each with a prominent ostiole. Ripe (mature) stromata reveal asci containing dark-colored ascospores. Perithecial stromata with ripe asci can be collected over the years.[39] This was confirmed by Stadler's group.[31] According to their unpublished results, *Hypoxylon Fragiforme* will often produce stromata already in the first season, just few weeks after the beach wood has been felled or damaged. The fungus may then persist for up to decades as saprotroph and regularly produce stromata.

Some may think that the dark pigment of the spore is probably melanin, located in a thicker inner layer.[31] It appears, and is proven that this is not the only pigment giving the color to the Xylariaceae fungi. *Hypoxylon fragiforme* possesses an ability to produce manifold stromatal red pigments. These red pigments are concentrated in the orange granules located beneath the stromatal surface.

2. Fungal metabolites and secondary metabolism

2.1 Biological activities of metabolites from Xylariaceae fungi

The structure - activity relationship among some mycotoxins was reviewed almost 20 years ago. [40] Important features that characterize common structural properties that influence biological activities of mycotoxins are:

- the **oxirane ring** (appears in cytochalasans and trichothecenes; some trichothecenes even have two **epoxy rings** in their structure)
- **quinoid moieties** (benzoquinone, naphthoquinone, and anthraquinone; for example, benzoquinone moiety of terreic acid, which is a diabetogenic mycotoxin)
- five-membered or six-membered **lactones**, either saturated or unsaturated. (for example, patulin can react as an alkylating agent with DNA molecules, why it shows mutagenic, carcinogenic, or teratogenic activity)
- **macrocyclic structures** (present in for example cytochalasans and some trichothecenes act as mycoestrogens) (**Figure 4**)
- **isocoumarins** (ochratoxins - dihydroisocoumarin moiety in combination with L- phenylalanin leads to inhibition of protein synthesis at the stage of amino acid activation.[41])

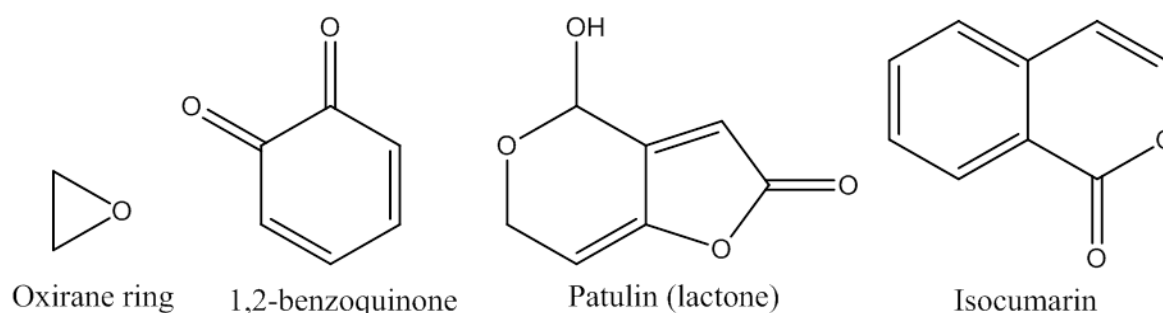


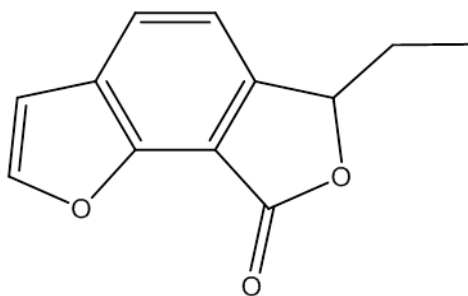
Figure 4: Examples of compounds with present functions that influence biological activities

Hundreds of natural substances and bioactive compounds were found in selected fungi on the basis of collection of fruiting bodies, strain preservation, biological screening and chemical investigation. For this reason, isolation process, structural

elucidation and biological activities of new and already known secondary metabolites have been revealed from many basidiomycetes and ascomycetes fungi. In the following chapters, there will be briefly depicted some of most interesting fungal secondary metabolites with characteristic bioactivities.

2.1.1 *Concentricolide*

Benzofuran lactone, concentricolide (**Figure 5**) was isolated from the fruiting bodies of xylariaceous ascomycete *Daldinia concentrica* along with four known compounds.[42, 43] Its main activity is that it inhibits HIV-1 induced cytopathic effects.

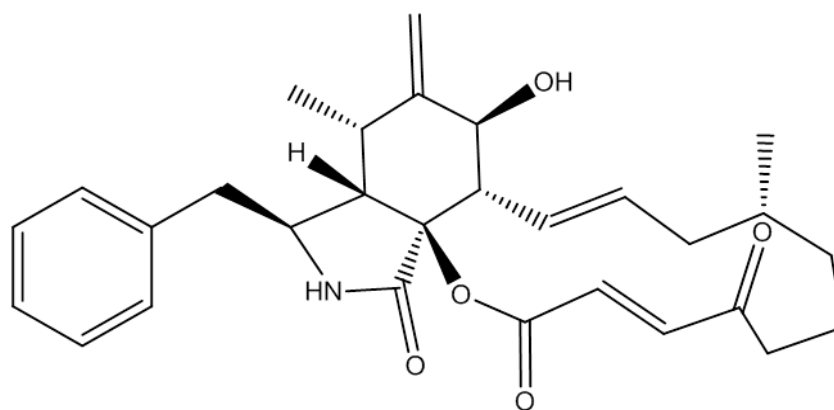


Concentricolide

Figure 5: Structure of concentricolide

2.1.2 *Cytochalasins*

The cytochalasins A-J (**Figure 6**) belong to a group of fungal metabolites related by a structure and biological activities. They share a number of unusual, interesting and characteristic effects on the cell, like inhibition of the division of cytoplasm, reversible inhibition of cell movement, inhibition of nuclear extrusion, inhibition of glucose transport, thyroid secretion and release of growth hormone, antibiotic, antitumor activity etc.



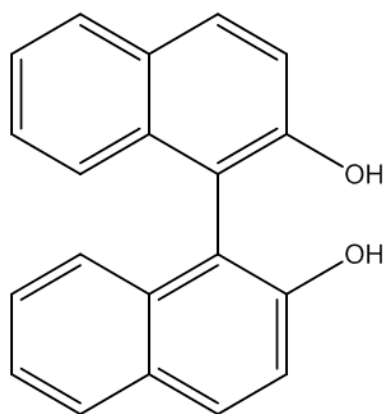
Cytochalasin A

Figure 6: Structures of Cytochalasin A

Cytochalasins from *Daldinia* have been shown to induce apoptosis,[44] and another cytochalasins from *Hypoxylon fragiforme* strongly inhibited human immunodeficiency virus (HIV-1) protease, by inducing apoptosis of viruses' cell.[31] That is why these compounds have been largely studied during the past decades in the sense of their biosynthesis (see below, Biosynthesis of azaphilones) and their activities.

2.1.3 Bynaphthyl

Bynaphthyl (**Figure 7**) from ascomycete fungus *Hypoxylon fuscum* exhibit quite high antioxidant activity that was almost the same as that of the ascorbic acid,[45] which is usually used for the comparison of decreasing the initial concentration of DPPH up to 50%. The antioxidative activity of BNT (4:5:4':5'-tetrahydroxy- 1:1'-binaphthyl) often found in Xylariaceae was almost the same as that of ascorbic acid.



Bynaphtyl

Figure 7: Structure of bynaphtyl

2.1.4 Azaphilones

Family of mitorubins is one of the first reported azaphilones,[46] which showed various bioactivities and some of them were even patented as antiprotzoan dihydrofolate reductase inhibitors.[47, 48] Mitorubins and rubiginosins (**Figure 8**) isolated from *Hypoxylon fragiforme* showed nematicidal activity, while not so high antifungal activity. Fragiformins A and B, isolated from the same species reported rather higher antifungal and nematicidal activity, even higher than that of cytochalashins. Mitorubins are known to moderately inhibit dihydrofolate reductase and geranylgeranyltransferase, with the latter reference including further reports on antifungal activity. However, the activities of most of the stromatal extrolites of *Hypoxylon* so far studied are apparently non-specific or insignificant. This also includes the other types of azaphilones from *Hypoxyloideae* and *Creosphaeria sassafras* such as daldinins, multiformins, and sassafrins (**Figure 8**), which have shown similar or even stronger broad-spectrum antimicrobial effects but have so far not been tested for nematicidal activities.[31] Sassafrins showed moderate antimicrobial activity and strong antifungal activity, as Quang and co-workers demonstrated in 2005.[49]

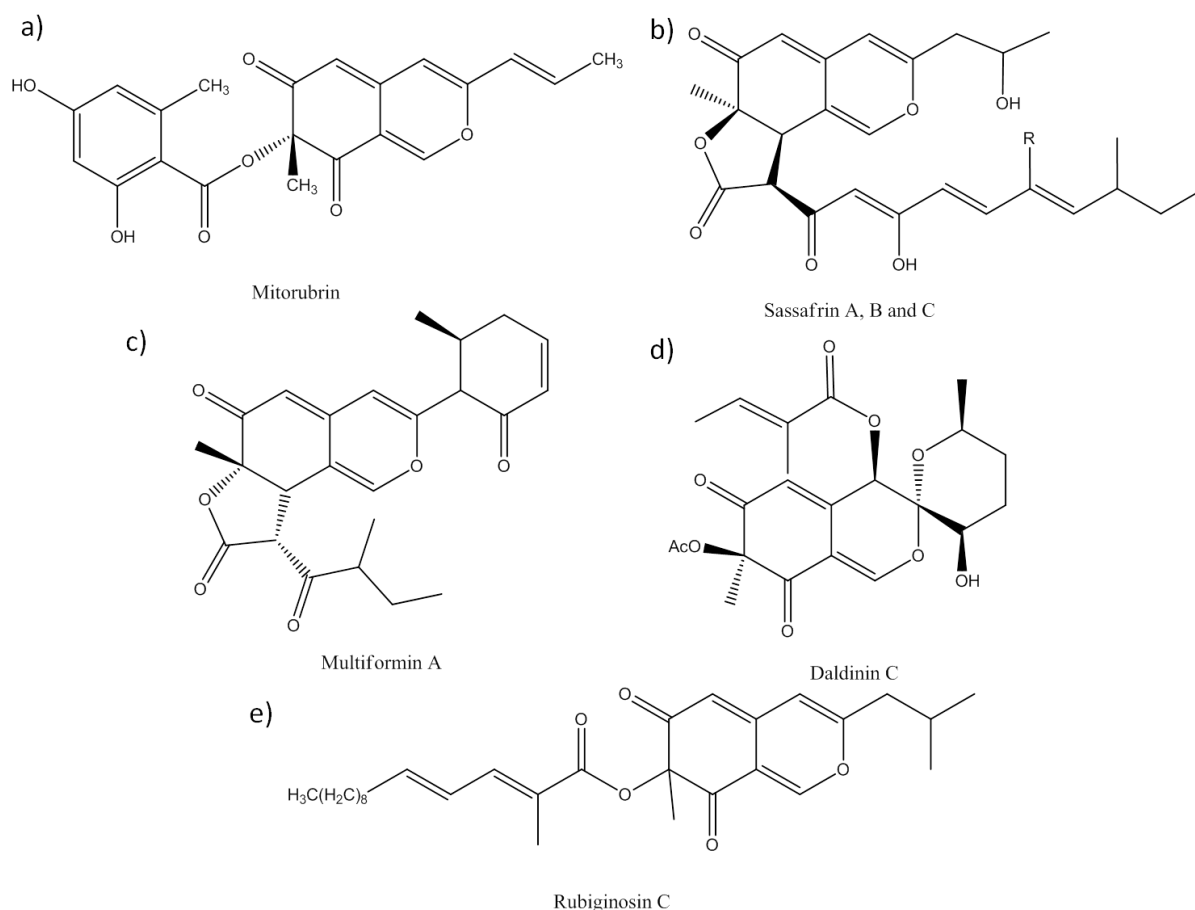


Figure 8: Structures of a) mitorubrin, b) sassafrin, where R=CH₃, H, CH₃ and double bond in lacton ring for A, B and C respectively c) multiformin, d) daldinin and e) rubiginosin

Daldinins E, F, and C do not show significant antioxidant activities. The presence of a lactone ring in multiformins and sassafrins plays an important role in their pharmacological activity. The *in vitro* antimicrobial activities of isolated azaphilones at a dose of 50 µg per paper disc were tested against a panel of laboratory control strains (*Staphylococcus aureus*, *K. pneumoniae*, *Pseudomonas aeruginosa*, *Salmonella enteritidis*, *Escherichia coli* bacteria, and fungal organisms *Aspergillus niger* and *Candida albicans*) and moderate to strong activity was observed against all tested strains.

Overproduction of NO by inducible nitric oxide synthase (iNOS) is included in various pathological processes including tissue damage following inflammation, rheumatoid arthritis. Therefore, suppression of NO production in macrophages could be a target for potential anti-inflammatory drugs. Inhibition of NO production was examined by Quang[50] and co-workers for fifteen azaphilones, isolated from

different Xylariaceae fungi (daldinins C, E and F from *Hypoxylon fuscum*, multiformin D from *Hypoxylon multiforme*, sassafrins A–C from *Creospharia sassafras*, entonaemin A and rubiginosins A–C from *Hypoxylon rubiginosin*, cohaerins A and B from *Hypoxylon cohaerens* and rutilins A and B from *H. rutilin*). The highest NO inhibition was observed for rutilins A and B (**Figure 9**), and for rubiginosin A, while cohaerins showed moderate NO inhibitory activity.[5, 51] Rutilins are formed by condensation of rubiginosin and mitorubrinol acetate, and thus possess in their structure two highly oxygenated skeletons which are probably responsible for such high NO inhibition response. Antioxidant activity was also examined for these azaphilones and the highest activity showed sassafrins B and C, cohaerins A and B and rubiginosin C [50], while cohaerins demonstrated also a strong and non-selective antimicrobial effects.[51]

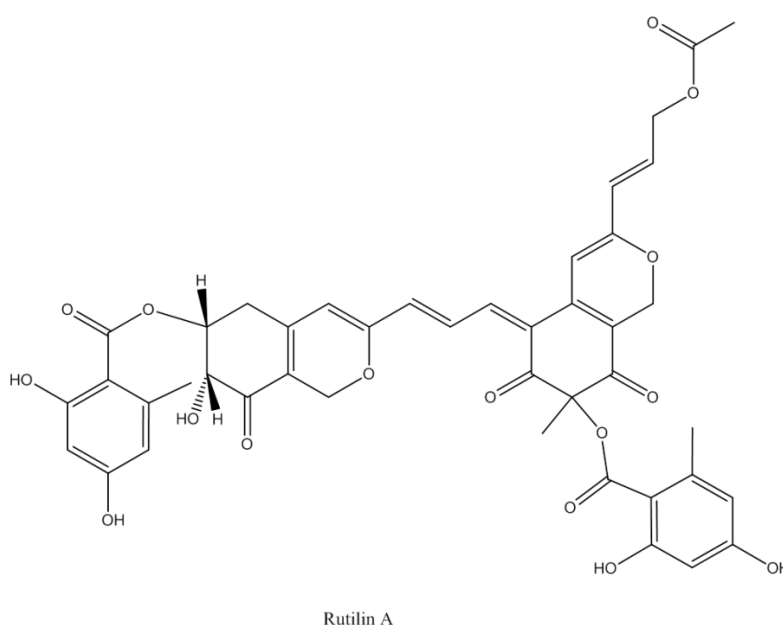


Figure 9: Structure of rutilin A

Talaromyce sp. are ascomycota that produce azaphilones kasinosins A and B (**Figure 10**), which were determined as specific inhibitors of eukaryotic DNA polymerases beta and lambda.[52]

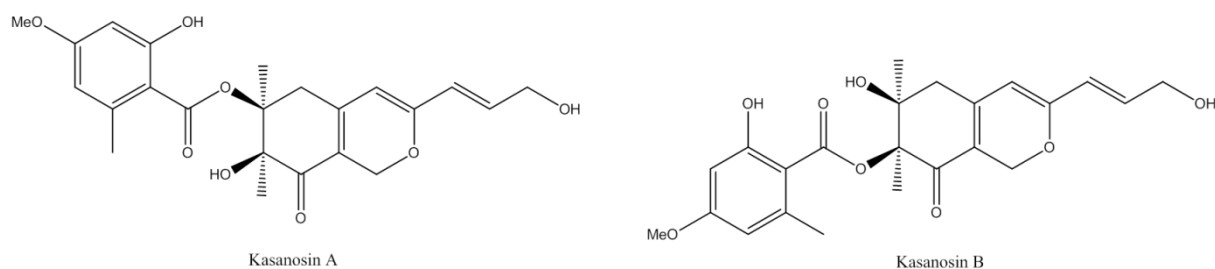


Figure 10: Structures of kansasins A and B

Organic solvent extracts of a Ascomycete subculture, *Helotialean* displayed inhibitory effect on HIV-1 replication in C8166 cells. This activity appears to be due to the azaphilones presents in this yet unidentified *Helotialean* species, *Helitalins A, B and C*. [53]

Azaphilones appears to show a large spectrum of biological activities against various target organisms, including bacteria, fungi, insects and nematodes and ultimately in repelling these enemies, which gives to Xylariaceae family a great importance. They are able to spontaneously incorporate ammonium ions and amines. [54] This may include biogenic amines such as free amino groups of proteins. Even though this has not yet been proven by experimental data but rather deduced from previously reported bioactivities of the chemical types of prevailing compounds, [55] they may be involved in a kind of chemical defense reaction. This is also suggested by the arrangement of anatomical structures that are typically found in the stromata of these fungi. [37]

In the **Table 3** are summarized biological activities of some Xylariaceae species and secondary metabolites that are charged for these activities.

Table 3: Biological activities of selected Xylariaceae species and compounds responsible for the activity

Xylariaceae species	Biological activities											Secondary metabolites			
	antibacterial gram positive	antibacterial gram negative	antifungal	antiviral	antitumor	immunosuppressive	free-radical scavenging	anti-inflammatory	anti-HIV	dihydrofolate reductase inhibition	nuclear extrusion inhibition of cell		nematicidal	NO inhibition	
<i>Daldinia Concentrica</i>	+	+	+						+					concentricolide, concentriols B, C and D (Figure 5)	
<i>Albatrellus confluens</i>			+		+									crifolin, albaconol	
<i>Thelephora ganbajun</i>							+							p-terphenyls	
<i>Thelephora aurantiotincta</i>							+							p-terphenyls	
<i>Boletopsis grisea</i>							+							p-terphenyls	
<i>Daldinia</i>	+	+			+						+	+		cytochalasins A-J (Figure 6)	
<i>Hypoxylon Fragiforme</i>	+	+	+						+				+	+	cytochalasins (Figure 6) , mitorubrins, rubignosins (Figure 8) , fragiformins A and B
<i>Hypoxylon Fuscum</i>							+						+	bynafthyl (Figure 7) , daldinins (Figure 8)	

<i>Creosphaeria sassafras</i>	+	+	+		+		daldinins, multiformins and sassafrins (Figure 8)
<i>Helotialean Ascomycete</i>						+	helitalins A, B and C (Figure 9)
<i>Hypoxylon rutilin</i>					+	+	rutilin A and B (Figure 9), BNT
<i>Hypoxylon rubiginosin</i>					+	+	dimeric azaphilones (Figure 9), rubiginosin A
<i>Hypoxylon cohaerens</i>	+	+	+		+	+	cohaerens
<i>Bulgaria inquinans</i>			+	+		+	bulgarialactone A and B
<i>Hypoxylon multiforme</i>	+	+					multiformins A - D (Figure 8)
<i>Hypoxylon</i>							hypomiltin
<i>Hypomiltum</i>							
<i>Annulohypoxylon cohaerens</i>			+			+	cohaerins
<i>Annulohypoxylon deflectus</i>	+	+	+	+			deflectins

- + - presence of biological activity

2.2 Fungal secondary metabolism

Secondary metabolism is commonly associated with sporulation processes in microorganisms,[56, 57] including fungi. [58, 59] Filamentous fungi produce a diverse array of secondary metabolites, small molecules that are not essential or necessary for normal growth and development. Secondary metabolites associated with sporulation[60] can be placed into three broad categories:

1. metabolites that activate sporulation,
2. pigments required for sporulation structures (for example, melanin is required for the formation of integrity of both sexual and asexual spores and overwintering bodies), and
3. toxic metabolites secreted by growing colonies at the approximate time of sporulation (mycotoxins).

Fungal secondary metabolites can be divided in few classes: polyketides (e.g. aflatoxin), non-ribosomal peptides, terpens and indole terpens.

2.2.1 *Expression and regulation of secondary metabolites*

Fungal pigments are natural products often associated with development of the structure (e.g. melanin is the most common). Some environmental factors affect mycotoxin production, such as temperature, availability of an air-surface interface and pH. Nutritional factors such as carbon and nitrogen source can also affect both mycotoxin production and morphological differentiation. [61]

The regulation of secondary metabolism in fungi has been comprehensively reviewed.[62-64] Secondary metabolite gene clusters often contain a transcription factor that acts specifically on the genes within the cluster. [65, 66] These regulators may also act on genes elsewhere in the genome. For example, transcription factor *aflR* that regulates aflatoxin cluster in *Aspergillus flavus* and *Aspergillus parasiticus* also regulates three genes outside the aflatoxin gene cluster.

Secondary metabolite production is also controlled at an upper hierarchic level by global transcription factors encoded by genes unlinked to the biosynthetic gene clusters. Such genes regulate multiple physiological processes and respond to environmental conditions (pH, temperature and nutrition).[62, 67]

Functional analysis of biosynthetic gene clusters usually relies on disrupting key genes in the cluster and observation of the resulted secondary metabolic profile. Genes in many clusters are produced at very low levels, and often particular metabolites cannot be detected at standard conditions, but under specific conditions, where they can be produced in much higher quantity level.

2.2.2 Functions and roles of defence secondary metabolites

There has been much speculation about the natural functions of secondary metabolites in the past. Until now it is almost completely accepted that these compounds are not randomly produced, but have important functions for the biology of their producers.

The role that secondary metabolites play in the life of fungi is unlimited.[5, 68] Many of these compounds are produced by pathogenic fungi, host-specifically. Host-specific toxins are often crucial for disease of host plant, as a benefit to the fungus. However, many of fungal toxins are often produced only after the death of fungi, thus does not contributes to the defense of the fungi, but only to the virulence to the plant, and are not considered as a defense metabolites. Nevertheless, the fungus is considered as pathogenic, and can involve disease of plant, or not.

The most likely advantage of secondary metabolite to a producing-organism is that they may allow an organism to survive in ecological niche. Many of such organisms live saprophetically (on dead or decaying organic matter) in the soil where they are exposed to a harsh environment with a diverse array of competing organisms. Fungal virulence has probably evolved to protect fungi in such environment against amoebae, nematodes or any other invertebrates that can feed on fungi. [69, 70]

2.2.3 Roles of secondary metabolites from Xylariaceae

Talking about Xylariaceae, their massive, conspicuous stromata have also been found to constitute a good source for such unique compounds. Since 1960, when the first secondary metabolites have been isolated,[71] Xylariaceae family revealed several hundreds of different active natural compounds until nowadays.

The vast majority of the known Xylariaceae secondary metabolites are polyketides. Their natural functions become quite evident in case of the numerous antibiotics, which are produced by these fungi, or in other cases where the metabolites act against specifically associated organisms. For instance, the plant pathogenic Xylariaceae produce a large number of phytotoxins that are involved in parasitism. However, most phytotoxins of the Xylariaceae that were so far characterized exhibited a quite broad-spectrum of bioactivities. They are not apparently specific, but their action may still facilitate the process of parasitism by weakening the defense of the host plants. The lack of knowledge on the natural functions of secondary metabolites in the saprotrophic and endophytic Xylariaceae is easily explained by the fact that most of the known compounds were obtained in the course of screening projects or basic research on the mechanisms of fungal metabolism, including their pigment chemistry.

Thanks to their characteristic chemical structure, a new group of secondary metabolites, azaphilones was formed. Formation of highly oxygenated bicyclic skeleton distinguishes them as new family of secondary metabolites. Azaphilones are increasingly analyzed, and it is important to explore their potentials.

2.3 Azaphilones, fungal secondary metabolites

It is known that fungi lack a protective outer layer (epidermis or bark), and they are forced to rely on their chemical defensive mechanisms.[72-74] For this reason fungi produce a wide range of biologically active secondary metabolites, and many different groups of such chemical compounds have been identified in fungi including organic acids, polyketides (such as quinones, antraquinones, xanthonones...), mono- to

tri - terpenes (volatiles and steroids), polysaccharides, lipopolysaccharides and N- and S- containing compounds.[47, 75, 76]

Azaphilones are interesting set of fungal secondary metabolites, having a polyketide structure. Some authors group the azaphilones into polyketides without giving them any higher significance or further definition.[47, 75] Still, polyketides often comprise structurally complex natural compounds produced by diverse organisms and includes classes such as like anthraquinones, flavonoid pigments, macrolid antibiotics, naphthalenes, polyenes, antibiotics, tetracyclines and tropolones. Azaphilones are later on classified as a separate group of natural products. They can be defined as:

“Structurally diverse class of fungal secondary metabolites (polyketide derivatives), namely pigments with pyrone-quinone structures containing a highly oxygenated bicyclic core and a chiral quaternary center”. [77, 78]

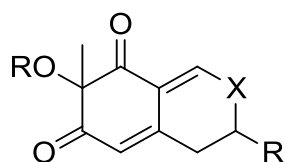


Figure 11: Common structure for all azaphilones (X = O, N)

The azaphilones share a common chemical structure (**Figure 11**). Their name arose as a result of their affinity for ammonia. They react with amino group present in proteins, amino acids and nucleic acids to form red or purple *vinyllogous γ -pyridones* due to the exchange of pyrane oxygen for nitrogen.[79] This is a characteristic reaction. It can take place both with ammonia alone as found in the case of monascorubramine and rubropunctamine, [80] or with the side chain of a macrocyclic polypeptide, as discovered for chlorofusin. [81] Later on, this reaction can be used for rapid synthesis of these compounds. [82]

As shown earlier, azaphilones exhibit a wide range of interesting but nonselective biological activities (see **Table 3**), such as antimicrobial, antifungal, antiviral, antioxidant, cytotoxic, nematocidal and anti-inflammatory activities. The potent

nonselective biological activities of azaphilones may be related to their production of vinylogous γ -pyridones. [68, 83]

2.3.1 *Biosynthesis of azaphilones*

Biosynthetically, most pigments produced by fungi are polyketide-based and involve complex pathways catalyzed by frequent type of polyketide synthases. The biosynthesis of azaphilones (**Figure 12**) uses both the polyketide pathway and the fatty acid synthesis pathway. The polyketide pathway assembles the main polyketide chain of the azaphilone pigments from acetic acid (the starter unit) and five malonic acid molecules (the chain extender unit) in a conventional way to generate the chromophore structure. The fatty acid synthesis pathway produces a medium-chain fatty acid (octanoic or hexanoic acid) that is then bound to the chromophore by a *trans*-esterification reaction.[84-86] For many azaphilones a biosynthetic pathways have been suggested until today (monascorubrin, mitorubrin,[87] monascusones, monascin, sassafrin, etc).

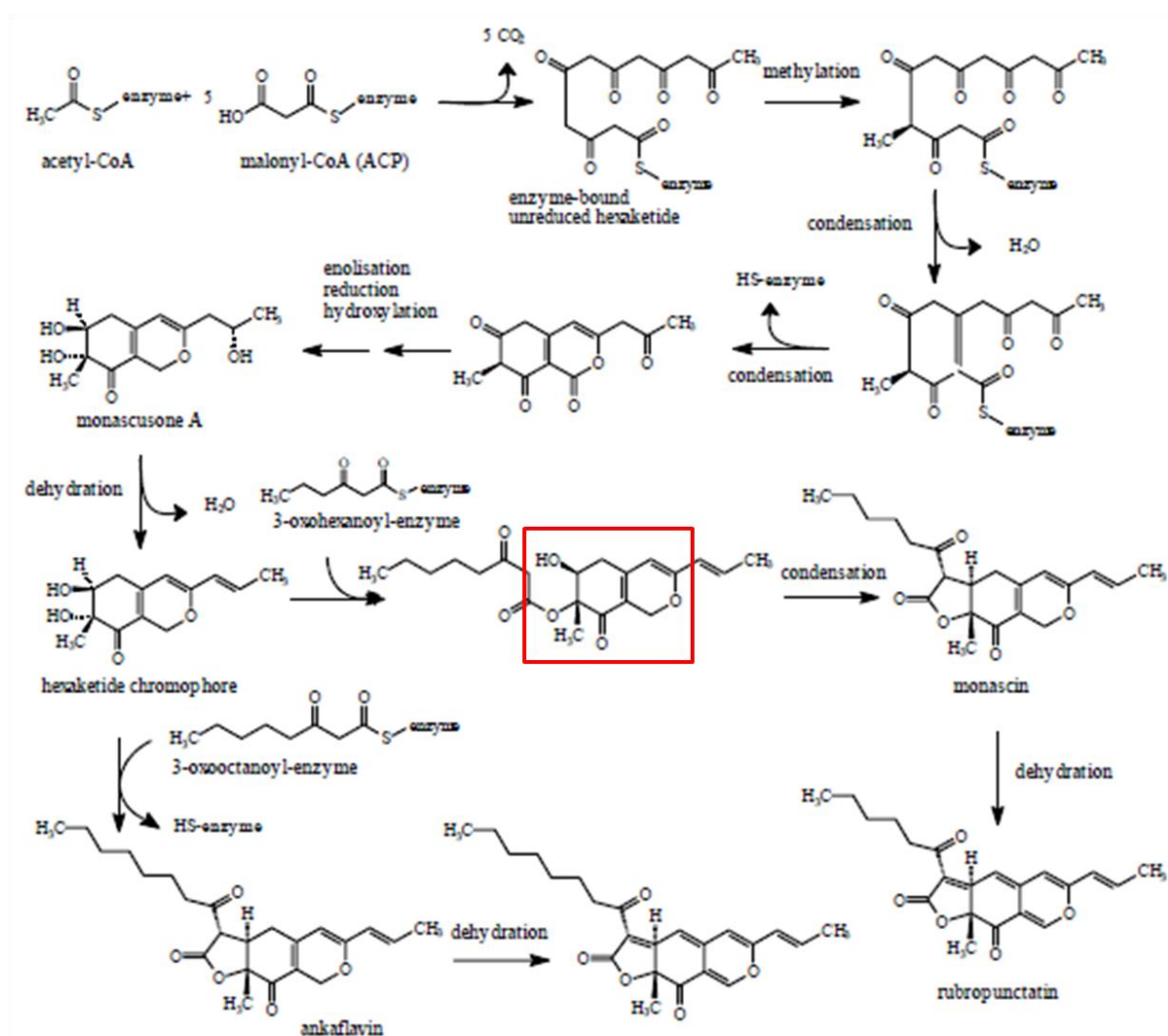


Figure 12: Proposed biosynthetic pathway for formation of azaphilone bicyclic core

The condensation of 1 equivalent of acetate with 5 equivalent of malonate leads to the formation of a hexaketide chromophore by the polyketide synthase. Then a medium-chain fatty acid such as octanoic acid, produced by the fatty acid biosynthetic pathway, is bound to the chromophore structure by a *trans*-esterification reaction to generate the orange pigment monascorubrin (or rubropunctatin upon *trans*-esterification with hexanoic acid).

Fungal polyketide biosynthesis typically involves multiple enzymatic steps, and the encoding genes are often found in gene clusters. It has been demonstrated that this biosynthesis is strongly dependent on the growth environment. The enzymatic

machinery for the formation of the polyketides consists of different modules characteristic of each fungus (e.g., keto synthases, acyl transferases, carboxylases, cyclases, dehydrases, aromatases, reductases, thioesterases, cyclases, laccases etc.) It is interesting to note that, while bacteria have similar enzymes, the folding of the growing polyketide chain deliver different structures. Depending on the chain length, different classes of mycotoxins are formed. Fungal polyketide biosynthesis typically involves multiple enzymatic steps and the encoding genes are often found in gene clusters.[41]

It is interesting to mention that the beginning of biosynthetic pathway of azaphilones and one of the cytochalasins (refer to **Figure 6**) are the same. The both involve condensation of acetate with five malonates. Further bounding of fatty acid is considered for azaphilones, while for cytochalasins is suggested bounding of one unit of phenylalanine and two units of methionine (**Figure 13**).[88]

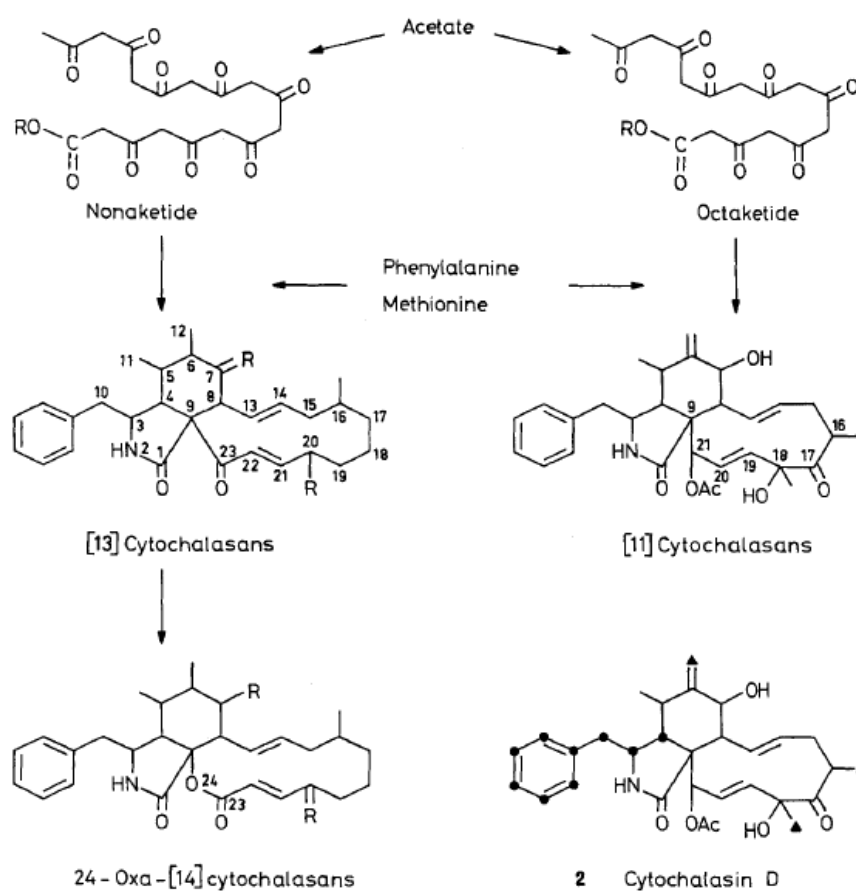


Figure 13: Proposed biosynthetic pathway of cytochalasins

2.3.2 Chemical synthesis of azaphilones

Although structurally similar, particularly in their bicyclic core, azaphilones differ in their properties. Reacting with amines, these molecules form pyridones irreversibly, which give them a high cytotoxicity. This gave to scientists a motivation to synthesize them, and different approaches have been published until nowadays.

Different retro-synthetic strategies have been proposed and published in the aim to obtain the simplest method for chemical synthesis of such molecules. Whalley and its group have proposed the first synthesis of azaphilones sclerotiorines.[89] Their approach was based on cyclization - dearomatization of an enol/aldehyde in the acidic environment and then catching the product with the oxidant (**Figure 14**). [90]

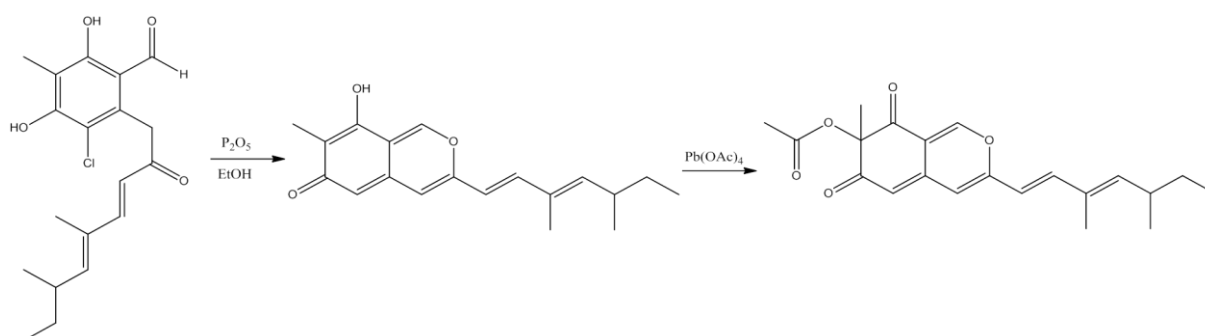


Figure 14: First synthesis of azaphilones proposed by Whalley

Many of upcoming synthesis have been based on this approach. Group of Suzuki [91] have used the same approach, but with different acid, thus changing the reagents as well as oxidants giving different derivatives.

In 2004, Porco's group published a synthesis of azaphilones,[82, 92, 93] that differs from others in the method of cyclisation - dearomatization. They were able to cyclize an enol of an alkyne through activation by a gold salt (AuCl_3). Intermediately, the same type of oxonium is also formed and led to azaphilones after oxidation.

Yao proposed a retro-synthetic pathway for the formation of azaphilones.[94] His group formed an chloroazaphilone by oxidation of 2- benzyzopyrylium salts (as

previously proposed Porco) (**Figure 15**), derived from the formyl ketones through the convergent coupling of substituted benzylic halides with masked acyllithium dithians and further protecting group adjustment.

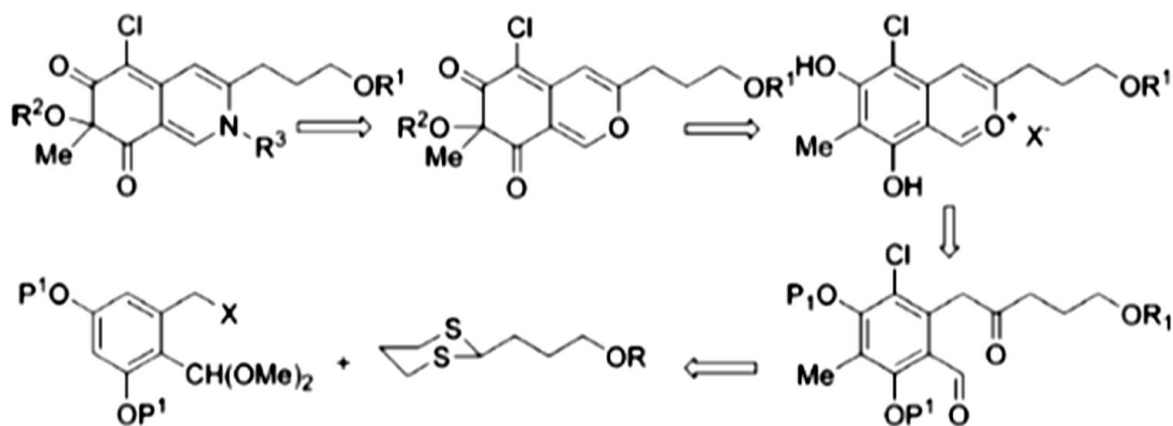


Figure 15: Proposed retro-synthetic pathway for chloroazaphilones[94]

2.3.3 Reaction with quaternary ammonium

Spontaneous reaction of azaphilones with amino group (azaphilone - “nitrogen loving”) from amino acids, proteins or nucleic acids is responsible for their wide range of biological activities. Many works have been based on determination of mechanism of this reaction to resolve its influence on such activities. Juzlova have proposed the biosynthetic pathway of formation of vinylogous γ -pyridones (**Figure 16**).[95] First nucleophilic primary amine is attached to C-10 by Michael addition, forming carbinolamine, which undergoes bond C-O cleavage. Nucleophilic attack on the C-2 carbonyl by the electron pair of enamine results in the closure of the ring and formation of hydroxyl group. Following elimination of water molecule results in the formation of nitrogen-containing azaphilone.

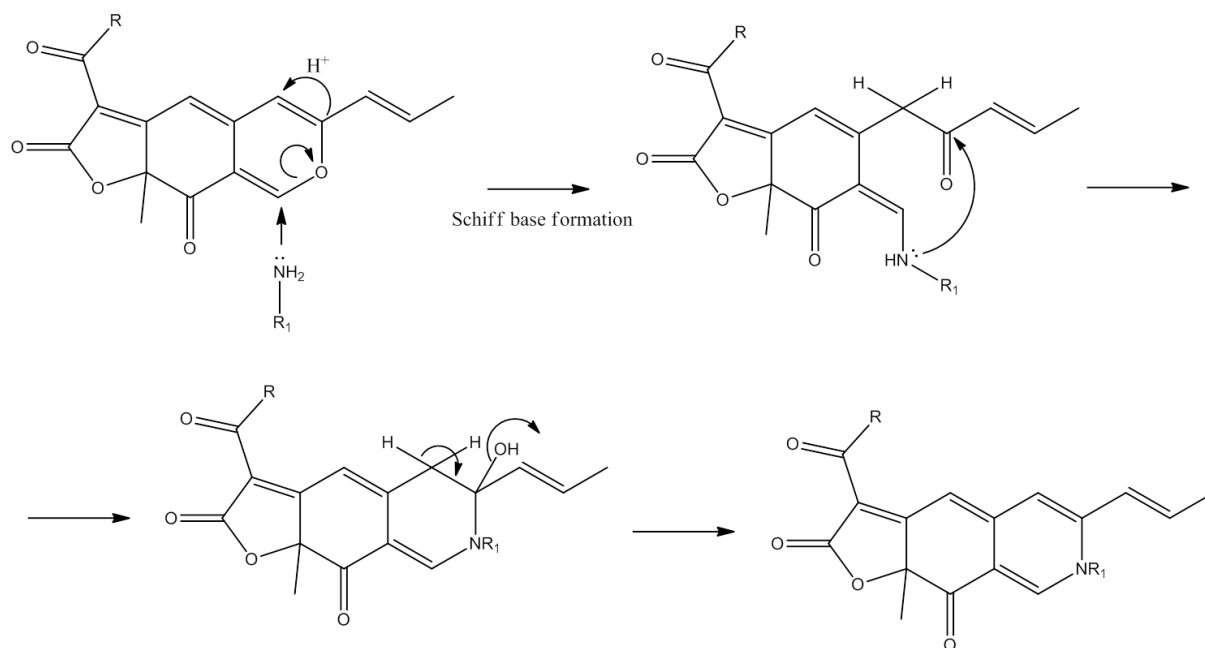


Figure 16 Proposed biosynthetic pathway for the formation of vinylogous γ -pyridones[95]

One of the mechanisms of synthesis of vinylogous γ -pyridones, proposed by Yao's group, is that pyranyl oxygen is replaced with nitrogen by insertion of primary amine.[94] This synthesis is in consistence with proposed biosynthetic pathway of Juzlova. Yao also investigated the reaction with primary amines having different substitution on their α -carbon. The reaction is fast, irreversible and with high yields, up to 98%. Less bulky amines give high yields of vinylogous γ -pyridones, while bulky amines, such as *tert*-butylamines give stable enamines.

Earlier in the manuscript was mentioned that azaphilones show nitric oxide (NO) inhibition, and that this activity is probably due to their reaction with amino group. Suppression of NO production is due to the inhibition of nitric oxide synthase (NOS), as Asakawa demonstrated on 2006.[50] NOS are a family of enzymes that catalyze production of NO from L-arginine. Knowing that azaphilone reacts with amino group from amino acids, it is quite evident that this reaction plays important role in inhibition of NO production. However, substituent group attached to the highly oxygenated bicyclic core shows an influence on this activity. Thus, different positions of orsellinic acid do not show high influence on the activity. Presence of

acetyl group shows an effect on the activity, while the presence of fatty acid side chain in some azaphilones have no influence or even decrease the activity.

3. Analytical methods for investigation of fungi

Generally, after being determined by mycologist, fungi are subjected to different analytical methods for their further determination. First, a sample preparation has to be considered to obtain a sample that is adequate for analysis. Then, prepared sample is subjected to separation methods to facilitate the study of analyzed components and increase the sensitivity. Finally, different analyzers and detectors are used to give complementary and helpful information about composition of sample and structures of the compounds.

Initially, chemical investigations of fungi were based on chemical spot tests, paper chromatography and thin layer chromatography (TLC). [96] Standardized methods for HPLC were later introduced allowing identification or at least partial characterization of many metabolites.[97, 98] For volatile secondary metabolites GC-MS has been used in taxonomy of *Penicillium*.

The introduction of a micro-scale agar plug extraction by Smedsgaard [99] made HPLC-Diode Array Detection (HPLC-DAD) an effective method for chemotaxonomic characterization of large amounts of strains. The method of choice for detailed chemotaxonomic studies of ascomycetes is HPLC-DAD mass spectrometry (HPLC-DAD-MS). [100] To facilitate even more the approach, direct inlet electrospray ionization mass spectrometry (diESI-MS) was introduced in chemotaxonomy by Smedsgaard and Frisvad,[101-103] and has later been applied in many studies.[104, 105]

A couple of automated methods have been developed for unbiased classification of analytical data for chemotaxonomic purposes. Effective methods have been made for aligning and comparing of both HPLC-DAD and MS data. Accelerated recognition of known secondary metabolites in the fungal kingdom, by a multi-detector HPLC platform supported by reference libraries has been proposed by Henkel and group.[106] In this working concept HPLC system is coupled with DAD, evaporative light scattering detector (ELSD) and MS, with possibilities of positive and negative ionization and automated MS/MS fragmentations. The collected information

obtained from all analytical methods used allowed a single search in reference libraries.

3.1 Sample preparation and extraction

Sample preparation is an important step, especially when complex biological matrixes are analyzed. [107, 108] Analytes have to be extracted from the sample matrix components and other impurities that may reduce the specificity and the sensitivity of detection.

Extraction is a method for the sample preparation that separates the compounds of interest from matrix. Different methods of extraction have been developed, such as sonication (or ultrasound) extraction, liquid-solid extraction (LSE) or solid phase extraction (SPE) etc. Here we briefly depict ones that are usually used for analysis of fungal extracts.

3.1.1 Sonication or ultrasound extraction

Sonication or ultrasound extraction is the simplest extraction procedure and is often used in laboratory for analytical separations. A given volume of solvent was coated over the analyte and the mixture incubated for a convenient time in a ultrasound bath. Ultrasonic radiation allows accelerating various steps of the analytical process. It is particularly helpful in the pre-treatment of solid samples as it facilitates and accelerates operations such as the extraction of organic and inorganic compounds, the homogenization, etc.[109] This method is often used as a first step for preparation of crude and very complex samples as it allows extracting the most of compounds from solid and rough matrix. For example, it is often used in preparation of crude extract of Xylariaceae fungi, to smash as much as possible its solid stromatal surface. [110]

3.1.2 Liquid-Solid Extraction

Liquid-solid extraction (LSE)[111] is the process of using a solvent for extracting compounds from a solid sample. The compounds to be extracted can be the analytes that have to be separated from the matrix or, less commonly, specific matrix compounds that have to be removed from the sample. For this kind of extraction, other operations are needed to help the extraction, such as cell disruption, sonication, grinding etc. This method is often used for preparation of crude extract from fungi, followed or not by purification methods. However, it is time-consuming and produces great amounts of solvent waste.

3.1.3 Solid Phase Extraction

Solid-phase extraction (SPE) uses a specific amount of finely divided porous solid phase (usually contained in a small column, a cartridge or a disc) to retain specific compounds from a solution. Retained compound is later released, using an eluent.

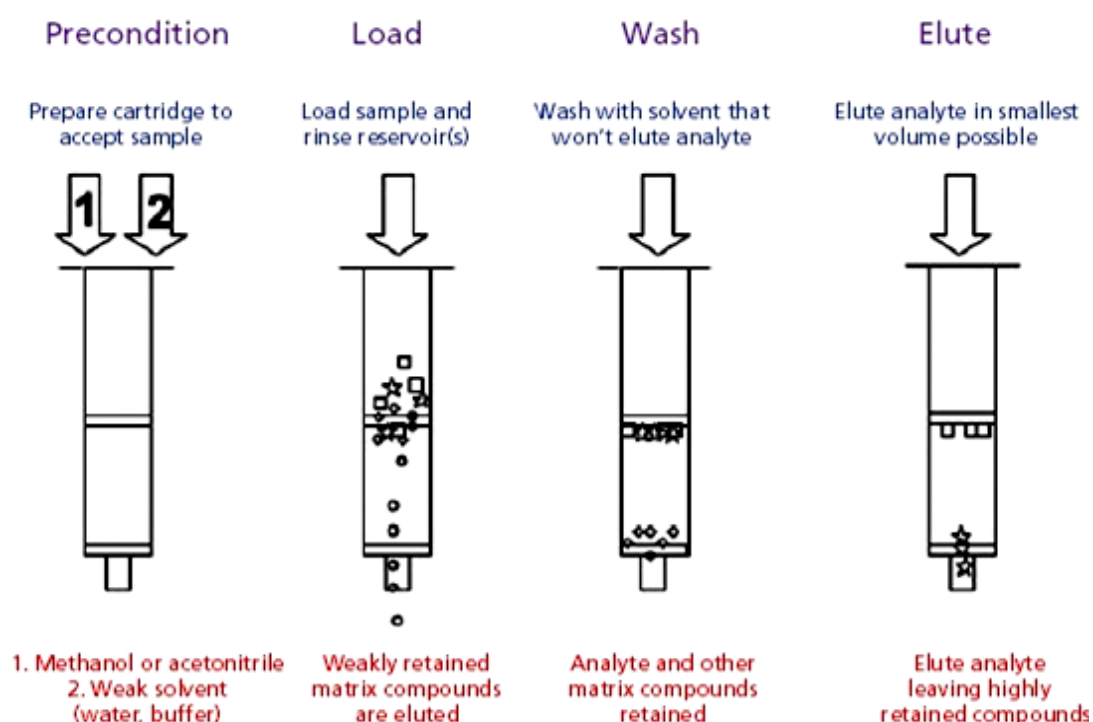


Figure 17: Schematic presentation of solid phase extraction for sample purification

This process is frequently used for sample cleanup and/or for sample pre-concentration. The cleanup process can be done in several ways. One basic procedure consists of the selective retention on the solid phase of the interfering compounds, while the analytes are eluted and collected for analysis (**Figure 17**). Another procedure consists of the retention of the analytes in the solid phase while the interfering compounds from matrix are rinsed away. After the elimination of the matrix compounds, the analytes retained on the solid phase are eluted with a different solvent and collected.[112]

The solid phase materials (sorbents) used in SPE are classified as non-polar, polar and ion-exchange types. For purification of crude extracts for determination of azaphilones, this method is used in purification purposes, thus, sometimes crude extract is simply filtered through the reverse phase SPE cartridge that retains non-polar compounds, and elutes compounds of interest (with the higher polarity).[113]

More recent extraction method is solid-phase micro-extraction (SPME). It is a simple and efficient method that uses negligible amounts of solvent, and is completely compatible with mass spectrometry. It simplifies a sample preparation step as it includes extraction of analyte from matrix, concentration and transfer to chromatograph in one step.[114] It uses a fused-silica fibre that is coated on the outside with an appropriate stationary phase. The analytes in the sample are directly extracted to the fibre coating. It is compatible with LC-MS interface, and also with GC-MS interface as it includes also the derivatization step.

3.2 High Performance Liquid Chromatography separation

Liquid chromatography is a separation process in which the sample mixture is distributed between two phases. The molecules to be separated (analytes) are carried by a liquid called mobile phase. Analytes interact or not with a fixed support (in a column), the stationary phase. There is a distribution or partition of analytes between the mobile and stationary phases. The fluid flow is continuous, so it is the shorter or longer retention of analytes on the column that leads to their separation. HPLC is a

powerful separation method able to resolve mixtures with a large number of similar analytes.[115]

A HPLC instrument has at least the following elements: solvent reservoir, transfer line with frit for solvent filtration, high pressure pumps, sample injector, column, detector and data recorder (**Figure 18**).

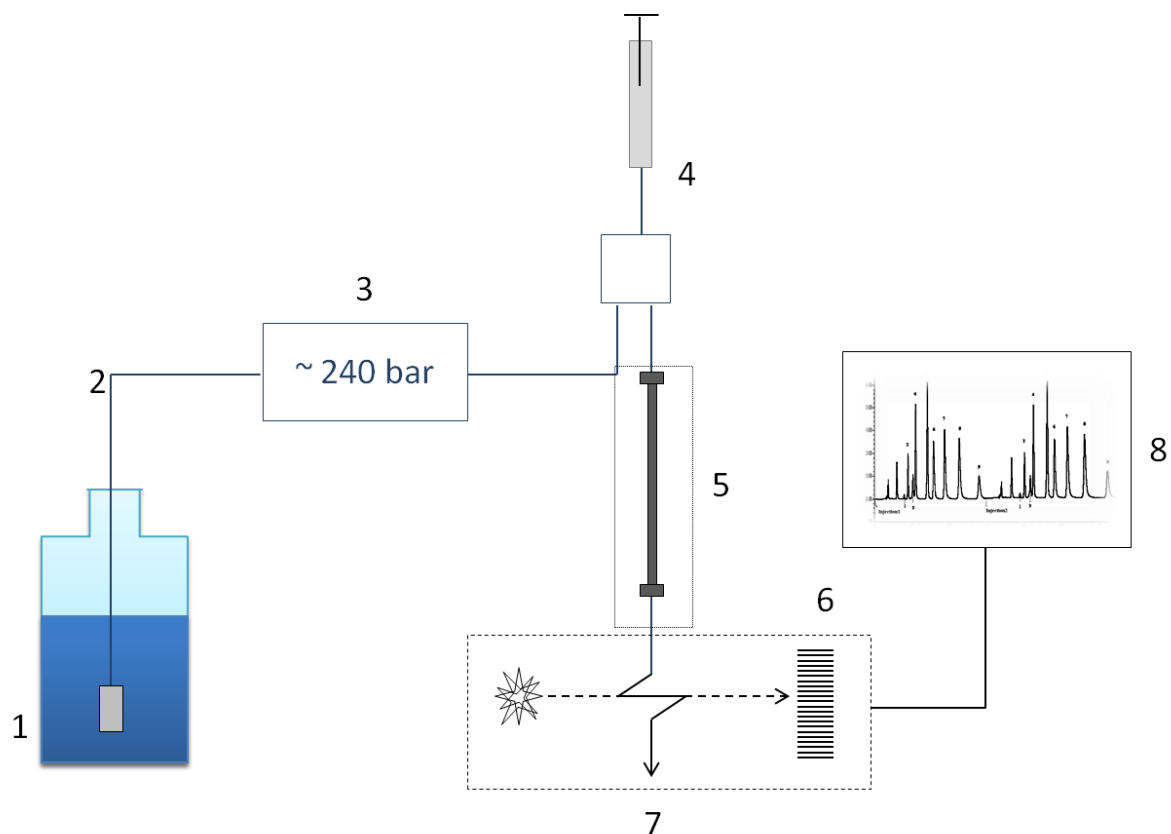


Figure 18: Schematic presentation of an HPLC system. 1-solvent reservoir; 2-transfer line with frit; 3-pump with manometer; 4-sample injector; 5-column and oven; 6-detector; 7-waste; 8-data acquisition

A degasser is also often used in HPLC system, for degassing solvents. If more than one solvent is used, a mixing chamber is required, and controller also. Different detector types are often interfaced with the HPLC system, such as ultraviolet and visible, infra-red detection, refractive index detection, fluorescence, light scattering, mass detection, etc. Coupling the HPLC with one or more spectroscopy techniques is of high importance and significance for achieving a wide range of information in as shorter time interval as possible.

Recently, a new more powerful technique was developed, ultra-high performance liquid chromatography (UPLC). It is in fact a miniaturization of HPLC in which the diameter size of the stationary phase particles is below than 2 μm .^[116] Decreasing the size of particles introduce higher capacity of peaks (number of peaks per time unit), better resolution and higher sensitivity.^[117] UPLC systems provide also better strength than the HPLC systems, particularly at the level of retention time.^[118] The retention times are decreased in comparison to HPLC, thus time analysis is shorter with the same resolution as classical HPLC columns.

3.2.1 Reverse-phase liquid chromatography

The most widely used columns contain a chemically modified silica stationary phase. A very popular stationary phase is reverse phase (RP) in which a C18 alkyl group is bonded to the silica surface (**Figure 19**).

Reverse phase liquid chromatography (RP-LC) is a high resolving chromatographic separation that can be coupled to mass spectrometer. It separates analytes according to their hydrophobicity by reversible non-covalent interactions with the hydrophobic surface (*i.e.*, hydrophobic ligand) of the medium.

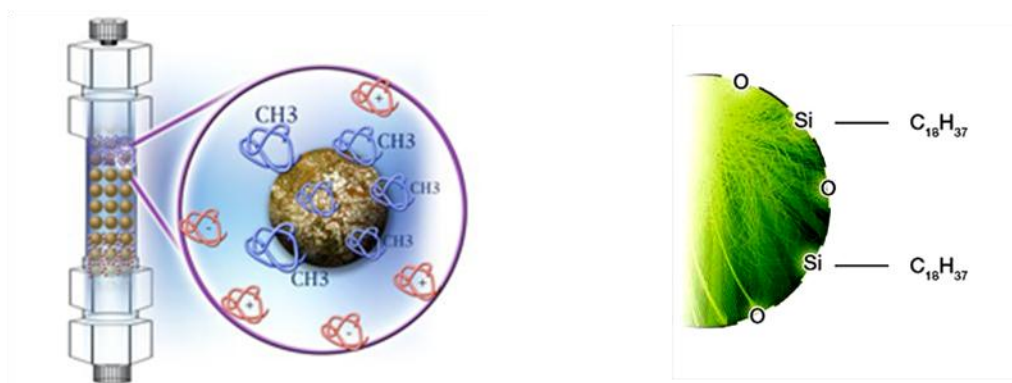


Figure 19: Reverse phase column and alkyl group binding to the silica surface

During separation, the sample is partitioned between the mobile phase and the stationary phase. The elution of the analytes is performed either by a gradient with increasing proportion of organic solvent, or by the isocratic elution with constant

percentage of solvent. Almost the totality of the samples is absorbed by the hydrophobic stationary, as the mobile phase is hydrophilic. Analytes are eluted in order of increasing hydrophobicity in function of the quantity of organic solvent (Figure 20).

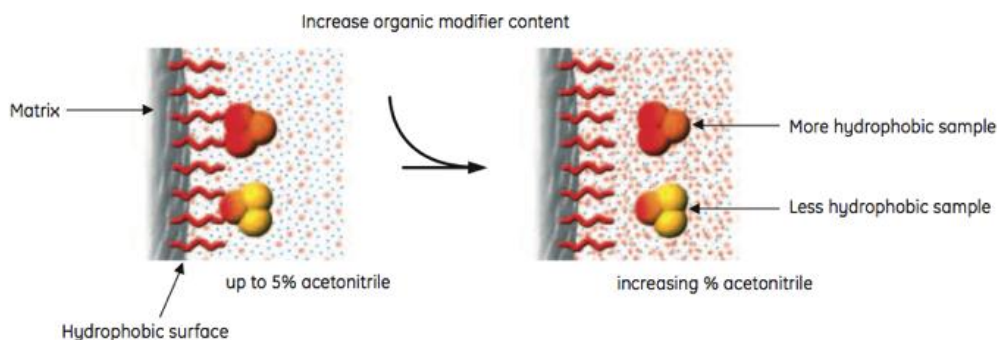


Figure 20: Schematic presentation of elution of compounds from the reverse phase.[119]

RP-LC is the most well suited LC technique to be combined with mass spectrometry as it commonly uses salt-free aqueous and organic solutions as mobile phases.

3.2.2 *Hydrophilic interaction liquid chromatography*

An alternative approach to RP-LC is hydrophilic interaction liquid chromatography (HILIC), often used for analysis of highly polar metabolites.[120] Stationary phase in HILIC chromatography is polar, while the mobile phase is highly organic (80% organic solvent) with a small amount of aqueous or polar solvent. Polar analytes partition into and out of adsorbed water layer, than the charged polar analyte can undergo cation exchange with charged silanol groups. Combination of these mechanisms results in enhanced retention of polar compounds.

3.2.3 *Preparative HPLC*

Preparative chromatography is used to separate and purify compounds for further analysis. Required amounts of desired compounds vary according to the application. For UV detection, few micrograms are sufficient for registration of spectrum while approximately ten of milligrams are required for ^1H and ^{13}C NMR analysis. Hundreds of milligrams are often required for the synthesis of derivatives. In this

purpose preparative HPLC is often utilized to isolate and purify efficiently compounds of interest.

An analytical chromatogram usually provides the starting point for preparative separation. Gradient are not recommended as they involve higher quantity of solvents. Consequently, it is used if no other possibility for good separation exists. A column for preparative HPLC is of bigger size, in the aim to enable the loading of higher amounts of sample. A 10 mm i.d (internal diameter) column accepts 10-100 mg of sample, while the column of 21 mm accepts up to 1 g of sample. The transfer from analytical to preparative conditions works best if the same stationary phase packing of column (meaning the size of pores) is used and if the length of columns is the same. With the increment of i.d. the flow increases for observing the same separation. Overloading effects are common in preparative chromatography. It can be obtained due to mass overload, volume overload or the two. If a great mass of sample is injected, the retention factor changes as well as the peak width, and a peak tailing can happened. If the injected volume is too high, the peak width can be affected (a sample mass low enough to avoid the mass overload). If the mass and the volume overload are present, the both phenomena are seen in the chromatogram.[119]

Used column should be the same that was used for the analytical purposes, thus if the RP column was used for determining the conditions of separation, the same stationary phase have to be used for preparative purposes. In preparative HPLC exists all the stationary phases as in the analytical HPLC.

The line between the detector and fraction collector must have a low size in comparison with the mobile phase flow rate, in the aim to accurately collect wanted fractions. The fraction collection can be controlled by time and by signal so the peaks can be guided into separate vessel without being intersected. If no peak appears, the eluate can be directed back to solvent reservoir, or to the waste.

3.3 Spectroscopic methods

3.3.1 Spectroscopy Methods

Spectroscopic techniques, often coupled with separation techniques, are performed for structural elucidation. Here, UV and NMR techniques are briefly described.

3.3.2 UV spectroscopy

Ultra-violet (UV) detector is the most commonly used detector because it has a high linear range of analysis and it is almost always integrated in the HPLC system.[121] It records compounds that absorb ultraviolet or visible light. Absorption takes place at a wavelength above 200 nm, provided that the molecule has at least a double bond adjacent to an atom with the lone pair, bromine, iodine or sulfur, carbonyl group, nitro group, conjugated double bond, aromatic ring. These groups absorb at different UV wavelengths. The absorption intensity and the wavelength of maximum absorption are affected by the neighboring atom groups in the molecule. The molar absorptivity, ϵ , is the measure of the light absorption intensity. The degree of absorption resulting from the passage of the light beam through the cell is a function of the molar absorptivity, molar concentration, c , of the compound and of length, d , of the cell. The product of these three parameters is known as absorbance, A , by Beer-Lambert law:

$$A = \epsilon cd,$$

and can be measured by UV detectors. Diode array detection creates a new dimension of analytical capability to liquid chromatography because it permits qualitative information to be obtained beyond simple identification by retention time. The UV absorption of the effluent is continuously measured at multiple wavelengths, and like this allows a higher range of compounds to be detected. It is often used method for fungal metabolite profiling, and in chemotaxonomy, where

the metabolites are identified by its retention times and with their UV fingerprints as well.[30, 35]

3.3.3 Nuclear magnetic resonance spectroscopy in structure elucidation of fungal secondary metabolites

NMR-Spectra are obtained from the precession frequency of nuclei with a magnetic moment in a static field. The position of the NMR signal (i. e the resonance frequency) is called the chemical shift δ . The values of the chemical shift δH and δC in ^1H -NMR and ^{13}C -NMR spectra give information on complete structures and functional groups contained in the studied molecule.

Coupling constants between protons which can be obtained from the fine structure of signals help to identify neighbor protons in building up of partial structures. However, the resolution of one dimensional ^1H -NMR spectra is rarely good enough to enable the calculation of all the important coupling constants. Together with the DEPT technique which enables the knowledge of the multiplicity of carbon atoms, two dimensional NMR offer powerful methods for the structure elucidation of natural products, such as homonuclear shift-correlation spectroscopy (COSY), nuclear overhauser spectroscopy (NOESY), heteronuclear multiple quantum-coherence (HMQC), heteronuclear multiple-bond correlation (HMBC). [122-124]

Main advantage of NMR spectroscopy is an ability to reach the complete structural elucidation On the other hand, its disadvantage is that it requires high amounts of sample (up to few mg), and the purity of the sample must be high. Only recently, direct analysis of mixture begins to be performed, where the NMR instrument is interfaced to liquid chromatography (LC-NMR),[125] but this technique appears to be difficult to perform and thus it is not popularized.

3.3.4 *Mass spectrometry*

In parallel with NMR, mass spectrometry for the access to structural information was developed, and gained much higher sensitivity. In the next chapter we will focus on mass spectrometry and describe this technique in detail.

4. Mass spectrometry

The importance of mass spectrometry has greatly increased in recent decades in large part due to the development of techniques for the analysis of biological macromolecules such as nucleic acids,[126, 127] proteins,[128] carbohydrates[129] or lipids.[130] Considerable resources and great effort invested in the development of ionization techniques for MS instruments culminated in the award of a Nobel Prize in 2002 to John B. Fenn (for electrospray, ESI), Koichi Tanaka (for soft laser desorption, SLD) [131] and Karas (for matrix assisted laser desorption ionization, MALDI)[132] for the development of soft desorption ionization methods for mass spectrometric analyses of biological macromolecules. While MALDI produces only mono-charged ions, ESI has advantage of producing multi-charged ions. This success enabled routine use of MS, in conjunction with separation techniques such as electrophoresis and HPLC, resulting in the development of so-called “hyphenated” techniques, e.g. LC-MS.

Advantage of mass spectrometry is mainly related to sensitivity, specificity and selectivity, and possibility to analyze the sample from the complex mixture as well. However, this technique can be useful if tandem MS is performed and/or high resolving power is achieved for structural elucidation. Without such high potentiality only molecular mass can be reached with no additional structural information, due to the soft ionization conditions under which low or no fragmentation is observed.

Several ionization methods can be interfaced to mass spectrometer, and the compatible one needs to be chosen according to the molecule properties. For not very polar and small size molecules, gas phase ionization (in vacuum) can be used, such as electron ionization (EI), chemical ionization (CI) etc. These modes can be coupled to GC/MS. Reversely, for less volatile small size molecules gas phase ionization methods at atmospheric pressure, such as atmospheric pressure chemical ionization (APCI) or atmospheric pressure photo ionization (APPI) condition can be applied. For larger and thermo-labile polar systems, desorption techniques can be used (ESI),

able to be coupled in LC-MS, also like API techniques. ESI appear to be more universal and for this reason it is more popularized.

Even though the ionization source can work in vacuum or under AP conditions, the analyzer and detector work only in vacuum, and under very low partial pressure ($P = \sum P_{gi}$) in water, which is real challenge when LC-MS is used, since the mixture of organic solvent and water is currently employed. To operate in vacuum (i.e. 10^{-6} to 10^{-7} mbar) it is required differential pumping which allows the ion from atmospheric pressure to go into vacuum region thanks to lens and skimmers between each part of the instrument for decreasing the pressure. Generally to reach such vacuum, two pumping are needed, primary pumping (rotary vacuum pump) associated with turbo molecular pump for high vacuum.

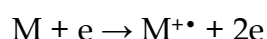
Mass spectrometers for HPLC coupling consists of three parts: interface between HPLC and MS where the ions are formed, mass analyzer and detector. Thanks to different ionization sources formed until nowadays, it is facilitated to interface these two techniques. Atmospheric pressure ionization (API) enables this coupling and formation and thus analysis of positive and negative ions as well.

4.1 Ionization techniques

Before any mass analysis, the ions need to be formed in the ionization source. For analysis of azaphilones, most used was electrospray ionization, though the first reports of analysis of azaphilones talks about electron impact mass spectra. Thus, in next two chapters the most used ionization techniques, electron impact and electrospray ionization will be described.

4.1.1 Gas Phase Ionization - Electron Ionization

Electron Ionization (EI) is one of the most utilized gas phase ionization sources that interface gas chromatography with mass spectrometry. EI is a technique that ionizes easily gas phase molecules, though it induces extensive fragmentations, and the molecular ions are often not well observed. This source consists of a heated filament that emits the electrons that after acceleration interact with the molecules that are previously transferred to a gas phase and introduced into the source. Kinetic energy of electrons is mainly about $80 \text{ eV} \pm 10 \text{ eV}$, and the associative wave allows interaction with electron of highest occupied molecular orbital (HOMO) orbital to eject it:



The resulting system is characterized by configuration distribution over the excited electronic and fundamental states by curve crossing and redistribution of electron excitation energy down to fundamental state (**Figure 21**). The internal energy is then constituted of residual vibrational energy in each electronic excited state (corresponding to the energy below the crossing point) and vibrational energy in fundamental state.

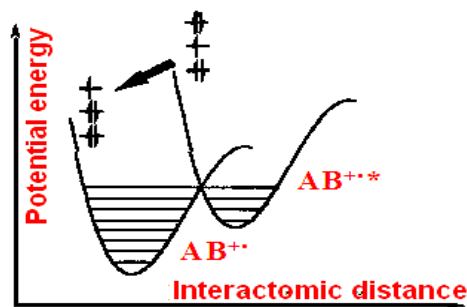
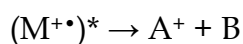


Figure 21: Potential energy curve crossing for polyatomic molecules and ions

The internal energy of resulting molecular ion is a convolution of electronic excited state vibrational energy and vibrational internal energy in the fundamental state. By this way is considered that the internal energy increases from 0 eV to 15 eV.

Electron ionization source work under vacuum (10^{-6} mbar) and a molecular ion can be considered as an isolated system. Thus, only the internal energy is present in the ion, except the energy released from the radiation. This internal energy distribution is characteristic of an ion, meaning that for the constant “in-source” residence time it is independent of the instrument.

With such internal energy, the molecular ion dissociates in the source. Dissociation is associated to the survival molecular ion yielding a mass spectrum independent of the instrument. The only difference that can appear using different mass spectrometers is the variation in ion abundance, but the appearance of the spectrum is always the same.



The variations in ion abundance appear due to the orientation of fragmentation pathways that are competitive or consecutive. This advantage was used to create data bases for identification of known molecular structures, especially from complex mixtures as the EI is “in-vacuum” ionization and it allows coupling of mass spectrometry with gas chromatography (GC).

For determination of characteristic secondary metabolites of Xylariceae, GC/MS was used. In this purpose ionization in the gas phase was the only choice, thus EI was

used to produce the ions. At the **Figure 22** is presented an EI spectrum of mitorubrin, a member of azaphilones from *Hypoxylon fragiforme*, but also present in *Penicillium rubrum*, [133] that was published in the early 1960's. A molecular ion of mitorubrin is present in the spectrum in quite low intensity, but still gives the important information about the molecular mass. Furthermore, an extensive fragmentation clarifies the chemical structure.

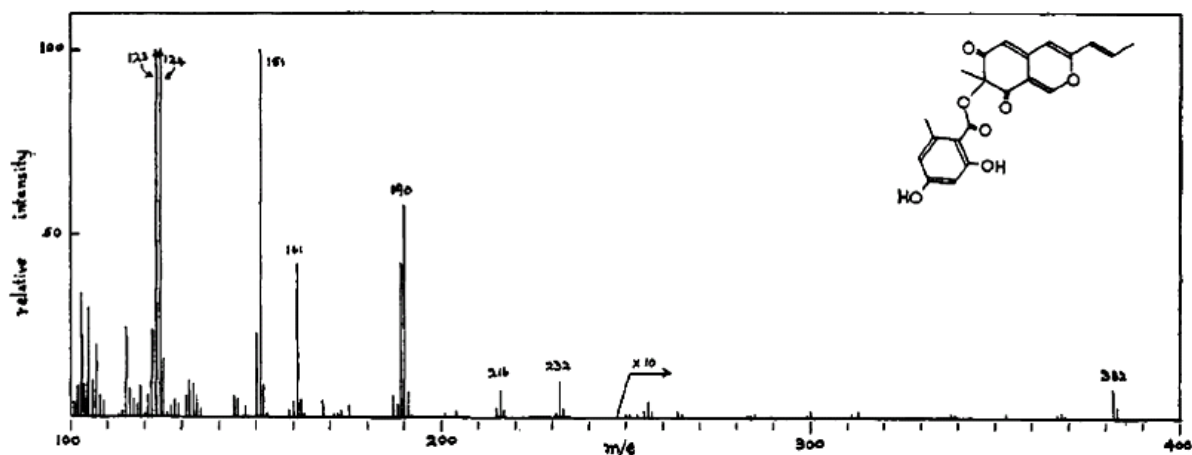


Figure 22: EI spectrum of mitorubrin [133]

There are various fragmentation pathway rules, because the structural characteristics play an important role. Mitorubrin is a good example for demonstration of some of the rules that leads the fragmentation. The two principle rules are simple cleavage and rearrangement. However, simple cleavage does not always lead directly to the formation of ion and neutral. During the simple cleavage an ion-dipole complex can be formed prior to dissociation. This dissociation is induced by the charge-radical site. Here, the H-migration can take place before the dissociation, leading to the formation of distonic ion, where the radical induces the dissociation, and the positive charge is a spectator. A last rule involves the electron parity of the fragment ion. The molecular ion can give odd or even electron species, yielding new even electron fragment ions by release of neutrals. This rule can be violated in the aromatic and nitrogen containing aromatic systems. These rules explains mass spectrum of mitorubrin obtained in EI.

In the spectrum of mitorubrin, the molecular ion at m/z 382 is observed with low abundance, which is expected due to the strong ionization conditions in EI, that induce internal energy of molecular ion high enough to cleave the single bond (about 0.8 eV to 2 eV) and a nature of odd electron nature of molecular ion that makes it unstable. Fragments that are formed during the ionization are observed at m/z 123, m/z 124 m/z 150, m/z 151, m/z 160, m/z 190 and m/z 232. The mechanism by which these product ions are formed is presented at **Figure 23**.

The approach that was used to explain the fragmentation of mitorubrin under EI conditions could be misused. We propose here our approach to the fragmentation mechanism, where the recent process, ion-dipole complex formation plays the main role, and it is also important for further results of the work.

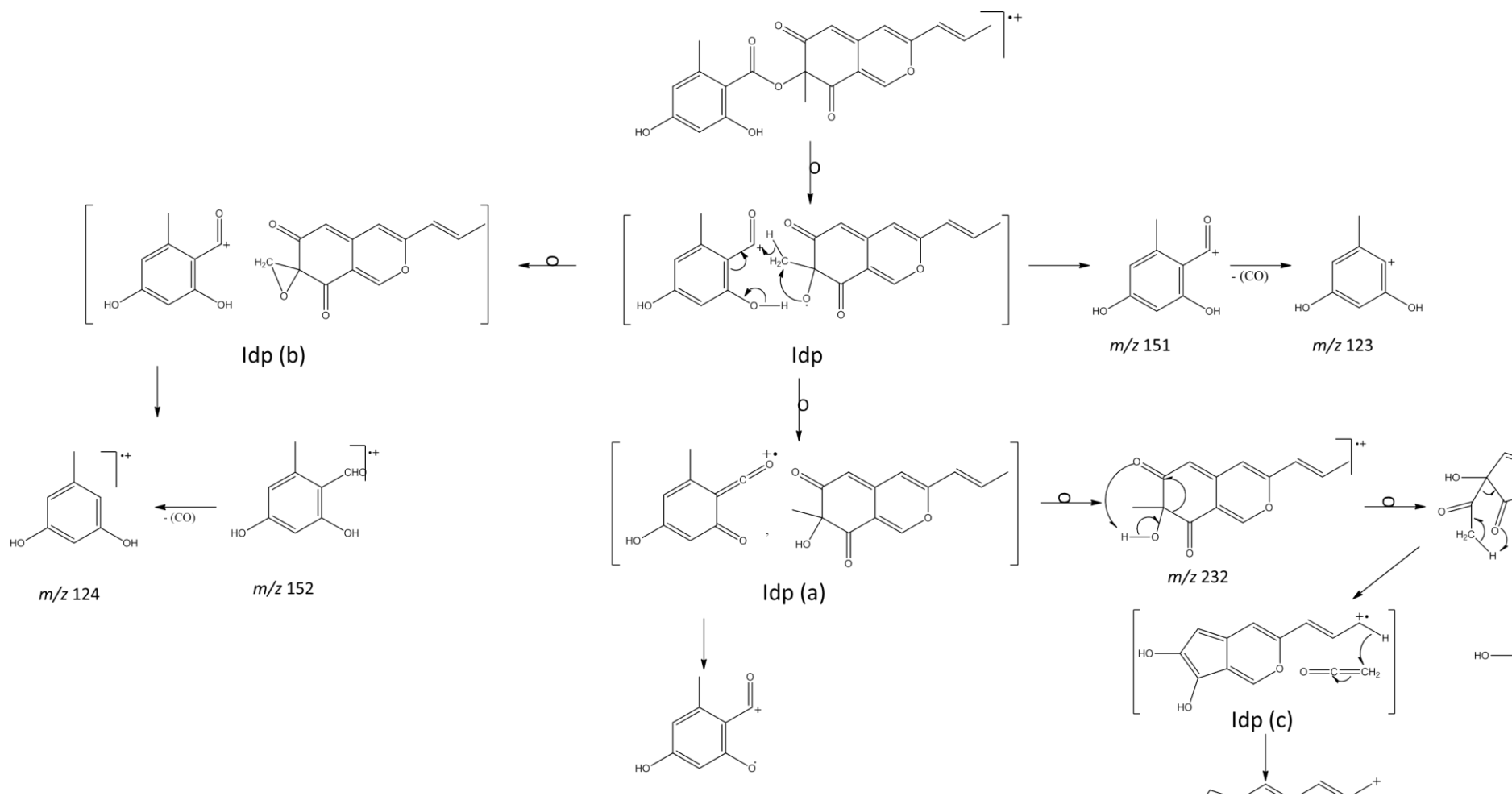


Figure 23: Proposed fragmentation mechanism of molecular ion from mitorubrin under EI conditions

Several complementary ions appear in the mass spectrum. They reflect the possible ion-dipole complex formation as a molecular isomerization prior to total dissociation. By the benzylic cleavage the ion-dipole complex (Idp) is formed as acylium ion accompanied by radical alcoxide. The direct dissociation of Idp gives m/z 151 (aromatic system). This ion is able to lose the C=O neutral (carbon monoxide) yielding the m/z 123. Idp can isomerizes by the H^o radical transfer from phenol site to radical partner giving a new ion-dipole complex, Idp(a), where the charge is distributed in to the bicyclic system, giving competition in the formation of m/z 232 and m/z 150, an odd-electron species. Here, the m/z 150 is more favored because of the strong delocalization of the charge through the system.

Idp can also isomerizes into the ion-dipole complex Idp(b) by H^o radical transfer from geminal methyl group (vicinal group) to the alcoxide site. This transfer is assisted by radical migration to give rise to (exocyclic) epoxide. Idp(b) dissociate into very unstable bi-phenol aldehyde, which release very promptly carbon-monoxide to yield m/z 124. All this ions can dissociate consecutively in to smaller species. For instance, the loss of acyl radical can occurs from m/z 232 through formation of new ion-dipole complex, Idp(c), constituted of bicyclic system and a keten. Direct release of keten yield m/z 190, and by allylic H-radical transfer from vinyl methyl group to keten allow losing radical acyl at m/z 189.

4.1.2 Atmospheric Pressure Ionization

Two main atmospheric pressure ionization modes are the gas-phase ionization (APCI, APPI, DART), that happen through the ion-molecule reactions and the desorption techniques, that happen through desorption from droplets. Desorption techniques are more popular for investigation of biological molecules of small and large size.

4.1.3 The case of Electrospray ionization

The contribution of mass spectrometry to current knowledge in biology is still relatively modest. However, electrospray mass spectrometry (ESI-MS) is now

considered as essential in this area. Emergence of this technique in MS started during the 60's by electro-dynamic studies, developed by Dole. The first step in the development of electro-spray has been forgotten. Abbot Nollet showed in the XVIII century the influence of the electric charge on the orientation of the small water jet.[134] After this, the electro-dynamics have not been developed more in the XIX century, only until its strong evaluation in mass spectrometry.

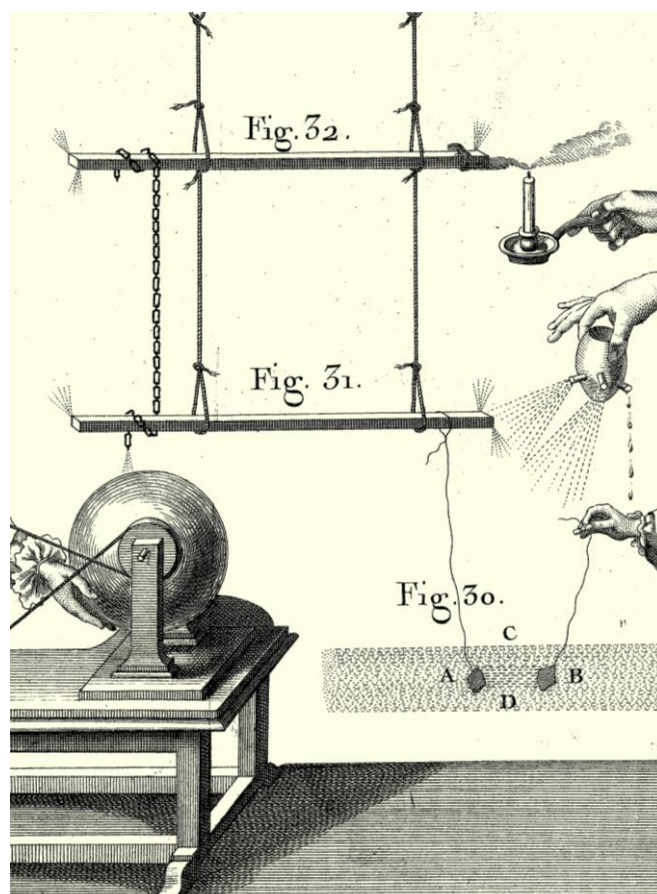


Figure 24 Influence of the electric charge on the orientation of small water jet; the origins of electrospray[134]

Through this evaluation, John Fenn developed electro-spray in 1992. Despite to this discovery, the mechanism of electro-spray is not yet well understood, the process can be just described, and two models are proposed, dependently on the size of ionizing molecules (see below). A sample solution is introduced into a capillary which is brought to a high electric potential. The electric field applied to the output of the capillary will formation of a cloud of charged droplets which pass through a

gradient of simultaneously electric field and a pressure gradient in the direction of the analyzer spectrometer mass.

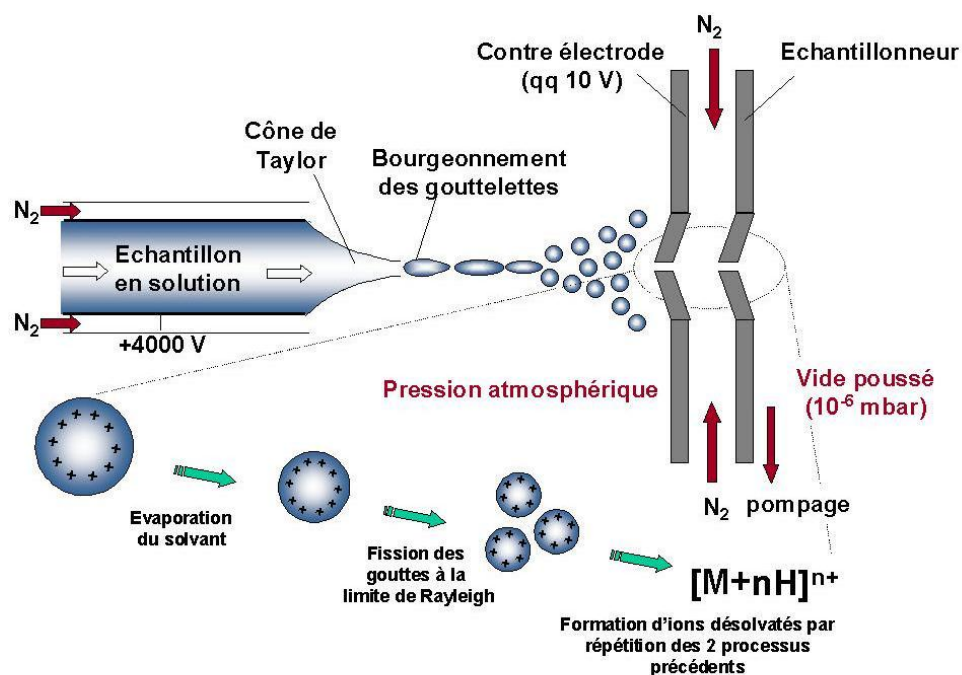


Figure 25: Schematic presentation of electrospray ionization process[135]

During this transport, the size of droplet decreases during evaporation of the solvent by successive "Coulomb" explosions (spontaneous divisions of the droplet form smaller droplets, caused by a very high surface potential) (Figure 25). The application of a pressure at the capillary inlet can facilitate nebulization, depending on the flow rate and composition of used solvent.[136] In addition, a gas flow (usually nitrogen) is applied to the interface to help evaporation of the solvent. In fact, Kebarle et al [137] showed that the smaller droplet can be produced very promptly and from this macroscopic approach desorption occurs from the deformed droplet creating an alembic shape. Desorbed species are macromolecular aggregates (strongly solvated molecules). The aggregate ions formed under atmospheric pressure are then focused through a set of ion optics, which enables them to pass toward the analyzer placed in vacuum region. The ions formed in positive mode are multi-protonated species. The exact mechanism of ion formation from charged droplets is under discussion.[138, 139]

The emission of ions from charged droplets to the gas phase is a kind of controversial process. Two models are accepted until today, the model of the residual charge proposed by Dole,[140] and model of ion evaporation proposed by Iribarne and Thomson.[141]

According to Dole's model of residual charge, successive stages of evaporation and Coulomb explosions result in the formation of smaller droplets having only one load (Figure 26).

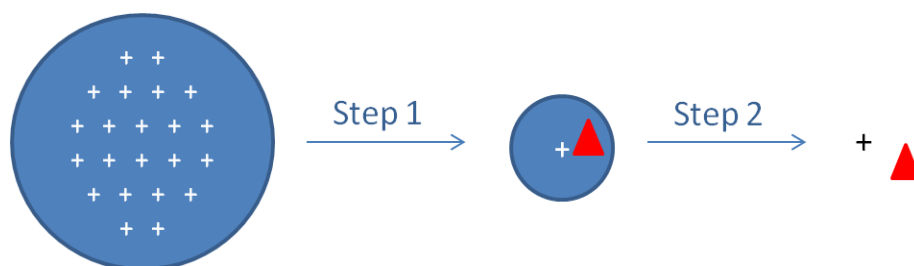


Figure 26: Schematic presentation of the ion emission in the gas phase during the ionization / desorption according to ES theory of Dole[140]

According to the theory of Iribarne and Thomson, when the droplets have a sufficient charge density, they no longer suffer the additional fission, but the ions are directly emitted to the gas phase (Figure 27).

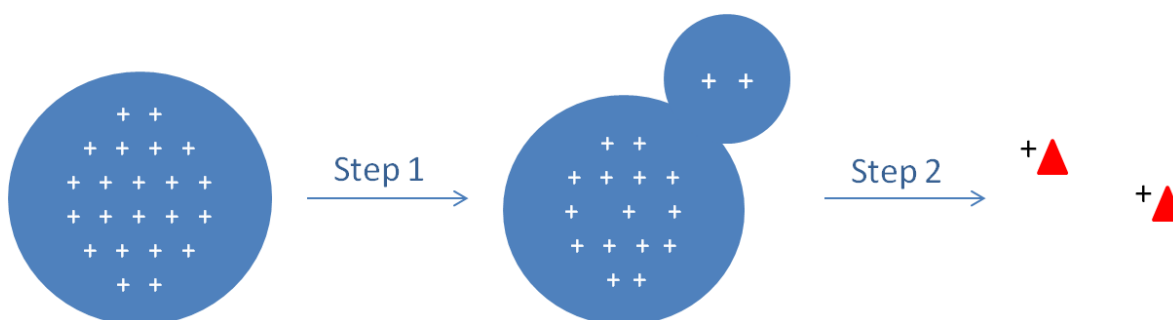


Figure 27: Schematic presentation of the ion emission in the gas phase during the ionization / desorption according to ES theory of Iribarne and Thomson [141]

Preparation of samples is quite simple. The analytes of interest should be dissolved in usually polar solvent that is compatible with electrospray, meaning acetonitrile or methanol, or mixture of these solvents with water.[142] It is often important to add acid or base (ammonium acetate etc) to facilitate the protonation or deprotonation.

With an eye kept on MS compatibility, phosphoric acid is unsuitable, due to its non-volatility. Trifluoroacetic acid (TFA) is a popular acidic modifier and however compatible with MS, it is not advisable due to its extensive ionization. The analytes of interest are less or not detectable when TFA is applied. Therefore in majority of the LC-MS investigations acetic acid or formic acid is used in concentrations ranging from 0.1% to 3%. However, surface active compounds, non-volatile substances and salts are poorly tolerated in ESI. Salts disrupt the electrospray process and form a series of cationized ions, as $[M+Na]^+$, $[M+K]^+$, $[M+H+Na]^{2+}$ etc., which complicates the spectrum and decreases sensitivity.

4.1.4 In-Source CID

Desolvation of ions is provided and helped by heated capillary or by applying a counter-flow of gas, but also by accelerating the ions in the interface region where the medium pressure of millibar range is provided. Acceleration of ions is obtained by applying a voltage between the different lenses and ion optics. Accelerated ions collide with residual gas increasing their internal energy, which helps the final desolvation and observation of single and desolvated ions on the micromolecular level. Furthermore, these collisions can give an extra energy to induce the ion fragmentation. At the end in the mass spectra are obtained a signals corresponding to the survival molecular ions and fragment ions that are formed in source. The extent of fragmentation depends on the amount of internal energy that ions observed in source.

In-source CID is often applied when a single-stage mass analyzers are used, (ESI-MS). In this case, mass spectrometer serves only for detection of ions, and not as analyzer, thus the in-source CID is used to obtain more structural information (as in case of EI or CI) and by interpretation of fragmentation pathways.

4.1.5 ESI-MS for analysis of azaphilones

Since its invention, electrospray ionization has been widely used in mass spectrometry approaches to classification of Xylariaceae. The most successful method

in fungal taxonomy has certainly been secondary metabolite profiling, particularly determined by HPLC. Interfacing liquid chromatography with mass spectrometry was surely facilitated with invent of ESI, allowing polar non- volatile molecules to be ionized in liquid phase. First was the group of Frisvad who started to use a ESI-MS as a rapid tool for chemotaxonomic classification, because observing mass spectrum directly from crude extracts takes advantage of high sensitivity and limited fragmentation.[101]

While techniques based on HPLC analysis suffers from spending time, by diESI-MS it is possible to distinguish species in a few minutes analysis. While ion suppression is of concern in ESI-MS, it does not seriously hamper the detection of expected metabolites although minor components may be lost. At the **Figure 28**, is presented an example of diMS spectra of three *Penicillium* species that are difficult to be distinguished by traditional phenotypic taxonomy. Most dominant peaks in spectra correspond to known and expected metabolites that appear in examined species in different abundances or missing in some species.

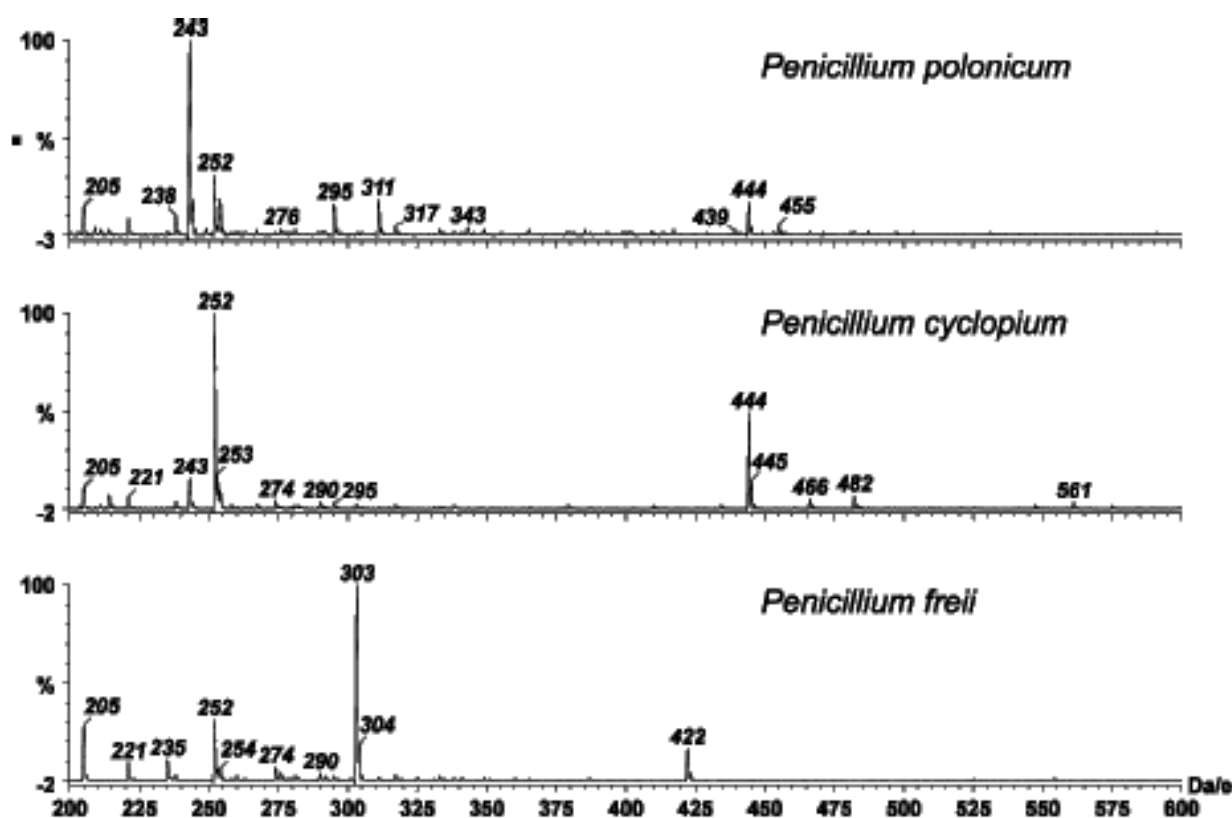


Figure 28: Nominal mass spectra from direct infusion of fungal extract into electrospray mass spectrometry, diESI-MS, shows the difference between three species which are difficult to distinguish by traditional phenotypic taxonomy.[101]

4.2 Mass analysers

Beside the selection of soft ionization (ESI, APCI or APPI), choosing the appropriate mass analyzer is crucial and strictly depends on the analytical aim.[143] For structure elucidation a tandem or multistage mass analyzer is a necessity which is well reflected in the trend of the last 5-6 years: single-stage analyzers have been displaced by tandem or multi-stage instruments. In tandem mass spectrometry only the analyte of interest is transmitted by the first analyzer which is then analysed by the second one. Multi-stage analyzers can repeat these steps consecutively. An iontrap (IT) or orbitrap analyzer allows fragmentation experiments up to MS⁷. [144] Hybrid constructions, like quadrupole-time-of-flight (Q-TOF), time-of-flight - time-of-flight (TOF-TOF) and classic tandem mass spectrometers, like the triple-quadrupole (TQ), especially offers an effective combination of qualitative and quantitative applications. The collision induced dissociation (CID) provides structural information on a selected ion.[145] If skimmer voltage is increased, in-source fragmentation may occur, thus MS³ can be reached with the TQ. Fragmentation in this case is not under the operator's control, nevertheless it can be useful.[146]

4.2.1 *High resolution mass spectrometry - Orbitrap mass spectrometer*

New demands for higher sensitivity and accuracy in mass measurements are of the highest importance since the global tendencies in analytical chemistry are focused on the fast and simple approaches. Orbitrap was developed for this kind of experiments as robust, rapid and sensitive mass instrument. It is a mass analyzer composed of an outer, barrel like electrode, and inner, central electrode around which the ions turns. Form of electrodes was made to allow ions to maintain the motion around the inner electrode as long as possible, thanks to high vacuum ion storage. Ions are injected in the orbitrap tangentially with kinetic energy of several keV. Under electrostatic field (direct current, DC voltage) like in ion trap, without radio-frequency (RF) voltage,

and high vacuum (10^{-10} mbar), they take a circular trajectory around the central electrode and oscillate simultaneously along the z axis (**Figure 29 a**).

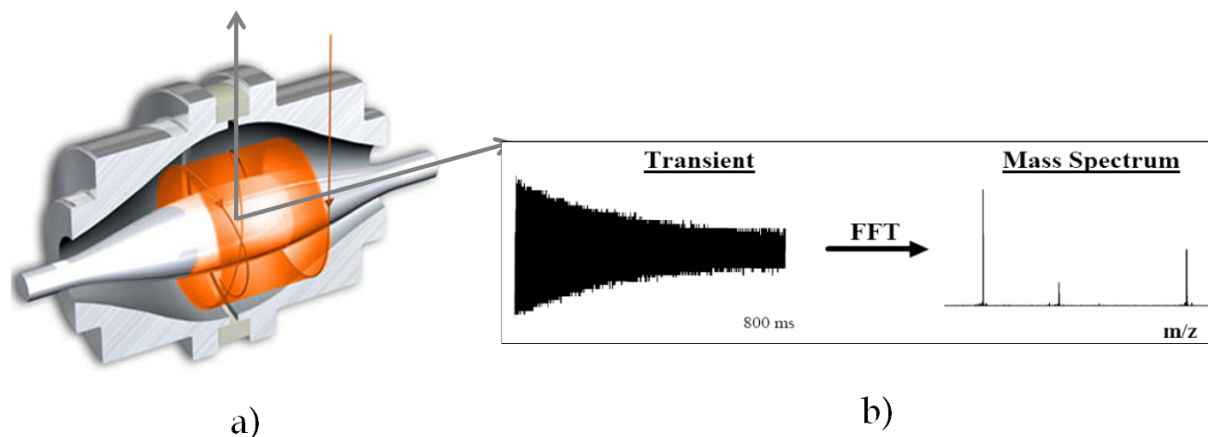


Figure 29: Orbitrap mass detector: a) Geometry of Orbitrap, b) Fast Fourier transformation signal treatment

The axial movement of ions is detected as an image of current when the ions move between two halves of the outer electrode. As a result of amplified current, the transient signal is recorded from the outer electrode (**Figure 29 b**). Ions with different masses oscillate with different frequencies. The set of frequencies which constitutes the transient are submitted to a mathematical treatment, Fourier transformation (FT) that converts this signal (time domain) into oscillation domain, and thus separates ions in m/z scale. Resolution of orbitrap is directly dependent on duration of transient signal. Longer the transient signal possesses higher number of data points, thus measurement accuracy of oscillating frequency is higher and resolution of ions better. For a longer transient signal collisions of ions with residual gas has to be avoided or at least reduced, and this is why the low pressure of 10^{-10} mbar is maintained. At the end, orbitrap can achieve a resolving power up to 100 000 (for m/z 400 FWHM, full width half maximum) and mass accuracy of less than 3 ppm.

4.2.2 LTQ-Orbitrap, a hybrid mass spectrometer with high resolving power

Orbitrap is considered as a mass detector, as no experiments are done in it, but it serves for a high resolution measurements. Thus, a good advance was made by

Hardman and Makarov, 2003 when they designed an LTQ-Orbitrap tandem mass spectrometer (**Figure 30**). It is consisted of linear ion trap (LTQ), C-trap and finally orbitrap.

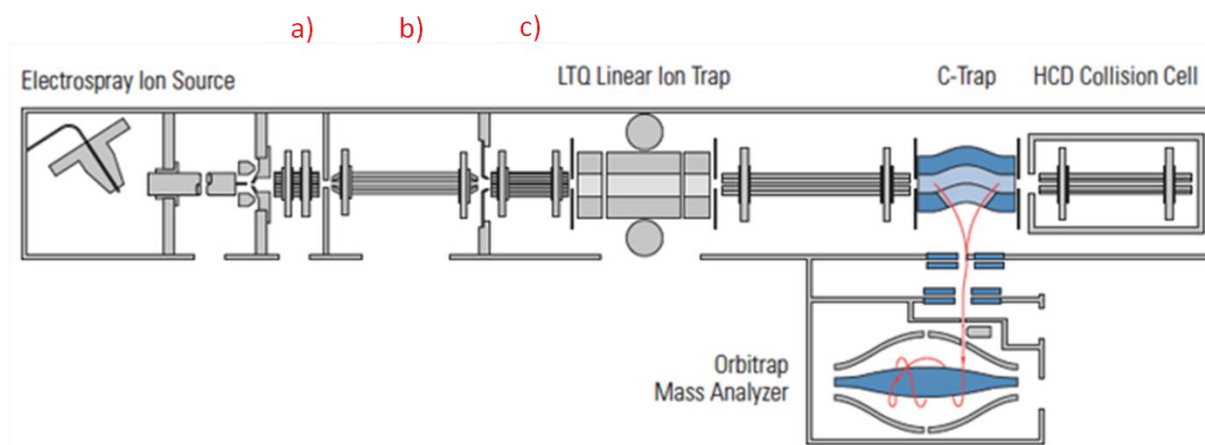


Figure 30: Schematic presentation of LTQ-Orbitrap XL hybrid mass spectrometer; a) aggregate ions desolvation region, b) ion transmission region, c) ion focalization

Aggregate ions formed in the API source are drawn into the ion-transfer tube to reach the tube lens – skimmer region (**Figure 30 a**) where they are desolvated in the collisions with residual gas and focused. In this point, ions meet a zone of lower pressure (10^{-3} mbar), where they pass through several multiples (**Figure 30 b**) and electrostatic lenses (**Figure 30 c**) and get trapped in the linear ion trap (10^{-5} mbar), called LTQ (linear trap quadrupole) (**Figure 31**).

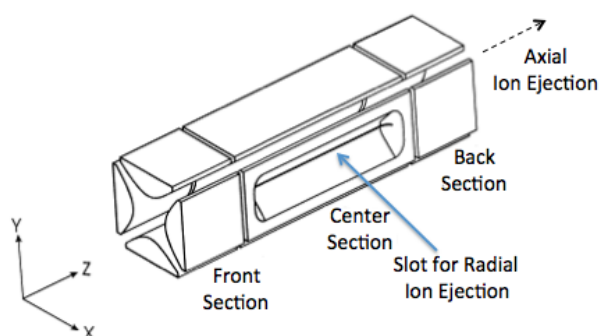
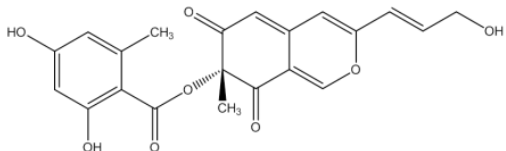
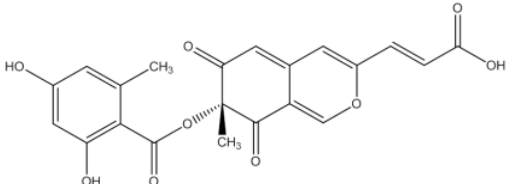
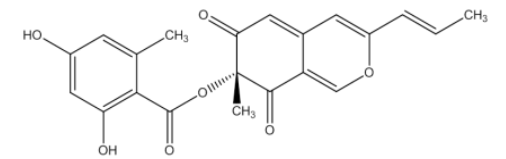


Figure 31: Schematic presentation of linear ion trap

LTQ is composed of four hyperbolic rods with parabolic inner edges. Rods are consisted of three sections, and on each section a DC voltage can be applied to allow trapping of ions in the center or along the z axis. This enables accumulation of higher number of ions and its focalization which for a purpose has higher sensitivity and accuracy. Furthermore, ions can be radially ejected and detected by low resolution. This ion trap allows to manipulate the ions either in MS mode for ion accumulation and storage) or in MSⁿ experiments. Moreover, the MSⁿ experiments can be done and detected by low or high resolution. High resolution detection is observed when ions are axially ejected toward the C-trap (RF-only quadrupole of a C letter shape), which ensure trapping a large number of ions and tangential injection into orbitrap. This way, electrostatic attraction toward the central electrode is compensated by injecting ions tangentially and resulting circular trajectory of ions.

Orbitrap mass spectrometer have never before been used for detection of azaphilones, thus they have never before been detected with such high resolution and accuracy. In the **Table 4**, main peaks that can appear in the mass spectra of azaphilones of interest (mitorubrins from *Hypoxylon fragiforme*), their structures, the monoisotopic masses of protonated ions and masses of adduct ions were summarized.

Table 4: Structures, monoisotopic masses and accurate masses of azaphilone adducts that can be formed in ESI and detected in orbitrap mass spectrometer during analysis of *Hypoxylone fragiforme*

Compound	Structure	Monoisotopic mass	Accurate mass of diagnostic peaks				
			[M+H] ⁺	[2M+H] ⁺	[M+Na] ⁺	[M+K] ⁺	[M+H ₂ O] ⁺
Mitorubrinol		398.1004	399.10744	797.2078	421.0902	437.1987	417.1174
Mitorubrinic acid		412.0797	413.0867	825.1664	435.0594	451.1780	431.0967
Mitorubrin		382.1055	383.1125	765.2180	405.0852	412.2038	401.1225

Mitorubrinol acetate		440.111	441.1180	881.2290	463.0907	479.2093	459.1280
Mitorubraminol		397.1164	398.1234	809.2191	420.0961	436.2147	416.1334
Mitorubraminic acid		411.0957	412.1027	823.1984	434.0754	450.1940	430.1127
Mitorubramin		381.1215	382.1285	763.2500	404.1012	420.2198	400.1385
Mitorubraminol acetate		439.1270	440.1340	879.261	462.1067	478.2253	458.1440
Orsellinic acid		168.0425	169.0495	337.0920	191.0222	207.1408	187.0596

4.2.3 Triple quadrupole

Briefly, based on the quadrupole device, a triple quadrupole (TQ) is consisted of three quadrupoles coupled either in axis or off-axis. The first (Q1) and the last (Q3) quadrupole are mass filters and the second one (Q2) works for the non-selective transmission and as activation cell. It can be quadrupole or multipole (hexapole or octapole), with a different geometry (linear, curved or half-circular). Mass filters scan both, DC and RF potential (see Annex) for selective m/z ion transmission. The activation cell is used either for collision induced dissociation (CID) or collision activated reaction (CAR) and it scans RF tension consistently with Q1 and/or Q3 RF potential.

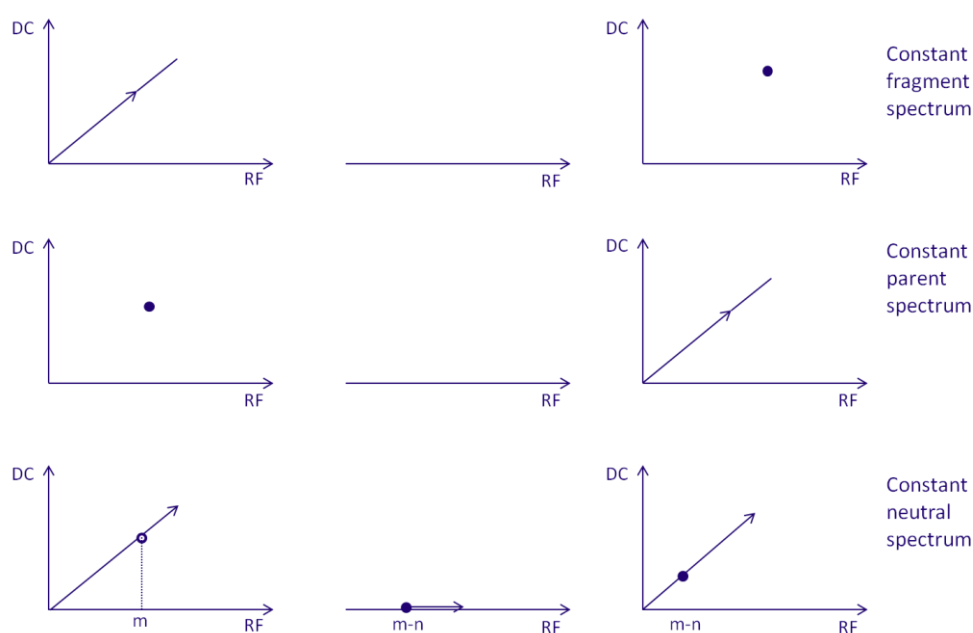


Figure 32: MS/MS experiments based on analysis using two spatially separate mass analysers. Q1 and Q2. Between the analyzers activation cell (for CID and CAR) (Q2)

From such link voltage, three different scans can be achieved: constant parent spectrum, constant fragment spectrum and a constant neutral loss spectrum (**Figure 32**). $DC_{(Q1)}$ and $DC_{(Q3)}$ as well as $RF_{(Q1)}$, $RF_{(Q2)}$ and $RF_{(Q3)}$ are linked scans. The properties of TQ tandem mass spectrometer are resolution of 3000-5000 FWHM, low m/z mass accuracy (± 0.2 Da) and a low m/z range (typically 25-6000 Th).

It is possible to study the collision induced dissociation (CID) using this type of analyzer. The CID works in two steps. First step is a collision with the target and the second step is dissociation. Due to the collision, ion-excitation occurs. During the collision, the ion kinetic energy (E_{lab}) is partially transformed into internal energy (10-100 eV, maximally up to 200 eV). Under such conditions only vibrational energy is carried out by the precursor ion. However, the maximum of internal energy corresponds only to the energy of the center of the mass:

$$E_{cm} = E_{lab} \times \left(\frac{m_{target}}{\sum m_{target} + m_{ion}} \right)$$

The best efficiency occurs when the collision complex of target plus ion is a long living. Only by these conditions, the efficiency in transformation of translational energy into vibrational energy is better. This means that at low kinetic energy, best efficiency is reached. Thus, the higher kinetic energy, the higher E_{lab} is reached, and the higher E_{int} would be reached if the life of complex is not shortened. Configuration of the potential applied to the quadrupole in the registration requirements of CID spectra is shown in **Figure 33**.

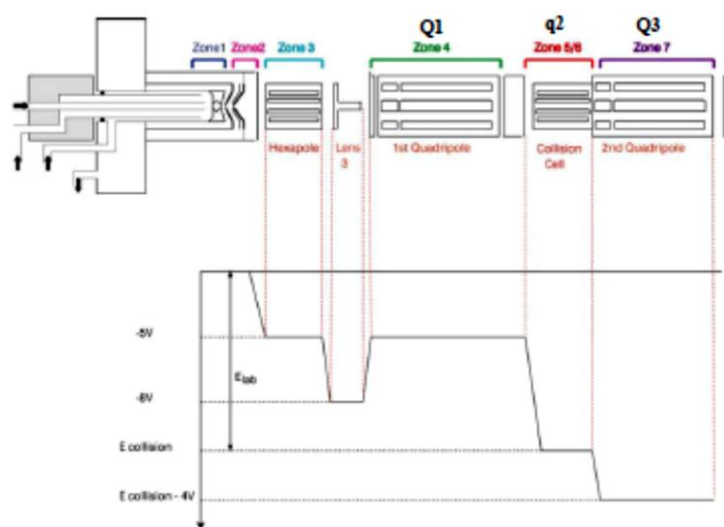


Figure 33: Schematic presentation of TQ with potential gradient

TQ mass spectrometers are typical examples of tandem-in-space instruments capable of operating in four main scanning modes: i) product ion scanning, ii) precursor ion scanning, iii) neutral loss scanning and iv) selected reaction monitoring (SRM).

4.3 Collision induced dissociation (CID) and collision activated reaction (CAR)

Collision Induced Dissociation (CID) is the most frequently used approach to fragment ions in mass spectrometry. When using soft ionization methods where protonated molecule is often the only one produced and observed ion in mass spectrum, CID becomes a necessary tool for further structural elucidation. It means the collision between ion and neutral reagent that induces transfer of kinetic to internal energy that causes dissociation. The yields of produced fragment ions depends on the activated precursor ion decomposition probability, regarding the quasi-equilibrium theory, RRKM. By this theory, CID is an ergodic process, which allows equal distribution of the excitation energy through the whole ion. Thus, the most probable sites in the ion where dissociation happens are the weakest bonds. Three important terms concerning CID are employed: collisions, energy transfer and dissociation.

CID works differently in time-separated (tandem in time) and space-separated (tandem in space) mass analyzers. In tandem in time mass analyzers, such as ion-cyclotron resonance (ICR) or ion trap, an inert gas is introduced in the mass analyzer, while in tandem in space inert gas is introduced in the collision cell which separates two mass analyzers. First mass analyzer serves then for isolation of precursor ion, while the second one serves for detection of all ions formed during the dissociation.

If a reagent gas is introduced instead of inert gas into the collision cell, and low energy collisions are performed, collision-activated reactions (CAR) or in other words ion-molecule reactions can take place.

4.3.1 Ion-molecule reactions in the gas phase

Time allowed for reaction between ion and introduced reactant gas is quite short and can be varied over only a limited range (several milliseconds). Moreover, it is difficult to achieve the very low collision energies that promote exothermic ion-molecule reactions. Nevertheless, product ion spectra arising from ion-molecule reactions can be recorded and serve as an alternative to CID for ion characterization. This method is widely used for gas phase reaction experiments, thus for H/D exchange in structural determination too.

4.3.2 Ion-dipole complexes

Ion-dipole complexes (Idp) were naturally introduced to explain the existence of molecular ion of alkanes in the EI. Indeed, for the alkane to be ionized, one electron needs to be removed from the δ -bond, because there is no lone electron pair or a π electron. Ion results from the cleavage of covalent bond. Two situations can occur:

- Separation of two fragments, one radical and one cation, and
- Both the partners are maintained together only by electrostatic interaction created by the dipole induced by the neighboring cation (**Figure 34**)

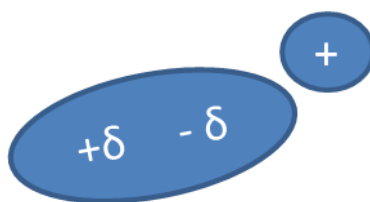


Figure 34 Electrostatic interaction between the dipole and cation

This means that in non-stabilized carbocation the charge needs to be solvated by the neutral radical partner. This situation characterizes the primary carbocation which presents molecular ions (ion-dipole), and is not applicable for the tertiary carbocation, for which the molecular ion is absent (the tertiary carbocation does not need to be solvated).

Concept of Idp was introduced simultaneously by two research groups to explain:

- i) Why the H^+ or H^\ominus can be transferred to the far site in the molecular ion,[147-149] and
- ii) Why particular fragmentations take place from the fragment ion produced in EI source.[150]

This concept has been extended and applied to other even electron ionic systems generated in CI (in positive or negative mode). However, under vacuum ionization conditions or in CI, where the pressure is increased, the relaxation by collisions is not sufficient for efficient internal energy relaxation, and then the corresponding even electron ions (protonated or deprotonated specie) are promptly decomposed in the ion source, from the ion-dipole complex. This situation is exacerbated when the basicity or acidity of both partners is too different, in positive or negative ionization mode, respectively. The formation of dimeric species have the same origin, however, they involve intramolecular interaction rather than intermolecular interactions. It is the same idea that Cooks introduced for the kinetic method to reach the basicity and acidity of the ions.[151, 152]

The total relaxation takes place under atmospheric pressure conditions. Consequently, by using API techniques (APCI, APPI, ESI...), the protonated (or deprotonated) molecular species that isomerizes into Idp, can survive the ionization step and soft ionization conditions.

4.3.3 Gas phase H/D exchange

H/D exchange reactions of natural organic compounds is an ancillary and practical technique for determination of different functional groups with heteroatoms such as alcohols, phenols, carboxylic acids, amines, amides, and mercaptans present in the molecular structures.[153]

This method is mostly used for structural elucidation of proteins' tertiary structure, but also for structural determination of small molecules. As the deuterium nucleus possess two neutrons and thus is twice heavier than the hydrogen nucleus, when the hydrogen is replaced by deuterium the final mass of molecule is higher. This fact is

largely used in mass spectrometry H/D exchange approach. The shift in m/z value of analyzed molecule after exposure of sample to a D-containing reagent provides a counting of active hydrogen atoms, which are bonded to hetero atoms, O, N or S. Different methods of H/D exchange have been developed in the past. Two approaches can operate: in solution, or in the gas phase. First, the most used was liquid phase H/D exchange where the replacement of hydrogen by deuterium takes place in solution, as the chemistry of living organisms occurs in bio-fluids. Further the products are analyzed by different analytical methods including classical mass spectrometry. The H/D exchange in the solution phase is not specific and is as the deuterium containing reagent is used D_2O , all mobile protons located on the amino, hydroxyl, amide, imine, enamine, carboxy groups and monosubstituted alkynes are fully exchanged.[154] This approach is currently applied for NMR and MS analysis. Still, intermolecular interactions and solvent effects are large in this method, thus some chemical properties of molecules, such as pK_a cannot be involved.

The gas phase H/D exchanges are specific processes due to the relative gas phase properties of both, the exchanging reagent (usually D_2O , MeOD or ND_3) and an analyzing ion (usually MH^+). These stepwise exchanges occur under particular gas phase basicity (in positive ion mode) or acidity (in negative ion mode) frame. For instance, in positive ion mode the process is a stepwise pathway and it considers:

- (i) Ion solvation - adduct ion formation, which is always exothermic, independently to the proton affinity (PA) of the exchangeable group in the ionized molecule
- (ii) Proton transfer from protonated molecule to the deuterated reagent into the ion-dipol complex. This reaction can be exothermic or endothermic relatively to the adduct ion energetic level
- (iii) Deuterium transfer from the protonated deuterium containing reagent to slightly more or less basic site to the neutral analyte and
- (iv) The comeback of the ionization of the exchangeable analytes takes place by simple cleavage (as desolvation).

If the PA of protonated analyte is lower than that of deuterium containing reagent (**Figure 35(a)**) this difference must not be too high otherwise the deuterium transfer process is in competition with the direct cleavage of $[RX, YD_xH]^+$ complex into the YD_xH^+ and the exchange does not take place.

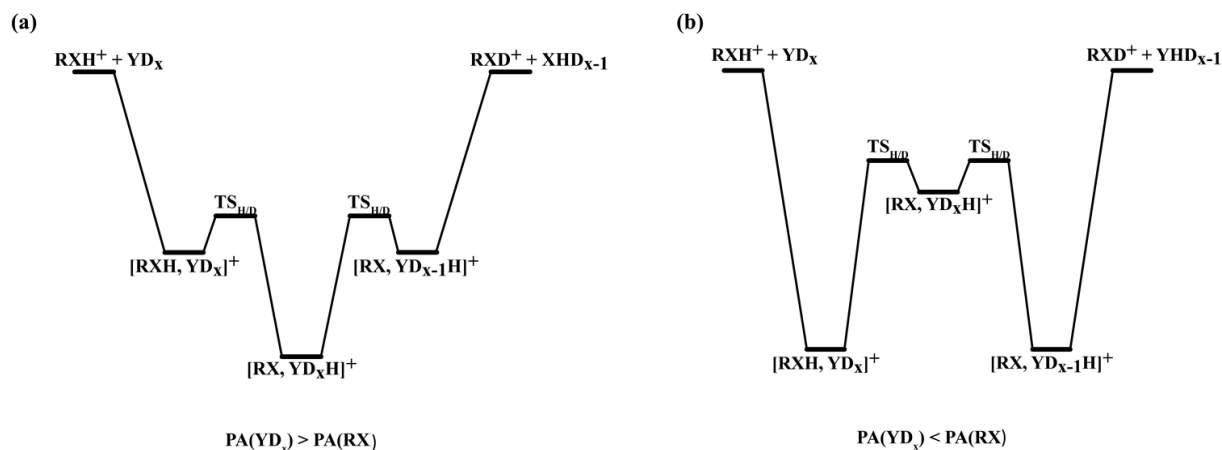


Figure 35 General mechanism of an H/D exchange process between a RXH^+ ion and YD_x ; case of exchange when (a) $PA(YD_x) > PA(RXH^+)$, and (b) $PA(YD_x) < PA(RXH^+)$.

If the PA of protonated analyte is higher than that of deuterium containing reagent, this difference must not be too high because the proton transfer to deuterated reagent is endothermic process relatively to the initial system, and thus does not occur. However, assistance can result in lowering of the energetic level of the $[RX, YD_xH]^+$ complex and thus allow the proton transfer as an exothermic process to the RX molecule and the exchanges can take place.

Further on, few approaches of in-source gas phase H/D exchange mass spectrometry have been developed to approach chemical properties of molecules and its structures. For example, an H/D exchange in ESI source have been developed requiring instrumental modifications in the source region of mass spectrometer.[155] In fact, the nebulization and/or curtain gas usually used (N_2 for example) was replaced with a deuterated reagent such as ND_3 or N_2/H_2O . This method shows a successful and complete exchange of active protons in small protonated or cationized molecules and is thus useful in structural elucidation of ionized molecules containing up to 25 labile protons. For bigger molecules the exchange can be incomplete. Such exchanges are clear for proton covalently bonded to heteroatom (vide infra).

Another method for gas phase H/D exchanges have been developed for the processes that happen in the mass analyzer. Applying this method intermolecular interactions and solvent effects can be neglected and gas phase chemistry can be utilized as very useful tool for understanding and studying important chemical properties of molecules. For this kind of research, utilized deuterium containing reagent in the gas phase can have important effect.[156] H/D exchanging rate depends on many factors. At first from protonated species, it depends of the type of exchangeable protons (amine, amide, hydroxyl, ...), and on presence of intermolecular hydrogen bonds and steric effects as well as other entropic effects that occurs with relay mechanism.[157] Positive ions of glycine oligomers were analyzed by H/D exchange by Beauchamp[158] with different deuterated reagent. This work showed that H/D exchange rate strongly depends on the gas phase basicity of deuterium containing reagent. More the reagent is basic, more the exchange rate is high. Thus, ND_3 exchanges mobile protons the most efficiently, while D_2O the slowest, due to its lowest gas phase basicity. Hunt analyzed hydrogen exchange of alkylbenzenes, oxygenated benzene, toluenes and some aromatic polycyclic hydrocarbons with D_2O , EtOD and ND_3 . [159] They demonstrated that for observation of complete exchange in protonated monofunctional compound, proton affinity difference between deuterated reagent and analyzed molecule should not exceed 20 kcal/mol. For polyfunctional molecules proton affinity difference between analyte and deuterated reagent gas can be higher. Gard showed that proton exchange of some amino acids with MeOD can occur even if their gas phase basicity exceeds 30 kcal/mol.[160] Onium ion and relay mechanism of H/D exchange were proposed by Beauchamp.[157]

H/D exchange reactions have been performed in the quadrupole, as well as in the trap mass spectrometers. Harrison performed exchange of enolate ions with MeOD and EtOD in the rf- only collision cell and demonstrated that exchange grows with collision energy and deuterated reagent increment.[161] Group of Cooks reported a study of the isotope exchange reactions of mass-selected molecular ions, M and protonated molecules, $[\text{M}+\text{H}]^+$, with CH_3OD and ND_3 , in the collision cell of a triple quadrupole mass spectrometer.[162] They reported that the use of ND_3 allowed

exchange of all active hydrogen atoms, while the use of CH₃OD allowed exchange of phenolic and carboxylic hydrogen atoms without exchanging the amino hydrogen atoms.

By this brief review of possibilities that H/D exchange can provide, it is evident its significance. It can also be used in much simpler purposes. Knowing the structures of azaphilones and their highly oxygenated bicyclic core, H/D exchange can be used for counting the number of labile hydrogen atoms in the aim of their structural elucidation. Furthermore, as the azaphilone react spontaneously with amino group giving the nitrogenized analogues, this family of molecules can be easily distinguished from their precursors, as they contains one hydrogen more in the structure, coming from enamine group formed during the reaction with amines. In our work, this method was used successfully for structural elucidation of nitrogenized azaphilone analogues, and will be explained in the Experimental part and Results and discussion chapters.

4.4 LC-MS interfacing

In the past 20 years the on-line combination of HPLC and MS has become a routinely applicable, extremely powerful and user-friendly analytical tool. The inability of gas chromatography-mass spectrometry (GC-MS) to analyze non-volatile and/or thermo-labile molecules of high polarity, such as plant phenolics, and the introduction of atmospheric pressure ionization (API) techniques, such as electrospray ionization (ESI), atmospheric pressure chemical ionization (APCI) and atmospheric pressure photo ionization (APPI) gave a massive contribution to LC-MS in gaining its position of today. The rapidly increasing number of papers convincingly proves that LC-MS is a unique technique capable of analyzing complex mixtures, like plant extracts, regardless to co-elution or other separation fault, which was a frequent problem when only UV or other usually LC associated detectors were used.

LC-MS requires atmospheric pressure conditions and coupling with mass spectrometry can occur only utilizing API sources. For volatile compounds gas phase

ionization can be used and reversely for larger system less volatile desorption method can be applied, especially ESI.

With the invention of electrospray ionization (ESI), [135, 163] a soft ionization technique at the atmospheric pressure, the analysis of macromolecules and polar and non-volatile molecules as well became feasible. Very often though a complex samples are to be analyzed. Analyzing these kinds of samples can be difficult due to the competition in the ionization of different molecules present in the sample. All the molecules will endeavor to ionize, and this will make a mass spectrum more complicate, and the ionization efficiency will be diminished. For this reason it is a good option to separate the analytes, and that is why mass spectrometry was coupled to HPLC, via ESI as interface. LC-MS has thus become one of the widest used methods for determination of low mass molecules, but the high mass molecules (such as proteins and peptides) as well.

Nowadays LC-MS coupling techniques have clearly become the most widely-used tool in analyzing drugs and their metabolites. Chromatographic separations are most commonly obtained using HPLC with reversed-phase columns. In the early phase of metabolite profiling, rapid generic chromatographic methods are often utilized, applying 5-80% acetonitrile or methanol and aqueous phase in a gradient run of few minutes.

For metabolic profiling studies the most common ionization methods in LC-MS applications are ESI and APCI. The ion sources are referred to as API sources, as the ionization does not take place in a vacuum but in atmospheric pressure. ESI is suitable for almost all drug-like molecules with at least one easily ionizing functional group,[164] whereas for steroids and other less polar compounds, APCI is often utilized.[165] Comparing these two methods, APCI is generally less susceptible to matrix effects.[166, 167]

MS data processing is nowadays highly automated and the developments of post-acquisition data mining techniques are strongly enabled by high mass resolution data. Metabolite screening is assisted by software that compares the acquired data

between the sample and negative control and suggests biotransformation and calculated elemental composition for the found metabolites using accurate mass measurements and information about compound of interest.

Experimental part

In this section are described chemical substances, instrumentation and methods used for the performed experiments. A chapter includes sample preparation, analytical HPLC separation of complex mixture, isolation and purification of compounds from the crude fungal extract, mass spectrometry techniques used for analysis of compounds in different experiments.

1. Solvents and chemicals

Hypoxylon fragiforme fungal samples were collected from the dead *Fagus sylvatica* tree at the forest in South-Eastern Serbia, characterized by Professor Mark Stadler, InterMed Discovery GmbH, Germany and deposited in the Herbarium Moesiacum, University of Nis (voucher number 5530). Methanol and acetonitrile were of HPLC grade (VWR, EC). Water was obtained from a Milli-Q Gradient system (Millipore, Brussels, Belgium). Formic acid was from SDS (Carlo Erba Reactifs, France). ND₃ (99.75%) was obtained from Eurisotop (CEA Group, France). Solvents used for HPLC and LC-MS were filtered through a 0.45 µm mixed cellulose ester membrane (Millipore, Bedford, MA, USA) and degassed in the degasser integrated in the HPLC system (or with the gentle stream of helium for different HPLC instruments used) before use.

2. Sample preparation

Air-dried stromata of *Hypoxylon fragiforme* fungi were carefully detached from the substrate and crushed using pestle and mortar. Sample of the obtained powder weighted 10 mg was extracted repeatedly with 1 mL methanol, 10 minutes each in ultrasonic bath, and at room temperature with a five-minute centrifugation after every extraction. Collected supernatants were combined and evaporated to dryness. Dry extract was further reconstituted in methanol for direct analysis by LC-MS, or supposed to purification by SPE.

2.1 Solid Phase Extraction

In order to pre-separate and purify the analytes of interest, samples were subjected to an SPE procedure prior to analysis, in aim to remove highly non polar components that could be harmful to the following HPLC column, applying Strata Phenomenex C18 SPE cartridge (**Figure 36**). Cartridges were conditioned with 2 mL of methanol, and the crude extract dissolved in small amount of acetonitrile: water was deposited onto the cartridge. 2 mL acetonitrile: water, 40:60 (v/v) was used for elution of analytes from the cartridge. Final concentration of extract is estimated to be up to 0.2

mg/mL, based on the bibliography references.[31] The sample was finally analyzed by LC/MS.

Sample preparation for isolation of pure compounds using preparative HPLC, was conducted as follows: 9 g of powdered fungi were measured in the 300 mL Erlenmeyer flask, and extracted with 180 mL of methanol for 30 min in ultrasonic bath. After extraction, the sample was centrifuged 10 min at 2000 r/min. Supernatant was poured off in a new flask and the precipitate was topped with a new portion of methanol. The procedure was repeated three times, and supernatants were combined and filtered through the filter-paper (black tape, Whatman No41), and evaporated in the rotary evaporator kept at 35°C.

As the crude methanol extract is a complex mixture rich in nonpolar compounds, additional purification of the sample is recommended before depositing the sample to the preparative column. Thus SPE was used for this purpose. For this purpose was used SPE manifold Phenomenex consisted of 18 places for SPE cartridge and vacuum pump. Reverse phase SPE cartridges, Phenomenex Strata C-18-E (55 μ m, 70 A) 500 mg/3 mL were conditioned with 3 mL of methanol, each. Crude extract is dissolved in solvent mixture acetonitrile/water=50/50, (v/v) up to the final concentration of 25 mg/mL. 3 mL of prepared sample was deposited on each conditioned cartridge and passed through. Elution of precipitated sample was done with 7 mL of solvent mixture acetonitrile/water=50/50, (v/v). Elutes were combined and evaporated in rotary evaporator. Final quantity of purified sample was 301 mg, supposed to be used for preparative purposes.

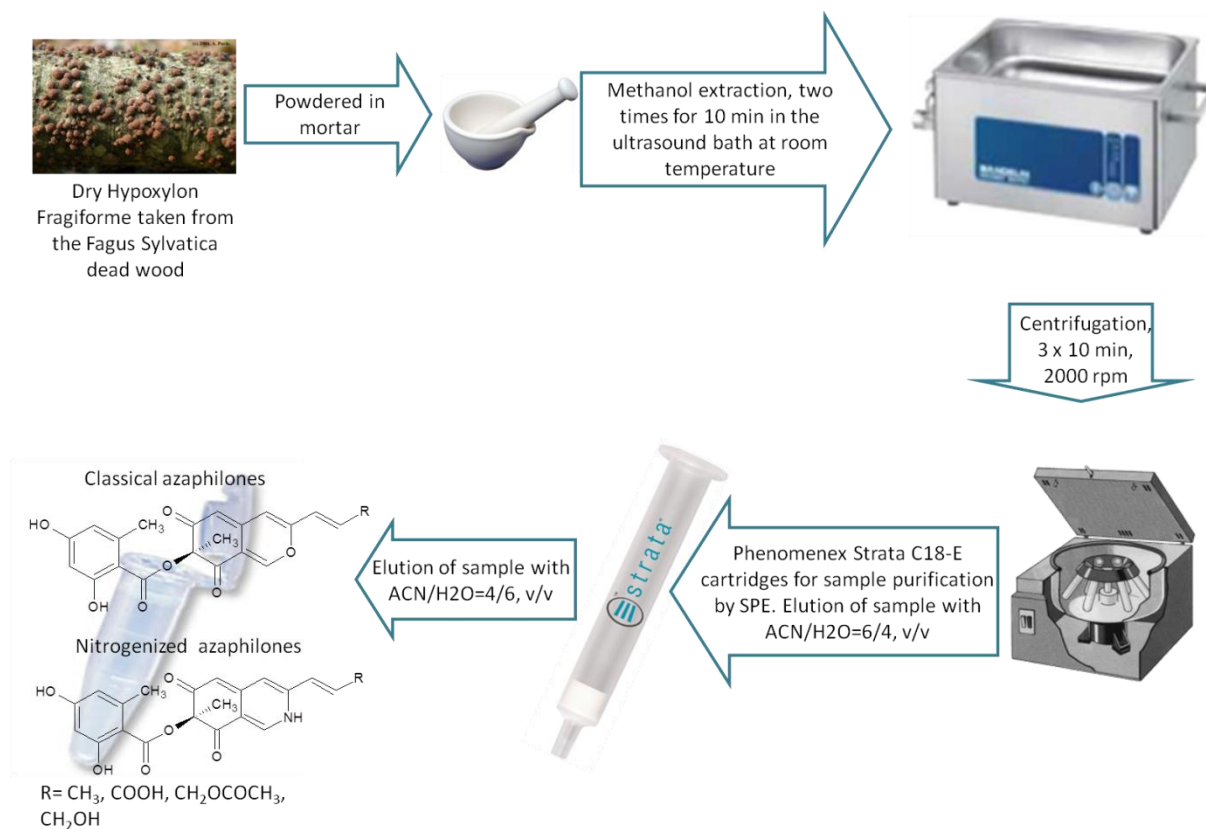


Figure 36 Step by step presentation for the sample preparation

3. Synthesis of vinillogous pyrodones

Synthesis of mitorubramin was performed as described. In 3mg/mL methanol solution of mitorubrinal obtained by preparative HPLC, equivalent volume of 0.88 M water solution of ammonium hydroxide was added. After agitation the solution was left for 5 minutes. After this, sample was evaporated and like this prepared for analysis by NMR.

4. Liquid Chromatography

4.1 Analytical High Performance Liquid Chromatography (HPLC)

For all experiments, 5 μL of extract (crude methanol extract or purified one) were injected into a reverse-phase C18 Symmetry (2,1 \times 150, 5 μm) column from Waters (Ireland). Separation of extract for analytical HPLC was done in different elution modes depending on the experiments performed. Isocratic mode using acetonitrile: water, 1:1 (v/v) with 0.1 % formic acid at a flow rate 200 $\mu\text{L}/\text{min}$ was done for gas-phase H/D exchange experiment (**Figure 37 a**)). When used gradient elution mode, starting point was 0,1% formic acid solutions in water and acetonitrile. 5 minutes elution with 90% of water was followed with a 55 minutes gradient to 90% of acetonitrile. After this, 40 minutes of 90% acetonitrile elution was performed (**Figure 37 b**)).

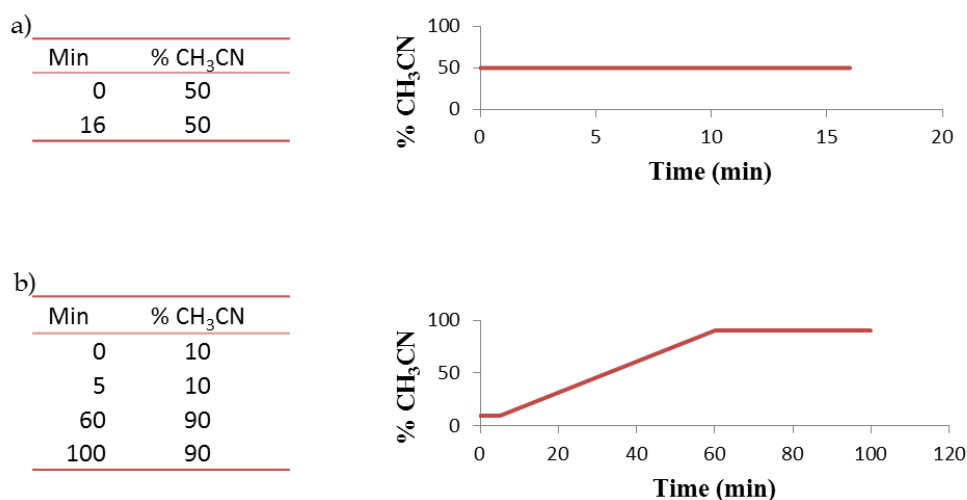


Figure 37 Elution conditions used for crude extract analysis: a) isocratic mode for gas-phase H/D exchange experiment, b) gradient mode for accurate mass measurements and CID experiments

Tableau 5 Parameters utilized for HPLC pumps and autosampler

Surveyor MS	Surveyor Auto sampler	Injection volume 15 μL
	Surveyor MS Pump Plus	Solvent A 0.1 % formic acid in H ₂ O
		Solvent B 0.1% formic acid in CH ₃ CN
		Solvent flow 200 $\mu\text{L}/\text{min}$

4.2 Preparative High Performance Liquid Chromatography

In aim to find new compounds of significance and to verify present and known ones, preparative HPLC was conducted. Instrumentation, materials and method used are summarized in **Table 6** and elution gradient is presented at **Figure 38**.

Table 6 Parameters used for preparative separation of azaphilones from methanol fungal extract

Shimadzu preparative liquid chromatograph	
Software	LCsolution
Equipment	
Degasser	FVC-130AL
Pump	LC-8A Shimadzu Preparative Liquid Chromatograph
Autosampler	SIL-10A Shimadzu Autosampler
Controller....	CBM-20A prominence Bus module
Fraction collector	FRC-10A Shimadzu Fraction Collector
Column	Agilent Prep-C18, 30 x 250mm, 10 μ m (Agilent, Montluçon, France)
Solvent A	H ₂ O
Solvent B	Acetonitrile
Injection volume	1200 μ L
Injected mass	600 mg
Diode Array Detection	190-450 nm
Cell temperature	40°C
LC Time program	
%B	Min
30	0
30	25
60	70
Acquisition time	70 min
Flow	40 mL/min
Fraction collector	
Width	2 sec
Slope	1000 μ V/sec
Level	-4500 μ V
Vial Volume	15 mL

Min	% CH ₃ CN
0	30
25	30
50	60
70	60

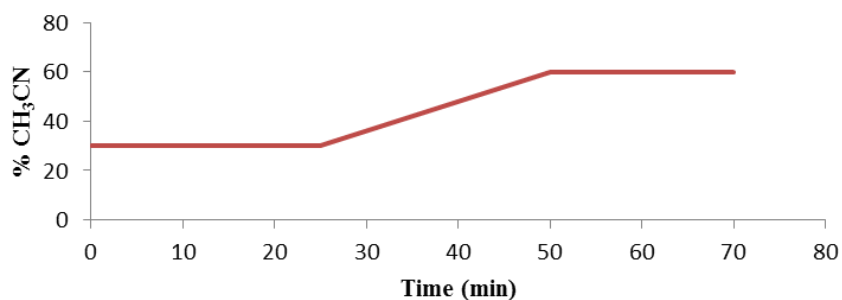


Figure 38 LC gradient for preparative isolation of azaphilones

Fraction collector was set to collect only the peaks with the slope higher 30 000 to avoid the collection of fractions with no or negligible quantities of samples. All peaks were collected, and the solvent (water and acetonitrile) from fractions was evaporated under vacuum and after under cold stream of nitrogen in liofilizator. Isolated substances were re-subjected into LC-MS to check their purity. The purity and quantity of isolated azaphilones was sufficient for further MS and NMR experiments.

5. Mass Spectrometry

The experiments were mostly done in positive ionization mode. For optimization of ionization conditions LCQ Deca (ThermoFisher Scientific, San Jose, CA, USA) ion trap mass spectrometer was used, interfacing with ESI source. Performed mass spectrometry experiments were preferentially based firstly on high resolving power yielding accurate mass measurements. For this purpose a hybrid mass spectrometer, LTQ Orbitrap XL (ThermoFisher Scientific, San Jose, CA, USA) was used. Furthermore, tandem mass spectrometer, triple quadrupole was used for gas-phase H/D exchange reactions. Experiments were performed in the collision cell of an instrument for structural elucidation. For this purpose Quatro II (Micromass, Manchester, U. K.) was used. In the following chapters a brief description of utilized instruments will be done.

5.1 Optimization of electrospray ionization conditions

After purification of crude methanol extract by SPE, 5 μ L of purified sample was deposited onto the column, and separated in the isocratic elution mode. Electrospray needle was kept at 3,5 kV for the positive ionization. Nebulizer gas was N₂ and it was kept at 70 arbitrary units (a.u.), while auxiliary gas, also N₂ was kept at 20 a.u. Temperature of heated capillary was kept at 250 °C, to help evaporation of solvents during the high LC flow. Capillary voltage and tube lens offset were modified, and used parameters are listed in **Table 7**. Mass spectra were recorded at the 100 - 900 m/z mass range.

Table 7 Utilized capillary voltages and tube lens offsets for optimization of ionization conditions and approach to the nitrogenized mitorubrin analogues

Tube lens offset (V)	Capillary voltage (V)	Tube lens offset (V)	Capillary voltage (V)
20	-30	-40	20
		-35	20
20	-20	-30	20
		-25	20
20	-10	-20	20
		-15	20
20	0	-10	20
		-5	20
20	10	0	20
		5	20
20	20	10	20
		15	20
20	30	20	20
		25	20
20	40	30	20
		35	20
		40	20

5.2 High resolution tandem mass spectrometry

Accurate mass measurements were performed on an LTQ Orbitrap XL from Thermo Fisher Scientific (San Jose, CA, USA) [168]. Positive ionization mode was chosen because more structural information are provided than those reached in the negative one. Parameters used for ESI ionization and mass analysis are as presented in the **Table 8**:

Table 8 Parameters used for HRMS and CID experiment

Electrospray	Sheath gas flow rate	70 a.u.
	Aux gas flow rate	20 a.u.
	ESI needle voltage	4 kV
	Capillary voltage	20 V
	Tube lens offset	80 V
	Capillary temperature	275 °C
Mass spectrometer	Acquire time	16 or 90 min
	Mass analyzer	Orbitrap XL
	Mass range	145 - 1000 Th
	Scan type	Full scan
	Microscan	3
	Maximum injection time	300 ms
	Mass lock (m/z)	214.089625
MS/MS	Mass range (m/z)	100-500 Th
	CID	15 % [169]
MS/MS/MS	Mass range	Depending on LMCO - 300 Th
	CID	22

5.3 Gas phase H/D exchange and TQ parameters

Gas-phase H/D exchange reaction studies on azaphilone compounds were undertaken on modified triple quadrupole mass spectrometer Quattro II (Micromass, Manchester, U. K.) (**Table 9**). The data were acquired using Masslynx software (Version 4.2). The ESI capillary voltage was maintained at 3,5 kV. Compounds were ionized with a cone voltage of 30 V, and “in source-CID” was performed with a cone voltage of 60 V. Nitrogen was used as the nebulization and desolvation gas. The source and desolvation temperatures were kept at 80°C and 20°C, respectively. ND₃ was introduced into the hexapolar collision cell at a pressure of 3.10⁻³ mbar (as read by the vacuum gauge attached to the pumping line leading from the quadrupole stage) for collision-activated reactions (CAR).[170] Analyzed protonated molecules and in-source fragment ions were mass selected in the first quadrupole with isolation *m/z* width equal to 1 Th and then sent to a radiofrequency (RF)-only hexapolar collision cell where they were submitted to ion-molecule reactions with labeled reagent gas. The collision voltage was set to $E_{\text{lab}} = 3 \text{ V}$ for all the CAR experiments. The use of set of lens voltage 7, 8 and 9 (250 V, 0 V and 0 V, respectively) was crucial for successful storage of the selected precursor ions for the CAR experiments. The reaction product ions were mass analyzed by scanning in the second quadrupole mass analyzer.

Table 9 Parameters used for H/D exchange experiments

Electrospray	ESI needle	3,5 eV
	Cone voltage	30 eV
	Cone voltage for in-source CID	60 eV
	Source temperature	80 °C
	Desolvation temperature	20 °C
Mass spectrometer	Reagent gas in collision cell	ND ₃
	Pressure of reagent gas	3.10 ⁻³ mbar
	Isolation width	1 Th
	Collision voltage	3 eV
	Lens 7	250 V
	Lens 8	0 V
	Lens 9	0 V

5.4 Density functional theory (DFT)

In parallel to gas phase H/D exchange experiments, quantum chemistry calculations have been performed using the Gaussian 09 program [171]. Geometry optimizations were obtained with the B3LYP functional [172, 173] and the def2-SVP split valence basis set [174]. Single-point energies were obtained with the same method and the Def2-TZVPE basis set. Structures were characterized either as minima or transition structures from vibrational analysis. Proton affinities (PA) were calculated for different sites of the mitorubrin compounds using atomization energies. Results presented are corrected by a linear factor obtained by comparing the results with well-defined proton affinities [175]. (PA) were calculated for the mitorubrin skeleton hetero atoms, not including the side chain hetero atoms. The mechanism of H/D exchange in the azaphilone ion structure was confirmed by the DFT calculation on the model system (**Figure 39**) of *iso*-propyl orsellinate. The model system was chosen in the aim to understand the H/D exchange mechanism in the orsellinic part of the molecule, where the side chain is chosen to observe the same proton affinity as for the analyzed molecule. Azaphilone bicyclic skeleton thus was replaced with *iso*-propyl alkyl chain.

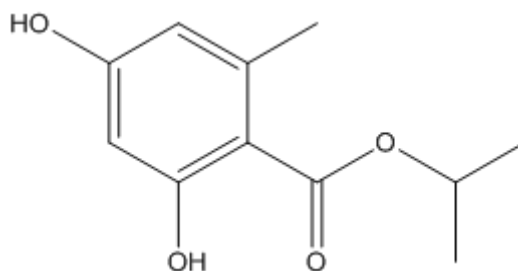


Figure 39 Structure of *iso*-propyl orsellinate, model system used for theoretical studies

6. NMR spectroscopy

^1H and ^{13}C NMR spectra were recorded at 600.40 and 150.99 MHz respectively, on a Bruker Avance III spectrometer fitted with a BBFO probe. All spectra were recorded in MeOD at 300K. Chemical shifts are reported in parts per million relative to MeOD (^1H δ 3.31; ^{13}C δ 49.15). ^{13}C direct detection was made difficult by small available quantities. ^1H Data are reported as follows: chemical shift, integration, multiplicity (s = singlet, d = doublet, t = triplet, q = quartet, m = multiplet), coupling constants. ^{13}C and ^1H assignments were made using ^1H , ^{13}C , DEPT, COSY, edHSQC and HMBC experiments.

Results and discussion

In the beginning, the separation methods and behavior of azaphilones during the reverse phase liquid chromatography are explained. Ionization of azaphilones and nitrogenized analogues showed a particular difference of behavior, and it is of interest to show the advantage of electrospray ionization for observation of different molecular species. Furthermore, the high resolution mass spectrometry (HRMS), accurate mass measurements and fragmentation pathways by using sequential fragmentation (MS^n) will be discussed as methods for distinguishing different molecular families. At the end, reaction of azaphilones during the ion-molecule reactions with deuterated reagents in the gas phase will be show and discussed in order to confirm those structures.

All the experiments performed have an aim to discover a novel family of secondary metabolites.

1. *Hypoxylon fragiforme* chemical composition

Chemical composition and particularly pigment composition of fruit body of macromycetes have been studied over the century, disclosing a hundreds of unique compounds that cannot be found in any other entity.[46] Furthermore, showing a high importance in the living circle of fungi and a large spectrum of biological activities, these chemical entities have been structurally determined, and their activities have been examined.

Beside the proteins, DNA, carbohydrates, fatty acids, a high percentage of secondary metabolites can be found in ascomycetes fungi, such as organic acids, polyynes, polyketides (such as quinones, anthraquinones, xanthenes, etc.), mono- to triterpenes (volatiles and low-volatile steroids), polysaccharides, lipopolysaccharides, and N- and S-containing compounds. When a methanol extract of ascomycetes, particularly Xylariaceae is examined, often the major constituents of the fruiting body are these particular secondary metabolites, indicating their importance in defense of fungi from environmental menaces.

Concerning the *Hypoxylon fragiforme*, major secondary metabolites found in their fruiting bodies are mitorubrin azaphilones. Still, the metabolic profile changes with many factors, for example the age of fungus or with the growth environment. Thus, in the following chapter a composition of *Hypoxylon fragiforme* collected in South-Eastern Serbia will be discussed.

1.2 Separation of mitorubrin azaphilones by reverse phase liquid chromatography

Fungal extract represent mixture of various metabolites and extreme attention should be paid to its analysis. For the separation of azaphilones from that kind of complex mixture by HPLC, different elution methods have been employed. Isocratic and gradient elution have been employed. A short isocratic separation was employed for fast detection of consisting compounds. After the purification of crude methanol extract by passing it through the SPE cartridge, a clear sample was deposited on the reverse phase HPLC column. The total ion current (TIC) obtained in positive electrospray HPLC-MS analysis is presented at the **Figure 40**.

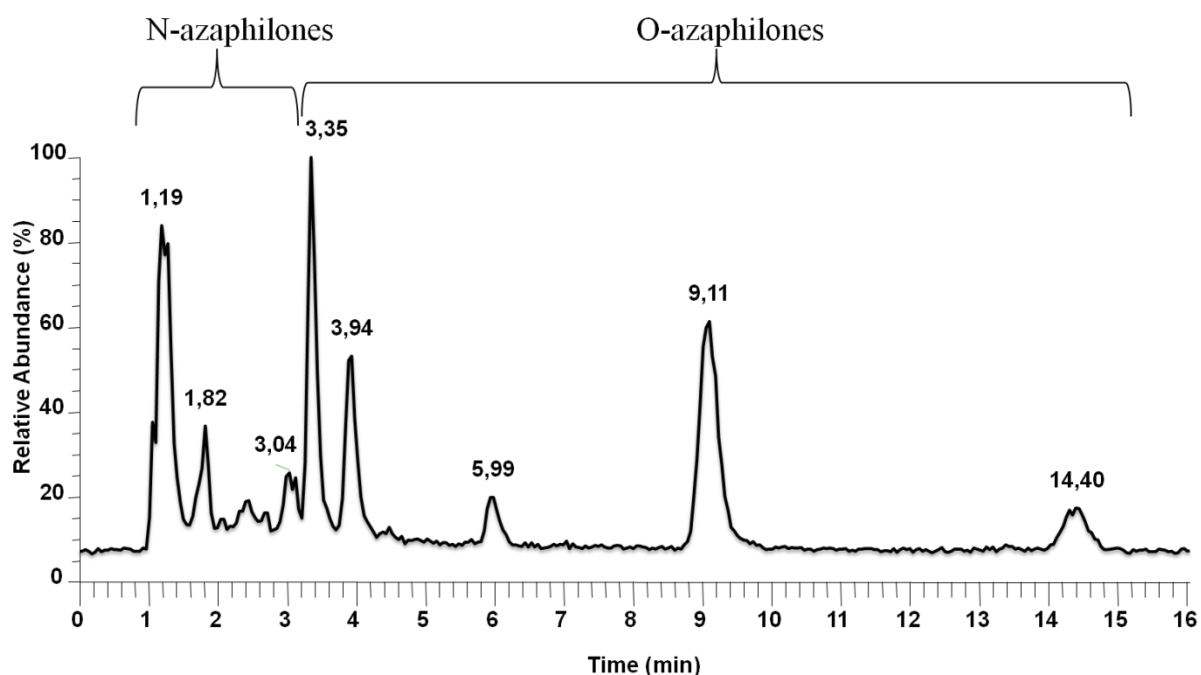


Figure 40 TIC chromatogram of *Hypoxylon fragiforme* methanol extract after purification by SPE, obtained in isocratic elution mode (0.1 % formic acid in MeOH / H₂O (50/50, v/v); flow rate: 200 μ L/min)[176]

In 2006, the chromatogram of *Hypoxylon fragiforme* has been shown in the work of Stadler's group[31] on the examination of stomatal ontogeny by following the

changes of secondary metabolite profiles in different ages of fungus (**Figure 41**). It appears that during stromatal ontogeny of *Hypoxylon fragiforme*, a profile of secondary metabolites changes, giving suppression of mitorubrin azaphilones and rising of another family of azaphilones, fragiformins. It is important to emphasize that UV detection was employed in mentioned experiments.

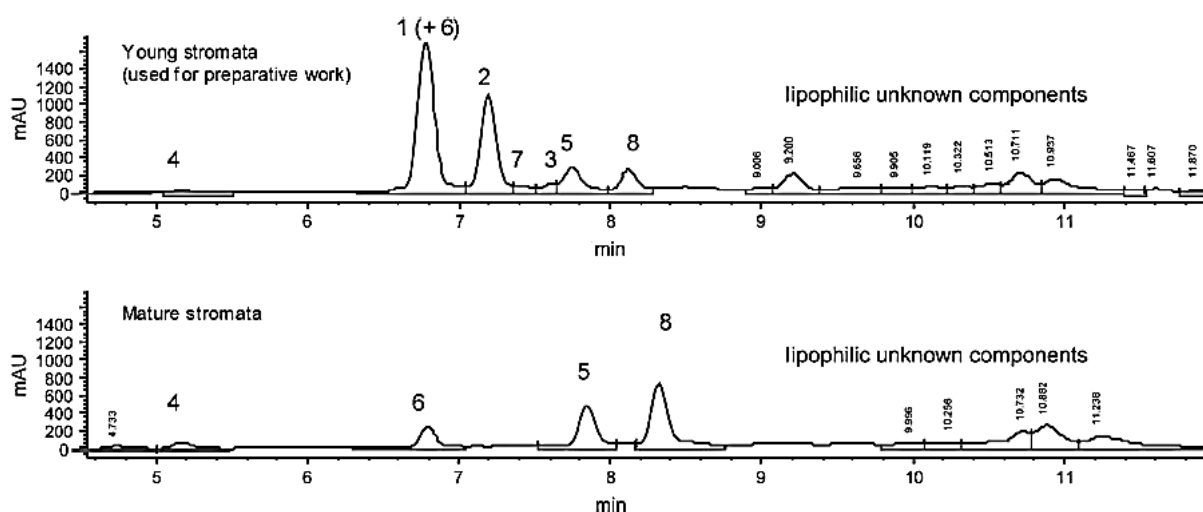


Figure 41 Section of the HPLC-UV chromatograms (210 nm) of MeOH extracts from stromata of *Hypoxylon fragiforme*. Top: young, maturing stromata; Bottom: Mature stromata [31] (0.01 M HCl-CH₃ CN; temperature 20°C; gradient: 90% 0.01 M HCl 1min; 90% 10% 0.01 M HCl 8 min; 10% 0.01 M HCl 15 min; 10-90% 0.01 M HCl 0.5 min; 90% 0.01 M HCl 2.5 min; flow-rate: 0.5 ml/min.[177]).

Differences between the published results and results herein obtained during our experiments are quite large. The elution mode we used was not the same as the one that Stadler's group used. Still, some expectations were satisfied, particularly concerning the mitorubrin azaphilones, which were detected in our samples. The chromatogram displays richer information about composition of extract. Nevertheless, we were primarily interested in the composition of secondary metabolites. In the TIC reconstituted chromatogram, beside the observed mitorubins, characteristic and always present in *Hypoxylon fragiforme*, additional chromatographic peaks were observed and did not correspond to any of additional peaks of fragiformins or other constituents in the chromatograms of young or old *Hypoxylon fragiforme* stromata (**Figure 41**). Concerned compounds exit the column at the beginning of elution, between first and fourth minute of elution, indicating a higher polarity of eluting compounds and suggesting the presence of new

compounds not usually detected in *Hypoxylon fragiforme* before. If these compounds were present in the samples of young or mature stromata used in previous work, they would appear at the beginning of the elution. Our tendencies were to determine the structures of these molecules, and assumptions were that these are potential mitorubrin nitrogen containing derivatives (refer to the **Chapter 2.3.3**).

Concerning the crude methanol extract of fungi with no further purification, a long separation method have been chosen purposely to obtain the separation as better as possible, especially for the more polar components of the extract that we were particularly interested in. A recorded TIC is presented at the **Figure 42**. It is obvious the complexity of crude extract, rich in many versatile compounds. During the 60 minutes long separation (5 min 90% of water followed by 55 min gradient up to 90% of acetonitrile, than 40 minutes of 90% acetonitrile) compounds characterized by different polarities were eluted. Mitorubrins appeared at the retention times lower than 45 minutes within high abundances which can be seen on the total ion current chromatogram. Possible nitrogenized mitorubrin analogues (pyrano quinon derivates) showed quite well abundance also, but taking into consideration higher polarity of amino group in comparison to mitorubrins (pyrano-quinone derivatives) ether group where hydrogen bonding is not favorable, they were eluted at lower retention times than 32 minutes. After 45 minutes of elution, unidentified compounds of non-polar character (as fatty acids and ergosterol derivatives) were observed.

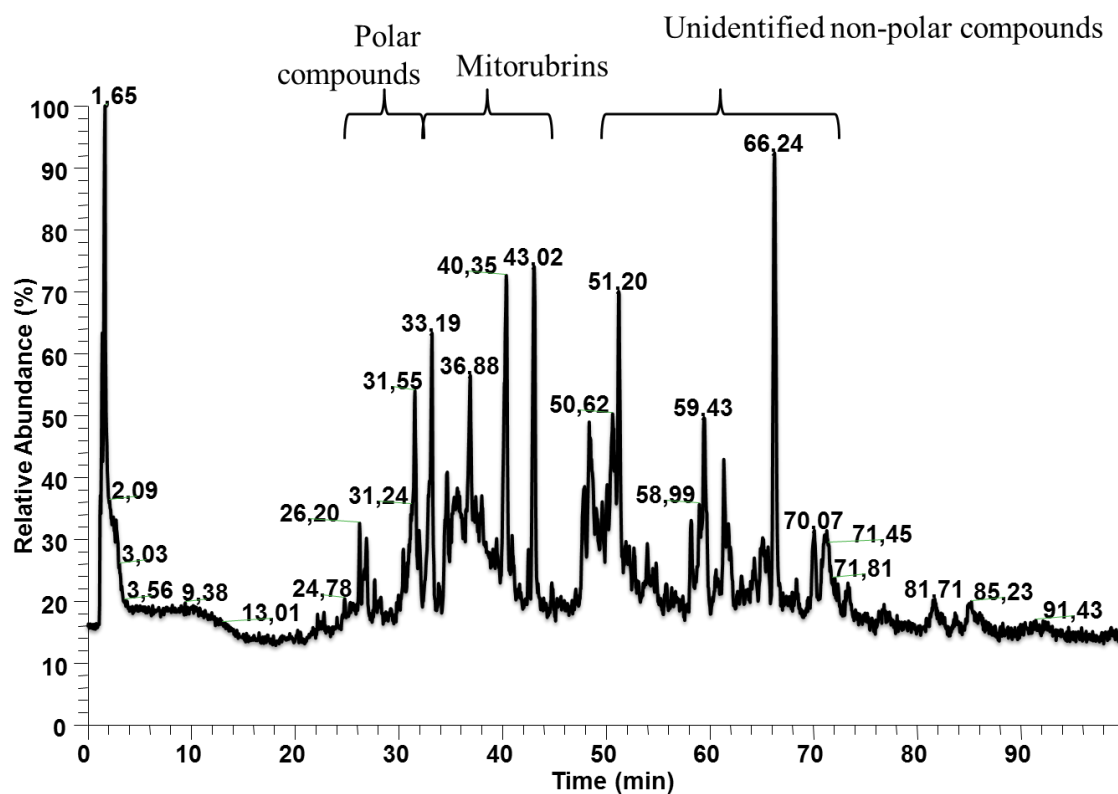


Figure 42 TIC of crude methanol extract of *Hypoxylon fragiforme* obtained by gradient elution (90% of water during first 5 min followed by linear gradient up to 90 % acetonitrile during 55 min, and thereafter isocratic 90 % acetonitrile elution during 40 min)[176]

1.3 Isolation of *Hypoxylon fragiforme* constituents by preparative HPLC

Preparative high performance liquid chromatography has been used to isolate mitorubrins and potentially novel metabolites from *Hypoxylone fragiforme*, to confirm the structures of mitorubrins and elucidate these new isolated compounds. For this purpose purification of crude methanol extract of fungi was done by SPE, and 301 mg was obtained to be separated by preparative HPLC. A gradient elution has been performed, as in the analytical HPLC it is obtained a difficult separation of polar compounds. In order to reach this, a preparative HPLC (LC-8A, Shimadzu preparative chromatograph) with Diode Array detection was used. Detection was performed at the UV wavelengths from 190 nm to 450 nm. Recorded chromatogram for the wavelength 254 nm and 3D presentation of chromatogram through the whole UV wavelength range (Figure 43), showing the UV spectra of separated compounds are presented at Figure 44.

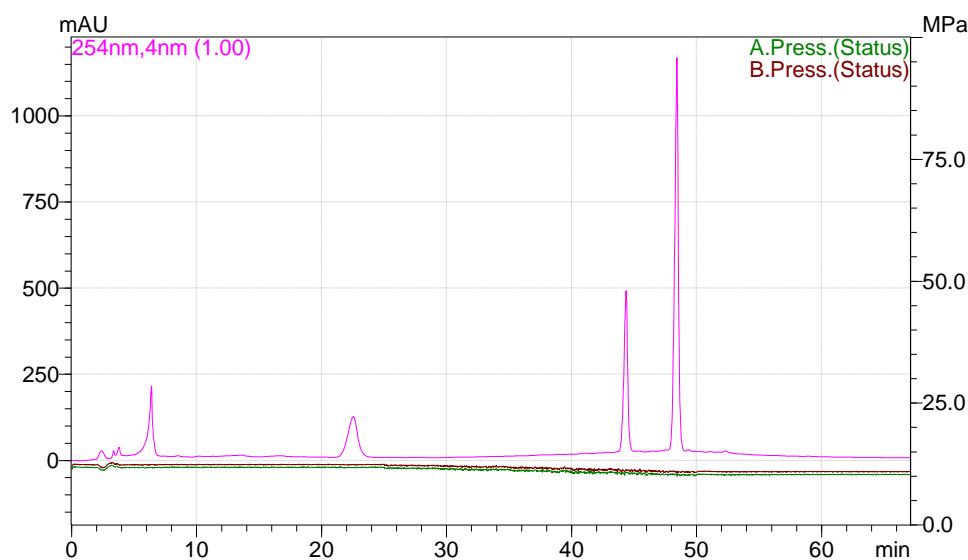


Figure 43 DAD chromatogram of *Hypoxylon fragiforme* extract (30 % MeOH during 25 min, than gradient up to 60 % MeOH during 45 min); UV, 254 nm.

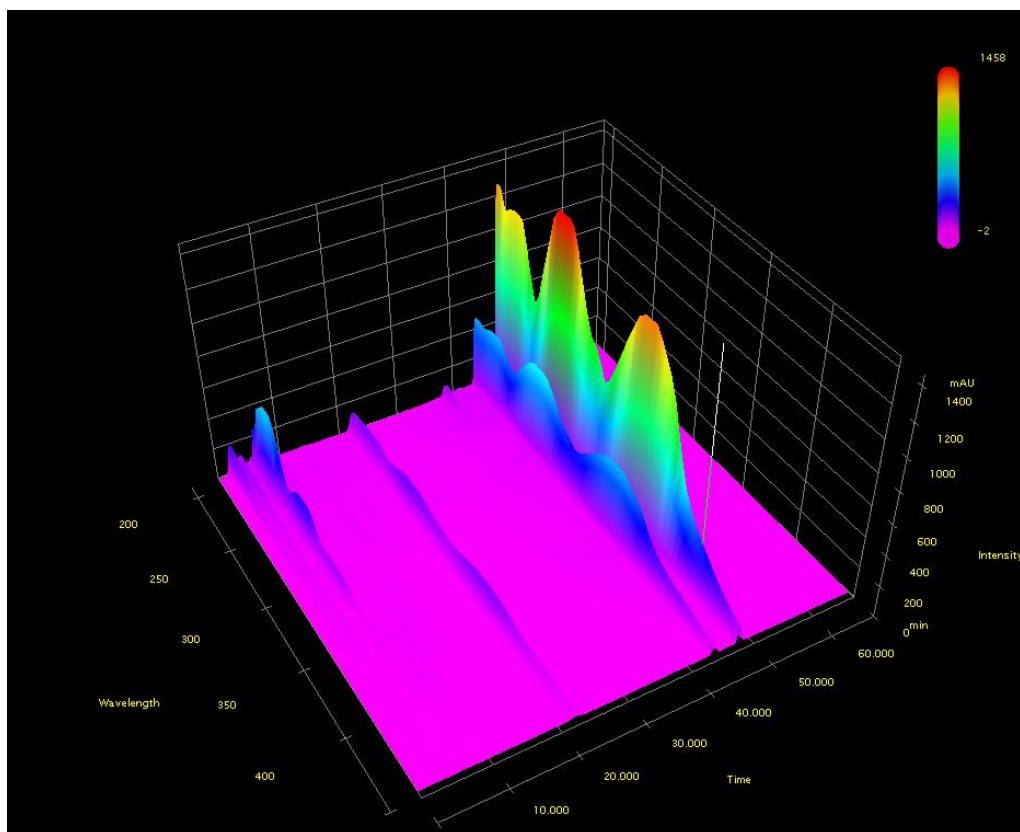


Figure 44 3D DAD chromatogram of *Hypoxylon fragiforme*, showing the UV spectra of constituents and their abundance in the extract (30 % MeOH during 25 min, than gradient up to 60 % MeOH during 45 min); UV, 190-254 nm.

Fraction collector was adjusted to collect the fractions from the slope point higher than 1000 uV/sec. In this way, the highest quantity of compounds is collected avoiding the collection of solvents and impurities. Also, negligible quantities of secondary metabolites have not been collected.

As the result several compounds were isolated. These compounds are listed in the **Table 10**.

Table 10 Secondary metabolites obtained in isolation by preparative HPLC, and quantities observed

Compound	Quantity (mg)
Mitorubrinol	2.8
Mitorubrinic acid	1.9
Mitorubrinol acetate	10.2
Mitorubrin	31.3
Orsellinic acid	5.1

Not all of expected secondary metabolites were isolated. For NMR analysis, a sufficient quantity has been obtained from mitorubrinol, mitorubrinol acetate and mitorubrin only. Thus, it was not possible to obtain NMR identification for mitorubrinic acid, though we expected to obtain a sufficient quantity for this analysis. More important was to isolate the polar compounds observed in analytical LC-MS, but their concentrations in the extract of fungi were too small for isolation and identification by NMR was not possible.

2. Synthesis of mitorubramine

As the quantity of mitorubrin obtained by preparative HPLC was more than sufficient for NMR analysis, one part of the isolate was used for the synthesis of mitorubramine, nitrogen containing mitorubrin, in aim to analyze it by NMR and MS techniques. This experiment was taken into consideration, because the assumption about the polar unknown product might have been novel group of azaphilones, or more particularly the nitrogenized azaphilones. The reaction of mitorubrin with ammonium hydroxide (refer to Chapter 2.3.3) as a fast reaction with high yield allowed us to obtain the NMR results for mitorubramine as a contribution for the future determination of such isolates directly from fungi. Furthermore, synthesized mitorubramine served as a standard compound for comparison and elucidation of polar compounds reached in previous experiments, which structures and origin were not known.

3. NMR spectroscopy results of isolated azaphilones

^1H and ^{13}C NMR spectra were recorded for isolated azaphilones and for synthesized mitorubramine. The NMR analysis confirmed the structures of present mitorubrins, and revealed information about the structure of mitorubramine. Obtained NMR spectra are presented in the Annex 1 and the obtained dataset is in the correlation with those of mitorubramines reported in the earlier works.[133, 178] dataset of mitorubramine was in the agreement with the proposed structure.

Mitorubrin				Mitorubrinol				Mitorubrinol acetate				Mitubramine				Orsellinic acid			
position	δ 13C	δ 1H	m	position2	d 13C3	d 1H4	m5	position6	d 13C7	d 1H8	m9	position10	d 13C11	d 1H12	m13	position14	d 13C15	d 1H16	m17
1	156,3	8,17	s	1	156,3	8,19	s	1	156,2	8,18	s	1	141,1	8,07	s				
3	158,0			3	152,1			3	156,8				98,5						
4	109,8	6,47	s	4	110,7	6,58	s	4	112,0	6,6	s	4	115,6	6,7	s				
4a	116,3			4a	116,0			4a	116,3			4a	116,2						
5	112,9	6,26	m	5	not seen	not seen		5	not seen	not seen		5	not seen	not seen					
6	194,9			6	194,9			6	194,0			6	196,7						
7	86,7			7	86,7			7	86,7			7	86,4						
7-Me	23,0	1,64	s	7-Me	23,0	1,65	s	7Me	22,9	1,65	s	7Me	24,0	1,62	s				
8	194,2			8	194,9			8	194,9			8	194,6						
8a	146,3			8a	145,4			8a	145,6			8a	154,4						
1"	171,2			1"	171,2			1"	171,3			1"	171,1			1"	not seen		
2"	105,0			2"	105,0			2"	105,0			2"	105,9			2"	167,1		
3"	164,7			3"	164,8			3"	164,8			3"	164,3			3"	163,8		
3"-OH	-	not seen		3"-OH	-	not seen		3"-OH	-	not seen		3"-OH	-	not seen		3"-OH	-	not seen	
4"	101,8	6,14	d	4"	101,8	6,15	d	4"	101,8	6,15	d	4"	101,8	6,14	d	4"	101,7	6,14	d
5"	166,6			5"	166,6			5"	166,6			5"	166,0			5"	167,1		
5"-OH	-	not seen		5"-OH	-	not seen		5"-OH	-	not seen		5"-OH	-	not seen		5"-OH	-	not seen	
6"	112,9	6,26	m	6"	112,9	6,26	dd	6"	113,0	6,26	d	6"	112,6	6,24	dd	6"	112,3	6,19	d
7"	145,4			7"	145,4			7"	145,4			7"	145,2			7"	145,4		
7"-Me	24,3	2,60	s	7"-Me	24,3	2,60	s	7"Me	24,3	2,60	s	7"Me	24,0	2,59	s	7"Me	24,4	2,49	s
1'	123,8	6,22	dq	1'	120,9	6,44	dt	1'	123,7	6,42	dt	1'	125,5	6,30	dq				
2'	137,2	6,68	dq	2'	140,3	6,74	dt	2'	133,9	6,64	dt	2'	136,0	6,66	dq				
3'	18,8	1,95	dd	3'	62,5	4,30	dd	3'	64,6	4,78	dd	3'	19,0	1,97	dd				
								4'	172,3			NH	-	not seen					
								5'	20,8	2,11	s								

5 and 6" signals are overlapped
6 and 8 signals may be inverted
3" and 5" signals may be inverted
exchangeables OH and NH are not seen in MeOD

Table 11 Results obtained from NMR analysis of isolates from preparative HPLC of Hypoxylon fragiforme (mitorubrin, mitorubrinic acid, mitorubamine acetate and orsellinic acid) and from synthesized mitorubramine

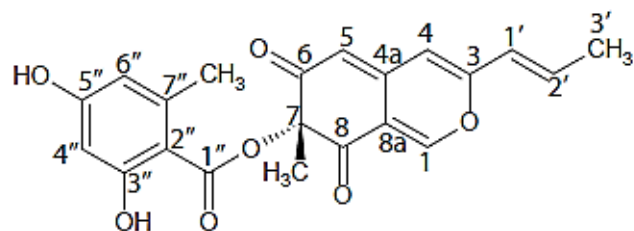


Figure 45 Nomenclature of mitorubrin for explanation of NMR spectra

4. Techniques used in MS investigation of mitorubrin azaphilones and polar compounds

The HPLC separation was coupled with mass spectral detection, and mitorubrins and polar compounds of interest have been revealed. Several MS techniques have been used in aim to determine compounds of interest. We started with optimization of electrospray source conditions to obtain as improved efficiency in desorption ionization of analyzed compounds as possible, and that we focused on the analysis of formed ionized molecular species of interest. In this approach, we have employed accurate mass measurements and a sequential CID for structural elucidation. Furthermore, a gas-phase H/D exchange reactions have been performed for further structural elucidation by counting the number of labile protons. The later experiment was performed because mitorubrins and polar compounds, assumed as nitrogen containing mitorubrins differ for one mass unit in their m/z values of single charged molecular species. Furthermore, this technique is helpful to detect a presence of amino group because, if the amino group is present in the structure, one labile proton more will be present in the molecule and exchanged with deuterium. Note that these results were consistent with differences in behavior of the protonated species toward CID processes.

4.1 High resolution mass spectrometry and accurate mass measurements

High resolution mass spectra were performed thanks to orbitrap mass spectrometer, in order to obtain the accurate mass measurements and elemental composition of containing azaphilones. Obtained accurate masses, their retention times and accurate elemental compositions of protonated analytes of interest are presented in the **Table 12**. Mentioned polar compounds that elutes at the beginning of the separation of *Hypoxylon fragiforme* extract were detected by mass spectrometry as singly charged ions with m/z for one mass unit lower than the mitorubrin azaphilones. Regarding their m/z values and retention times they can correspond to the nitrogen containing mitorubrins. Their retention times assign their higher polarity in comparison to the ones of mitorubrins. If these polar compounds are nitrogen containing mitorubrins, it is understandable that they elute before the mitorubrins due to the higher polarity of the amino group which replace the divinyl ether group of mitorubrins. Low resolution mass spectrometry and nominal mass measurements are not sufficient in elucidation of the structures of these polar compounds, which is why we employed high resolving mass measurements, which can give much more information about the elemental composition of both the precursor and product ions, by the means of ESI and CID spectra, respectively.

Table 12 Retention times, obtained azaphilones and nitrogenized analogues, *m/z* of their characteristic peaks and elemental composition by LC/HR-MS

Retention time (min)	Compound	Measured <i>m/z</i>	Elemental composition of observed ions	Experimentally observed ions	Relative error (ppm)
26.2	Mitorubraminol	398,12496	C ₂₁ H ₂₀ O ₇ N	[M+H] ⁺	1.4
29.1	Mitorubraminic acid	412,10324	C ₂₁ H ₁₈ O ₈ N	[M+H] ⁺	1.5
31.5	Mitorubramin	382,12903	C ₂₃ H ₂₂ O ₈ N	[M+H] ⁺	1.4
31.9	Mitorubraminol acetate	440,13443	C ₂₁ H ₂₀ O ₆ N	[M+H] ⁺	1.1
33.2	Mitorubrinol	399,10773	C ₂₁ H ₁₉ O ₈	[M+H] ⁺	0.9
		797.20892	C ₄₂ H ₃₇ O ₁₆	[2M+H] ⁺	1.6
34.6	Mitorubrinic acid	413,08719	C ₂₁ H ₁₇ O ₉	[M+H] ⁺	1.2
		825.16754	C ₄₂ H ₃₃ O ₁₈	[2M+H] ⁺	1.6
		151,03879	C ₈ H ₇ O ₃	[MH-217] ⁺	-1.3
40.3	Mitorubrin	383,11261	C ₂₁ H ₁₉ O ₇	[M+H] ⁺	1.2
		765,21930	C ₄₂ H ₃₇ O ₁₄	[2M+H] ⁺	1.6
43.1	Mitorubrinol acetate	441,11856	C ₂₃ H ₂₁ O ₉	[M+H] ⁺	0.4
		881.23004	C ₄₆ H ₄₁ O ₁₈	[2M+H] ⁺	1.8

First eluting compound was observed at 26 min and the main ion in mass spectrum was observed at m/z 398, which corresponds to a nitrogen containing mitorubrinol. From now on this compound will be assigned as **mitorubraminol** (Figure 46). High resolving mass measurement gave an elemental composition that corresponds with a high accuracy to such compounds, where the oxygen of heterocyclic part of mitorubrinol is replaced by amino group. Second eluting product was observed at 29 min and in mass spectrum a main peak was obtained at m/z 412, which is a value for one m/z unit (Th) lower than that of the mitorubrinic acid. We named a new compound **mitorubraminic acid** (Figure 47), because its elemental composition corresponded to such compound. At 32nd min of elution, two compounds eluted together and their elemental composition corresponded to the nitrogen containing mitorubrin and mitorubrinol acetate. These compounds were named **mitorubramine** and **mitorubraminol acetate** (Figure 48). Their structures will be enlightened later.

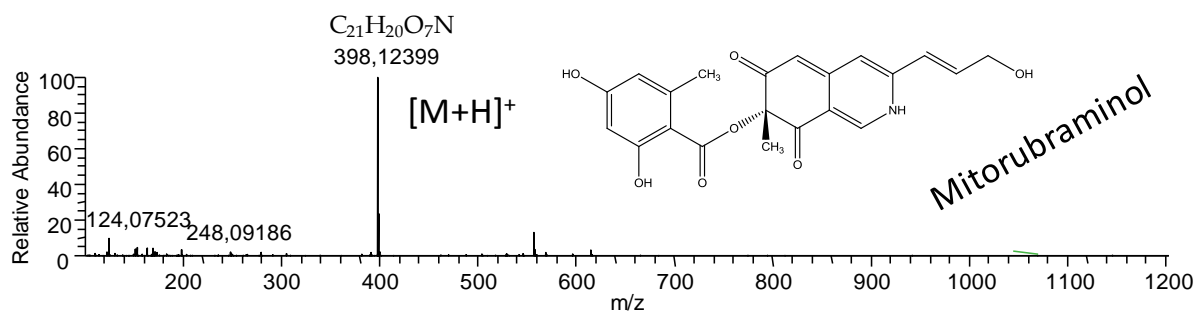


Figure 46 Mass spectrum of assumed mitorubraminol

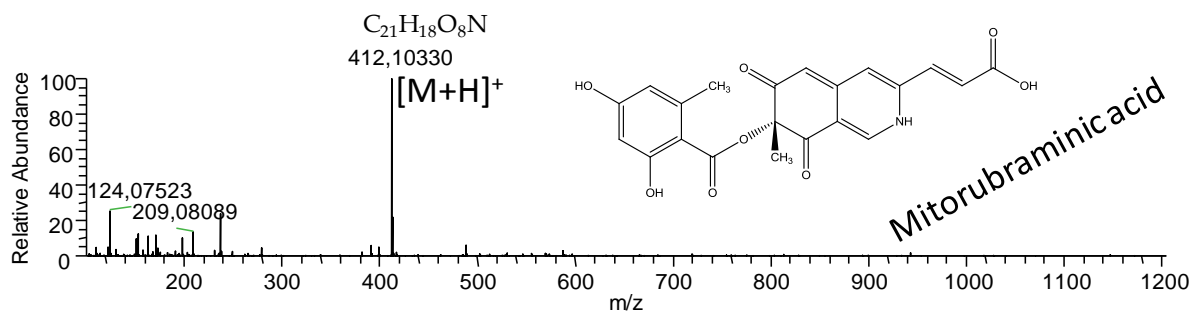


Figure 47 Mass spectrum of assumed mitorubraminic acid

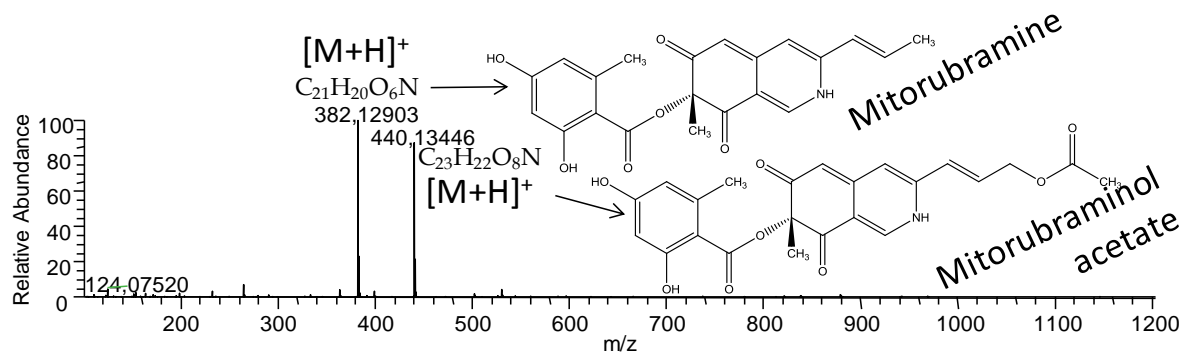


Figure 48 Mass spectrum of assumed mitorubramine and mitorubraminol acetate

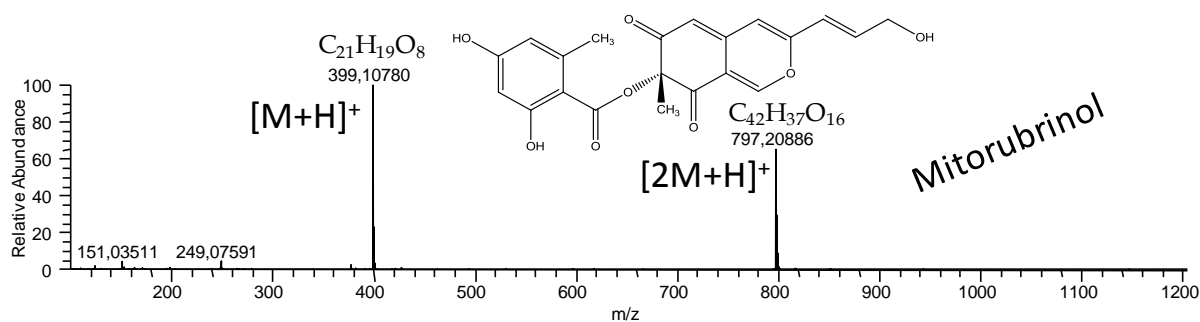


Figure 49 Mass spectrum of mitorubrinol

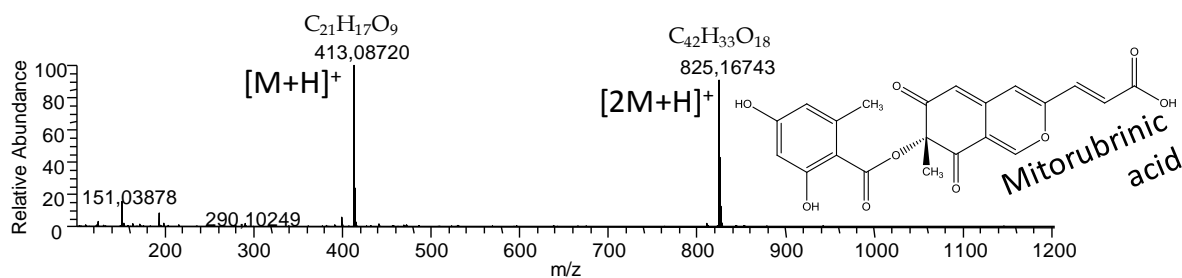


Figure 50 Mass spectrum of mitorubrinic acid

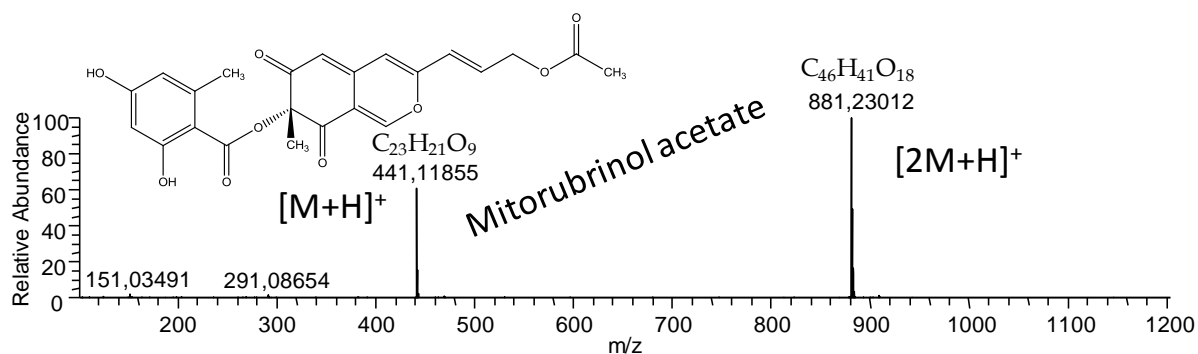


Figure 51 Mass spectrum of mitorubrinol acetate

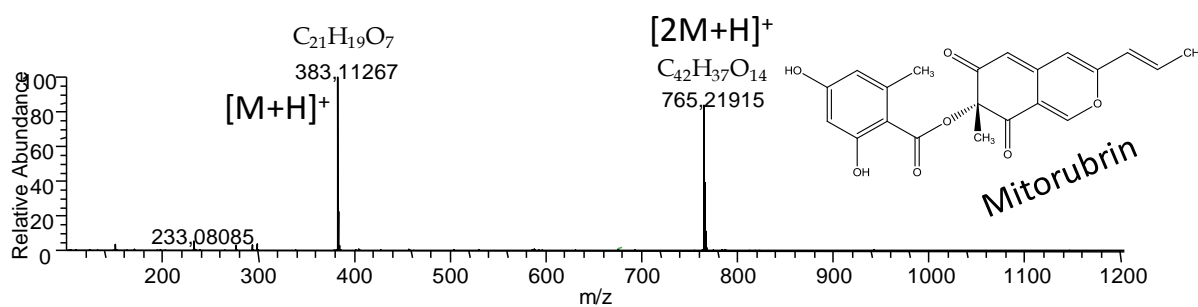


Figure 52 Mass spectrum of mitorubrin

Considering mass spectra, mitorubramines gave peaks only for protonated molecules, except mitorubraminol acetate, for which adduct with water was observed. Still, high resolving power of orbitrap mass spectrometer gave a confident data about their molecular mass and elemental composition with the accuracy of 1 ppm. The mass spectra of mitorubrin azaphilones showed protonated molecules (**Figure 49**, **Figure 50**, **Figure 51**, **Figure 52**), but also protonated dimer signals, which may be provoked by higher concentration in the extract, comparing to mitorubramines. Formation of dimeric ions depends on two factors: concentration and proton affinity (PA) of azaphilone ion. If this PA of ion is relatively high, the tendency toward the formation of complex will be lower, because its desolvation will be characterized by relatively high rate constant. If the PA is lower, the tendency to the formation of dimers will be higher. On the other hand, this can be comparable only if the ions of interest form dimeric ions with the same interacting site. Thus, if the mitorubrins and polar mitorubramines would have formed dimers at the same site, which would be the site of protonation (carbonyl group of the hetero bicyclic part of ion as the site of the highest PA; see later), it would be expected that mitorubrins easily form dimers, and mitorubramines not, due to the higher PA of nitrogen system (see later **Table 15**) in comparison to that of oxygen. Regarding the previous consideration, at least three order of magnitude lower concentration is predicted for the mitorubramines, in comparison to mitorubrin azaphilones. This can be a reason why mitorubramines present in *Hypoxylon fragiforme* methanol extract are not well detectable by other spectroscopy methods coupled to HPLC, such as UV/VIS detection.

4.2 Optimization of desorption ionization conditions for detection of nitrogenized mitorubrin analogues

Appearance of polar compounds in LC-MS profile of *Hypoxylon fragiforme* motivated us to understand their detection from the sample by analyzing their behavior in different desolvation conditions of ESI source, by varying both, the capillary voltage and a tube lens offset.

Use of ESI is a pertinent ionization approach to study structures of mitorubrins, because the formation of intact protonated molecules can be obtained in high abundance giving the information about the elemental composition, when combined with high resolving power analyzers. Further structural information can be reached by harder desolvation conditions (using “in-source CID”), or by sequential MSⁿ. Many parameters can have an influence on the formation and detection of the protonated molecules, such as choice of solvent and concentrations of the analyte, choice of additives to the solution, choice of the flow rates of the solution through the electro-spray capillary, the electrical potentials applied to the spray needle, potentials on the electrodes leading to the *m/z* ion analysis. Different compounds are always ionized with a different efficiency, and this will depend on many conditions.

The behavior on azaphilone derivatives under different ESI conditions, such as capillary voltage and tube lens potential difference was examined, since these parameter can have high influence at the desolvation of ions during their acceleration, desolvation and focalization, and thus on their appearance and abundance in mass spectrum.

Different desolvation conditions have been applied to register the appearance of novel family of secondary metabolites. Such species are unexpected in ESI, at least, they corresponds to the compounds which carry odd number of nitrogen atom(s).

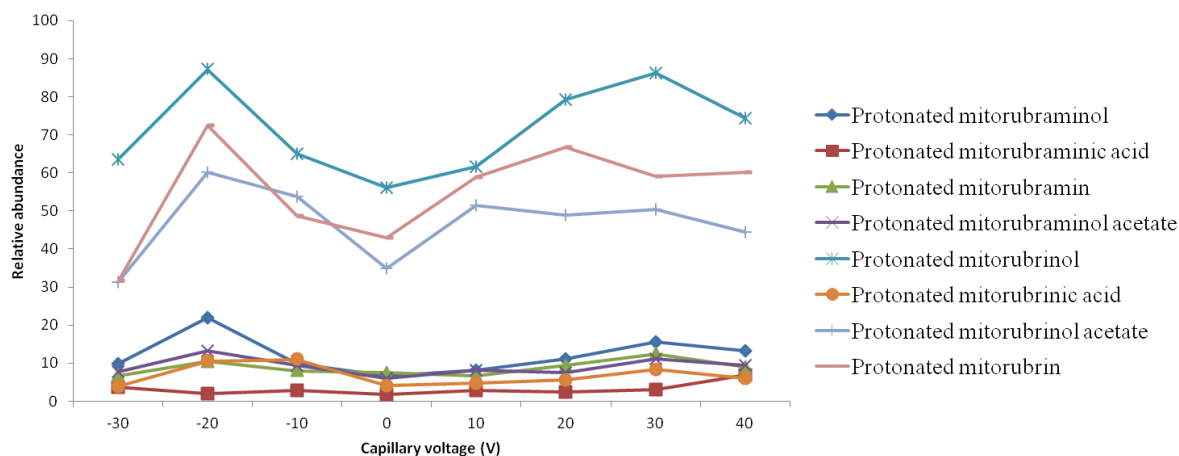


Figure 53 Dependence of normalized intensities of mitorubrins and polar components at different capillary voltage conditions

On the **Figure 53** is presented the dependence of both the mitorubrin and mitorubramine abundances in ESI mass spectra on the capillary voltage. It is visible that the abundance of mitorubramines is far lower than that of the oxygenized ones, which is due to their low concentrations. When increasing the capillary voltage values, change in azaphilone abundance is not observed. This can be expected since the capillary voltage, not really favoring desolvation and dissociations, but influences ion transfer and acceleration toward the mass analyzer through the atmospheric pressure region for all the compounds. The most important effects are those that happen due to the processes at the exit of the heated capillary and interfacing the ion optics, such as tube lens and skimmers.

Tube lens potential difference has an influence on the behavior of mitorubrins and its nitrogenized analogues. Potential and pressure gradient and focusing lens position lead to the formation of solvent free ions. Before passing through the lens section of ion source, ions are solvated, and dependently on their proton affinity they are harder or easier desolvated under the same conditions. Proton affinity of oxygen is lower than that of nitrogen and for this reason, ions containing nitrogen in the structure will be easier desolvated and thus it will be more visible at mass spectrum. This process is less endothermic than desolvation of oxygenized ions. For this kind of ions higher internal energy is necessary to be desolvated. For this reason, they are better desolvated at higher tube lens offsets the nitrogenized derivatives. At a very

low desolvation conditions it is visible enhancement of all ion intensities. This can be explained with the relatively high basicity of all analyzed nitrogenized compounds and thus, high energy is not needed for the complete desolvation. This is important cognition for better assessment of mitorubramine species because of their very low concentration in the natural samples. At higher desolvation conditions, ion abundance decrease due to the high energy collisions in the vacuum region, and thus the “in-source” collision induced dissociation (**Figure 54**). Therefore, it is very difficult to observe nitrogenized species of this kind.

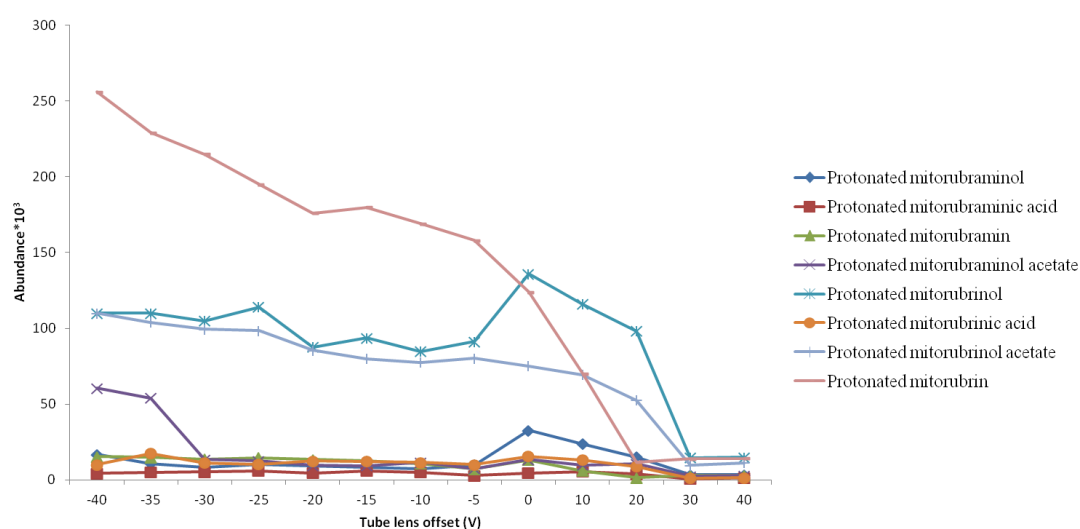


Figure 54 Ion abundance dependence upon the tube lens potential difference

At **Figure 55** is presented ratio of the abundances of nitrogenized analogues and mitorubrines, and dependence of this ratio upon different desolvation conditions at the tube lens. At higher desolvation conditions is observed increment of this ratio, which can be explained with a higher stability of nitrogenized compounds in regard to the natural azaphilones, due to the resonance stabilization and negative inductive effect of nitrogen that is lower than the oxygen ones. Hence, at higher desolvation conditions, natural azaphilones are easier dissociated than the nitrogenized ones and their abundance decrease rapidly.

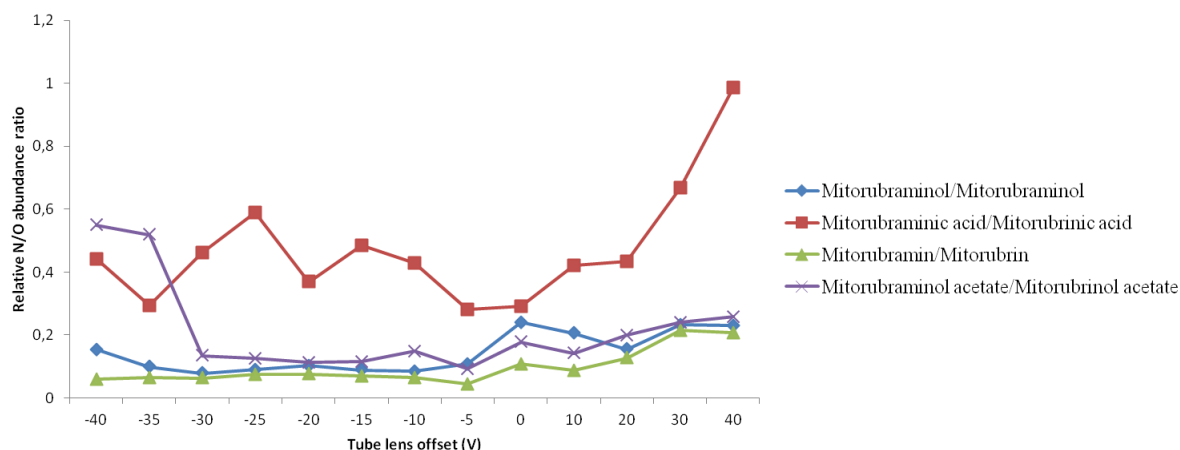


Figure 55 Variation of the intensity ratio of mitorubramines and mitorubrins with the tube lens potential difference

4.3 Collision induced dissociation

CID is the method the mostly utilized in tandem mass spectrometry for the structural elucidation. In order to reach maximum of structural information, sequential MS^n experiments, under CID conditions on protonated species under LC-ESI-MS became a very popular tool. Furthermore, sequential MS^3 experiments have been also performed. It was of interest to get as much information about the nitrogenized analoges of mitorubrins, mitorubramines as possible, because the quantity of these compounds was strictly limited, and certainly not sufficient for NMR analysis, which would gave us complete picture about their respective structure. The presence of mitorubramines is suggested by their retention times and accurate mass measurements. Still, theoretically the position of nitrogen can be different in different isomers, and this cannot be directly proven by accurate mass measurements. For example the nitrogen does not have to necessarily be present in these molecules in the form of amino group, but it can be present as an amide as well. This hypothesis can be very well developed by the means of tandem mass spectrometry. Thus, the resonant CID experiments are of crucial importance for their structural elucidation.

4.3.1 Behavior of protonated mitorubrins and mitorubramines under resonant CID conditions

The separated mitorubrins and assumed mitorubramines have been then mass-selected and studied by the means of CID experiments of protonated mitorubrins (M_0H^+) and mitorubramines (M_NH^+), which we have signed m/z [368+R] and m/z [367+R], respectively, to keep one general structure per secondary metabolite family. Resulting CID spectra are presented in **Figure 56**.

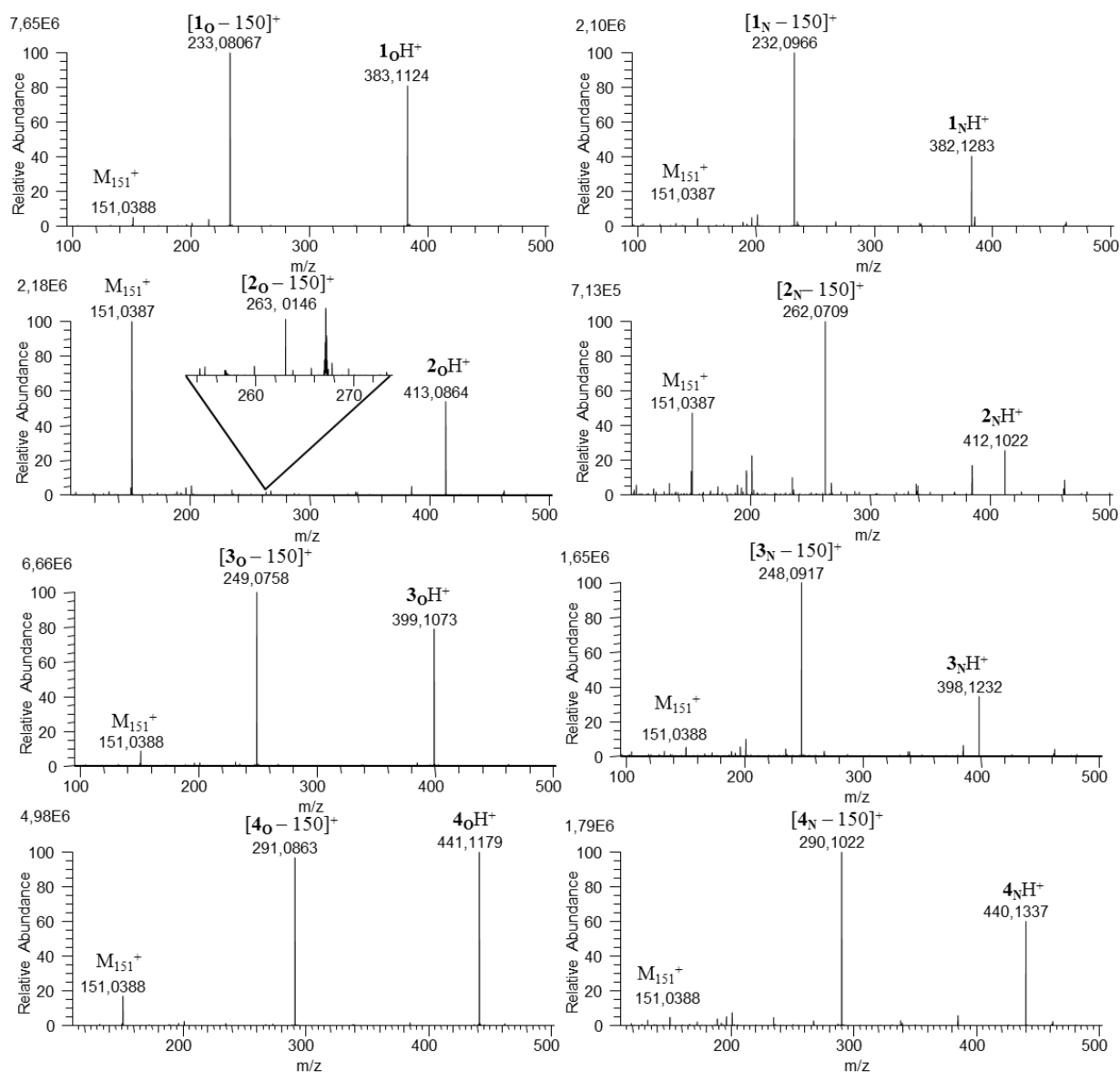


Figure 56 CID spectra of mitorubrins and mitorubramines (normalized collision energy, 22 %; 1_0H^+ -mitorubrin, 2_0H^+ -mitorubrinic acid, 3_0H^+ -mitorubrinol, 4_0H^+ -mitorubrinol acetate, 1_NH^+ -mitorubramin, 2_NH^+ -mitorubraminic acid, 3_NH^+ -mitorubraminol, 4_NH^+ -mitorubraminol acetate)

Fragmentations of protonated mitorubrins and mitorubramines occur *via* stepwise mechanism, involving the formation of initial ion-dipole complex, which is consisted of orselinyl ion and a hetero bicyclic system, where the intra-complex proton transfer can take place. Extensive studies have shown that species consisted of cation and neutral which are held together by ion-dipole attractive forces frequently play an important role in the chemistry of isolated ions.[179-181] From such complexes, often two ions are formed in the competitive processes through the internal proton transfer. The complex may either fragment to form carbonyl cation and release a hetero bicyclic neutral, or can release the orselinyl neutral and form the protonated hetero bicyclic ion. Proposed mechanism of fragmentation of protonated mitorubrins and mitorubramines is presented at **Figure 57**. According to their relative PA values, two possible neutrals are complementary present in the complex. In fact, α,β -unsaturated keton can remove proton to the protonated like-methylene quinone ion and reversely.

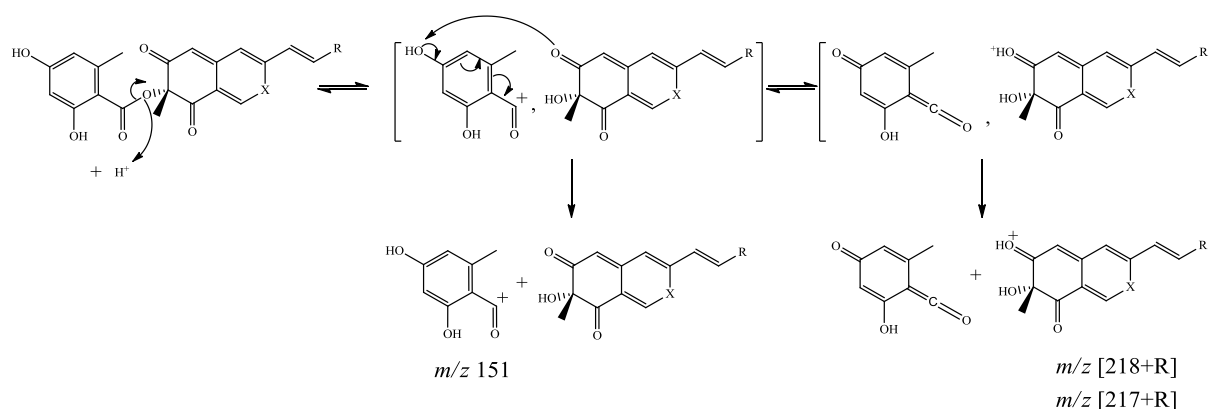


Figure 57 Proposed mechanism of fragmentation of protonated mitorubrins and mitorubramines during the CID of normalized collision energy of 15 %; X = -O or -NH.

For all protonated mitorubrins and mitorubramines subjected to the resonant CID, a common ion at m/z 151 is observed. This ion corresponds to the orselinyl ion, which is released from the ion-dipole complex by a simple cleavage. Its formation occurs by stepwise process *via* isomerization of protonated molecules into an ion-dipole complex [182], as given in **Figure 57**. Another ion that can be released from this ion-dipole complex is yielded after the proton transfer from the p -hydroxyl group of

orselinylium ion to the carbonyl group of bicyclic system, forming a new ion-dipole complex consisting of orselinylium neutral and protonated hetero bicyclic system. This process is favored by the electron delocalization through the whole carbonyl (orselinylium) system. As products, protonated mitorubrin hetero bicyclic ions are observed in the mass spectra and their m/z values differ due to different side chains. We have signed them as m/z [218+R] where R is concerned to the side chain. The same results are obtained from mitorubramines which we have signed as m/z [217+R] ion. The m/z values displayed in CID spectra are presented at **Table 13**.

The relative abundances of the complementary m/z 151 and m/z [218+R] (or m/z [217+R] for nitrogenized analogues) product ions vary accordingly to the side chain group. Constantly, the common m/z 151 ions are characterized by a very low abundance (except for 2_{O}H^+ and 2_{N}H^+). In general, protonated mitorubramines yield stronger fragmentations than protonated mitorubrins. Note that in the case of protonated mitorubrinic acid (m/z 413), the abundance of m/z 151 is higher than that of the complementary m/z [218+R] product ion (m/z 263). This can be explained by the electron withdrawing effect of the conjugate carboxylic group of the side chain, that can diminish the proton affinity of the oxygen $\text{O}_{(5)}$. The formation of the common m/z 151 ion is thus strongly favored, rather than the m/z 263 or m/z 262 product ions. In case of protonated mitorubrinic acid nitrogenized analogue (m/z 412), this effect is decreased with the mesomeric effect assistance of nitrogen atom at $\text{N}_{(7)}$. Consequently, the complementary m/z 262 and m/z 151 fragment ions appear in more comparable abundances. The abundance ratio of observed peaks in CID spectra is mostly rationalized in the terms of equilibration between the ion-dipole complexes proposed as isomeric intermediates in the fragmentation of protonated molecules.

4.3.2 Sequential MS³ experiments of bicyclical product ions

4.3.2.1 Differences in behaviour of mitorubrins and mitorubramines

As protonated mitorubrins and mitorubramines gave quite similar CID spectra and exhibited the same mechanism of fragmentation, this experiment was not sufficient for complete structural elucidation of mitorubramines, though the accurate mass measurements gave the exact masses that correspond to those of the protonated mitorubramines and CID experiments gave first information about their structures.

4.3.2.2 Main product ions

To obtain more informative data for the structural elucidation, sequential MS³ experiments have been performed on the all product ions observed from the protonated molecules (m/z 151, m/z [217 + R] and m/z [218 +R] ions). The characteristic bicyclic product ions which distinguish the mitorubrins and mitorubramins, meaning m/z [218+R] and m/z [217+R] respectively have been mass selected and submitted to collisions with helium in the 2D ion trap of tandem LTQ-Orbitrap, at 22 % of normalized collision energy, meaning the 1.1 V_{p-p} for resonance excitation amplitude. The obtained spectra are presented in the **Figure 58** and obtained product ions are listed in the **Table 13**.

Table 13 Displayed main product ions in CID spectra of selected product ions generated from the [M+H]⁺ precursors

Selected protonated ions [M+H] ⁺	<i>m/z</i> of selected ions	Accurate elemental composition	Obtained product ions	Accuate elemental composition	Error (ppm)
Mitorubraminol	248.09152	C ₁₃ H ₁₄ O ₄ N	230.08104	C ₁₃ H ₁₂ O ₃ N	-0.6
			206.08125	C ₁₁ H ₁₂ O ₃ N	-0.4
			204.10193	C ₁₂ H ₁₄ O ₂ N	-0.1
			202.08629	C ₁₂ H ₁₂ O ₂ N	-0.2
Mitorubraminic acid	262.07080	C ₁₃ H ₁₂ O ₅ N	244.06018	C ₁₃ H ₁₀ O ₄ N	-1.1
			220.06011	C ₁₁ H ₁₀ O ₄ N	-1.5
			219.05226	C ₁₁ H ₉ O ₄ N	-1.6
			218.08072	C ₁₂ H ₁₂ O ₃ N	-2.1
			216.06504	C ₁₂ H ₁₀ O ₃ N	-2.2
Mitorubramine	232.09689	C ₁₃ H ₁₄ O ₃ N	214.05726	C ₁₃ H ₁₂ O ₂ N	-0.1
			190.08656	C ₁₁ H ₁₂ O ₂ N	-2.5
			189.07875	C ₁₁ H ₁₁ O ₂ N	-2.4
			188.10745	C ₁₂ H ₁₄ ON	2.3
			186.09177	C ₁₂ H ₁₂ ON	2.1
Mitorubraminol acetate	290.10272	C ₁₅ H ₁₆ O ₅ N	272.09188	C ₁₅ H ₁₄ O ₄ N	0.8
			248.08984	C ₁₃ H ₁₄ O ₄ N	-0.8
			247.07837	C ₁₃ H ₁₃ O ₄ N	-1
			246.10913	C ₁₄ H ₁₆ O ₃ N	-13.57
			244.09833	C ₁₄ H ₁₄ O ₃ N	6.19
Mitorubrinol	249.07581	C ₁₃ H ₁₃ O ₅	231.06521	C ₁₃ H ₁₁ O ₄	0.1
Mitorubrinic acid	263.009128	C ₁₃ H ₁₁ O ₆	245.08059	C ₁₃ H ₉ O ₅	-0.9
Mitorubrinol acetate	291.08649	C ₁₅ H ₁₅ O ₆	273.07583	C ₁₅ H ₁₃ O ₅	-0.3
			231.06537	C ₁₃ H ₁₁ O ₄	-0.8
Mitorubrin	233.08086	C ₁₃ H ₁₃ O ₄	215.07019	C ₁₃ H ₁₁ O ₃	-0.4

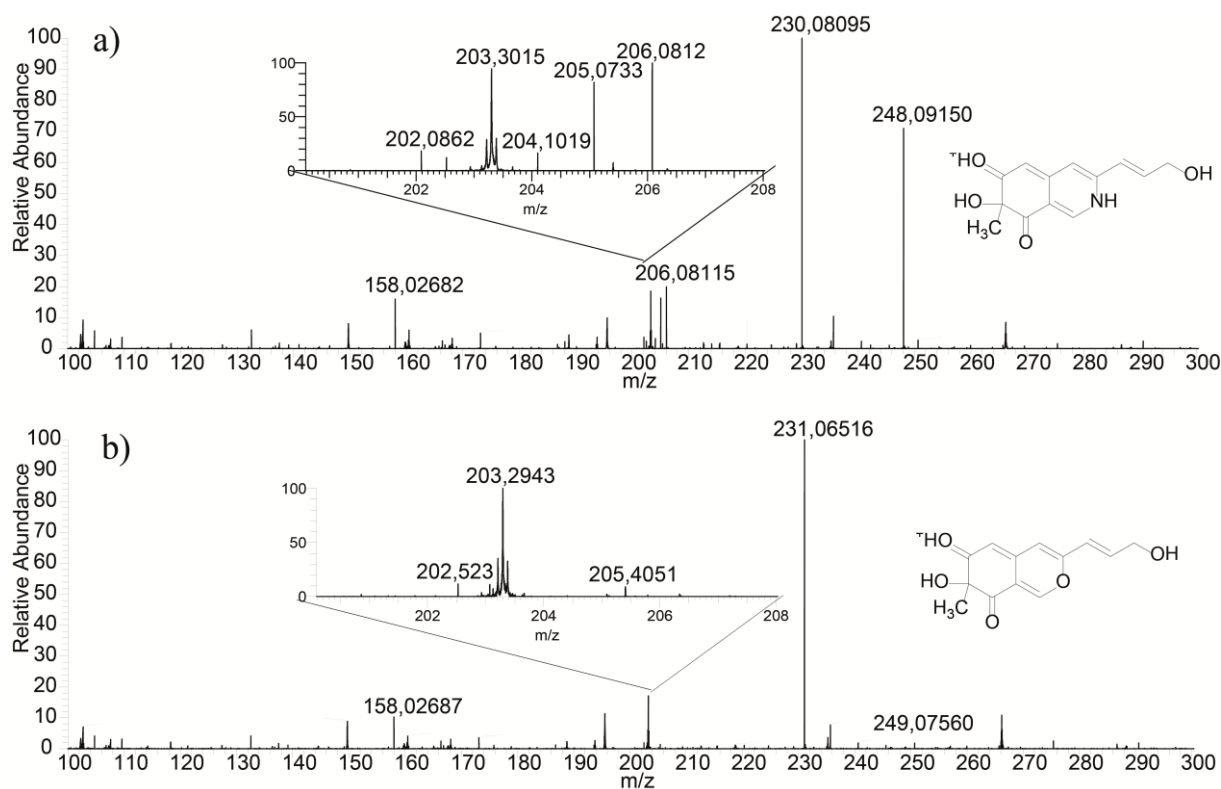


Figure 58 Sequential CID spectra of product ions from protonated a) mitorubrinol and b) mitorubraminol; (normalized collision energy, 22%)

➤ *Ring contraction and a water loss as assumed release*

CID spectra of sequential MS³ experiments of the [217+R]⁺ ions of mitorubramines are significantly different compared to the ones of mitorubrin azaphilones (i.e., [218+R]⁺ ions). For all analyzed ions, both mitorubrins and mitorubramines, in the sequential MS³ experiment, a main and common loss of water molecule was observed. The fragmentation mechanism of the water release is presented at **Figure 59**. The loss of water can be expected, since protonation happens at the hydroxyl di-keto ring due to the highest proton affinity of the keto site. Indeed, the nitrogen atom of the heterocyclic moiety in the mitorubramines (or oxygen atom in the mitorubrins) is characterized by the lower PA than the oxygen atom. The protonation of keto group can result due to the proton transfer to the vicinal hydroxyl group, inducing the water release in spite of the endothermic proton transfer. Furthermore, the water loss is assisted by ring contraction, whereby the more stable carbocation is attained.

Indeed, the ring contraction results from the vicinal carbocation, which is stabilized by the proton migration to the keton to produce regenerated keton, stabilized by long distance delocalization from nitrogen atom. Furthermore, the reaction can be directed by the two keto groups in competition, giving the isomeric product (**Figure 59, a)** and **b)**).

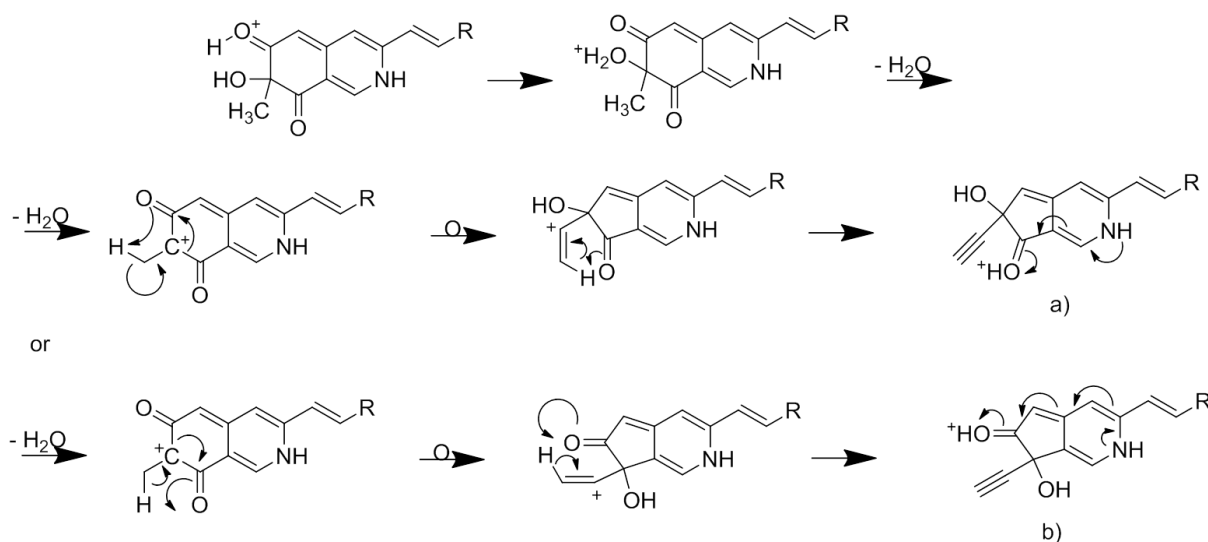


Figure 59 Proposed mechanism for the water loss from bicyclic product ion from mitorubraminol

4.3.2.3 Formation of diagnostic product ions

In the high resolution sequential MS³ spectra of protonated mitorubramines, additional peaks were observed, suggesting quite complicate fragmentation pathways, favored by the presence of nitrogen atom. These ions are: m/z 214, m/z 190, m/z 189, m/z 188 and m/z 186 for mitorubramin, m/z 230, m/z 206, m/z 205, m/z 204 and m/z 202 for mitorubraminol, m/z 244, m/z 220, m/z 219, m/z 218 and m/z 216 for mitorubraminic acid and m/z 272, m/z 248, m/z 247, m/z 246 and m/z 244 for mitorubraminol acetate (**Table 13**). These ions correspond to fragment ions obtained by the losses of 42, 43, 44 and 46 Da, respectively, which is referred to the losses of C₂H₂O, C₂H₃O, CO₂ and HCOOH, thanks to high resolution measurements. Accordingly to the proposed fragmentation pathways, losses of CH₂CO and CH₃CO^o radical are competitive processes, as well as the losses of CO₂ and HCOOH.

➤ *Ring contraction and ketene neutral and acetyl radical losses*

Losses of CH_2CO and $\text{CH}_3\text{CO}^\circ$ radical and mechanism of $[(217+\text{R})-\text{C}_2\text{H}_2\text{O}]^+$ and $[(217+\text{R})-\text{C}_2\text{H}_3\text{O}]^{+\circ}$ ions formation is presented on **Figure 60**. These losses are competitive releases, and they could be promoted by the ring contraction, which is referred to the losses of 42 and 43 u, respectively. Instead of proton or hydroxyl group migration, 1,2-migration of a carbonyl site occurs, like in Wagner-Meerwein rearrangement. [183, 184] This process is assisted by electron lone-pair migration from hydroxyl group to the opened C-CO bond. The produced cyclopentenone system can isomerizes into protonated cyclopentenone system (**Figure 60 a**)), allowing formation of ion-dipole complex (**Figure 60 b**)) induced by acetyl bond cleavage. The formed ion-dipole complex is constituted of the alkyl cyclopenta-pyridine-6,7-diol and an acylium moiety. From this intermediate, two competitive pathways occur further. By direct internal proton transfer from acylium moiety to bicyclic system, a ketene (*i.e.* 42 u) is released giving rise to formation of protonated alkyl cyclopenta-pyridine-6,7-diol. Competitively, electron transfer from tetraenic system to acylium moiety occurs, giving $\text{CH}_3\text{CO}^\circ$ radical release (*i.e.*, loss of 43 u), and formation of odd-electron alkyl cyclopenta-pyridine-6,7-diol.

Formation of ion-dipole complex and proton transfer from acylium to heterocyclic nitrogen, can give losses of CH_2CO and $\text{CH}_3\text{CO}^\circ$ radical. However, this process cannot occur in mitorubrin azaphilones. In addition, electron transfer is known to take place specifically in heterocyclic systems with nitrogen, rather than with oxygen. For all these reasons, the multi decomposition pathways observed for mitorubramines, cannot take place for mitorubrins.

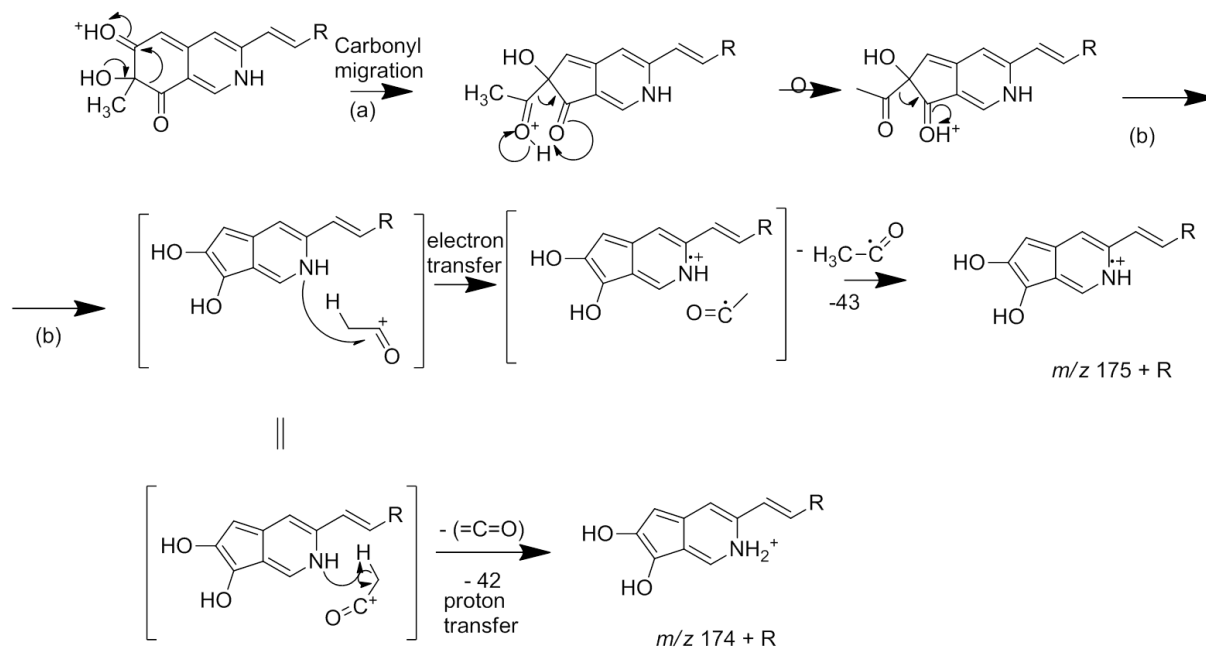


Figure 60 Proposed mechanism for the losses of keten and methoxy radical from the bicyclic product ion from mitorubraminol

➤ *Ring contraction for the CO₂ and HCOOH releases*

Losses of CO₂ and HCOOH are competitive processes independent of CH₂CO and CH₃CO[•] radical releases pathways, giving the formation of [(217+R)-CO₂]⁺ and [(217+R)-HCOOH]⁺ ions. The assumed fragmentation and formation of these neutral species is presented on **Figure 61**. First, 1,2-hydroxy group migration induced by the protonated ketone yield as a geminated diol and tertiary carbocation. The latter is stabilized by a 1,2-hydride transfer with the ring opening.[185, 186] This pathway yields unsaturated carboxylic acid linked to monocyclic cation. The charge migration can lead to the formation of *p*-ethanolic pyridinium species. This form is able to generate ion-dipole complex by benzyl bond cleavage induced through the charge migration. This ion-dipole complex is constituted of protonated carbon dioxide and the heterocyclic system. Internal proton transfer from CO₂H⁺ to nitrogen of heterocyclic system initiates elimination of neutral - carbon dioxide (e.g. loss of 44 u) yielding the m/z [188 + R] ion. Reversely, hydride transfer from the NH site of heterocyclic system to the protonated carbon dioxide results into the release of formic acid (e.g. loss of 46 u) and detection of m/z [171 + R].

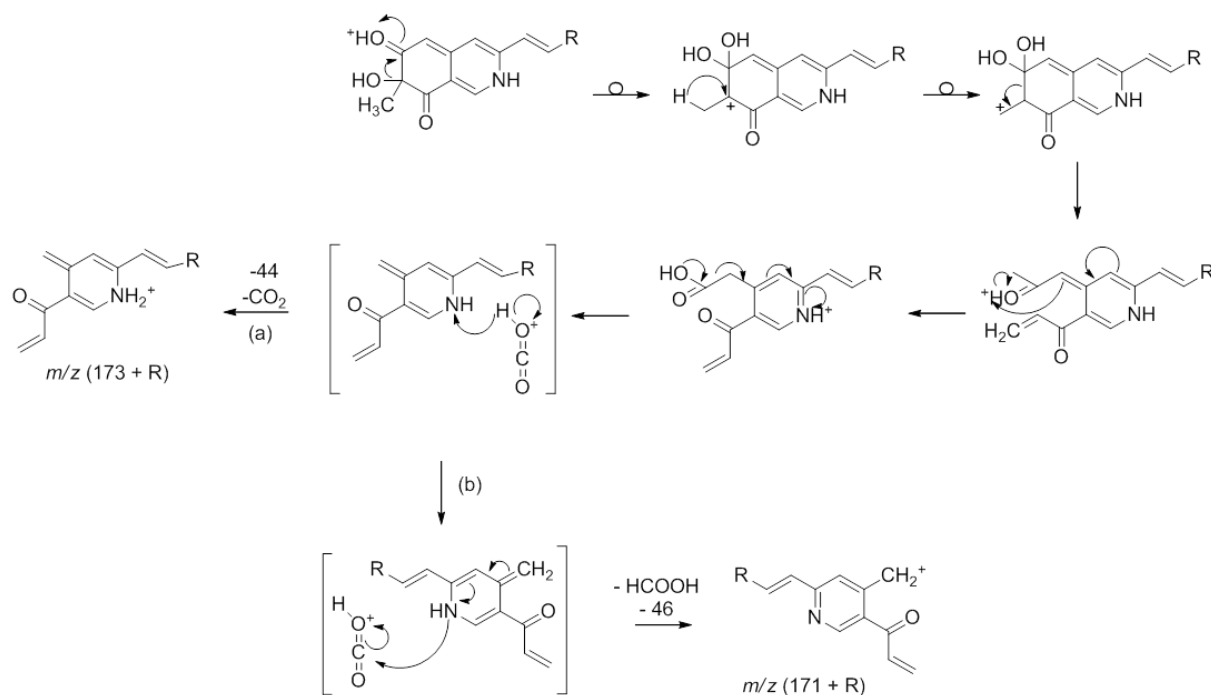


Figure 61 Proposed mechanism of losses of formic acid and carbon dioxide from bicyclic product ion from mitorubraminol

Isomerization is possible for both mitorubrins and mitorubramines, but only the later ones can assist the proton transfer from exocyclic carbon to α -carbon, because of the presence of lone-pair on nitrogen atom. Positively charged nitrogen, promotes the allylic bond cleavage. Ion-dipole complex formed by this way can directly release carbon dioxide, not possible from mitorubrins.

Dissociations displayed at **Figures 59** and **60** are specific for the mitorubramines. This gives us unambiguous results about the structure and presence of these molecules in the crude extract of *Hypoxylon fragiforme*. The diagnostic fragmentations are of a crucial importance for structural identification of vinylogous 4-pyridone derivatives-mitorubramines, and to establish the exact position of nitrogen in the molecule as well, but also for their structural distinction from the oxygen containing analogues.

4.4 Gas-phase H/D exchange for structural elucidation

To analyze structurally these derivatives more accurately, gas phase H/D exchange mass spectrometry was performed in the collision cell of a modified triple quadrupole. Approach was performed by H/D exchange reaction on the mass selected ions under the low-energy gas phase collisions ($E_{\text{lab}} < 3\text{eV}$) with the suitable mobile deuterium containing reagent. Mass selection is an efficient approach because it eliminates the interference of the natural isotopic ions and consequently the isotopic ratio of exchanged species is more accurate. For determination of labile protons of N-containing and natural azaphilones, after LC separation and ionization, parent ions are isolated in the first mass filter of triple quadrupole and let to collide with introduced ND_3 in the collision cell. Then, the exchanged ions can be detected in the second quadrupole. In the ion source, fragment ions were analyzed in the same manner. Kinetic energy of ions is lowered. In fact, ion-molecule reactions occur. To perform such experiment, the kinetic energy of the ion must be decreased to allow the production of the ion-neutral complex. This means that kinetic energy (E_{lab}) must be lower than few eV. E_{lab} values correspond to the potential difference between the source and collision cell. Generally, the potential of Q2 (RF-only) quadrupole is lower than that of first quadrupole filter (Q1). Herein, the potential of the collision cell is relatively higher than that of Q1. Under such collision conditions, ion-molecule reactions occur instead of CID. Such processes are called collision induced reactions (CAR). Under these conditions, H/D exchange between ion and ND_3 become possible.

Table 14 Proton affinities for different reagent used in gas phase H/D exchange ion-molecule reactions

Molecule	Proton affinity (kcal/mol)
H_2O (D_2O)	165.1
NH_3 (ND_3)	204.1
CH_3OH (CH_3OD)	180.2
$\text{C}_2\text{H}_5\text{OH}$ ($\text{C}_2\text{H}_5\text{OD}$)	185.5
<i>i</i> - $\text{C}_3\text{H}_7\text{OH}$ (<i>i</i> - $\text{C}_3\text{H}_7\text{OD}$)	189.5

The ND₃ has been chosen as the reagent gas because of its high PA and thus ability to exchange the most of the labile protons in the analyzed molecule (**Table 14**). Beside the fact that in the gas phase, in reactions with different D-containing reagents chemical properties can be achieved, there are other advantages of such technique performed in the gas phase. Thus, selective gas-phase chemistry can be investigated in order to enlighten particular reactivity as well as for the elucidation molecular structures. For the structural elucidation, H/D exchange is used in particular to reach conformation which allows or not the exchange by reaching the endothermic or exothermic barrier. The possibility of the interaction between two basic sites can allow activation energy to decrease, which depends on the relative basicity of exchangeable site and the label neutral. Furthermore, mass selection of ion before the reaction with labeled reagent enables the elimination of the interferences. In fact, after the isolation of mass selected ion, this is unique species of ions that will further react with a reagent. In this way, it is certain that isotopic peaks are not included in the yield of H/D exchange reaction, since they were ejected from the trap before the ion-molecule reaction.

4.4.1 Gas-phase H/D exchange of protonated mitorubins and mitorubramines in collision cell

Gas-phase H/D exchange reactions have further been performed in a collision cell of triple quadrupole instrument under very low collision energy conditions ($E_{\text{lab}} = 3$ eV). Precursor ions were isolated in the first mass filter of triple quadrupole and have undergone reactive collisions with a labeled reagent gas. ND₃ was chosen as a gas-phase labeled reagent because of its relatively high PA (204 kcal/mol) and is thus expected to exchange most of the labile protons. The obtained CAR spectra are presented in **Figure 62**.

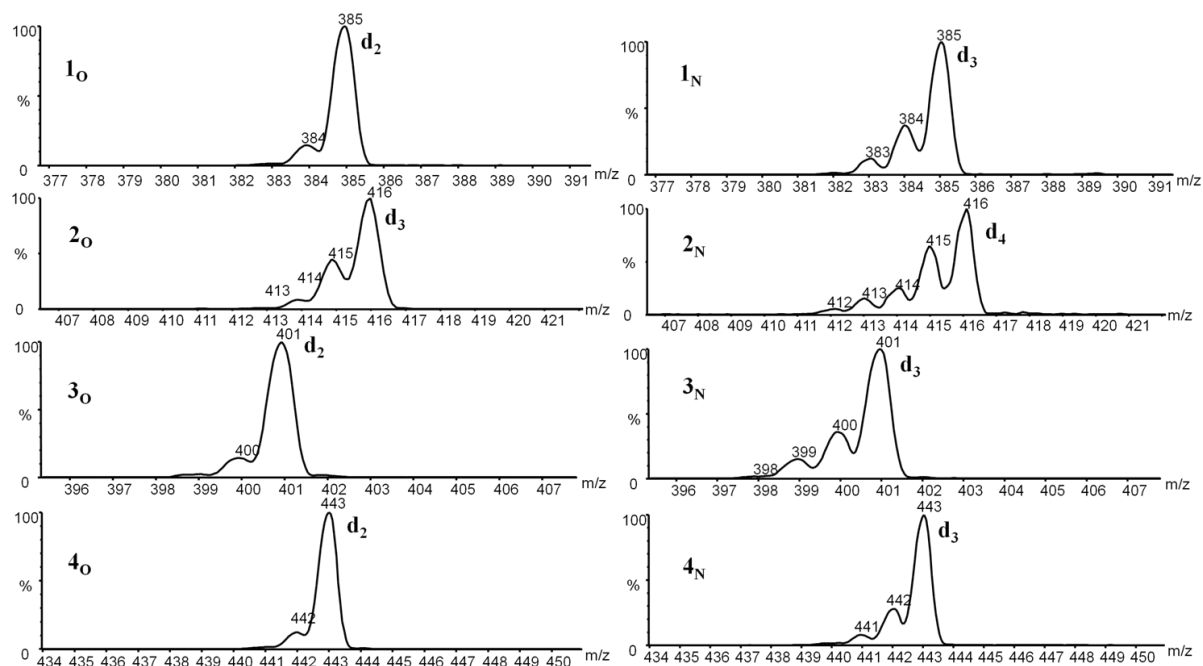


Figure 62 CAR spectra of gas-phase exchange of mitorubins ($X_O = 1_O, 2_O, 3_O, 4_O$) and mitorubramines ($X_N = 1_N, 2_N, 3_N, 4_N$); $E_{lab} = 3$ eV

Expected exchangeable protons on protonated mitorubins (X_O) (**Figure 63**) are (i) the one of protonation (position $O_{(4)}$), (ii) those positioned on the $O_{(1)}$ and $O_{(2)}$ atoms and eventually (iii) on the R group. This makes thus at least three protons to be exchanged. Concerning mitorubramines, four protons should be at least exchanged as the compounds possess, in addition, a secondary amine unit with a labile proton. Quite unexpectedly, precursor ions of all compounds show a number of exchanged protons lower by one than what was expected. Thus, only two protons are exchanged on protonated mitorubins 1_OH^+ , 3_OH^+ and 4_OH^+ although three were thought to be exchangeable and three are exchanged on 2_OH^+ with four expected. Furthermore, as expected, nitrogenized mitorubins (X_N) did exchange one more proton than corresponding oxygenated derivatives.

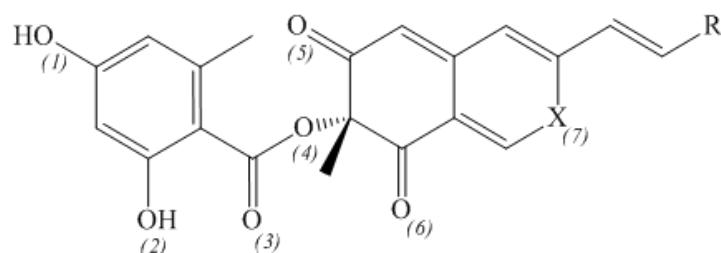


Figure 63 Sites of mitorubins and mitorubramines where the H/D exchange is possible

Complementary $[M_{OH-150}]^+$ and $[M_{NH-150}]^+$, and common orsellinic part (m/z 151) fragment ions formed in source have been studied in gas-phase H/D exchange CAR experiments, under the same condition used previously. Hence, they were isolated in the first mass filter of triple quadrupole and have undergone the very low energy reactive collision with ND_3 in the collision cell. The obtained CAR spectra are presented in **Figure 64**.

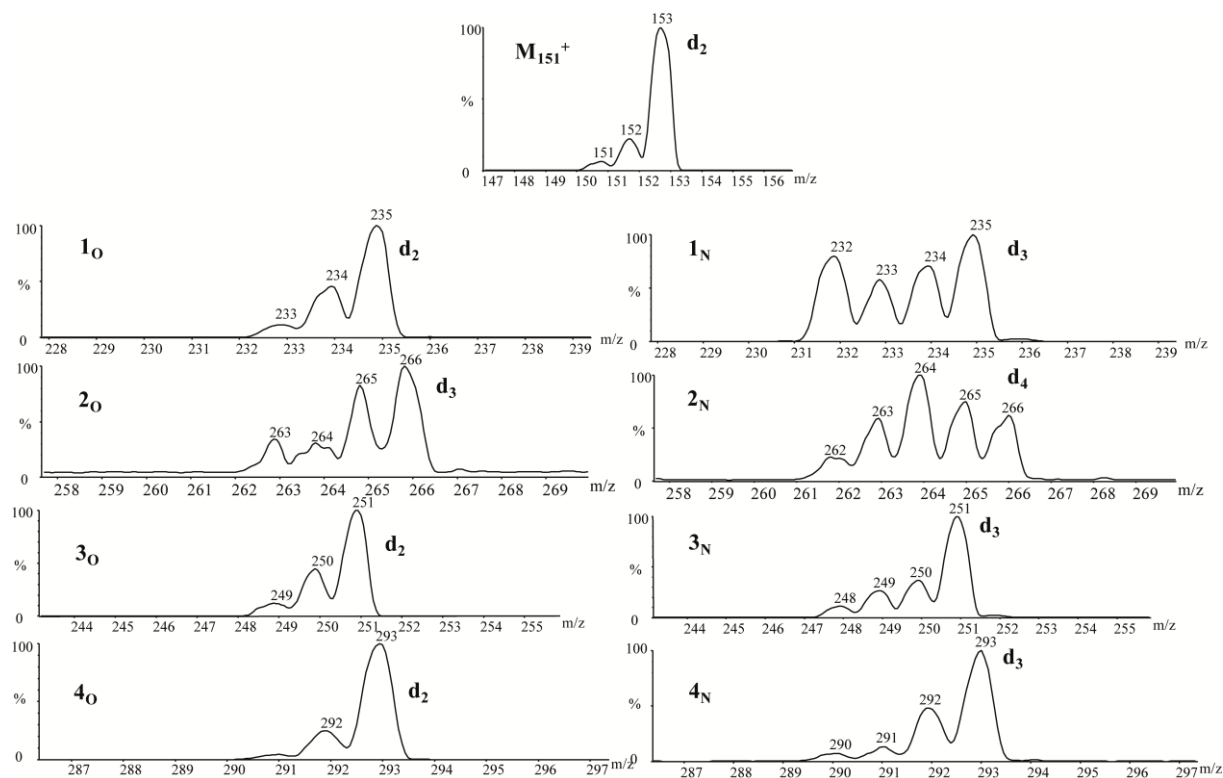


Figure 64 Gas phase H/D exchanges from CAR spectra ($E_{lab} = 3$ eV) of fragment m/z 151 (M_{151}^+) and $[MH-(150)]^+$ ions from protonated mitorubrins (X_O) and nitrogenized derivatives (X_N)

In the bicyclic fragment ion of mitorubrin azaphilones, at least two sites with labile protons are present, at the $O_{(4)}$ and $O_{(5)}$ positions after the rearrangement during the fragmentation processes, whereas for the nitrogenized analogues there is also an $N_{(7)}$ site with the labile proton that could be exchanged. Thus, 1_{OH}^+ , 3_{OH}^+ and 4_{OH}^+ exchange two protons by deuterons, while 2_{OH}^+ exchanges three. Concerning nitrogenized analogues, fragment ions of 1_{NH}^+ , 3_{NH}^+ and 4_{NH}^+ exchange three protons by deuterium, while 2_{NH}^+ exchanges four. Hence, no side chain H/D exchange happens at $R = CH_3$, CH_2OH and CH_2OCOCH_3 , but for $R=COOH$, one H/D exchange takes place.

On the other hand, orsellinic part ion (m/z 151) exchanges two protons by deuterium at the $O_{(1)}$ and $O_{(2)}$ positions, which can be referred to the $O_{(a)}$ and $O_{(b)}$ positions of the model system. This suggest that the protonated molecule isomerization into ion-dipole complex does not occur prior to CID processes since, if it is the case, additional H/D exchanges could be expected through three body complex formation.

The question is: which one of the protons does not succumb to the exchange and why? These questions got an answer by theoretical calculations.

4.4.2 Theoretical calculations and a model system

To understand these unexpected features, we have undertaken a theoretical study on a model system shown in **Figure 65**. The density functional theory (DFT) is the approach to calculate the electronic structure of many-body systems as atoms, molecules, and the condensed phases. DFT provides the ground state properties of a system, which are completely determined by the charge density. DTF predicts a variety of molecular properties molecular structures, vibrational frequencies, ionization energies, atomization energies, reaction paths, etc. DTF is often used to properly describe intermolecular interactions, especially van der Waals forces (dispersion); charge transfer excitations; transition states etc.[187] In many cases the results of DFT calculations for solid-state systems agree quite satisfactorily with experimental data.

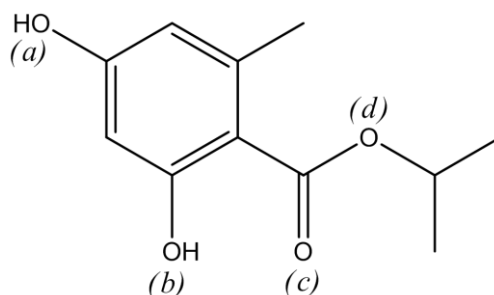


Figure 65 Structure of model system (MS) used for the theoretical explanation of gas-phase H/D exchange of mitorubins and mitorubramines

A propyl orselylate was used as a model system (*MS*) and contains only the orsellinic part of the mitorubins. There was indeed no need to consider the bicyclic azaphilone core of the compounds as gas phase H/D exchanges taking place on this side of the molecule concern either the R group or the amine in the case of the nitrogenized analogues.

MS has been chosen with an isopropyl ester form because it possesses similar PA values of its $O_{(a)}$, $O_{(c)}$ and $O_{(d)}$ sites (**Figure 65**) as on the $O_{(1)}$, $O_{(3)}$ and $O_{(4)}$ sites (**Figure 63**) of mitorubins and nitrogenized analogues (respectively, 182.6, 225.1 and 215.7 kcal/mol to be compared with the PA values given in **Table 15**). It may be noticed that PA values were defined for each oxygen (and nitrogen) atom of the molecule except for $O_{(2)}$ because calculations showed that protonation at this site leads to a prompt proton transfer to the $O_{(3)}$ atom.

Table 15 Calculated proton affinities of different sites of mitorubins (1_O) and mitorubramines (1_N)

Site	Proton affinities (kcal/mol)	
	1_O	1_N
$O_{(1)}$	182.6	184.7
$O_{(3)}$	225.1	239.2
$O_{(4)}$	213.8 ^a	214.1 ^a
$O_{(5)}$	231.9	238.5
$O_{(6)}$	215.7	217.8
$O_{(7)}$ or $N_{(7)}$	167.2	188.7

^aOn the $O_{(4)}$ site, protonation results in the formation of an ion-dipole complex.

4.4.3 *Explanation of gas-phase H/D exchange of mitorubrins and mitorubramines*

No protons are exchanged at the side chain of mitorubrin ($R = \text{CH}_3$) or mitorubrinol acetate ($\text{CH}_2\text{OCOCH}_3$) because these groups do not contain labile protons. For mitorubrinic acid, one proton is exchanged as expected, on the hydroxyl group of the side chain carboxyl group ($R = \text{COOH}$). In the case of mitorubrinol, it could be expected that one proton would be exchanged on the side chain allylic hydroxyl group ($R = \text{CH}_2\text{OH}$). Still, in this position no exchanges happen. Earlier was described the mechanism by which H/D exchange in the gas-phase occurs (refer to General part, 4.3.3) and that it depends on the energy of the transition state (TS) which is conducted by the PAs of reacting compounds. The behavior of each protonated form describes the reaction of the $[\text{MSH}^+, \text{ND}_3]$ complex within a protonated canonic structure when

- (i) the ionizing proton is exchanged, or
- (ii) in the case of relay mechanism.

However, zwitterion-like form could be involved into this complex, meaning the $[(\text{MS-H})\text{-H}^+, \text{NHD}_3^+]$ structure. In this case, the transferred proton to ND_3 comes from the $\text{O}_{(a)}\text{H}$ site to give rise to formation of salt-bridge complex, in which the ionizing proton at the ester site is spectator. From such an ion-dipole complex, H/D exchange can take place in the salt-bridge position. This can occur only if the formation of the complex requires relative low TS. This situation does not characterize the calculated transition state with $\text{O}_{(a)}$, since it appears slightly endothermic (**Table 16**), and rules out such salt-bridge intermediate (**Figure 66 a**). On the other hand, as protonation takes place during ESI, at this position, due to the presence of water from eluting solvents, within the protonated canonic form, then the H/D exchange is hindered, because of the too weak PA value of the $-\text{OH}$ site (184.7 kcal/mol) comparing to that of ND_3 . The deuteron attachment to this position is thus too much endothermic.

Table 16 Relative energies (in kcal/mol) of the ions, complexes and transitions structures involved in the H/D exchange process between MSH^+ and ND_3

Site	$MS_HH^+ + ND_3$	$[MS_HH^+, ND_3]$	$TS_{H/D}$	$[MS_H, NHD_3^+]$	$TS_{H/D}$	$[MS_DH^+, ND_2H]$	$MS_DH^+ + ND_2H$
$O_{(a)}$	0.0	-16.0	0.3	-9.4	0.3	-16.0	-0.1
$O_{(b)}$	0.0 ^a	-19.7	-8.9	-16.2	-8.9	-19.7	-0.1
	$MS_HH^+ + N$ D_3	$[MS_HH^+, ND_3]$	$TS_{H/D}$	$[MS_H, NHD_3^+]$	$TS_{H/D}$	$[MS_HD^+, NH_2D]$	$MS_HD^+ + NH_2D$
$O_{(c)}$	0.0	-4.9	-11.0	-16.2	-11.0	-4.9	-0.1

Theoretical results obtained for the gas phase H/D exchange reaction on the three possible oxygen atoms, $O_{(a)}$, $O_{(b)}$ and $O_{(c)}$, of the protonated model system, MSH^+ are presented in **Table 16**. For each reaction (which will be further termed accordingly to the name of the oxygen atom, *i.e.* reaction a), b) or c)) energies are given relatively to the starting system ($MSH^+ + ND_3$). Formation of the ion-dipole $[MSH^+, ND_3]$ complex as a solvation step allows isomerization of the complex into the $[MS, NHD_3^+]$, which is an exothermic process for these pathways but releases more energy in the case of b) and c) (up to 16.2 kcal/mol for b) and c) pathways in comparison to -9.4 kcal/mol for a) pathway). Then, the transition states, $TS_{H/D}$, which structures are presented at the **Figure 66**, are located at -8.9 and -11.0 kcal/mol under the starting system for the b) and c) paths, respectively, in contrast to +0.3 kcal/mol above the entrance system for path a). Furthermore, as the barriers for the reactions b) and c) are crossed over, $[MS_DH^+, ND_2H]$ and $[MS_HD^+, ND_2H]$ complexes are formed competitively with releasing the exchanged MS_DH^+ and MS_HD^+ , respectively. Transition state of the reaction b) leads to the H/D exchange, because this process occurs with assistance of the ionizing proton interaction from the $O_{(c)}$ site, through the hydrogen bond to the $O_{(b)}$ site, process impossible in the case of the $O_{(a)}$. Thus, these results show that the exchange is exclusively favorable at the $O_{(b)}$ and $O_{(c)}$ sites but not on $O_{(a)}$. With the help of this model system, we can therefore understand processes which have been taking place in the reaction of protonated mitorubins and analogues with ND_3 and, why one proton less as expected is exchanged on the systems under study.

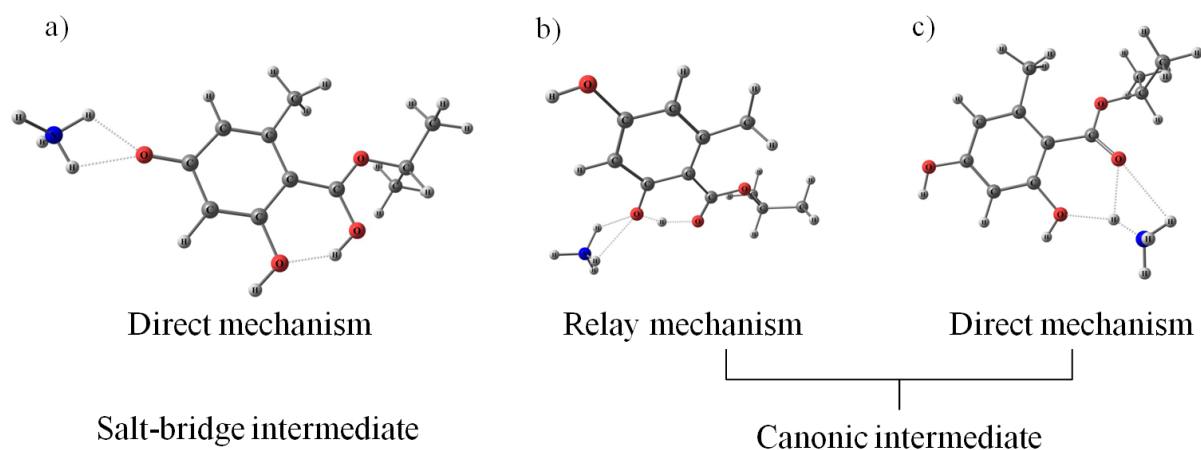


Figure 66 Transition states for the H/D exchanges between MSH^+ and ND_3 occurring on the sites a) $O_{(a)}$, b) $O_{(b)}$ and c) $O_{(c)}$ of model system MS .

Theoretical results obtained for the gas phase H/D exchange reaction of orsellinic acid fragment ion at m/z 151 are presented at **Table 17**.

Table 17 Relative energies (in kcal/mol) of the ions, complexes and transitions structures involved in the gas-phase H/D exchange process between m/z 151 (M_{151}^+) and ND_3 on three different sites

Site	$151^+ + ND_3$	$[151^+, ND_3]$	$TS_{H/D}$	$[152^+, NHD_2]$	$152^+ + NHD_2$
$O_{(a)}$	0.0	-20.9	-8.0	-20.9	-0.2
$O_{(b)}$	0.0	-20.7	-8.6	-20.7	-0.2

For both reactions named (a) and (b) for the $O_{(a)}$ and $O_{(b)}$ sites respectively, formation of ion-dipole complex $[151^+, ND_3]$ is an exothermic process (-20.9 kcal/mol for (a) and -20.7 kcal/mol for (b)) relatively to the starting system ($151^+ + ND_3$). The release of energy during the H/D exchange in (a) is quite the same as in the case of (b) (-20.9 kcal/mol for (a) and -20.7 kcal/mol for (b)), and the transition state for both path are exothermic, -8.0 kcal/mol for (a) and -8.6 kcal/mol for (b). Relatively high transition state for this stepwise process is due to relatively high PA of neutral coming from m/z 151 acylium, which is presented on the **Figure 67**.

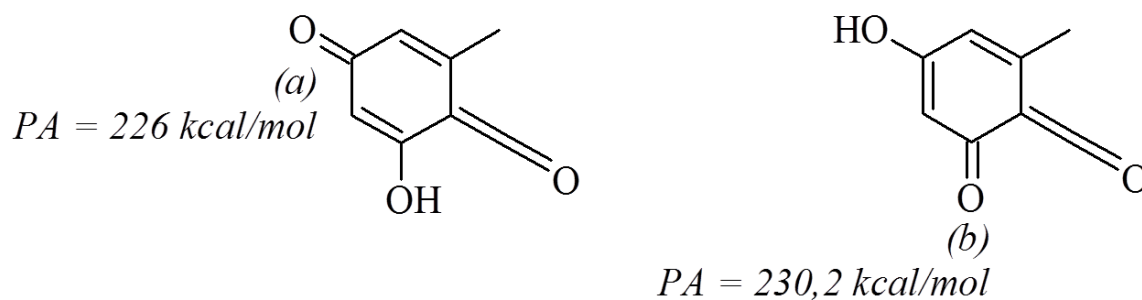


Figure 67 Structures of neutrals from m/z 151 and their PA

Indeed, the PAs of such neutrals with *p*- and *o*-quinone-like forms are higher than that of ND_3 , thus 226 kcal/mol and 230 kcal/mol, respectively, obtained by the calculations. This result explains the final exchange on both sites leading to the H/D exchange on $\text{O}_{(a)}$ and $\text{O}_{(b)}$. Though, in both reactions (a) and (b), no isomerization in a second complex has been detected. This is probably due to its high stability of the complexes, which results into a fast H/D exchange in a particular transition state only reached by calculations.

Conclusion

Identification of novel secondary metabolites has become a tendency during the last decades, simply because of the wide range of bioactivities that these small natural products exhibit. Fungal kingdom appears to be very rich and divers in area of secondary metabolites among of which some families are quite specific for this kingdom. Speaking of that, more and more novel azaphilones are identified. During this research, nitrogenized analogs of mitorubrins, mitorubramines have been identified in the *Hypoxylon fragiforme*, utilizing mass spectrometric approaches, meaning HRMS, CID with sequential MSⁿ experiments and gas-phase H/D exchange in CAR experiments.

ESI conditions in positive mode appears do not have such high influence on the detection of mitorubrins, and more important on their nitrogen containing analogues. Compounds with that kind of structures are relatively easily ionized under soft ionization/desorption conditions under atmospheric pressure, and their observation is facilitated thanks to their chemical properties (*i.e.*, basicity). It seems that ESI is an ionization method of choice for the formation of protonated mitorubramines and their further identification. The advantage of the experimental control of desolvation steps in API modes in a means to favor one of the examined families, mitorubrins versus mitorubramines. Skimer potential allows favoring the one type products without dissociation (“in-source CID”). This is based on the thermochemistry of protonation.

Use and advantage of HRMS is in our work was completely justified. With a mass accuracy of 2 ppm, and resolving power of 60 000, we have quite certainly obtained the elemental composition of protonated mitorubrins, but more important the elemental composition of protonated mitorubramines, and product ions observed in sequential CID. Supported by these powerful methods, we were able to determine new secondary metabolites, not found in nature before.

Sequential MSⁿ experiments, under CID conditions, give a large amount of information that can and is often used in the structural elucidation. In our work, MS²

experiment was not sufficient to determine the structures of novel secondary metabolites, because same decomposition pathways are involved for both the analyzed families. However, the MSⁿ approved its advantage. In the sequential MS³ experiments of protonated mitorubrins and mitorubramines, structural distinction have been obtained. The sequential CID of product ions gave the most important information about the structure of mitorubramines because of lot of competitive cleavage pathways. They enlighten the position of nitrogen atom in the protonated molecule, which is based on the original fragmentation pathways. Indeed, they involved unusual mechanisms, such as hydroxyl migration or ring contractions, giving the small neutral releases. In this case, nitrogen atom and its lone-pair are shown to play the main role, enabling in that way clear structural distinction between two very similar families of molecules, directly from the crude extract, applying just MS methods. The presence of nitrogen atom was very useful for true and relevant ally for the structural determination.

Gas-phase H/D exchange is a method widely used for structural elucidation of small and large molecules. In our case, this technique helped us to distinguish two families of molecules, basically counting the number of exchanged protons with deuterium ones. Disadvantage (or advantage in other cases of research) is that this method depends on the utilized deuterium reagent (and thus the reaction rate, too), and not complete exchange may occur. This is advantage when the method is used for determination of basicity of analyzed compounds in positive ionization mode. However, it may pose problem when the aim of the methods is counting the number of labile protons, when some protons may not be exchanged. In our research, we have obtained one less hydrogen atom exchanged than expected, but the results was comparable for the both families of analyzed compounds, and thus helped us to distinguish them and confirm the assumptions, *i.e.* dihydropyridine moiety rather than amide possibility. This approach is very pertinent for elucidation of novel azaphilone structures, not revealed before.

Perspectives

Many new ideas arise from this work. Some of them are listed below:

- a) Find new secondary metabolites as a contribution to the mycochemistry and pharmacy. Concerning the mycochemistry, these achievements can be of a great importance for further development of classification of fungi by chemotaxonomy.
- b) Concerning the pharmaceutical science, finding new secondary metabolites enriches and enlarges the possibilities of new drugs discoveries.
- c) Investigation of mitorubramines' bioactivities is a next step for determining of their purpose in the nature, as they have never before been examined in this manner.
- d) In conclusion, the HRMS and CID can be routinely applied for identification of new azaphilones in fungi and of their chemical structure.

References

1. Merzendorfer, H. and Zimoch L., *Chitin metabolism in insects: structure, function and regulation of chitin synthases and chitinases*. J Exp Biol, **2003**. 206: p. 4393-412.
2. S., M.R. and A.K. R, *An Introduction to Mycology*. New Age International Publishers (Google books http://books.google.fr/books?id=0iA2ytCR2IEC&printsec=frontcover&hl=fr&source=gs_bse_ge_summary_r&cad=0#v=onepage&q&f=false).
3. Lindahl, B.D., et al., *Spatial separation of litter decomposition and mycorrhizal nitrogen uptake in a boreal forest*. New Phytol, **2007**. 173(3): p. 611-20.
4. Barea, J.M., et al., *Microbial co-operation in the rhizosphere*. J Exp Bot, **2005**. 56(417): p. 1761-78.
5. Quang, D.N., Hashimoto T., Y. Asakawa, *Inedible mushrooms: a good source of biologically active substances*. Chem Rec, **2006**. 6(2): p. 79-99.
6. Frisvad, J., et al., *Mycotoxins, drugs and other extrolites produced by species in Penicillium subgenus Penicillium*. STUDIES IN MYCOLOGY, **2004**. 49: p. 201-241.
7. Guimaraes, D.O., et al., *Biological activities from extracts of endophytic fungi isolated from Viguiera arenaria and Tithonia diversifolia*. FEMS Immunol Med Microbiol, **2008**. 52(1): p. 134-44.
8. Dos Reis Vieira, F., et al., *Biological activities of the fermentation extract of the endophytic fungus Alfernaria alternata isolated from Coffea arabica L.* **2009**, 45.
9. Liu, J.K., *Secondary metabolites from higher fungi in China and their biological activity*. Drug Discov Ther, **2007**. 1(2): p. 94-103.
10. Hawksworth, D.L., *The fungal dimension of biodiversity: magnitude, significance, and conservation*. Mycol. Res., **1991**. 95(6): p. 641-655.
11. Whalley, A.J.S. and Edwards R.L., *The Xylariaceae: A Case Study in Biological and Chemical Diversity*. **1999**.
12. Hibbett, D.S., et al., *A higher-level phylogenetic classification of the Fungi*. Mycol Res, **2007**. 111(5): p. 509-47.
13. Kirk, P.M., et al., *Dictionary of the Fungi 10th ed*. Wallingford: CABI **2008**: p. 55.
14. Ju, Y.M. and Rogers J.D., *A Revision of the Genus Hypoxylon*. APS Press, **1996**.
15. Lonsdale, D., Pautasso M., Holdenrieder O., *Wood-decaying fungi in the forest: conservation needs and management options*. Eur. J. For. Res., **2008**. 127(1): p. 1-22.
16. Rossman, A.Y. and Palm-Hernandez M.E., *Systematics of Plant Pathogenic Fungi: Why It Matters*. Plant Dis., **2008**. 92(10): p. 1376-1386.
17. Tang, A.M.C., Jeewon R., Hyde K.D., *A re-evaluation of the evolutionary relationships within the Xylariaceae based on ribosomal and protein-coding gene sequences*. Fungal divers., **2009**. 34: p. 127-155.
18. Rogers, J.D., *Xylaria bulbosa, Xylaria curta, and Xylaria longipes in Continental United States*. Mycologia, **1983**. 75(3): p. 457-467.
19. Rogers D. J, *Xylaria cubensis and its anamorph Xylocoremium flabelliforme, Xylaria allantoides, and Xylaria poitei in continental United States*. Mycological Society of America, **1984**. 76.

20. Whalley, A.J.S. and Whalley M.A., *Stromal pigments and taxonomy of Hypoxylon*. Mycopathologia, **1977**. 61(2): p. 99-103.
21. Stadler, M., Fournier J., Granmo, A., Beltran-Tejera, E., *The "red Hypoxylons" of the Temperate and Subtropical Northern Hemisphere*. Pacific Northwest Fungi, **2008**. 3(7): p. 73-125.
22. Boddy, L. and Rayner A.D.M., *Origins of Decay in Living Deciduous Trees: The Role of Moisture Content and a Re-appraisal of the Expanded Concept of Tree Decay*. New Phytologist, **1983**. 94(4): p. 623-641.
23. Pointing, S.B., Parungao M.M., Hyde K.D., *Production of wood-decay enzymes, mass loss and lignin solubilization in wood by tropical Xylariaceae*. Mycol Res, **2003**. 107(2): p. 231-5.
24. Pointing, S.B., et al., *Screening of basidiomycetes and xylariaceous fungi for lignin peroxidase and laccase gene-specific sequences*. Mycol Res, **2005**. 109(1): p. 115-24.
25. Shary, S., Ralph, S.A., Hammel K.E., *New insights into the ligninolytic capability of a wood decay ascomycete*. Appl Environ Microbiol, **2007**. 73(20): p. 6691-4.
26. Davis, E.C., et al., *Endophytic Xylaria (Xylariaceae) among liverworts and angiosperms: phylogenetics, distribution, and symbiosis*. Am J Bot, **2003**. 90(11): p. 1661-7.
27. Müller, *Phycomyceten und Ascomyceten. Untersuchungen aus Brasilien*. **1901**, Jena: G. Fischer.
28. Miller, J.H., *A monograph of the world species of Hypoxylon* Athens, **1961**.
29. Whalley, A.J.S., *Numerical taxonomy of some species of Hypoxylon*. Mycopathologia, **1976**. 59(3): p. 155-161.
30. Stadler, M. and Wollweber H., *Secondary metabolite profiling, genetic fingerprints and taxonomy of Daldinia and allies*. Mycotaxon, **2001**. 77: p. 379-429.
31. Stadler, M., et al., *Changes in secondary metabolism during stromatal ontogeny of Hypoxylon fragiforme*. Mycol Res, **2006**. 110(7): p. 811-20.
32. Stadler, M., Ju Y.M., Rogers J.D., *Chemotaxonomy of Entonaema, Rhopalostroma and other Xylariaceae*. Mycol Res, **2004**. 108(3): p. 239-56.
33. Stadler, M. and Keller N.P., *Paradigm shifts in fungal secondary metabolite research*. Mycol Res, **2008**. 112(2): p. 127-30.
34. Stadler, M. and Fournier J., *Pigment chemistry, taxonomy and phylogeny of the Hypoxyloideae (Xylariaceae)*. Rev Iberoam Micol, **2006**. 23(3): p. 160-70.
35. Stadler, et al., *Molecular chemotaxonomy of Daldinia and other Xylariaceae*. Mycol Res, **2001**,105(10): p. 1191-1205.
36. Radulovic, N., *Novi azafiloni, steroidi i terfenili iz gljiva Creosphaeria sassafras, Hypoxylon Multifforme i Theleophora terrestris*. Doctoral disertation, **2006**.
37. Hellwig, V., et al., *Hypomiltin, a novel azaphilone from Hypoxylon hypomiltum, and chemotypes in Hypoxylon sect. Hypoxylon as inferred from analytical HPLC profiling*. Mycol. Prog., **2005**. 4(1): p. 39-54.
38. Hsieh, H.M., Ju Y.M., J.D. Rogers, *Molecular phylogeny of Hypoxylon and closely related genera*. Mycologia, **2005**. 97(4): p. 844-65.
39. Webster, J. and Weber R.W.S., *Teaching Techniques for Mycology: 23. Ecllosion of Hypoxylon fragiforme ascospores as a prelude to germination*. Mycologist, **2004**. 18(04): p. 170-173.
40. Betina, V., *Structure-activity relationships among mycotoxins*. Chem Biol Interact, **1989**. 71: p. 105-146.
41. Brase, S., et al., *Chemistry and biology of mycotoxins and related fungal metabolites*. Chem Rev, **2009**. 109(9): p. 3903-90.

42. Chang, et al., *Absolute Configuration of Anti-HIV-1 Agent (-)-Concentricolide: Total Synthesis of (+)-(R)-Concentricolide*. 76. **2011**, Washington, DC, ETATS-UNIS: American Chemical Society. 4.
43. Fange, et al., *First Synthesis of Racemic concentricolide, an Anti-HIV-1 agent isolated from the fungus *Daldinia concentrica**. *Heterocycle*, **2009**, 78(8): p.2107-2113.
44. Nagasawa, H., et al., *Apoptosis induction in HCT116 cells by cytochalasins isolated from the fungus *Daldinia vernicosa**. *Phytomedicine*, **2000**. 6(6): p. 403-9.
45. Quang, D.N., et al., *Cyclic azaphilones daldinins E and F from the ascomycete fungus *Hypoxylon fuscum* (Xylariaceae)*. *Phytochemistry*, **2004**. 65(4): p. 469-73.
46. Gil, et al., *Progress in the Chemistry of Organic Natural Products*. **1987**: p. 51.
47. Quang, D.N., et al., *Cohaerins A and B, azaphilones from the fungus *Hypoxylon cohaerens*, and comparison of HPLC-based metabolite profiles in *Hypoxylon* sect. *Annulata**. *Phytochemistry*, **2005**. 66(7): p. 797-809.
48. Hayashi, K., et al., Japanese patent, JP 08217673, 1996.
49. Dang Ngoc, Q., et al., *Sassafrins A-D, new antimicrobial azaphilones from the fungus *Creosphaeria sassafras**. *Tetrahedron*, **2005**, 61(7): p. 1743-1748.
50. Quang, D.N., et al., *Inhibition of nitric oxide production in RAW 264.7 cells by azaphilones from xylariaceous fungi*. *Biol Pharm Bull*, **2006**. 29(1): p. 34-7.
51. Quang, et al., *Cohaerins C-F, four azaphilones from the xylariaceous fungus *Annulohypoxylon cohaerens**. *Tetrahedron*, **2006**, 62(26): p. 6349-6354.
52. Kimura, T., et al., *Novel azaphilones, kasanosins A and B, which are specific inhibitors of eukaryotic DNA polymerases beta and lambda from *Talaromyces* sp.* *Bioorg Med Chem*, **2008**. 16(8): p. 4594-9.
53. Zou, X.-W., et al., *Helotialins A-C, Anti-HIV Metabolites from a Helotialean Ascomycete*. *Chinese J. Nat. Med.*, **2009**. 7: p. 140-144.
54. Powell, et al., *Survey of the chemistry of the azaphilones to that date*. *Chemical Society*, **1956**. 5.
55. Park, J.H., et al., *Antifungal activity against plant pathogenic fungi of chaetoviridins isolated from *Chaetomium globosum**. *FEMS Microbiol Lett*, **2005**. 252(2): p. 309-13.
56. Hopwood, D.A., *The Leeuwenhoek lecture, 1987. Towards an understanding of gene switching in *Streptomyces*, the basis of sporulation and antibiotic production*. *Proc R Soc Lond B Biol Sci*, **1988**. 235(1279): p. 121-38.
57. Maplestone, R.A., Stone M.J., Williams D.H., *The evolutionary role of secondary metabolites--a review*. *Gene*, **1992**. 115(1-2): p. 151-7.
58. Bu'Lock, J.D., *Intermediary metabolism and antibiotic synthesis*. *Adv Appl Microbiol*, **1961**. 3: p. 293-342.
59. Sekiguchi, J. and Gaucher G.M., *Conidiogenesis and secondary metabolism in *Penicillium urticae**. *Appl Environ Microbiol*, **1977**. 33(1): p. 147-58.
60. Calvo, A.M., et al., *Relationship between secondary metabolism and fungal development*. *Microbiol Mol Biol Rev*, **2002**. 66(3): p. 447-59.
61. Kronstad, J., et al., *Signaling via cAMP in fungi: interconnections with mitogen-activated protein kinase pathways*. *Arch Microbiol*, **1998**. 170(6): p. 395-404.
62. Yu, J.H. and Keller N., *Regulation of secondary metabolism in filamentous fungi*. *Annu Rev Phytopathol*, **2005**. 43: p. 437-58.
63. Shwab, E.K. and Keller N.P., *Regulation of secondary metabolite production in filamentous ascomycetes*. *Mycol Res*, **2008**. 112(2): p. 225-30.

64. Keller, N.P., Turner G., Bennett J.W., *Fungal secondary metabolism - from biochemistry to genomics*. Nat Rev Microbiol, **2005**. 3(12): p. 937-47.
65. Brown, D.W., et al., *Twenty-five coregulated transcripts define a sterigmatocystin gene cluster in Aspergillus nidulans*. Proc Natl Acad Sci U S A, **1996**. 93(4): p. 1418-22.
66. Fernandes, M., Keller N.P., Adams T.H., *Sequence-specific binding by Aspergillus nidulans AfIR, a C6 zinc cluster protein regulating mycotoxin biosynthesis*. Mol Microbiol, **1998**. 28(6): p. 1355-65.
67. Hoffmeister, D. and Keller N.P., *Natural products of filamentous fungi: enzymes, genes, and their regulation*. Nat Prod Rep, **2007**. 24(2): p. 393-416.
68. Osmanova, et al., *Azaphilones: a class of fungal metabolites with diverse biological activities*. Phytochemistry reviews, **2010**. 9(2): p. 315-342.
69. Mylonakis, E., Casadevall A., Ausubel F.M., *Exploiting amoeboid and non-vertebrate animal model systems to study the virulence of human pathogenic fungi*. PLoS Pathog, **2007**. 3(7): p. 101.
70. Fox, E.M. and Howlett B.J., *Secondary metabolism: regulation and role in fungal biology*. Curr Opin Microbiol, **2008**. 11(6): p. 481-487.
71. Stadler, et al., *Chemotaxonomy of the Xylariaceae and remarkable bioactive compounds from Xylariales and their associated asexual stages*. Phytochemistry **2005**. 9
72. Ying, J., et al., *Icons of medicinal fungi from China*. Science press, **1987**.
73. Molitoris, H.P., *Mushrooms in medicine, folklore and religion*. Feddes Repertorium, **2002**. 113(1-2): p. 165-182.
74. Hobbs and Christopher, *Medicinal mushrooms: an exploration of tradition, health and culture*. Botanica press, **2003**.
75. Gill, M. and Steglich W., *Pigments of fungi (Macromycetes)*. Fortschr Chem Org Naturst, **1987**. 51: p. 1-317.
76. Steglich W, Fugmann B, L.-F. S, *Encyclopedia natural products*. Thieme Verlag, New York, **2001**.
77. Strudikova, M., et al., *Mikrobiálna produkcia farbnych azaphilonovych metabolitov*. Chem Listy, **2000**. 94: p. 105-110.
78. Dong, J., et al., *New nematocidal azaphilones from the aquatic fungus Pseudohalonestria adversaria* Microbiol Lett, **2006**. 264(1): p. 65-9.
79. Stadler, M., et al., *Novel Bioactive Azaphilones from Fruit Bodies and Mycelial Cultures of the Ascomycete Bulgaria inquinans (Fr.)*. Natural Product Letters, **1995**. 7(1): p. 7-14.
80. Akihisa, et al., *Anti-tumor-initiating effects of monascin, an azaphilonoid pigment from the extract of Monascus pilosus fermented rice (Red-Mold Rice)*. Chem Biodivers **2005**. 2(10): p. 1305-9.
81. Duncan, S.J., et al., *Isolation and structure elucidation of Chlorofusin, a novel p53-MDM2 antagonist from a Fusarium sp.* J. Am. Chem. Soc, **2001**. 123(4): p. 554-560.
82. Zhu, J., Germain A.R., Porco J.A., *Synthesis of Azaphilones and Related Molecules by Employing Cycloisomerization of o-Alkynylbenzaldehydes*. Angewandte Chemie International Edition, **2004**. 43(10): p. 1239-1243.
83. Park, et al., *Antifungal activity against plant pathogenic fungi of chaetoviridins isolated from Chaetomium globosum*. FEMS microbiology letters, **2005**, 252(2): p. 309-313.
84. Hajjaj, et al., *Medium-chain fatty acids affect citrinin production in the filamentous fungus Monascus tuber*. American Society for Microbiolog **2000**, 66.
85. Velisek, et al., *Biosynthesis of Food Constituents: Natural Pigments. Part 2 -a Review*. Czech journal of food sciences, **2008**, 26(2): p. 73-98.

86. Velišek J. and C. K., *Pigments of higher fungi - a review*. Czech Journal of Food Science, 2011. **29**.
87. Turner, W.B. and Aldridge D.C., *Fungal metabolites*. **1971**, London, New York: Academic Press.
88. Graf, W., et al., *Biosynthesis of the Cytochalasans. Part III. 13C-NMR. of cytochalasin B (phomin) and cytochalasin D. Incorporation of [1-13C]- and [2-13C]-sodium acetate*. Helvetica Chimica Acta, **1974**. 57(6): p. 1801-1815.
89. Birchall, G.R., et al., *The chemistry of fungi. Part LX. The synthesis of tetrahydro-sclerotioramine, tetrahydro-sclerotoquinone, and tetrahydro-sclerotiorin*. Journal of the Chemical Society C: Organic, **1971**: p. 3559-3566.
90. Chong, R., King R.R., Whalley W.B., *The synthesis of sclerotiorin and of an analogue of rotiorin*. Journal of the Chemical Society D: Chemical Communications, **1969**, 24: p. 1512-1513.
91. Suzuki, T., et al., *Synthesis of 7-acetyloxy-3,7-dimethyl-7,8-dihydro-6H-isochromene-6,8-dione and its analogues*. Journal of Heterocyclic Chemistry, **2001**. 38(6): p. 1409-1418.
92. Zhu, J., et al., *Synthesis of the Azaphilones Using Copper-Mediated Enantioselective Oxidative Dearomatization*. J Am Chem Soc, **2005**. 127(26): p. 9342-9343.
93. Zhu, J. and J.A. Porco, *Asymmetric Syntheses of (â~)-Mitorubrin and Related Azaphilone Natural Products*. Organic Letters, **2006**. 8(22): p. 5169-5171.
94. Wei, W.-G. and Yao Z.-J., *Synthesis Studies toward Chloroazaphilone and Vinylogous γ -Pyridones: Two Common Natural Product Core Structures*. The Journal of Organic Chemistry, **2005**. 70(12): p. 4585-4590.
95. Juzlova, et al., *Secondary metabolites of the fungus Monascus : a review*. Journal of Industrial Microbiology Biotechnology **1996**, 16(3).
96. Frisvad, et al., *Analysis and screening for mycotoxins and other secondary metabolites in fungal cultures by thin-layer chromatography and high-performance liquid chromatography*. Archives of environmental contamination and toxicology, **1989**, 18 (3): p. 331-335.
97. Frisvad C. J, *High-performance liquid chromatographic determination of profiles of mycotoxins and other secondary metabolites*. J Chromatogr., **1987**, 392: p. 333-347
98. Frisvad C. J, *The use of high-performance liquid chromatography and diode array detection in fungal chemotaxonomy based on profiles of secondary metabolites*. Botanical journal of the Linnean Society, **1989**, 99(1): p. 81-95.
99. Nielsen, et al., *Fungal metabolite screening: database of 474 mycotoxins and fungal metabolites for dereplication by standardised liquid chromatography-UV-mass spectrometry methodology*. Antimicrob Agents Chemother. **2010**, 54(1): p. 509-512.
100. Nielsen, K.F., et al., *Chemical identification of fungi: metabolite profiling and metabolomics*. Fungal biotechnology in agricultural, food, and environmental applications, **2004**: p. 6.
101. Smedsgaard, et al., *Using direct electrospray mass spectrometry in taxonomy and secondary metabolite profiling of crude fungal extracts*. Journal of microbiological methods, **1996**, 25(1): p. 5-17.
102. Smedsgaard J, *Terverticillate Penicillia Studied by Direct electrospray Mass Spectrometric Profiling of Crude Extracts. II. Database and Identification*. Biochemical Systematics and Ecology, **1997**, 25(1): p. 65-71,
103. Smedsgaard, J.r. and Frisvad J.C., *Terverticillate penicillia studied by direct electrospray mass spectrometric profiling of crude extracts. I. Chemosystematics*. Biochemical Systematics and Ecology, **1997**. 25(1): p. 51-64.
104. Smedsgaard, J., *Classification of terverticillate Penicillia by electrospray mass spectrometric profiling*. Studies in Mycology, **2004**. 49: p. 243-251.

105. Frisvad J. C. and S.R. A., *Polyphasic taxonomy of Penicillium subgenus Penicillium. A guide to identification of the food and air-borne terverticillate Penicillia and their mycotoxins*. *Studies in Mycology*, **2004**, 49(173): p. 1-173.
106. Bitzer, et al., *Accelerated dereplication of natural products, supported by reference libraries*. *Chimia*, **2007**, 61(6): p. 332-338.
107. Novakova, et al., *A review of current trends and advances in modern bio-analytical methods: Chromatography and sample preparation*. *Anal Chim Acta*. **2009**, 656(1-2):8-35.
108. Kataoka and Hiroyuki, *New trends in sample preparation for clinical and pharmaceutical analysis*. *TrAC. Trends in analytical chemistry*, **2003**, 22: p. 232-244
109. Herrera, et al., *Ultrasound-assisted extraction of phenolic compounds from strawberries prior to liquid chromatographic separation and photodiode array ultraviolet detection*. *J Chromatogr A*. **2005**, 1100(1):p. 1-7
110. *Sample preparation in chromatography*. p. 297.
111. *Sample preparation in chromatography*. *Journal of chromatograph library*. **65**: p. 304.
112. *Sample preparation in chromatography*. *Journal of chromatograph library*. **65**: p. 341.
113. *Sample preparation in chromatography*. *Journal of chromatograph library*: p. 346.
114. VAS, et al., *Solid-phase microextraction: a powerful sample preparation tool prior to mass spectrometric analysis*. *J Mass Spectrom*, **2004**. 39(3): p. 22.
115. PANG, et al., *Validation study on 660 pesticide residues in animal tissues by gel permeation chromatography cleanup/gas chromatography-mass spectrometry and liquid chromatography-tandem mass spectrometry*. *Journal of chromatography*, **2006**. 1125(1): p. 30.
116. Plumb, et al., *Ultra-performance liquid chromatography coupled to quadrupole-orthogonal time-of-flight mass spectrometry* *Rapid Comm Mass Spectrom*, **2004**. 18(19): p. 6.
117. Wilson, I.D., et al., *HPLC-MS-based methods for the study of metabonomics*. *Journal of Chromatography B*, **2005**. 817(1): p. 67-76.
118. Leandro, C.C., et al., *Comparison of ultra-performance liquid chromatography and high-performance liquid chromatography for the determination of priority pesticides in baby foods by tandem quadrupole mass spectrometry*. *Journal of Chromatography A*, **2006**. 1103(1): p. 94-101.
119. *Hydrophobic Interaction and Reversed Phase Chromatography-Principles and Methods*. GE Healthcare: p. 91.
120. Staples, et al., *A chip-based amide-HILIC LC/MS platform for glycosaminoglycan glycomics profiling*. *Proteomics*. **2009**, 9(3): p. 686-95 .
121. Scott, R.P.V., *Chromatographic detectors, Design, Function and Operation*. *Chromatographic Science Series*. **73**: p. 180.
122. Martin, G.E. and Crouch R.C., *Inversed-Detected Two-Dimensional NMR Methods: Applications in Natural Products Chemistry*. *Journal of Natural Products*, **1991**. 54: p. 1- 70.
123. Sanders J. K. and B.K. Hunter, *Modern NMR Spectroscopy*. Oxford University Press, **1990**.
124. Atta-Ur-Rahman and M.I. Choudhary, *Solving Problems with NMR Spectroscopy*. Academic Press, **1996**.
125. Exarchou, V., et al., *LC-NMR coupling technology: recent advancements and applications in natural products analysis*. *Magnetic Resonance Chemistry*, **2005**. 43(9): p. 681-7.
126. Huber, C.G. and H. Oberacher, *Analysis of nucleic acids by on-line liquid chromatography-mass spectrometry*. *Mass Spectrom Rev*, **2001**. 20(5): p. 310-43.

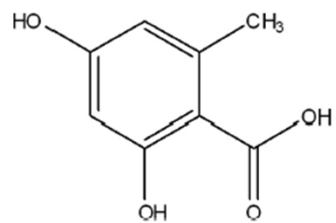
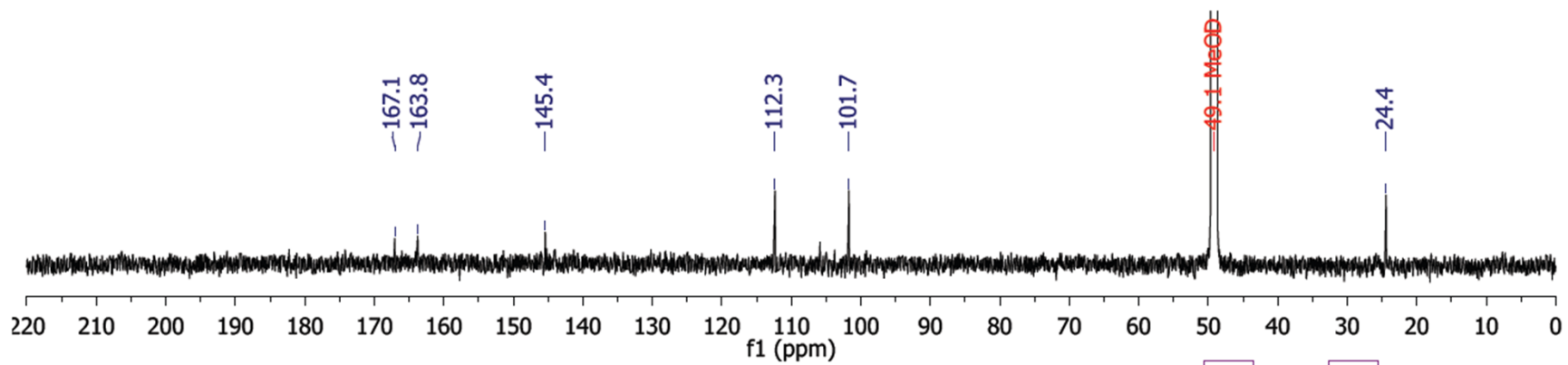
127. Il'ina, E.N. and V.M. Govorun, *Mass spectrometry of nucleic acids in molecular medicine*. Bioorg Khim, **2009**. 35(2): p. 149-64.
128. Mamone, G., et al., *Analysis of food proteins and peptides by mass spectrometry-based techniques*. J Chromatogr A, **2009**. 1216(43): p. 7130-42.
129. Rodrigues, J.A., et al., *Mass spectrometry of carbohydrates: newer aspects*. Adv Carbohydr Chem Biochem, **2007**. 61: p. 59-141.
130. Hoofnagle, A.N. and Heinecke J.W., *Lipoproteomics: using mass spectrometry-based proteomics to explore the assembly, structure, and function of lipoproteins*. J Lipid Res, **2009**. 50(10): p. 1967-75.
131. Tanaka, et al., *Protein and polymer analyses up to m/z 100 000 by laser ionization time-of-flight mass spectrometry*. Rapid Comm Mass Spectrom, **1988**. 2(8): p. 3.
132. Karas, M. and Hillenkamp F., *Laser desorption ionization of proteins with molecular masses exceeding 10,000 daltons*. Anal Chem, **1988**. 60(20): p. 2299-301.
133. Buchi, G., White J.D., Wogan G.N., *The Structures of Mitorubrin and Mitorubrinol*. Journal of the American Chemical Society, **1965**. 87(15): p. 3484-3489.
134. Abbé Nollet Jean-Antoine, *Lettre de electricité*. Paris, 1755 (Tome 1) Edit: Hippolyte-Louis Guérin, & Louis-François Delatour **6**: p. 156.
135. Gaskell and J. S, *Electrospray : Principles and practice*. J Mass Spectrom, **1997**, 32(7): p. 677-688.
136. Whitehouse, C.M., et al., *Electrospray interface for liquid chromatographs and mass spectrometers*. Anal Chem, **1985**. 57(3): p. 675-9.
137. Kebarle, P. and Tang L., *From ions in solution to ions in the gas phase - the mechanism of electrospray mass spectrometry*. Analytical Chemistry, **1993**. 65(22): p. 972A-986A.
138. Wilm, M.S. and Mann M., *Electrospray and Taylor-Cone theory, Dole's beam of macromolecules at last?* Internat J Mass Spectrom and Ion Processes, **1994**. 136(23): p. 167-180.
139. Fenn B. J, *Ion formation from charged droplets: roles of geometry, energy, and time*. J Am Soc Mass Spectrom, **1993**, 4(7): p. 524-535.
140. Dole, M.M., et. al., *Molecular Beams of Macroions*. Journal of Chemical Physics, **1968**. 49: p. 9.
141. Iribarne, J.V. and Thomson B.A., *On the evaporation of small ions from charged droplets*. The Journal of Chemical Physics, **1976**. 64(6): p. 2287-2294.
142. Cole, R., *Electrospray and MALDI mass spectrometry : fundamentals, instrumentation, practicalities, and biological applications*. John Wiley & Sons, Inc., Hoboken, New Jersey, 2010. **Second edition**(Part one): p. 9.
143. de Rijke, E., et al., *Analytical separation and detection methods for flavonoids*. J Chromatogr A, **2006**. 1112(1-2): p. 31-63.
144. Hoffmann E.D., *Mass spectrometry Principles and applications*. John Wiley & sons LTD., Chichester, 2002: p. 33-39, 45-47, 72-78, 159-162, 186-193.
145. Kazuno, S., et al., *Mass spectrometric identification and quantification of glycosyl flavonoids, including dihydrochalcones with neutral loss scan mode*. Anal Biochem, **2005**. 347(2): p. 182-92.
146. Hvattum, E. and D. Ekeberg, *Study of the collision-induced radical cleavage of flavonoid glycosides using negative electrospray ionization tandem quadrupole mass spectrometry*. J Mass Spectrom, **2003**. 38(1): p. 43-9.
147. Longevialle, P., *Ion-neutral complexes in the unimolecular reactivity of organic cations in the gas phase*. Mass Spectrometry Reviews, **1992**. 11(3): p. 157-192.

148. Longevialle, P. and R. Botter, *Electron impact mass spectra of bifunctional steroids. The interaction between ionic and neutral fragments derived from the same parent ion.* *Organic Mass Spectrometry*, **1983**, 18(1): p. 1-8.
149. Longevialle, P. and R. Botter, *Evidence for intramolecular interaction between ionic and neutral fragments in the mass spectrometer.* *Journal of the Chemical Society, Chemical Communications*, **1980**, 17: p. 823-825.
150. Bowen, R.D., *Reactions of isolated organic ions. Alkene loss from the immonium ions CH₃CH[double bond, length half m-dash]N+HC₂H₅ and CH₃CH[double bond, length half m-dash]N+HC₃H₇.* *Journal of the Chemical Society, Perkin Transactions 2*, **1989**, 7: p. 913-918.
151. Cooks, R.G., Koskinen J.T., Thomas P.D., *The kinetic method of making thermochemical determinations.* *J mass spectrom*, **1999**, 34(2): p. 85-92.
152. Jianhua, R.E.N., Patel, and G. Chirag, *Determination of the gas-phase acidity of methylthioacetic acid- using the cooks' kinetic method.* *J Am Soc Mass Spectrom*, **2005**, 16(4): p. 535-541.
153. Hunt, D., McEwen C., Upham R., *Determination of active hydrogen in organic compounds by chemical ionization mass spectrometry.* *Analytical chemistry*, **1972**, 44(7): p. 1292-1294.
154. Mohamed, R., et al., *Mass spectral characterization of ergot alkaloids by electrospray ionization, hydrogen/deuterium exchange, and multiple stage mass spectrometry: Usefulness of precursor ion scan experiments.* *Rapid Commun Mass Spectrom*, **2006**, 20(19): p. 2787-99.
155. Hemling, M.E., et al., *Gas phase hydrogen/deuterium exchange in electrospray ionization mass spectrometry as a practical tool for structure elucidation.* *Journal of the American Society for Mass Spectrometry*, **1994**, 5(5): p. 434-442.
156. Takàts, Z., Schlosser G., Vékey K., *Hydrogen/deuterium exchange of electrosprayed ions in the atmospheric interface of a commercial triple quadrupole mass spectrometer.* *International Journal of Mass Spectrometry*, **2003**, 228: p. 729-741.
157. Campbell, S., et al., *Structural and Energetic Constraints on Gas Phase Hydrogen/Deuterium Exchange Reactions of Protonated Peptides with D₂O, CD₃OD, CD₃CO₂D, and ND₃.* *J Am Chem Soc*, **1994**, 116(21): p. 9765-9766.
158. Campbell, et al., *Deuterium Exchange Reactions as a Probe of Biomolecule Structure. Fundamental Studies of Gas Phase H/D Exchange Reactions of Protonated Glycine Oligomers With D₂O, CD₃OD, CD₃CO₂D and ND₃.* *J Am Chem Soc* **1995**, 117(51): p. 12840-12854.
159. Hunt, D.F. and S.K. Sethi, *Gas-phase ion/molecule isotope-exchange reactions: methodology for counting hydrogen atoms in specific organic structural environments by chemical ionization mass spectrometry.* *Journal Name: J. Am. Chem. Soc.* **1980**, 102(23): p. 6953-6963.
160. Gard, E., et al., *Gas-phase hydrogen/deuterium exchange as a molecular probe for the interaction of methanol and protonated peptides.* *Journal of the American Society for Mass Spectrometry*, **1994**, 5(7): p. 623-631.
161. Ni, J. and A.G. Harrison, *Reactive collisions in quadrupole cells. 2. H/D exchange reactions of enolate ions with CH₃OD and C₂H₅OD.* *Journal of the American Society for Mass Spectrometry*, **1992**, 3(8): p. 853-858.
162. Asoka, R., et al., *Selective isotopic exchange of polyfunctional ions in tandem mass spectrometry : methodology, applications and mechanism.* *Organic mass spectrometry*, **1992**, 27(2): p. 77-88.,.
163. Fenn, J.B., et al., *Electrospray ionization for mass spectrometry of large biomolecules.* *Science*, **1989**, 246(4926): p. 64-71.
164. Cech, et al., *Practical implications of some recent studies in electrospray ionization fundamentals.* *Mass Spectrom Rev.* **2001**, 20(6): p. 362-387.

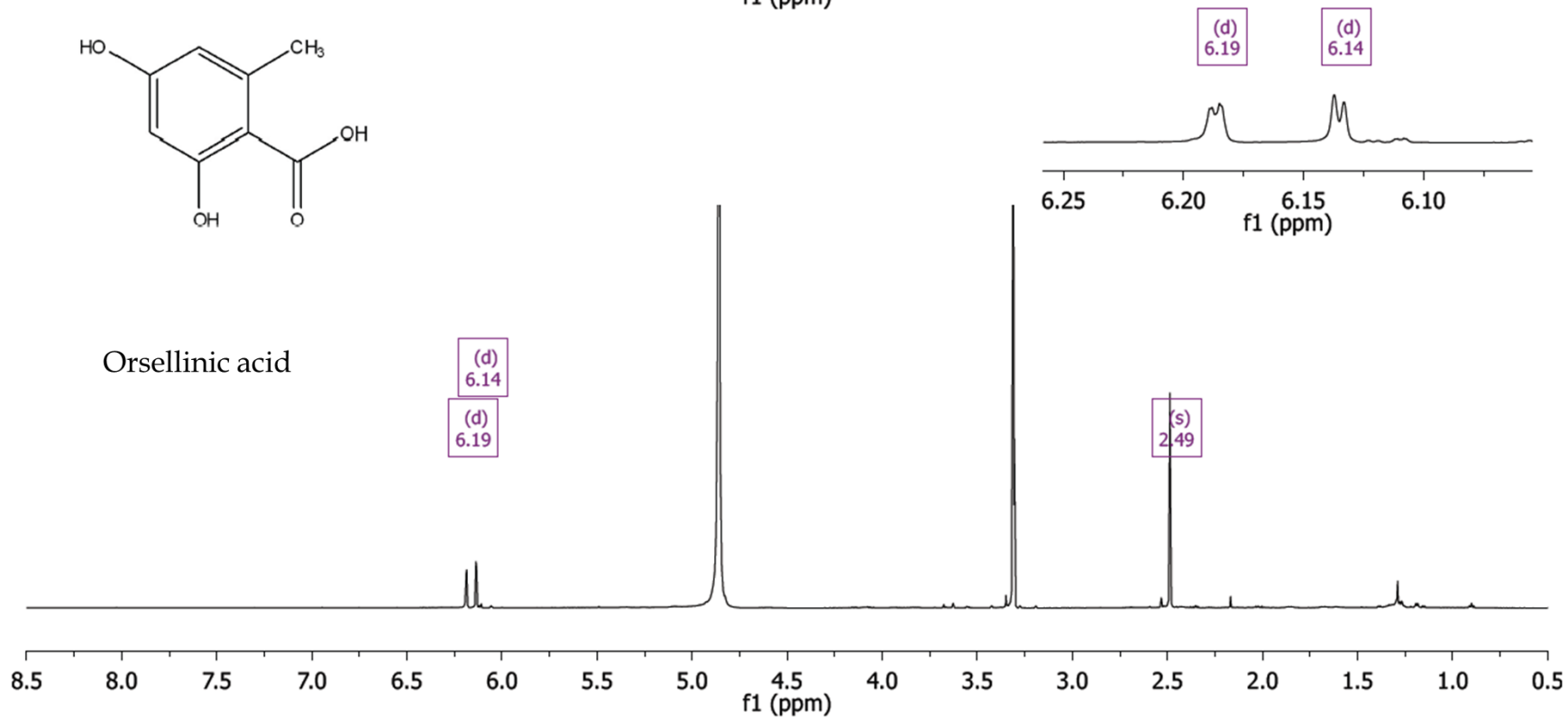
165. Leinonen, et al., *Liquid chromatography/mass spectrometry in anabolic steroid analysis: optimization and comparison of three ionization techniques: electrospray ionization, atmospheric pressure chemical ionization and atmospheric pressure photoionization*. *J Mass Spectrom.* **2002**, 37(7): p.693-698.
166. Dams, et al., *Matrix effect in bio-analysis of illicit drugs with LC-MS/MS: Influence of ionization type, sample preparation, and biofluid*. *J Am Soc Mass Spectrom.* **2003**, 14(11): p. 1290-1294.
167. Niessen, et al., *Matrix effects in quantitative pesticide analysis using liquid chromatography-mass spectrometry*. *Mass Spectrom Rev.* **2006**, 25(6):p. 8818-99.
168. Qizhi, H.U., et al., *The orbitrap : a new mass spectrometer*. *J Mass Spectrom.* **2005**, 40(4): p. 430-43.
169. Lopez, L.L., et al., *Automated strategies for obtaining standardized collisionally induced dissociation spectra on a benchtop ion trap mass spectrometer*. *Rapid Communications in Mass Spectrometry*, **1999**. 13(8): p. 663-668.
170. Baumgarten, S., et al., *The Role of Water in Platinum-Catalyzed Cycloisomerization of 1,6-Enynes: A Combined Experimental and Theoretical Gas Phase Study*. *ChemCatChem*, **2009**. 1(1): p. 138-143.
171. Frisch, M.J., et al., *Gaussian 09, Revision B.01*, in *Gaussian 09, Revision B.01*, Gaussian, Inc., Wallingford CT. 2009: Wallingford CT.
172. Lee, C.T.Y. and R.G. Parr, *Development of the Colle-Salvetti correlation-energy formula into a functional of the electron density*. **1988**, 37: p. 785-789.
173. Becke, A.D., *Density-functional thermochemistry. III. The role of exact exchange*. *The Journal of Chemical Physics*, **1993**. 98(7): p. 5648-5652.
174. Weigend, F. and R. Ahlrichs, *Balanced basis sets of split valence, triple zeta valence and quadruple zeta valence quality for H to Rn: Design and assessment of accuracy*. *Physical Chemistry Chemical Physics*, **2005**. 7(18): p. 3297-3305.
175. Lindstrom, P.J. and W.G. Mallard, *NIST Chemistry WebBook, NIST Standard Reference Database National Institute of Standards and Technology, Gaithersburg MD, 20899*. **69**.
176. Svilar, L., et al., *Distinctive gas-phase fragmentation pathway of the mitorubramines, novel secondary metabolites from Hypoxylon fragiforme*. *Rapid Communication in Mass Spectrometry*, **2012**(just accepted).
177. Stadler, et al., *Identification of alkaloids and polyketides in an Actinomycete by high-performance liquid chromatography with mass spectrometric and UV-visible detection*. *Journal of chromatography*, **1998**, 818(2): p. 187-195.
178. Li, L.-Q., et al., *A New Azaphilone, Kasanosin C, from an Endophytic Talaromyces sp. T1BF*. *Molecules*, **2010**. 15(6): p. 3993-3997.
179. Morton, T.H., *Ion-molecule complexes in unimolecular fragmentations of gaseous cations. Alkyl phenyl ether molecular ions*. *Journal of the American Chemical Society*, **1980**. 102(5): p. 1596-1602.
180. Bowen, R.D. and D.H. Williams, *Unimolecular reactions of isolated organic ions. The importance of ion-dipole interactions*. *Journal of the American Chemical Society*, **1980**. 102(8): p. 2752-2756.
181. Moylan, C.R. and J.I. Brauman, *Mechanistic information from infrared multiple photon decomposition. The ethylisopropylamine proton-transfer system*. *Journal of the American Chemical Society*, **1985**. 107(4): p. 761-765.
182. Garver Jm Fau - Yang, Z., et al., *Gas phase reactions of 1,3,5-triazine: proton transfer, hydride transfer, and anionic sigma-adduct formation*. **2011**. 22: p. 1260.
183. Tutar, et al., *Bromination of an N-carbethoxy-7-aza-2,3-benzonorbornadiene and synthesis of N-carbethoxy-7-aza-2,3-dibromo-5,6-benzonorbornadiene: high temperature bromination. Part 14*. *Tetrahedron*, **2002**, 58(44): p. 8979-8984.

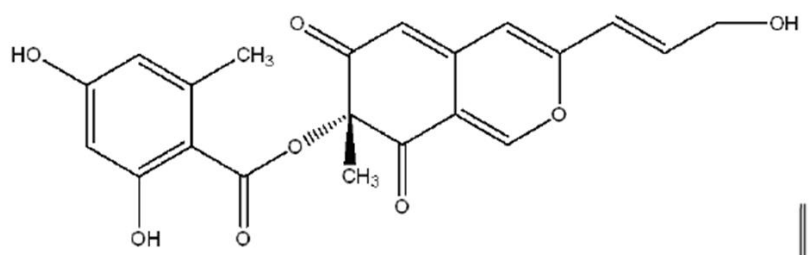
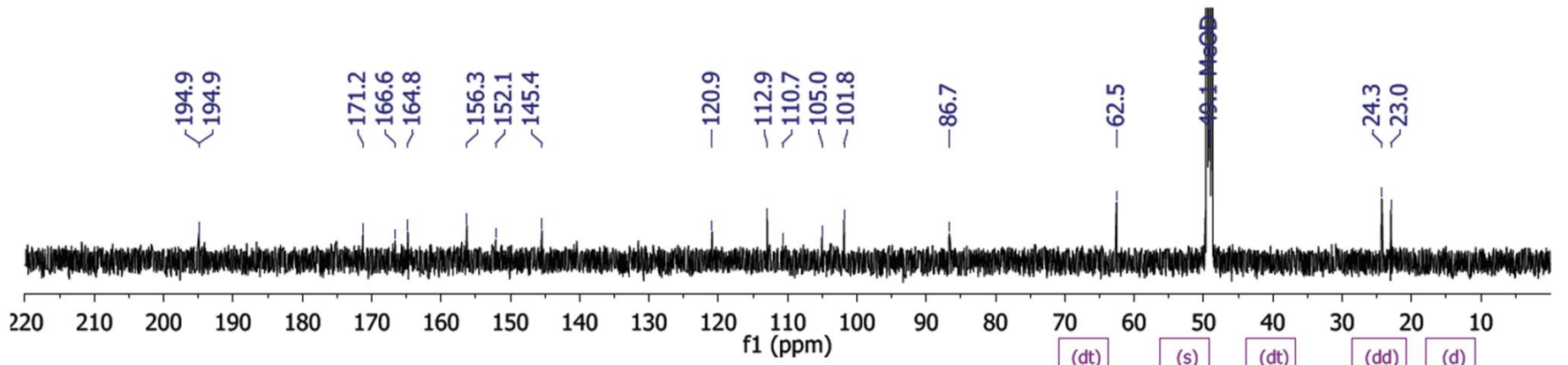
184. Nikitina, et al., *First synthesis of 6-spiro[5-aza-2-oxatricyclo[6.2.1.0[3][,][9]]undec-3-ene-6,1'-cyclohexane]*. *Chemistry of Heterocyclic Compounds* **2003**, 39(1): p. 130-131.
185. Morlender, V., et al., *The role of hydrogen migration in the mechanism of alcohol elimination from MH[+] ions of ethers upon chemical ionization*. *J Mass Spectrom.* **1997**, 32(10): p. 1124-1132.
186. Kuzmenkov, et al., *Role of hydrogen migration in the mechanism of acetic acid elimination from MH[+] ions of acetates on chemical ionization and collision-induced dissociation*. *J Mass Spectrom.* **1999**, 34(8): p. 797-803.
187. Fiolhais, C., F. Nogueira, and M.A.L. Marques, *A Primer in Density Functional Theory*. *Lecture Notes in Physics*, **2003**. **620**(13): p. 256.

Annex 1 - NMR spectra

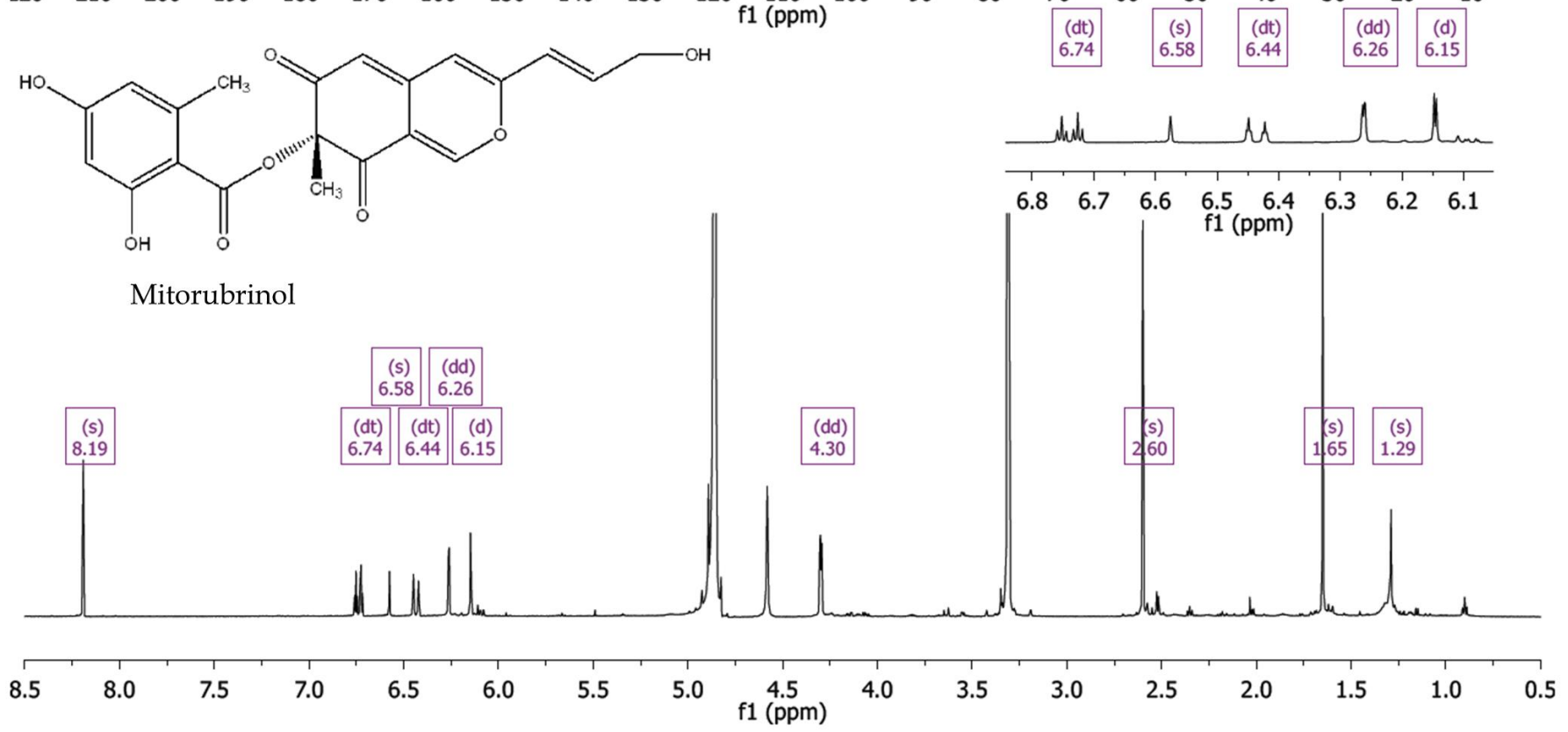


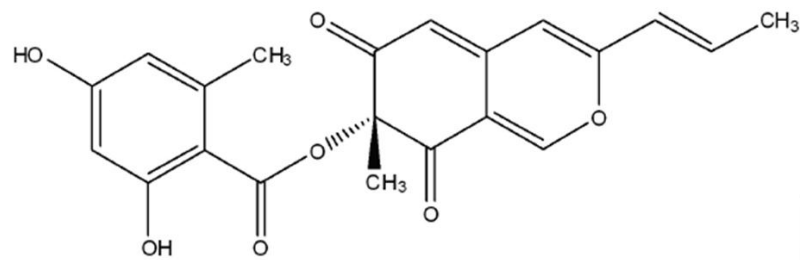
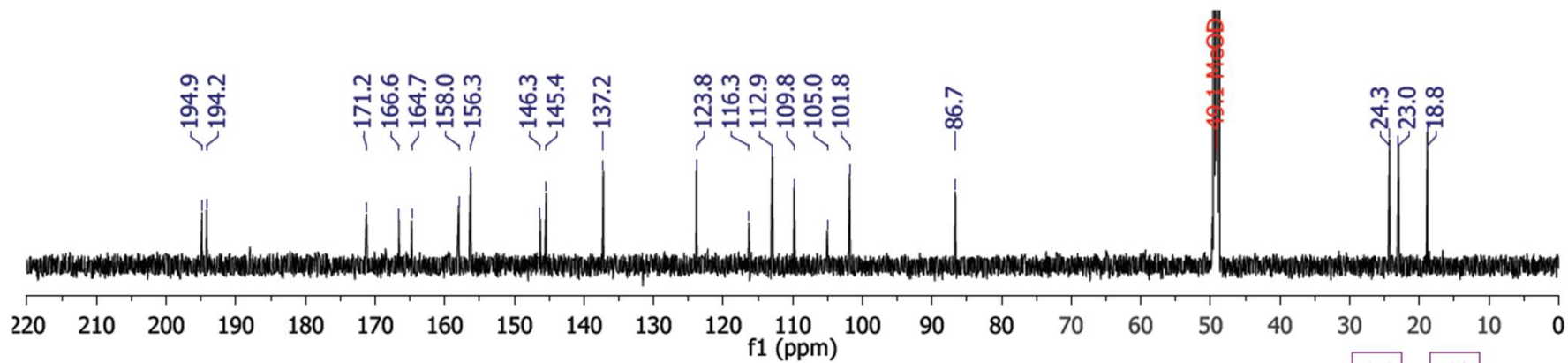
Orsellinic acid



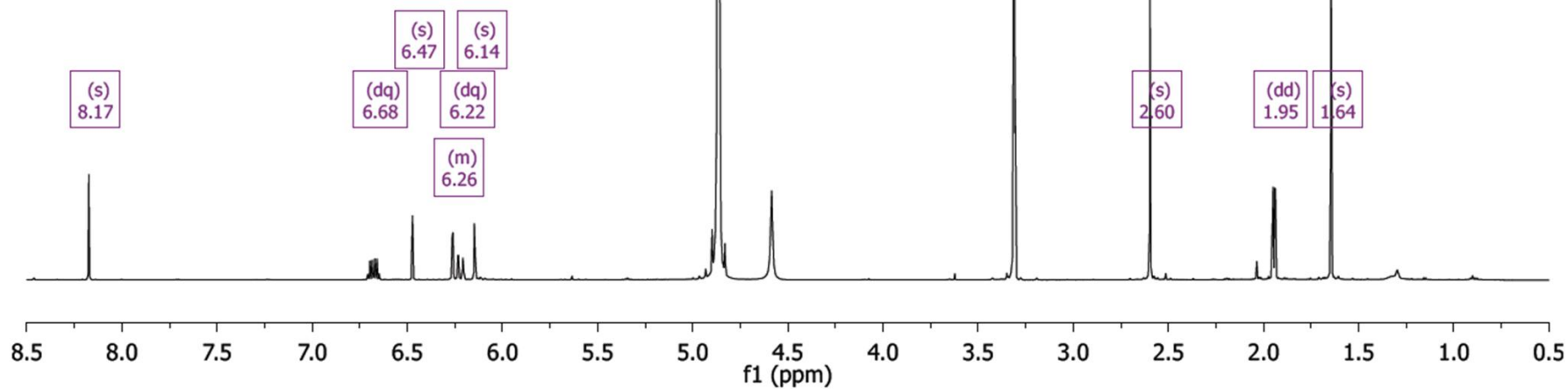


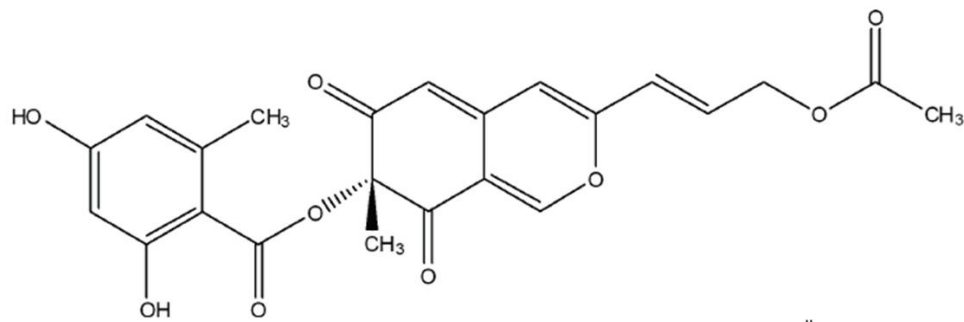
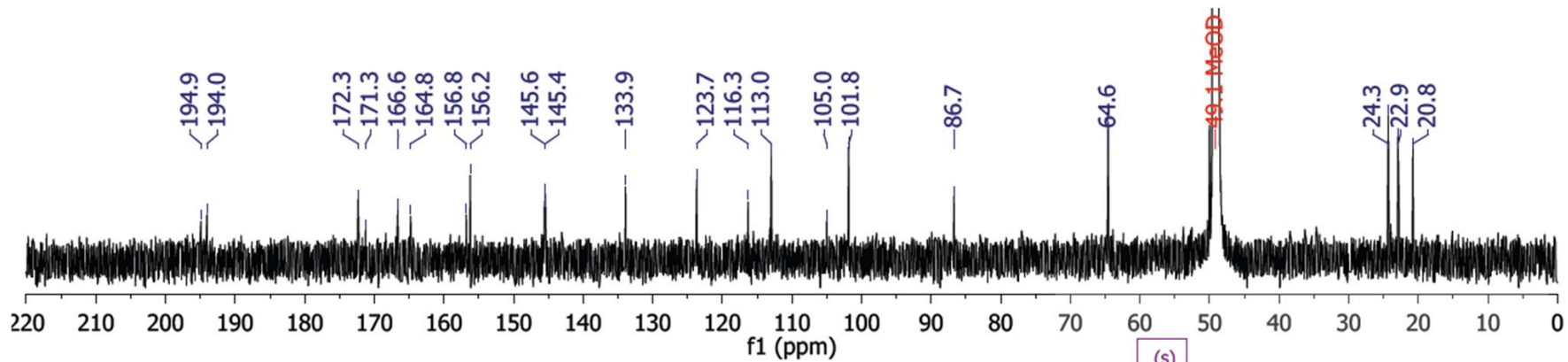
Mitorubrinol



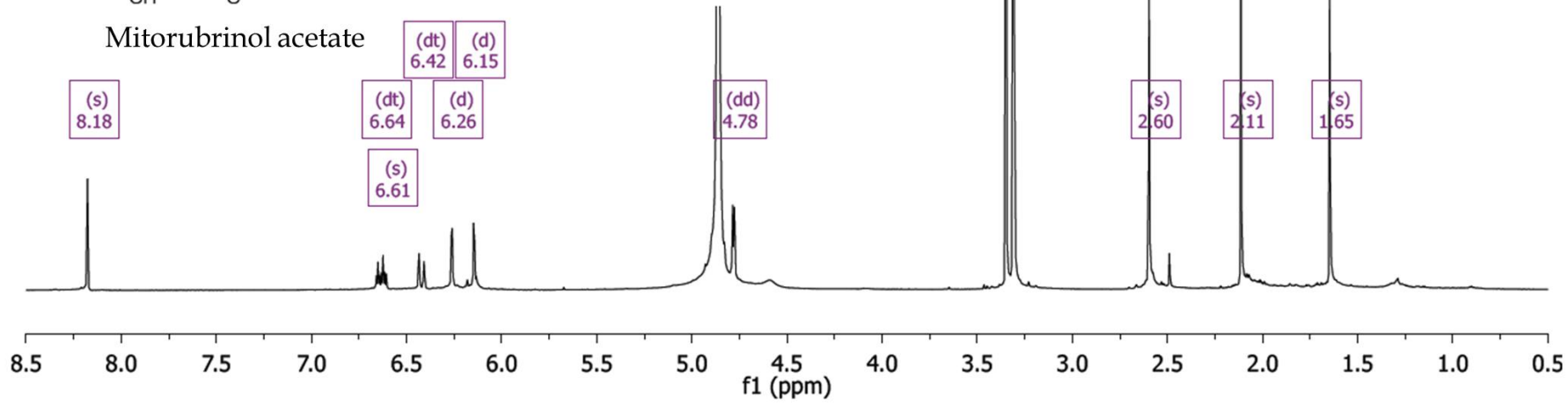


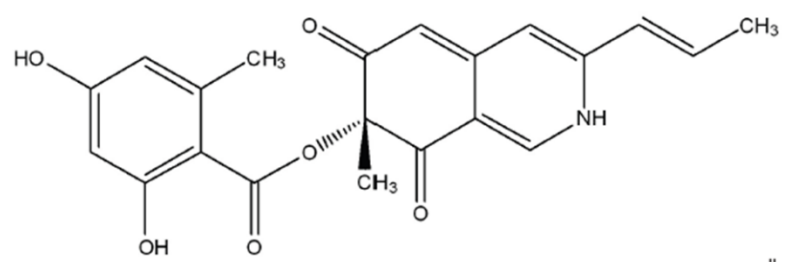
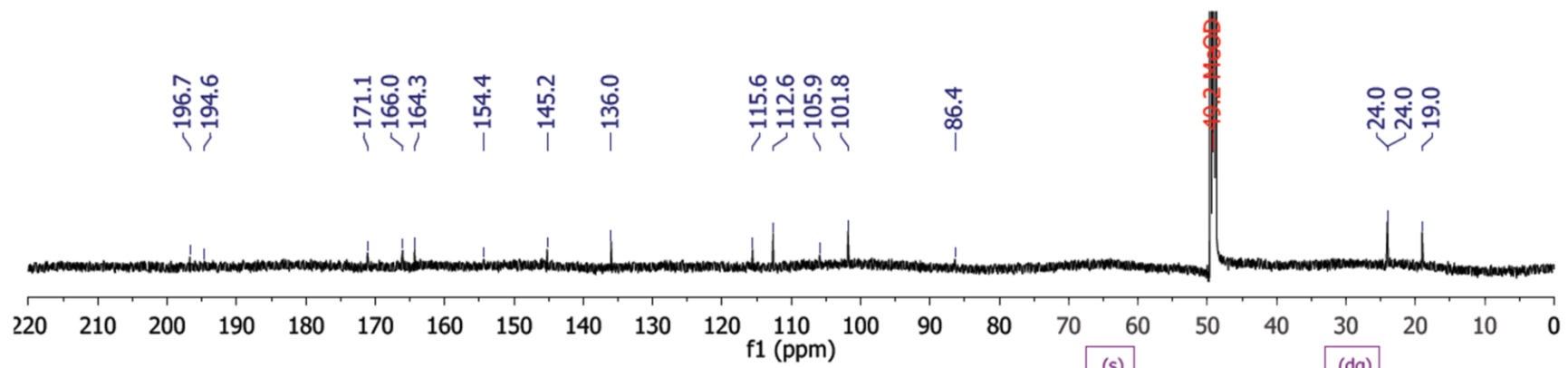
Mitorubrin



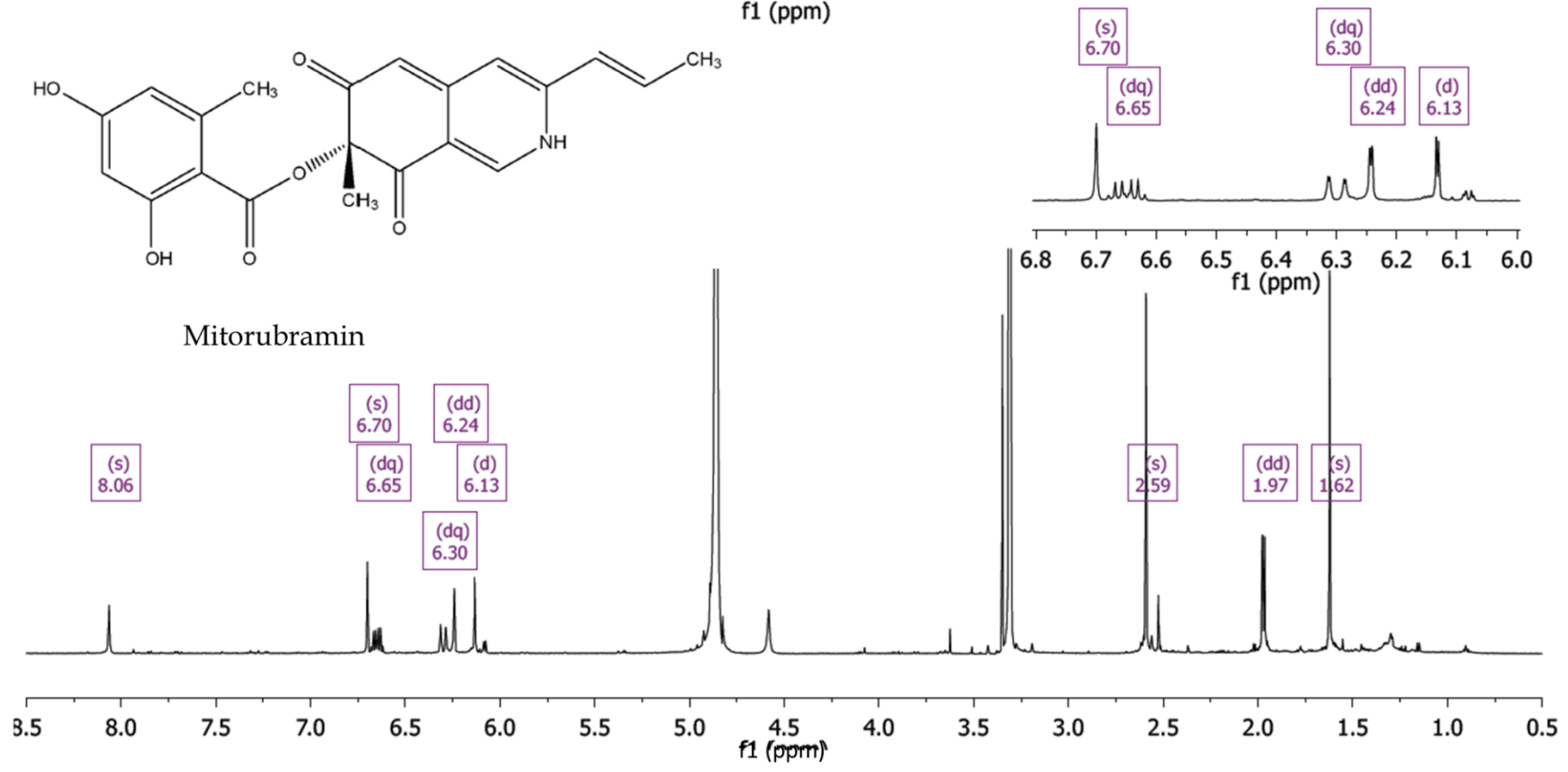


Mitorubrinol acetate





Mitorubramin



Annex 2 - High-resolution mass spectrometry and hydrogen/deuterium exchange study of mitorubrin azaphilones and nitrogenized analogues

High-resolution mass spectrometry and hydrogen/deuterium exchange study of mitorubrin azaphilones and nitrogenized analogues

Ljubica Svilar,^{a,b} Vesna Stankov-Jovanovic,^{b*} Denis Lesage,^a Héloïse Dossmann^a and Jean-Claude Tabet^{a*}

Azaphilones represent numerous groups of wild fungal secondary metabolites that exhibit exceptional tendency to bind to nitrogen atoms in various molecules, especially those containing the amine group. Nitrogenized analogues of mitorubrin azaphilones, natural secondary metabolites of *Hypoxyton fragiforme* fungus, have been detected in the fungal methanol extract in very low concentrations. Positive electrospray ionization interfaced with high-resolution mass spectrometry was applied for confirmation of the elemental composition of protonated species. Collision-induced dissociation (CID) experiments have been performed, and fragmentation mechanisms have been proposed. Additional information regarding both secondary metabolite analogue families has been reached by application of gas-phase proton/deuterium (H/D) exchanges performed in the collision cell of a triple quadrupole mass spectrometer. An incomplete H/D exchange with one proton less than expected was observed for both protonated mitorubrin azaphilones and their nitrogenized analogues. By means of the density functional theory, an appropriate explanation of this behavior was provided, and it revealed some information concerning gas-phase H/D exchange mechanism and protonation sites. Copyright © 2012 John Wiley & Sons, Ltd.

Supporting information may be found in the online version of this article.

Keywords: mitorubrins; LC-ESI-FT/MS; CID; gas-phase H/D exchange; density functional theory

INTRODUCTION

Azaphilones are secondary metabolites and natural fungal pigments which representatives have various structures and manifest a number of biological activities such as antimicrobial, antibacterial, nematocidal, antimalarial, cytotoxic and antioxidant.^[1–4] Their name ('nitrogen loving') comes from their ability to react spontaneously with the amino groups from amino acids, proteins or nucleic acids to form nitrogenized analogues by the exchange of pyran-oxygen by a nitrogen atom. Among the different families of azaphilones, mitorubrins present a class that can be often found in the *Hypoxyton fragiforme* fungus and which is usually used as a fingerprint of these species.^[5–7] The general structure of mitorubrins consists an orsellinic acid moiety attached to a bicyclic azaphilone core by an ester bond. The different members of the mitorubrin family differ by the substituent R group located at the side chain end of the bicyclic core (Scheme 1a). By reacting with an amino group,^[8] a nitrogenized mitorubrin analogue is formed (Scheme 1b).^[9]

Various structural studies of mitorubrins can be found in the literature,^[10,11] some of them use mass spectrometry techniques mostly *via* electrospray ionization (ESI) and time of flight or quadrupole mass analyzers.^[12,13] Quite surprisingly, we were not able to find any work related to a structural characterization of nitrogenized analogues, although different synthesis routes to form these compounds are described.^[14,15] This is mostly due to the fact that these molecules exist only as traces in natural samples, which thus avoid any further characterization with classical analytical

methods. By studying extracts of some samples of *H. fragiforme* fungus, we recently found out that they contain two classes of compounds, one corresponding to mitorubrins and the other to nitrogenized analogues. To our knowledge, this is the first time that these nitrogenized analogues could be detected in this fungi species. We have thus decided to undertake a complete structural study of these compounds using high-resolution mass spectrometry (FT/MS), coupled to high-performance liquid chromatography (HPLC). The use of HPLC was justified as we were working with complex mixtures of mitorubrins and analogues.

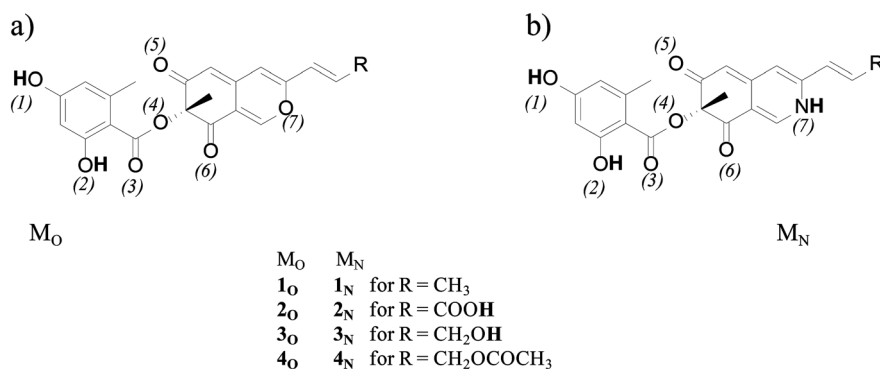
Furthermore, to secure higher confidence data, we decided to apply additional analytical techniques. The studied molecules have

* Correspondence to: Jean-Claude Tabet, Université Pierre et Marie Curie, Institut Parisien de Chimie Moléculaire, UMR 7201-FR2769, Case Courrière 45, Bâtiment F, 716, 4, place Jussieu, 75252 Paris CEDEX 05, France. E-mail: jean-claude.tabet@courrier.upmc.fr

* Vesna Stankov-Jovanovic, University of Nis, Faculty of Science and Mathematics, Department of Chemistry, Visegradska 33, 18000 Nis, Serbia. E-mail: sjvesna@pmf.ni.ac.rs

a Université Pierre et Marie Curie, Institut Parisien de Chimie Moléculaire, UMR 7201-FR2769, Case Courrière 45, Bâtiment F, 716, 4, place Jussieu, 75252 Paris CEDEX 05, France

b University of Nis, Faculty of Science and Mathematics, Department of Chemistry, Visegradska 33, 18000 Nis, Serbia



Scheme 1. General structure of (a) mitorubrin M_O and (b) the nitrogenized mitorubrin derivatives M_N (hydrogen atoms displayed with bold letters are possibly exchangeable).

been indeed represented in a very low concentration in fungi extract and were thus impossible to separate in adequate amounts for analysis. This reduced the number of reliable and powerful analytical methods such as NMR and IR/UV-VIS spectroscopy by which we could strengthen our first findings. The information that protonated nitrogenized analogues contain one exchangeable proton (see possible exchangeable hydrogen atoms at Schemes 1a and b) more than the oxygenized azaphilones gave us idea to apply the gas-phase proton/deuterium (H/D) exchange method.^[16,17] The H/D exchange between selected gaseous ions and suitable deuterated agents is a well-established mass spectrometry method.^[18] It is an ancillary and practical technique for determination of different compounds, with functions containing mobile protons often bounded to heteroatom(s) such as alcohols, phenols, carboxylic acids, amines, amides and mercaptans, which are present in natural organic compound.^[19,20] Gas-phase H/D exchange rate constants depend mostly on the nature of exchangeable protons and the used labeled reagent (i.e. the respective proton affinities (PAs) of reagent and exchangeable site). Furthermore, the presence of intermolecular hydrogen bonds, steric effects as well as other entropic effects can influence the gas-phase H/D exchanges that can, for instance, occur with the relay mechanism.^[16,19]

In the present work, we are showing a mass spectrometric study of mitorubrins and nitrogenized analogues originating from *H. fragiforme* fungus. This study includes the use of FT/MS coupled to HPLC as well as gas-phase H/D exchange reactions to validate our findings. Some calculations based on the density functional theory have also been performed to help understand the mechanisms involved in the course of the gas-phase H/D exchanges.

EXPERIMENTAL

H. fragiforme fungal samples were collected from the dead *Fagus sylvatica* tree in the forest in southeastern Serbia, and fungi material was deposited in the Herbarium Moesiacum, University of Nis (voucher number 5530). Methanol and acetonitrile were of HPLC grade (VWR, EC). Water was obtained from a Milli-Q gradient system (Millipore, Brussels, Belgium). Formic acid was from SDS (Carlo Erba Reactifs, France). ND₃ (99.75%) was obtained from Eurisotop (CEA Group, France). Standard mixtures used for the external calibration of the MS instrument, Calmix (caffeine, L-methionyl-arginyl-phenylalanyl-alanine acetate) and Ultramark 1621, were from Thermo Fisher Scientific (Les Ulis, France).

Samples of fungi were crushed with pestle and mortar. Ten milligrams of the obtained powder was extracted with methanol

two times for 10 min in ultrasonic bath at room temperature with a 5-min centrifugation after each extraction. Collected supernatants were evaporated and purified by solid-phase extraction to remove highly nonpolar components that could be harmful to the HPLC column. They were then eluted *via* a Strata Phenomenex C18 cartridge with 2 ml acetonitrile : water (40 : 60, v/v). Final concentration is estimated to be up to 0.2 mg/ml.^[21] The sample was finally analyzed by liquid chromatography coupled to ESI-mass spectrometry (LC/MS). To this end, 5 μ l of the sample was injected into a reverse-phase C18 Symmetry (2.1 \times 150.5 μ m) column from Waters (Ireland). Separation of the different species was done in isocratic mode using acetonitrile : water (1:1, v/v) with 0.1% formic acid at a flow rate 200 μ l/min.

Accurate mass measurements were performed on an LTQ Orbitrap XL from Thermofisher Scientific (San Jose, CA, USA),^[21] with the external calibration of the instrument, which specification of accuracy is up to 5 ppm. Parameters for positive ESI were the following: ESI needle 4 kV, capillary voltage 20 V, capillary temperature 275 °C, nebulizer gas N₂ 70 arbitrary units (a.u.), auxiliary gas 20 a.u. and tube lens offset 80 V. Mass spectra were recorded in the 145–900 Th range. Collision-induced dissociation (CID) experiments were done in the linear ion trap using helium as a collision gas in the 100–500 Th range, with 1 Th isolation width and 15% of normalized collision energy.^[22] The mass resolving power (full width at the half maximum height) was set at 6×10^4 for signal at mass m/z 400.^[23]

Gas-phase H/D exchange reaction studies on azaphilone compounds were undertaken on modified triple quadrupole mass spectrometer Quattro II (Micromass, Manchester, UK). The data were acquired using the Masslynx software (version 4.2). The ESI capillary voltage was maintained at 3.5 kV. Compounds were ionized with a cone voltage of 30 V, and in-source CID was performed with a cone voltage of 60 V. Nitrogen was used as the nebulization and desolvation gas. The source and desolvation temperatures were kept at 80 °C and 20 °C, respectively. ND₃ was introduced into the hexapolar collision cell at a pressure of 3×10^{-3} mbar for collision-activated reactions (CAR) on selected precursor ion.^[24,25] CAR describes multiple collision ion–molecule reactions that occur in the radiofrequency (rf)-only quadrupole cell of triple quadrupole between selected ion beam (from the first quadrupole filter) and neutral reagent introduced *via* the helium line at the pressure, as higher as possible.^[26] These ion–molecule reactions occur at very low energy collision conditions for exothermic processes (E_{lab} of few electron volts) in contrast to CID. However, for slightly endothermic ion–molecule reactions, higher ion kinetic energies are required, without reaching the CID threshold.^[27] Under these low-energy

collision conditions (i.e. herein as $E_{\text{lab}}=3$ eV or $E_{\text{CM}}\approx 0.15$ eV), multiple neutral-ion interactions take place, yielding relaxation of both ion kinetic and internal energy, resulting in relatively long-life ion-dipole complexes. Analyzed protonated molecules and in-source fragment ions were mass selected in the first quadrupole with isolation width equal to 1 Th and then sent to a rf-only hexapolar collision cell where they were submitted to ion-molecule reactions with labeled reagent gas. The use of a set of lens voltage 7, 8 and 9 (250, 0 and 0 V, respectively) was crucial for successfully storing the selected precursor ions for the CAR experiments. The reaction product ions were mass analyzed by voltage scanning in the second quadrupole mass analyzer.

In parallel to experiments, quantum chemistry calculations have been performed using the Gaussian 09 program.^[28] Geometry optimizations were obtained with the B3LYP functional^[29,30] and the def2-SVP split valence basis set.^[31] Single-point energies were obtained with the same method and the Def2-TZVPE basis set. Structures were characterized either as minima or transition structures from vibrational analysis. PAs were calculated for different sites of the mitorubrin compounds using atomization energies. Results presented were corrected by a linear factor obtained by comparing the results with well-defined PAs.^[32]

RESULTS AND DISCUSSION

H. fragiforme methanol extract was at first separated using HPLC. The corresponding total ion current is shown in Fig. 1, and retention times and accurate elemental compositions are listed in Table 1.

Each separated ion could further be identified *via* its elemental composition obtained by the high resolution of the instrument and given within 1 ppm of accuracy. In the first 3.5 min of chromatographic separation, ions with an elemental composition corresponding to nitrogenized analogues, M_N (**1_N**, **2_N**, **3_N** and **4_N**, see Scheme 1) were observed, whereas ions corresponding to mitorubrin azaphilones, M_O (**1_O**, **2_O**, **3_O** and **4_O**, see Scheme 1) have a retention time larger than 3 min. A possible explanation for the nitrogenized analogues fast elution is their high polarity due to the presence of cyclic diene amine in comparison with cyclic diene ether group in mitorubrin.

The separated mitorubrins and their nitrogenized analogues have been then mass selected and studied by means of CID experiments of M_OH^+ and M_NH^+ (m/z [368+R] and m/z [367+R], respectively). The resulting CID spectra are shown in Fig. 2.

For all compounds, a common m/z 151 ion is observed. Its formation occurs by stepwise process *via* isomerization of protonated molecules into an ion-dipole complex,^[33] prior to

dissociation, as given in Scheme 2. Within this complex, proton transfer may occur, leading to the formation of m/z [218+R] (or m/z [217+R]) ion, also observed in the CID spectra.

The relative abundances of m/z 151 and m/z [218+R] (or m/z [217+R] for nitrogenized analogues) ions vary accordingly to the side chain group. In general, nitrogenized analogues exhibit a stronger fragmentation than do the protonated mitorubrin azaphilones. In the particular case of mitorubric acid (m/z 413), the abundance of m/z 151 is higher than that of the complementary m/z [218+R] ion (m/z 263). This can be explained by the mesomeric effect of carboxylic group of the side chain, which can decrease the PA of oxygen $O_{(5)}$ (see Scheme 1), and the formation of the common m/z 151 ion is thus strongly favored. In case of mitorubric acid nitrogenized analogue (m/z 412), this effect is decreased with the mesomeric effect assistance of nitrogen atom at $N_{(7)}$, thus the complementary m/z 262 and m/z 151 fragment ions appear in comparable abundances.

Gas-phase H/D exchange reactions have further been performed in a collision cell of triple quadrupole instrument under very low collision energy conditions ($E_{\text{lab}}=3$ eV). Parent ions were isolated in the first mass filter of triple quadrupole and have undergone reactive collisions with a labeled reagent gas. ND_3 was chosen as a gas-phase labeled reagent because of its relatively high PA (204 kcal/mol),^[27] thereby expecting exchange of the majority labile protons. The obtained spectra are presented in Fig. 3.

Expected exchangeable protons on protonated mitorubrins are (i) the one of protonation, (ii) $O_{(1)}$ and $O_{(2)}$ atoms and (iii) those within the side chain. At least three protons are thus possibly exchanged. Concerning nitrogenized mitorubrin analogues, four protons at least should be exchanged as these compounds possess in addition a secondary amine unit with an exchangeable proton. All precursor ions exhibit a number of exchanged protons lower by one than expected. Hence, protonated mitorubrins **1_OH⁺**, **3_OH⁺** and **4_OH⁺** exchange of only two protons, whereas **2_OH⁺** exchanges three. The corresponding nitrogenized mitorubrin analogues exchange one proton more than the corresponding oxygenated derivatives.

Generally, ionizing proton is exchanged with a suitable labeled reagent. However, this proton can be a spectator of the H/D exchange process, in the case of relay mechanism, where the exchange takes place from a labile proton distant to the former one (*vide infra*). In the present case, the H/D exchange at the $N_{(7)}$ site is somewhat unexpected because of its low PA value (Table 2), compared with ammonia. To explain this behavior, delocalization of the $N_{(7)}$ atom electron lone pair, when the $O_{(5)}$ atom is protonated, should be considered. Under these conditions, the withdrawing-electron effect takes place, yielding electron

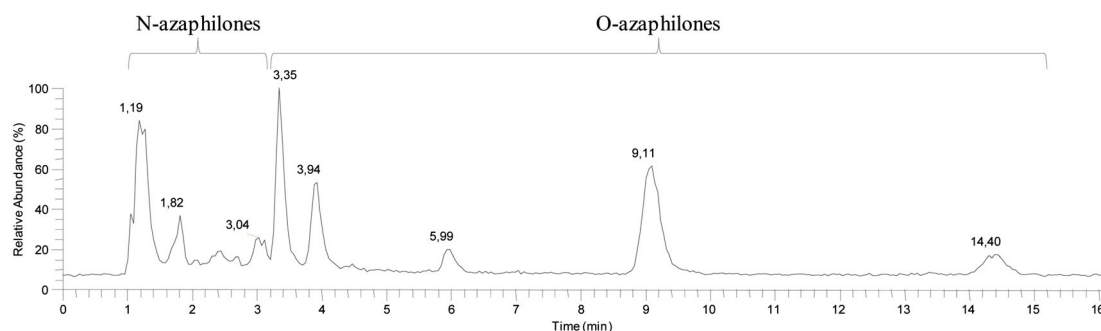
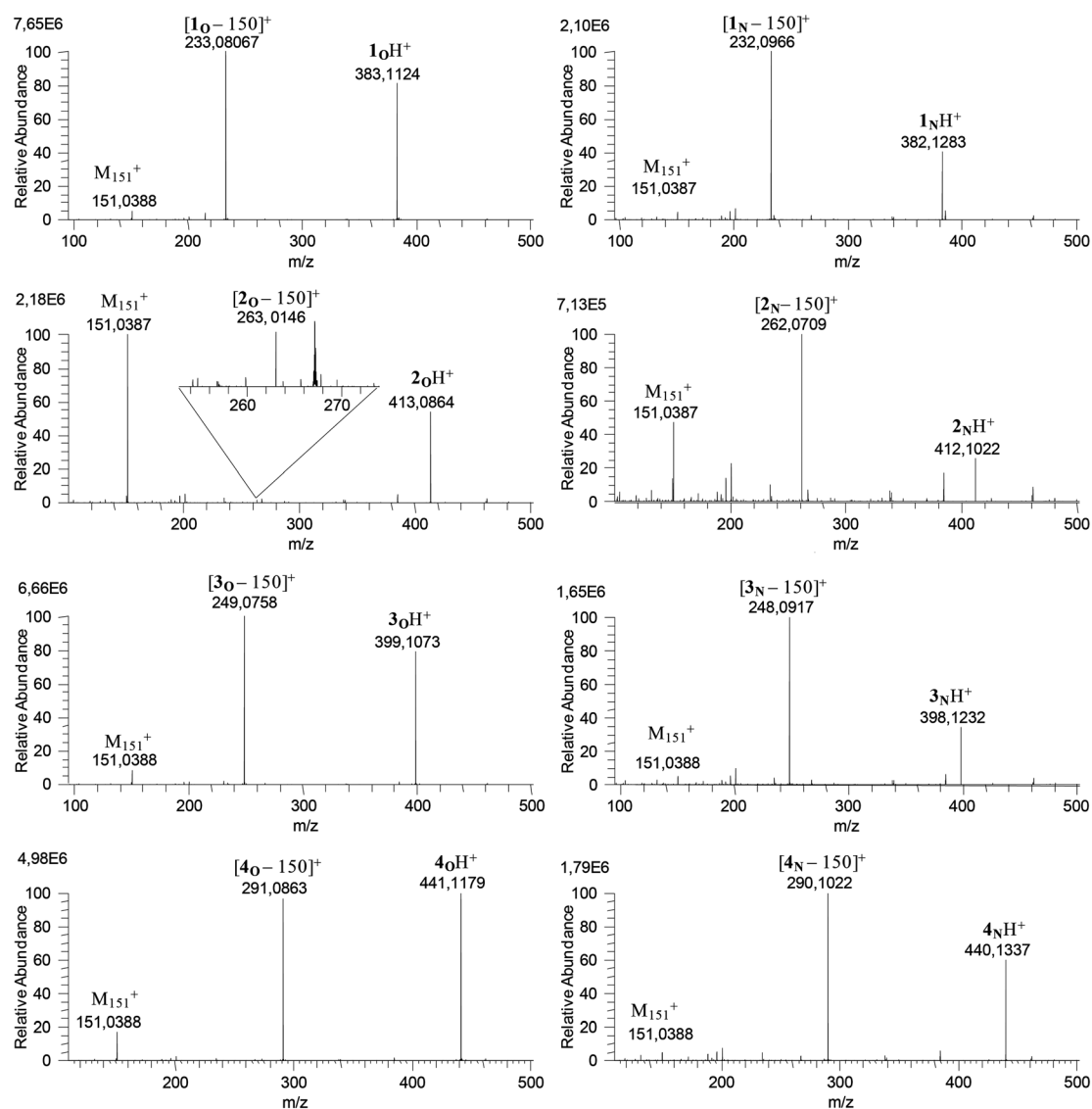


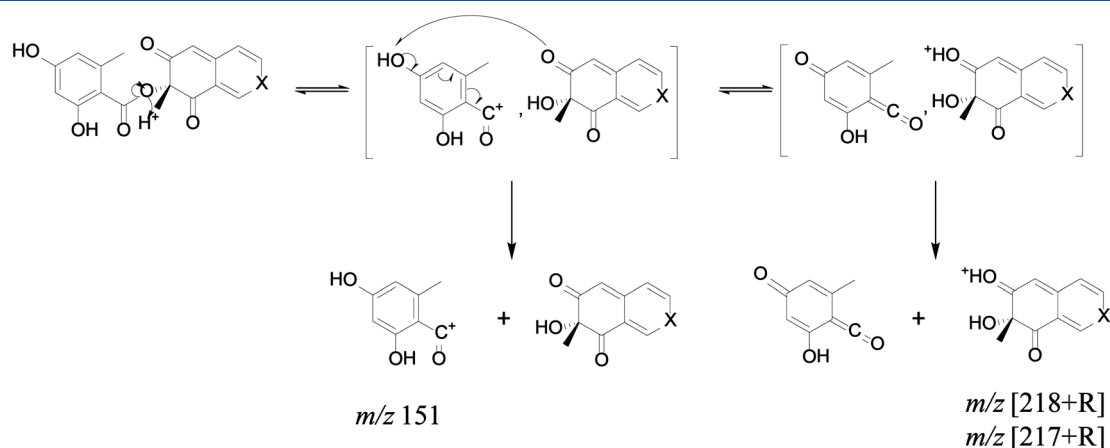
Figure 1. Total ion chromatogram of the *Hypoxylon fragiforme* methanol extract.

Table 1. Retention time, m/z and deduced elemental composition for protonated molecules of *Hypoxylon fragiforme* methanol extract separated by LC-MS and their corresponding specific fragment ions

Retention time (min)	m/z	Elemental composition	Ion	Relative error ^a (ppm)	Product ion (m/z)	Elemental composition	Relative error ^a (ppm)
1.82	398.1236	C ₂₁ H ₂₀ O ₇ N	3 _N H ⁺	0.5	248.0917	C ₁₃ H ₁₄ O ₄ N	0.0
2.35	412.1028	C ₂₁ H ₁₈ O ₈ N	2 _N H ⁺	0.2	262.0709	C ₁₃ H ₁₂ O ₅ N	-0.3
3.04	440.1340	C ₂₃ H ₂₂ O ₈ N	4 _N H ⁺	0.0	290.1022	C ₁₅ H ₁₆ O ₅ N	-0.2
3.07	382.1286	C ₂₁ H ₂₀ O ₆ N	1 _N H ⁺	0.1	232.0967	C ₁₃ H ₁₄ O ₃ N	-0.7
3.35	399.1075	C ₂₁ H ₁₉ O ₈	3 _O H ⁺	0.1	249.0759	C ₁₃ H ₁₃ O ₅	0.4
3.94	413.0868	C ₂₁ H ₁₇ O ₉	2 _O H ⁺	0.3	263.0548	C ₁₃ H ₁₁ O ₆	-0.8
9.11	441.1180	C ₂₃ H ₂₁ O ₉	4 _O H ⁺	-0.1	291.0862	C ₁₅ H ₁₅ O ₆	-0.3
14.40	383.1125	C ₂₁ H ₁₉ O ₇	1 _O H ⁺	-0.2	233.0807	C ₁₃ H ₁₃ O ₄	-0.8

^aRelative error is obtained by comparing the observed m/z value with the calculated monoisotopic m/z value corresponding to the elemental composition.

**Figure 2.** CID (normalized collision energy 15%) spectra of protonated molecules of mitorubrin (M_O : 1_OH⁺, 2_OH⁺, 3_OH⁺ and 4_OH⁺) and nitrogenized derivatives (M_N : 1_NH⁺, 2_NH⁺, 3_NH⁺ and 4_NH⁺).



Scheme 2. Proposed mechanism for the observed dissociation of protonated azaphilones and nitrogenized azaphilones *via* ion–dipole isomerization ($R=CH_3$, CH_2OCOCH_3 , $COOH$, CH_2OH , and $X=O$, NH).

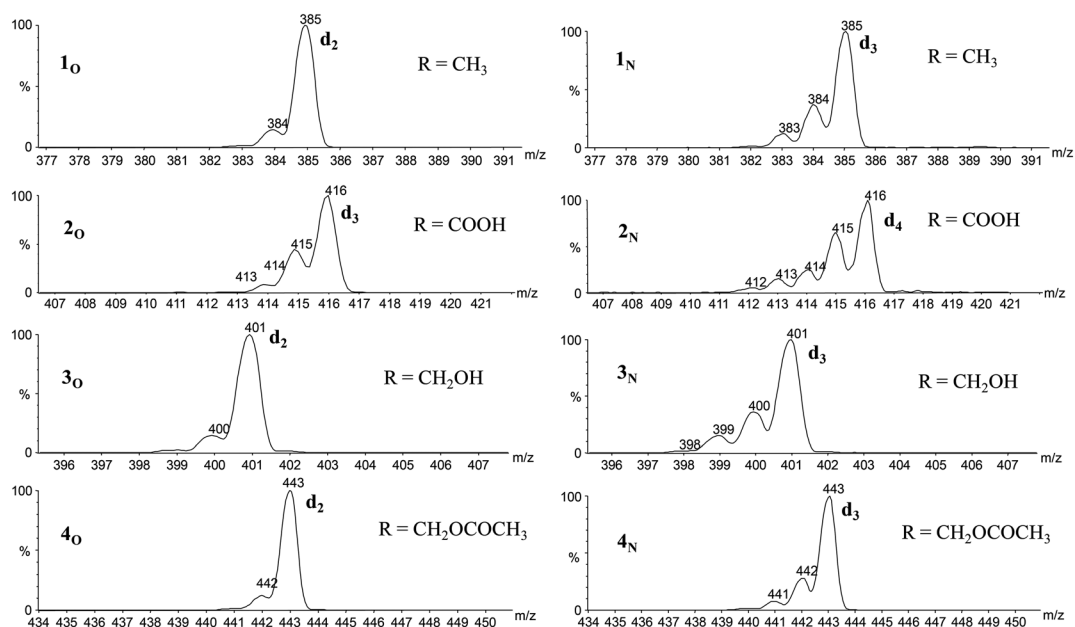


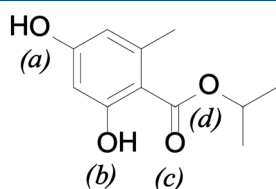
Figure 3. Gas-phase H/D exchange CAR spectra ($E_{lab}=3$ eV) of selected protonated mitorubrins (1_OH^+ , 2_OH^+ , 3_OH^+ , 4_OH^+) and the corresponding protonated nitrogenized derivatives (1_NH^+ , 2_NH^+ , 3_NH^+ , 4_NH^+).

Table 2. Calculated proton affinities of different sites of 1_O and 1_N molecules		
Site	Proton affinities (kcal/mol)	
	1_O	1_N
$O_{(1)}$	182.6	184.7
$O_{(3)}$	225.1	239.2
$O_{(4)}$	213.8 ^a	214.1 ^a
$O_{(5)}$	231.9	238.5
$O_{(6)}$	215.7	217.8
$O_{(7)}$ or $N_{(7)}$	167.2	188.7

^aOn the $O_{(4)}$ site, protonation results in the formation of an ion–dipole complex.

delocalization from the distant $N_{(7)}H$ site to $O_{(5)}H$. Consequently, it results with possibility of the ND_3 reagent to remove the former proton, leading to formation of ion–dipole complex between HND_3^+ and neutral. The latter one is tautomer to the initial nitrogen mitorubrin analogue molecular form. In this way, the $N_{(7)}$ atom within the formed pyridine ring can receive deuteron from the HDN_3^+ part of the complex (see Supporting Information, Scheme S3).

To understand these unexpected features, we have undertaken a theoretical study on a model system shown in Scheme 3. This system contains only the orsellinic part of the mitorubrins, because there was no need to consider the bicyclic azaphilone core of the compounds, because gas-phase H/D exchanges take place on this side of the molecule including either the R group, or the amine, in the case of the nitrogenized analogues. Hence, no protons are exchanged for $R=CH_3$ or CH_2OCOCH_3 because these groups do



Scheme 3. Structure of molecule **5** used as a model system for calculations.

not contain labile protons. For $R=COOH$, one proton was exchanged as expected. In the case of $R=CH_2OH$, one proton exchange could be assumed. However, in this case, the mechanism would imply most likely that protonation of 3_OH^+ (or 3_NH^+) is carried by oxygen leading immediately to a loss of water, favored by its allylic position. Thus, no proton is actually exchanged at this site because fast water release occurs instead.

To achieve better insight in mechanism, model system **5** has been chosen with an isopropyl ester form because it possesses similar PA values of its $O_{(a)}$, $O_{(c)}$ and $O_{(d)}$ sites as on the $O_{(1)}$, $O_{(3)}$ and $O_{(4)}$ sites of mitorubins and nitrogenized analogues (respectively, 182.6, 225.1 and 215.7 kcal/mol to be compared with the PA values given in Table 2). It may be noticed that PA values were defined for each oxygen (and nitrogen) atom of the molecule except for $O_{(2)}$ because calculations showed that protonation at this site leads to a prompt proton transfer to the $O_{(3)}$ atom.

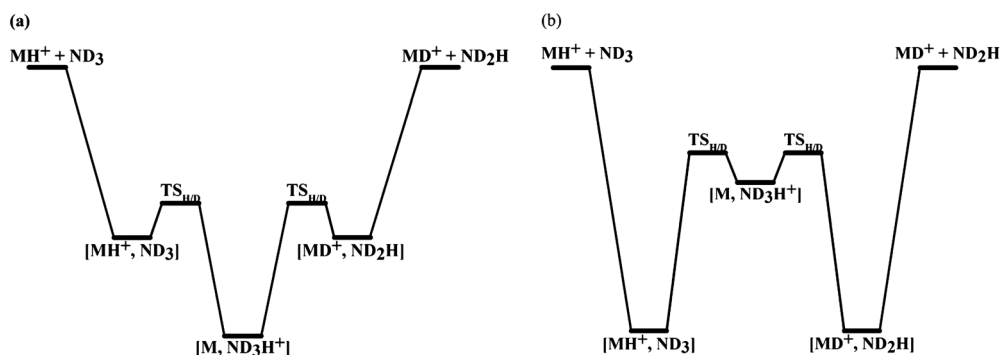
Gas-phase H/D exchange processes have been extensively studied since now.^[17,34] The general mechanism of H/D exchange between an MH^+ ion and ND_3 is depicted in Scheme 4. Two cases can be distinguished, depending on the nature of the proton exchanged. If the PA of M is lower than that of ND_3 , the solvated $[MH^+, ND_3]$ form can isomerize into $[M, NHD_3^+]$, which is much more

stable and can lead to formation of the $[MD^+, NHD_2]$ complex (Scheme 4a). The latter one gives labeled MD^+ and NHD_3^+ ions by competitive dissociation. Reversely, when PA of M is higher than that of ND_3 , the TS energy is significantly increased and becomes close to the initial energetic level. This can be lowered by assistance (relay mechanism)^[19] (Scheme 4b), meaning that the ionizing proton is not necessarily exchanged during this stepwise process (*vide supra*).

The behavior of each protonated form describes the reaction of the $[5H^+, ND_3]$ complex within a protonated canonic structure when (i) the ionizing proton is exchanged or (ii) a relay mechanism takes place. However, zwitterion-like form could be involved into assumed canonic structure $[(5-H)^+H^+, NHD_3^+]$. In this case, the proton transferred to ND_3 comes from the $O_{(a)}H$ site to give rise to formation of the salt-bridge complex, in which the ionizing proton at the ester site is a spectator. From such ion-dipole complex, H/D exchange can take place in the salt-bridge position. This can occur only if the formation of the complex requires relatively low-energy TS. Because the calculated transition state with $O_{(a)}$ appears slightly endothermic (Table 3), previous considerations need to be disregarded, as well as assumed salt-bridge intermediate.

On the other hand, as protonation takes place during ESI, within the protonated canonic form, the H/D exchange is hindered because of very low PA value of the $-OH$ site (184.7 kcal/mol) in comparison with that of ND_3 . The deuteron attachment to this position is thus highly endothermic.

The results of theoretical calculations obtained for the gas-phase H/D exchange reaction on the three possible oxygen atoms, $O_{(a)}$, $O_{(b)}$ and $O_{(c)}$, of the protonated $5H^+$ molecule are presented in Table 3. For each reaction (which will be further annotated according to the mark of the oxygen atom, i.e. reaction (a), (b) or (c)) energies are given to the starting system ($5H^+ + ND_3$). Formation of the ion-dipole $[5H^+, ND_3]$ complex (an ion solvation



Scheme 4. General mechanism of an H/D exchange process between MH^+ ion and ND_3 , in the case of exchange of (a) $PA(NH_3) > PA(M)$ and (b) $PA(NH_3) < PA(M)$.

Table 3. Relative energies (in kcal/mol) of the ions, complexes and transition structures involved in the H/D exchange process between $5H^+$ and ND_3 on three different sites

Site	$5_HH^+ + ND_3$	$[5_HH^+, ND_3]$	$TS_{H/D}$	$[5_H, NHD_3^+]$	$TS_{H/D}$	$[5_DH^+, ND_2H]$	$5_DH^+ + ND_2H$
$O_{(a)}$	0.0	-16.0	0.3	-9.4	0.3	-16.0	-0.1
$O_{(b)}$	0.0 ^a	-19.7	-8.9	-16.2	-8.9	-19.7	-0.1
$O_{(c)}$	$5_HH^+ + ND_3$	$[5_HH^+, ND_3]$	$TS_{H/D}$	$[5_H, NHD_3^+]$	$TS_{H/D}$	$[5_HD^+, NH_2D]$	$5_HD^+ + NH_2D$
	0.0	-4.9	-11.0	-16.2	-11.0	-4.9	-0.1

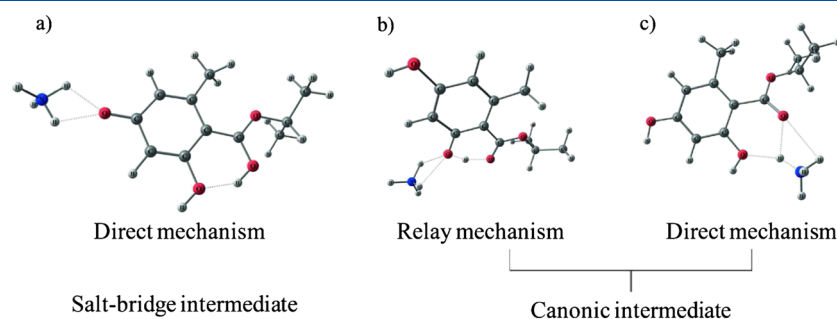


Figure 4. Transition states for the H/D exchanges between 5H^+ and ND_3 occurring on the sites (a) $\text{O}_{(a)}$, (b) $\text{O}_{(b)}$ and (c) $\text{O}_{(c)}$ of model system **5**.

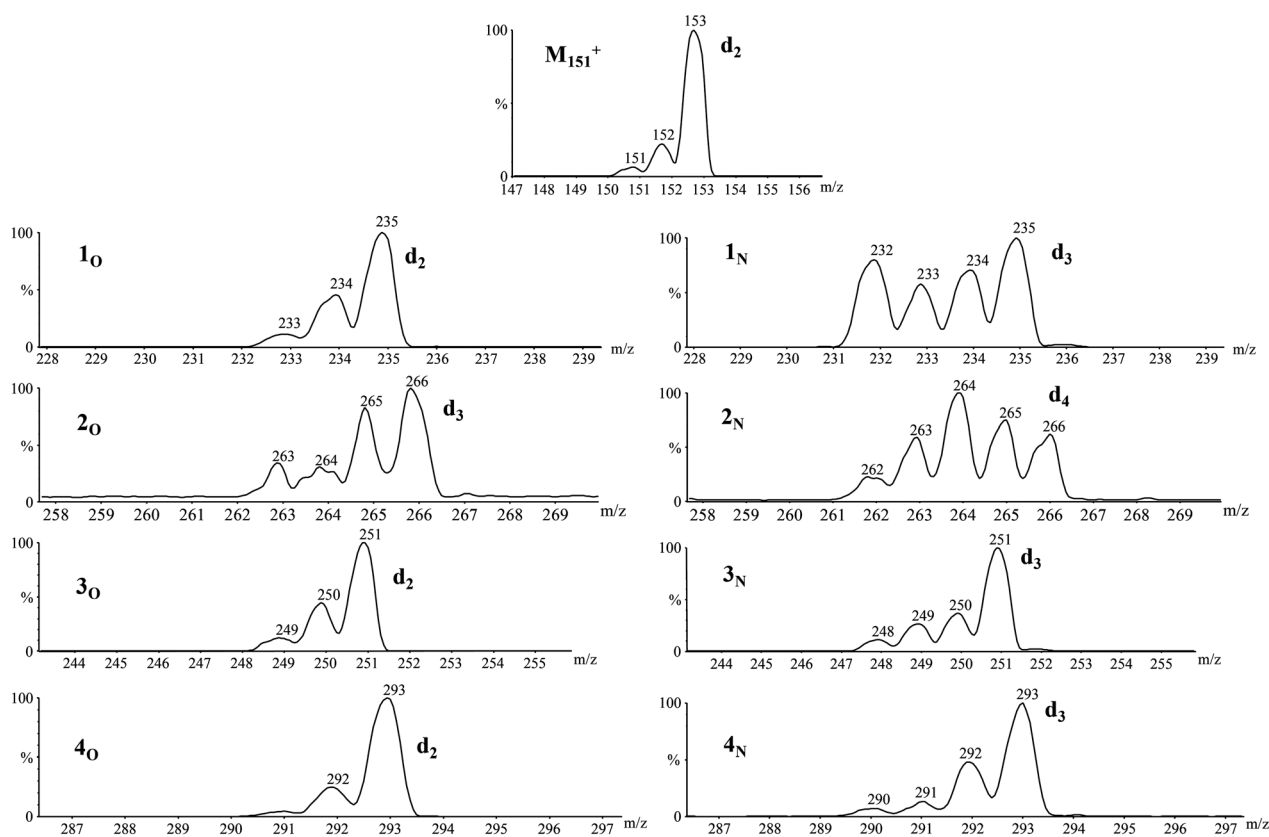


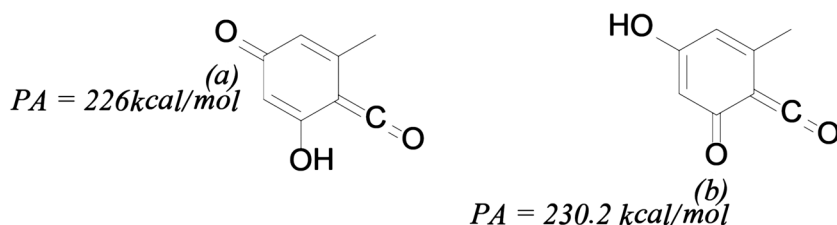
Figure 5. Gas-phase H/D exchanges from CAR spectra ($E_{\text{lab}} = 3$ eV) of fragment m/z 151 and $[\text{MH} - (150)]^+$ ions from protonated azaphilones and nitrogenized derivatives.

Table 4. Relative energies (in kcal/mol) of the ions, complexes and transitions structures involved in the gas-phase H/D exchange process between m/z 151 (M_{151}^+) and ND_3 on three different sites

Site	$151^+ + \text{ND}_3$	$[151^+, \text{ND}_3]$	$\text{TS}_{\text{H/D}}$	$[152^+, \text{NHD}_2]$	$152^+ + \text{NHD}_2$
$\text{O}_{(a)}$	0.0	-20.9	-8.0	-20.9	-0.2
$\text{O}_{(b)}$	0.0	-20.7	-8.6	-20.7	-0.2

step) allows isomerization into the $[\text{5}, \text{NHD}_3^+]$ complex, which is an exothermic process releasing more energy in the case of (b) and (c) pathways (up to 16.2 kcal/mol) in comparison with the

(a) pathway (9.4 kcal/mol). The transition states energies, $\text{TS}_{\text{H/D}}$, (Fig. 4), are located at -8.9 and -11.0 kcal/mol, under the initial energy of the system for the (b) and (c) paths, respectively, in contrast to $+0.3$ kcal/mol, for path (a). Furthermore, as the barriers for the reactions (b) and (c) are crossed over, the $[\text{5}_\text{D}\text{H}^+, \text{ND}_2\text{H}]$ and $[\text{5}_\text{H}\text{D}^+, \text{ND}_2\text{H}]$ complexes are formed competitively, releasing the exchanged $\text{5}_\text{D}\text{H}^+$ and $\text{5}_\text{H}\text{D}^+$, respectively. Transition state of reaction (b) leads to the H/D exchange because this process occurs with assistance of the ionizing proton interaction from the $\text{O}_{(c)}$ site, through the hydrogen bond with the $\text{O}_{(b)}$ site. This process is impossible in the case of $\text{O}_{(a)}$. These considerations suggest that the exchange is favorable at the $\text{O}_{(b)}$ and $\text{O}_{(c)}$ sites exclusively.



Scheme 5. Structures of neutrals from m/z 151 and their PA.

Complementary $[M_OH-150]^+$ (or $[M_NH-150]^+$) and common orsellinic part (m/z 151) fragment ions formed in source have been studied in gas-phase H/D exchange experiments, under the same CAR condition used previously. Hence, they were isolated in the first mass filter of triple quadrupole and undergone the low-energy collisions. The obtained CAR spectra are presented in Fig. 5.

In the bicyclic fragment ion of mitorubrin azaphilones, at least two sites with labile protons are present, at the $O_{(4)}$ and $O_{(5)}$ positions, after the rearrangement during the fragmentation processes, whereas for the nitrogenized analogues, there is also an $N_{(7)}$ site with the labile proton that could be exchanged. Thus, $1_O H^+$, $3_O H^+$ and $4_O H^+$ exchange two protons by deuterons, whereas $2_O H^+$ exchanges three. Concerning nitrogenized analogues, fragment ions of $1_N H^+$, $3_N H^+$ and $4_N H^+$ exchange three protons by deuterium, whereas $2_N H^+$ exchanges four. Hence, no side chain H/D exchange happens at $R=CH_3$, CH_2OH and CH_2OCOCH_3 , but for $R=COOH$, one H/D exchange takes place.

On the other hand, orsellinic part ion (m/z 151) exchanges two protons by deuterium at the $O_{(1)}$ and $O_{(2)}$ positions, which can be referred to the $O_{(a)}$ and $O_{(b)}$ positions of the model system. This suggests that the protonated molecule isomerization into the ion–dipole complex does not occur prior to CID processes. Otherwise, if it were the case, additional H/D exchanges could be expected through three body complex formations (Scheme 2).

Results of theoretical calculations obtained for the gas-phase H/D exchange reaction of orsellinic acid fragment ion at m/z 151 are presented in Table 4.

For both reactions named (a) and (b), the formation of ion–dipole complex $[151^+, ND_3]$ is an exothermic process (-20.9 kcal/mol for (a) and -20.7 kcal/mol for (b)), relatively to the starting system ($151^+ + ND_3$). The release of energy during the H/D exchange in (a) is almost the same as in the case of (b) (-20.9 kcal/mol for (a) and -20.7 kcal/mol for (b)), and the transition states for both path are exothermic, -8.0 kcal/mol for (a) and -8.6 kcal/mol for (b). Relatively high transition state energy for this stepwise process is due to relatively high PA of neutral coming from m/z 151, which is presented in Scheme 5.

The PAs of such *p*- and *o*-quinon-like neutral forms are higher than that of ND_3 , 226 and 230 kcal/mol, respectively. In that way, final exchange at both sites leading to the H/D exchange on $O_{(a)}$ and $O_{(b)}$ could be explained, although, in both reactions, no isomerization in the second complex has been detected. This is probably due to the high stability of the complexes, resulting in fast H/D exchange in the particular transition state.

CONCLUSION

Mitorubrin azaphilone secondary metabolites from the *H. fragiforme* fungus were characterized applying high-resolution and gas-phase H/D exchange mass spectrometry. Differentiation between the

already known oxygenized derivatives and their nitrogenized analogues was investigated. CID studies were performed and showed similarity between the ion structures as well as the fragmentation pathways for both families of mitorubrin analogues. Concerning the H/D experiments performed by CAR, one proton less was exchanged in all analyzed compounds. H/D exchange mechanism involves the formation of ion–dipole complex, after the activation process. Complex yields a product ion in dependence of the PA values of both partners of the complex.

Theoretical studies of the gas-phase H/D exchange reaction mechanism have been applied to explain the earlier mentioned phenomenon. In that way, the H/D exchange has been shown as a powerful tool for structural distinction of both the mitorubrin metabolite groups, oxygenated and nitrogenized. Calculations showed that a relay mechanism can take place from a phenolic site that is adjacent to the ester group of mitorubrins or nitrogenized analogues. Finally, the low PA values of the dienamine group can explain at least partially why this proton was not exchanged.

Acknowledgements

The authors thank the Ministry of Education and Science Republic of Serbia (Grant 172051) and the SM³P Platform for financial support.

We are thankful to Professor Mark Stadler (Department Microbial Drugs, Helmholtz-Centre for Infection Research, Inhoffenstrasse 8, 38124 Braunschweig, Germany) for determination of the fungi. Ljubica Svilar expresses her sincere gratitude to the French Government and Embassy of France in Serbia for the scholarship provided for her Ph.D. program. We thank Dr E. Derat who is in charge of the calculation cluster at IPCM for the calculation time he provided us and his availability to answer any of our questions.

Supporting Information

Supporting information may be found in the online version of this article.

REFERENCES

- [1] S. Jongrungruangchok, P. Kittakoop, B. Yongsmith, R. Bavovada, S. Tanasupawat, N. Lartpornmatulee, Y. Thebtaranonth. Azaphilone Pigments From a Yellow Mutant of the Fungus *Monascus kaoliang*. *Phytochemistry* **2004**, *65*, 2569.
- [2] M. Stadler, D. N. Quang, A. Tomita, T. Hashimoto, Y. Asakawa. Changes in Secondary Metabolism During Stromatal Ontogeny of *Hypoxylon fragiforme*. *Mycol. Res.* **2006**, *110*, 811.
- [3] D. N. Quang, T. Hashimoto, Y. Nomura, H. Wollweber, V. Hellwig, J. Fournier, M. Stadler, Y. Asakawa. Cohaerins A and B, Azaphilones From the Fungus *Hypoxylon cohaerens*, and Comparison of HPLC-based Metabolite Profiles in *Hypoxylon Sect. Annulata*. *Phytochem.* **2005**, *66*, 797.
- [4] D. N. Quang, T. Hashimoto, M. Tanaka, M. Stadler, Y. Asakawa. Cyclic Azaphilones Daldinins E and F From the Ascomycete Fungus *Hypoxylon fuscum* (Xylariaceae). *Phytochemistry* **2004**, *65*, 469.

- [5] D. N. Quang, T. Hashimoto, Y. Asakawa. Inedible Mushrooms: A Good Source of Biologically Active Substances. *Chem. Rec.* **2006**, *6*, 79.
- [6] M. Stadler, N. Keller. Paradigm Shifts in Fungal Secondary Metabolite Research. *Mycol. Res.* **2008**, *112*, 127.
- [7] J. C. Frisvad, B. Andersen, U. Thrane. The Use of Secondary Metabolite Profiling in Chemotaxonomy of Filamentous Fungi. *Mycol. Res.* **2008**, *112*, 231.
- [8] L. Wu, D. Liu, A. Kord. Gas-Phase Meerwein Reaction of Epoxides with Protonated Acetonitrile Generated by Atmospheric Pressure Ionizations. *J. Am. Soc. Mass Spectrom.* **2010**, *21*, 1802.
- [9] A. Germain, D. Bruggemeyer, J. Zhu, C. Genet, P. O'Brien, J. Porco. Synthesis of the Azaphilones (+)-Sclerotiorin and (+)-8-O-Methylsclerotiorinamine Utilizing (+)-Sparteine Surrogates in Copper-Mediated Oxidative Dearomatization. *J. Org. Chem.* **2011**, *76*, 2577.
- [10] N. Osmanova, W. Schultze, N. Ayoub. Azaphilones: a Class of Fungal Metabolites with Diverse Biological Activities. *Phytochem. Rev.* **2010**, *9*, 315.
- [11] V. Hellwig, Y. M. Ju, J. D. Rogers, J. Fournier, M. Stadler. Hypomiltin, a Novel Azaphilone from *Hypoxylon hypomiltum*, and Chemotypes in *Hypoxylon* sect. *Hypoxylon* as Inferred from Analytical HPLC Profiling. *Mycol. Prog.* **2005**, *4*, 39.
- [12] J. Bitzer, B. Kopcke, M. Stadler, V. Hellwig, Y. M. Ju, S. Seip, T. Henkel. Accelerated Dereplication of Natural products, Supported by Reference Libraries. *Chimia* **2007**, *61*, 332.
- [13] M. Stadler, H. Wollweber. Secondary Metabolite Profiles, Genetic Fingerprints and Taxonomy of *Daldinia* and Allies. *Mycotaxon* **2001**, *77*, 379.
- [14] J. Zhu, A. Germain, J. Porco. Synthesis of Azaphilones and Related Molecules by Employing Cycloisomerization of *o*-alkynylbenzaldehyde. *Angew. Chem. Int. Ed.* **2004**, *43*, 1239.
- [15] L. Musso, S. Dallavalle, L. Merlini, A. Bava, G. Nasini, S. Penco, G. Giannini, C. Giommarelli, A. De Cesare, V. Zuco, L. Vesci, C. Pisano, F. Dal Piaz, N. De Tommasi, F. Zunino. Natural and Semisynthetic Azaphilones as a New Scaffold for Hsp90 Inhibitors. *Bioorg. Med. Chem.* **2010**, *18*, 6031.
- [16] A. Ranasinghe, G. Cooks, S. Sethi. Selective Isotopic Exchange of Polyfunctional Ions in Tandem Mass Spectrometry: Methodology, Applications and Mechanism. *Org. Mass Spectrom.* **1992**, *27*, 77.
- [17] J. Ni, A. Harrison. Reactive Collisions in Quadrupole Cells. 2. H/D Exchange Reactions of Enolate Ions with CH₃OD and C₂H₅OD. *J. Am. Soc. Mass Spectrom.* **1992**, *3*, 853.
- [18] M. Hemling, J. Conboy, M. Bean, M. Mentzer, S. Carr. Gas Phase Hydrogen/Deuterium Exchange in Electrospray Ionization Mass Spectrometry as a Practical Tool for Structure Elucidation. *J. Am. Soc. Mass Spectrom.* **1994**, *5*, 434.
- [19] D. Hunt, C. McEwen, R. Upham. Determination of Active Hydrogen in Organic Compounds by Chemical Ionization Mass Spectrometry. *Anal. Chem.* **1972**, *44*, 1292.
- [20] S. Campbell, M. Rodgers, E. Marzluff, J. Beauchamp. Structural and Energetic Constraints on Gas Phase Hydrogen/Deuterium Exchange Reactions of Protonated Peptides with D₂O, CD₃OD, CD₃COOD and ND₃. *J. Am. Chem. Soc.* **1994**, *116*, 9765.
- [21] Q. Hu, R. Noll, H. Li, A. Makarov, M. Hardman, G. Cooks. The Orbitrap: a New Mass Spectrometer. *J. Mass Spectrom.* **2005**, *40*, 430.
- [22] L. Lopez, P. Tiller, M. Senko, J. Schwartz. Automated Strategies for Obtaining Standardized Collisionally Induced Dissociation Spectra on a Benchtop Ion Trap Mass Spectrometer. *Rapid Commun. Mass Spectrom.* **1999**, *13*, 663.
- [23] T. Liu, M. Belov, N. Jaitly, W.-J. Qian, R. Smith. Accurate Mass Measurements in Proteomics. *Chem. Rev.* **2007**, *107*(8), 3621.
- [24] R. Cole, J.-C. Tabet. Stereospecific Ion-Molecule Reactions of Nucleophilic Gas-phase Reagents with Protonated Bifunctional Tetracyclic Terpene Epimers in the Triple Quadrupole Collision Cell. *J. Mass Spectrom.* **1997**, *32*, 413.
- [25] S. Baumgarten, D. Lesage, V. Gandon, J.-P. Goddard, M. Malacria, J.-C. Tabet, Y. Gimbert, L. Fensterbank. The Role of Water in Platinum-Catalyzed Cycloisomerization of 1,6-enynes: A Combined Experimental and Theoretical Gas Phase Study. *Chem. Cat. Chem.* **2009**, *1*, 138.
- [26] S. Gronert, A. Fagin, K. Okamoto. Stereoselectivity in the Collision-Activated Reactions of Gas Phase Salt Complexes. *J. Am. Soc. Mass Spectrom.* **2004**, *15*, 1509.
- [27] M. Kinter, M. Bursley. Ion/Molecule Reactions of Ammonia with Two Translationally Excited C₂H₅O⁺ Isomers. *J. Am. Chem. Soc.* **1986**, *108*, 1797.
- [28] M. J. Frisch, G. W. Trucks, H. B. Schlegel, G. E. Scuseria, M. A. Robb, J. R. Cheeseman, G. Scalmani, V. Barone, B. Mennucci, G. A. Petersson, H. Nakatsuji, M. Caricato, X. Li, H. P. Hratchian, A. F. Izmaylov, J. Bloino, G. Zheng, J. L. Sonnenberg, M. Hada, M. Ehara, K. Toyota, R. Fukuda, J. Hasegawa, M. Ishida, T. Nakajima, Y. Honda, O. Kitao, H. Nakai, T. Vreven Jr., J. A. Montgomery, J. E. Peralta, F. Ogliaro, M. Bearpark, J. J. Heyd, E. Brothers, K. N. Kudin, V. N. Staroverov, R. Kobayashi, J. Normand, K. Raghavachari, A. Rendell, J. C. Burant, S. S. Iyengar, J. Tomasi, M. Cossi, N. Rega, N. J. Millam, M. Klene, J. E. Knox, J. B. Cross, V. Bakken, C. Adamo, J. Jaramillo, R. Gomperts, R. E. Stratmann, O. Yazyev, A. J. Austin, R. Cammi, C. Pomelli, J. W. Ochterski, R. L. Martin, K. Morokuma, V. G. Zakrzewski, G. A. Voth, P. Salvador, J. J. Dannenberg, S. Dapprich, A. D. Daniels, Ö. Farkas, J. B. Foresman, J. V. Ortiz, J. Cioslowski, D. J. Fox. Gaussian 09, Revision A.1. Gaussian, Inc.: Wallingford CT, **2009**.
- [29] C. T. Lee, W. T. Yang, R. G. Parr. Development of the Colle-Salvetti Correlation-Energy Formula into a Functional of the Electron Density. *Phys. Rev. B* **1988**, *37*, 785.
- [30] A. D. Becke. Density-Functional Thermochemistry III. The Role of Exact Exchange. *J. Chem. Phys.* **1993**, *98*, 5648.
- [31] F. Weigend, R. Ahlrichs. Balanced Basis Sets of Split Valence, Triple Zeta Valence and Quadruple Zeta Valence Quality for H to Rn: Design and Assessment of Accuracy. *Phys. Chem. Chem. Phys.* **2005**, *7*, 3297.
- [32] P. J. Lindstrom, W. G. Mallard (Eds). NIST Chemistry WebBook, NIST Standard Reference Database Number 69. National Institute of Standards and Technology: Gaithersburg MD, 20899, **2011**. <http://webbook.nist.gov> [11/28/2011].
- [33] J. Garver, Z. Yang, S. Kato, W. Wren, K. Vogelhuber, C. Lineberger, V. Bierbaum. Gas phase Reactions of 1,3,5-triazine: Proton Transfer, Hydride Transfer, and Anionic σ -adduct Formation. *J. Am. Soc. Mass Spectrom.* **2011**, *22*, 1260.
- [34] S. Campbell, T. M. Rodgers, M. E. Marzluff, J. L. Beauchamp. Deuterium Exchange Reactions as a Probe of Biomolecule Structure. Fundamental Studies of Gas Phase H/D Exchange Reactions of Protonated Glycine Oligomers with D₂O, CD₃OD, CD₃CO₂D, and ND₃. *J. Am. Chem. Soc.* **1995**, *117*, 12840.

Annex 3 - Distinctive gas-phase fragmentation pathway of the mitorubramines, novel secondary metabolites from *Hypoxylon fragiforme*

Rapid Commun. Mass Spectrom. 2012, 26, 2612–2618
(wileyonlinelibrary.com) DOI: 10.1002/rcm.6382

Distinctive gas-phase fragmentation pathway of the mitorubramines, novel secondary metabolites from *Hypoxylon fragiforme*

Ljubica Svilar^{1,2}, Vesna Stankov-Jovanovic^{1*}, Marc Stadler³, Hristo Nedev² and Jean-Claude Tabet^{2*}

¹University of Nis, Faculty of Science and Mathematics, Department of Chemistry, Visegradska33, 18000 Nis, Serbia

²University Pierre and Marie Curie, Paris Institut of Molecular Chemistry, UMR 7201-FR2769, Case Courrier 45, Batiment F, 716, 4, place Jussieu, 75252 Paris cedex 05, France

³Department Microbial Drugs, Helmholtz-Centre for Infection Research, Inhoffenstrasse 8, 38124 Braunschweig, Germany

RATIONALE: Azaphilones, belonging to the class of mitorubins usually produced in *Hypoxylon fragiforme*, react easily with amino groups, giving amine derivatives, mitorubramines. These secondary metabolites exhibit a wide range of biological activities. Finding new secondary metabolites from fungi is important, and electrospray ionization (ESI) high-resolution mass spectrometry (HRMS) coupled with sequential MSⁿ experiments has become a method of choice for the chemotaxonomic classification of fungi.

METHODS: High-performance liquid chromatography of methanol extracts coupled to positive electrospray ionization, high resolving power for accurate mass measurements and resonant excitation for selective ion collision-induced dissociation (CID) have been conducted with the aim of resolving the structures of possible novel compounds.

RESULTS: Soft desolvation conditions in the ESI source enabled the detection of intact mitorubramines present in the extract. HRMS provided unambiguous information about the elemental composition of the mitorubramines and their product ions, while sequential MS³ experiments were essential for the structural discernment of already reported mitorubins and newly discovered mitorubramines. Indeed, specifically from the latter, a series of consecutive dissociations takes place under CID conditions that are useful for structural elucidation.

CONCLUSIONS: A distinctive method for two families of secondary metabolites has been developed. Information observed using HRMS and sequential MSⁿ experiments gave unambiguous information about the structure of mitorubramines, especially the position of the nitrogen atom, which was strengthened by proposed unusual fragmentation mechanisms, such as the rearrangement yielding the release of CO₂ from the hydroxyl-diketone structures. These experiments demonstrated that the fragmentations are facilitated by the nitrogen electron lone-pair in mitorubramines, which does not occur in mitorubins. Copyright © 2012 John Wiley & Sons, Ltd.

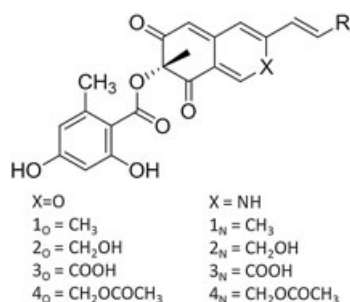
Mitorubrin azaphilones from *Hypoxylon fragiforme* (Scheme 1), containing a pyrone-quinone group, have been reported, and elucidation of their structures was performed by a range of analytical methods,^[1,2] such as liquid chromatography (LC) with ultraviolet/diode-array detection (UV/DAD), nuclear magnetic resonance (NMR), infrared (IR) and mass spectrometry (MS), using pure, isolated compounds.^[3–5] Because of their versatile biological activities (anti-fungal activity, inhibition of dihydrofolate reductase and geranylgeranyl transferase),^[6] these compounds represent a group of highly interesting secondary

metabolites. Azaphilones generally react with nitrogen from amines to form vinylogous 4-pyridone derivatives. However, very few azaphilone vinylogous 4-pyridone derivatives have been found to be present as natural products in biological samples,^[7–9] although some syntheses of these derivatives have been reported.^[10,11]

To the best of our knowledge, there have been no reports on the presence of vinylogous 4-pyridone derivatives in *Hypoxylon fragiforme* or other species of the Xylariaceae. Mitorubramines (Scheme 1) have been detected in the current study in the methanolic stromatal extract of *Hypoxylon fragiforme*, although in low concentration. LC was coupled to high-resolution mass spectrometry (HRMS) and collision-induced dissociation (CID) to provide unambiguous information about the structures, molecular masses and some chemical properties of this novel group of secondary metabolites. Mass spectra obtained by soft ionization techniques often do not provide sufficient information about the molecular structure of interest, and consequently further tandem mass spectrometric (MS/MS) fragmentation must be undertaken to obtain more detailed data. CID MS/MS is widely utilized in forming reference libraries for the

* Correspondence to: V. Stankov-Jovanovic, University of Nis, Faculty of Science and Mathematics, Department of Chemistry, Visegradska33, 18000 Nis, Serbia.
E-mail: sjvesna@pmf.ni.ac.rs

** Correspondence to: J.-C. Tabet, University Pierre and Marie Curie, Paris Institut of Molecular Chemistry, UMR 7201-FR2769, Case Courrier 45, Batiment F, 716, 4, place Jussieu, 75252 Paris cedex 05, France.
E-mail: jean-claude.tabet@courriel.upmc.fr



Scheme 1. Mitorubrin and mitorubramine molecular structures with variation in the R group (1_O – mitorubrin, 2_O – mitorubrinol, 3_O – mitorubrinic acid, 4_O – mitorubrinol acetate, 1_N – mitorubramin, 2_N – mitorubraminol, 3_N – mitorubraminic acid, 4_N – mitorubraminol acetate).

recognition of substructures and chemotaxonomic classification.^[12,13] The fragmentation of a precursor ion from a specific compound under CID conditions will depend on its structure, and will be directed by its functional groups. Thus, two families of similar molecules may react differently under CID conditions. Sequential MSⁿ experiments will provide even more information about the molecular structures.

EXPERIMENTAL

Water was obtained from a Milli-Q Gradient system (Millipore, Brussels, Belgium). Methanol and acetonitrile were of HPLC grade (VWR, Lutterworth, UK). Formic acid was from SDS (Carlo ErbaReactifs, Val de Rueil, France). The fungal sample was collected from a dead *Fagus sylvatica* tree in a forest in south-eastern Serbia, and determined morphologically and by chemotaxonomic studies. Fungal material was deposited in the Herbarium Moesiacum, University of Nis, Nis, Serbia (HMN), voucher number 5530.

Powdered stromata (5 mg) were extracted twice in methanol for 10 min in an ultrasonic bath, at room temperature, and centrifuged for 5 min. The resulting supernatants were filtered through a 45 μm membrane filter, and then analyzed by LC/MS. A volume of 10 μL of approximately 100 μg/mL extract was injected into the reversed-phase C18 column (Symmetry, 2.1 × 150 mm, 5 μm; Waters, Wexford, Ireland). For the separation of compounds of interest from the complex methanol extract, a solvent system of 0.1% formic acid solution in water and acetonitrile was used in the following gradient: 90% of water in isocratic condition during the first 5 min was followed by a linear gradient from 10% acetonitrile to 90% acetonitrile for 55 min, and thereafter isocratic 90% acetonitrile elution for 40 min.

Detection of accurate masses was obtained in positive electrospray ionization (ESI) mode using a LTQ Orbitrap XL (hybrid, 2D ion trap-orbitrap) mass spectrometer (Thermo Fisher Scientific, Bremen, Germany).^[14] The parameters for ionization of compounds were adjusted to obtain the best efficiency and desolvation of adduct ions. The electrospray needle was kept at a voltage of 4 kV, and the sheath gas and auxiliary gases were both N₂ at flow rates of 45 and 10 arbitrary units (a. u.), respectively. The capillary temperature was maintained at 275 °C, and the capillary voltage at 50 V. The tube lens offset was

maintained at 40 V. MS scanning was performed from *m/z* 100 to 1200. The mass resolution (full width at half maximum height, FWHM) was 60 000 at *m/z* 400. For accurate mass measurements, a lock mass was used for internal calibration in real time.^[15] The ion at *m/z* 214,08963 corresponding to protonated *N*-butylbenzene sulfonamide, which was present in the solvent system, was used for this purpose. CID experiments were performed by radial resonant excitation in the LTQ 2D ion trap mass spectrometer. The normalized CID collision energy,^[16] resonant excitation amplitude of 0.85 mV_{P-P} and 1.1 mV_{P-P} for sequential MS² and MS³ experiments, respectively, was 15% and 22%. Product ions were detected in the orbitrap mass spectrometer with a mass resolving power of 60 000 (FWHM).

RESULTS AND DISCUSSION

The crude methanol extract was chromatographed and the total ion chromatogram (TIC) is presented in Fig. 1, while the corresponding data are reported in Table 1. A long separation time was chosen, to obtain an efficient separation, especially for the more polar components of the extract, particularly the mitorubramines. The mitorubrans were eluted at retention times of less than 45 min, in quite high abundance (Fig. 1). Mitorubramines were also present in quite high abundances and, because of their higher polarity, eluted at retention times of less than 32 min. Mitorubramin and mitorubraminol acetate eluted at similar retention times, suggesting that they are of similar polarity. After 45 min of elution, unidentified non-polar compounds (probably fatty acids and ergosterol derivatives), often present in crude extracts of many fungi, were detected. The good separation of compounds enables us to observe mitorubramines despite them being present only at low levels in the extracts.

The positive ion ESI spectra of all the mitorubramines gave only peaks that corresponded to the protonated molecules. The high-resolution mass measurements gave confident data about their accurate molecular masses and elemental compositions, with an accuracy of better than 2 ppm. In the mass spectra of mitorubrans, in addition to protonated molecules, protonated dimers were also obtained. Furthermore, the higher ionization efficiency of mitorubramines, resulting from their higher proton affinity (PA), enabled their detection, despite their low concentration in the samples. On the other hand, the formation of mitorubrin protonated dimers decreased the chromatographic peak height in that area of the chromatogram, thus enabling the facile detection of protonated mitorubramines, which do not form dimeric ions. These soft ionization conditions allow the survival and transmission of dimeric ions, decreasing the height of the mitorubrin chromatographic peaks, making it possible to detect the mitorubramines by ESI-MS.

MS methods can provide a wealth of additional information about the structures of analyzed compounds, and, for this purpose, additional experiments were conducted. Sequential MS² and MS³ experiments were performed to confirm the postulated structures (i.e. divinyllogous secondary amine), and to gain more information about the position of the nitrogen atom in the postulated vinylogous 4-pyridone structures in different mitorubramines. The data on ions observed in the sequential MSⁿ experiment are presented in Table 2. CID experiments on the protonated mitorubrans (oxygen containing) and mitorubramines (nitrogen containing) gave product ions at *m/z* [218+R]⁺ and

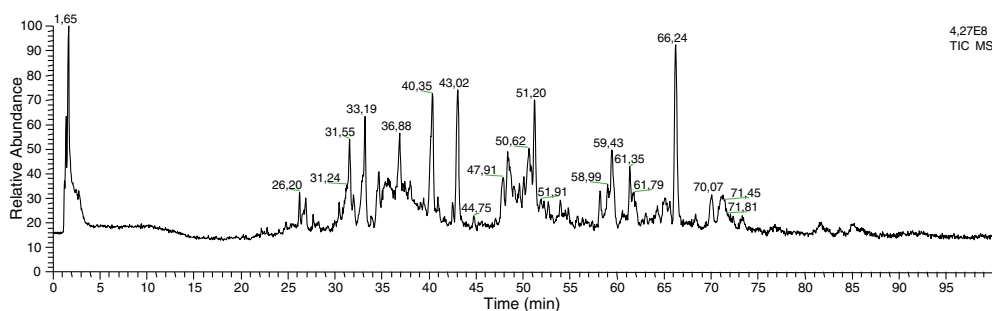


Figure 1. LC/MS TIC of *Hypoxylon fragiforme* crude methanol extract from ESI experiment.

Table 1. LC/MS data of crude methanol extract of *Hypoxylon fragiforme*: retention times of analyzed ions, their accurate molecular masses and elemental compositions, obtained by HRMS

Compound	Retention time (min)	Observed mass (m/z)	Elemental composition of molecule	Observed ions	Error (ppm)
Mitorubraminol (2_N)	26.2	398.12496	$C_{21}H_{20}O_7N$	$[M + H]^+$	1.4
Mitorubraminic acid (3_N)	29.1	412.10324	$C_{21}H_{18}O_8N$	$[M + H]^+$	1.5
Mitorubramin (1_N)	31.5	382.12903	$C_{21}H_{20}O_6N$	$[M + H]^+$	1.4
Mitorubraminol acetate (4_N)	31.9	440.13443	$C_{23}H_{22}O_8N$	$[M + H]^+$	1.1
Mitorubrinol (2_O)	33.2	399.10773	$C_{21}H_{19}O_8$	$[M + H]^+$	0.9
Mitorubrinic acid (3_O)	34.6	797.20892	$C_{42}H_{37}O_{16}$	$[2M + H]^+$	1.6
		413.08719	$C_{21}H_{17}O_9$	$[M + H]^+$	1.2
		825.16754	$C_{42}H_{33}O_{18}$	$[2M + H]^+$	1.6
Mitorubrinol acetate (4_O)	40.3	151.03879	$C_8H_7O_3$	$[MH-262]^+$	-1.3
		441.11856	$C_{23}H_{21}O_9$	$[M + H]^+$	1.2
		881.23004	$C_{46}H_{41}O_{18}$	$[2M + H]^+$	1.6
Mitorubrin (1_O)	43.1	383.11261	$C_{21}H_{19}O_7$	$[M + H]^+$	0.4
		765.21930	$C_{42}H_{37}O_{14}$	$[2M + H]^+$	1.8

m/z $[217+R]^+$, respectively, which clearly correspond to the bicyclic moieties. These ions are formed by loss of a common neutral species (orsellinic acid - H_2O , 150 Da), derived from the orsellinic acid that forms part of the mitorubrin and mitorubramine structures. Protonated mitorubrins and mitorubramines showed the same behavior under CID, preventing their distinction one from another. It was also not possible to determine the exact position of the secondary amino group. Thus, the results obtained from sequential MS^3 experiments performed on these bicyclic structures provide much more information and are essential for differentiation between the two families of compounds.

An example of behavior of product ions from protonated mitorubramines and mitorubrins under MS^3 conditions is shown in Fig. 2. It is important to note that CID spectra of sequential MS^3 experiments of mitorubramines are significantly different from those of mitorubrin azaphilones. A peak at m/z 203, present in both spectra, corresponds to detector noise, and does not arise from the fragmentation pathway. The high-resolution actually shows that this ion has a mass default, which differs strongly from those of the other product ions and, thus, its inconsistency with the precursor structure. For all analyzed ions, both mitorubrins and mitorubramines, in the sequential MS^3 experiments, a main and common loss of a water molecule was observed.

The loss of water (Scheme 2) is expected, since protonation occurs at the hydroxyl diketo ring due to the proton affinity being highest at this position. The nitrogen atom of the

heterocyclic moiety in the mitorubramines (or oxygen atom in the mitorubrins) has a lower proton affinity than the oxygen of the keto group from the hydroxy diketo ring. After the release of the water molecule, a keto group is protonated, due to the presence of a vicinal hydroxyl group, in spite of the endothermic proton transfer required. Furthermore, the formed intermediate ion can be subjected to ring contraction, to yield the more stable carbocation. This ring contraction results from the vicinal carbocation, which is stabilized by proton migration to the ketone to produce a protonated ketone, stabilized by long distance delocalization from the nitrogen atom. The reaction can also be directed by the two keto groups, giving the isomeric product.

In the sequential MS^3 spectra of protonated mitorubramines, additional peaks were observed, suggesting quite complicated fragmentation pathways, favored by the presence of nitrogen. These product ions are reported in Table 2. They correspond to losses of 42, 43, 44 and 46 Da, which are assigned to the neutral loss of C_2H_2O , $C_2H_3O^\circ$, CO_2 and $HCOOH$, respectively. We have proposed fragmentation mechanisms by which the diagnostic peaks in the CID spectra could be obtained. Mechanisms for the losses of CH_2CO and the CH_3CO° radical, yielding the $[(217+R)-C_2H_2O]^+$ and $[(217+R)-C_2H_3O]^{+\circ}$ ions, are presented in Scheme 3. Ring contraction could also occur where, instead of proton or hydroxyl group migration, 1,2-migration of a carbonyl site occurs as in the Wagner-Meerwein rearrangement.^[17,18] The ring contraction is assisted by electron lone-pair migration from the hydroxyl group to the tetra-substituted carbon,

Table 2. Main product ions in CID spectra of selected precursor ions produced in sequential MS² and their product ions obtained in the sequential MS³ experiments

Compound	MH ⁺	Product ions from MS ²		Elemental composition of precursor ion	Error (ppm)	Obtained product ions from MS ³ (<i>m/z</i>)	Elemental composition of product ions	Error (ppm)
		(a) <i>m/z</i> [217+R] ⁺ for mitorubramines	(b) <i>m/z</i> [218+R] ⁺ for mitorubrins					
2 _N	398	248.09152		C ₁₃ H ₁₄ O ₄ N	-0.7	230.08104	C ₁₃ H ₁₂ O ₃ N	-0.6
						206.08125	C ₁₁ H ₁₂ O ₃ N	-0.4
3 _N	412	262.07080		C ₁₃ H ₁₂ O ₅ N	-0.7	205.07341	C ₁₁ H ₁₁ O ₃ N	-0.3
						204.10193	C ₁₂ H ₁₄ O ₂ N	-0.1
						202.08629	C ₁₂ H ₁₂ O ₂ N	-0.2
						244.06018	C ₁₃ H ₁₀ O ₄ N	-1.1
						220.06011	C ₁₁ H ₁₀ O ₄ N	-1.5
						219.05226	C ₁₁ H ₉ O ₄ N	-1.6
1 _N	382	232.09689		C ₁₃ H ₁₄ O ₃ N	0.3	218.08072	C ₁₂ H ₁₂ O ₃ N	-2.1
						216.06504	C ₁₂ H ₁₀ O ₃ N	-2.2
						214.05726	C ₁₃ H ₁₂ O ₂ N	-0.09
						190.08656	C ₁₁ H ₁₂ O ₂ N	-2.5
						189.07875	C ₁₁ H ₁₁ O ₂ N	-2.4
4 _N	440	290.10272		C ₁₅ H ₁₆ O ₅ N	1.5	188.10745	C ₁₂ H ₁₄ ON	2.3
						186.09177	C ₁₂ H ₁₂ ON	2.1
						272.09188	C ₁₅ H ₁₄ O ₄ N	0.8
						248.08984	C ₁₃ H ₁₄ O ₄ N	-0.8
						247.07837	C ₁₃ H ₁₃ O ₄ N	-1.0
2 _O	399	249.07581		C ₁₃ H ₁₃ O ₅	0.2	246.10913	C ₁₄ H ₁₆ O ₃ N	-13.57
						244.09833	C ₁₄ H ₁₄ O ₃ N	6.19
						231.06521	C ₁₃ H ₁₁ O ₄	0.1
						245.08059	C ₁₃ H ₉ O ₅	-0.9
						273.07583	C ₁₅ H ₁₃ O ₅	-0.3
3 _O	413	263.09128		C ₁₃ H ₁₁ O ₆	-0.5	231.06537	C ₁₃ H ₁₁ O ₄	-0.8
4 _O	441	291.08649		C ₁₅ H ₁₅ O ₆	0.6	215.07019	C ₁₃ H ₁₁ O ₃	-0.4
1 _O	383	233.08086		C ₁₃ H ₁₃ O ₄	0.1			

*A high error obtained for observed product ions for MS³ of 4_N is due to the small number of precursor ions. Thus the experiment was repeated using the LTQ, and the obtained spectrum is presented in Supplementary Fig. S1 (see Supporting Information).

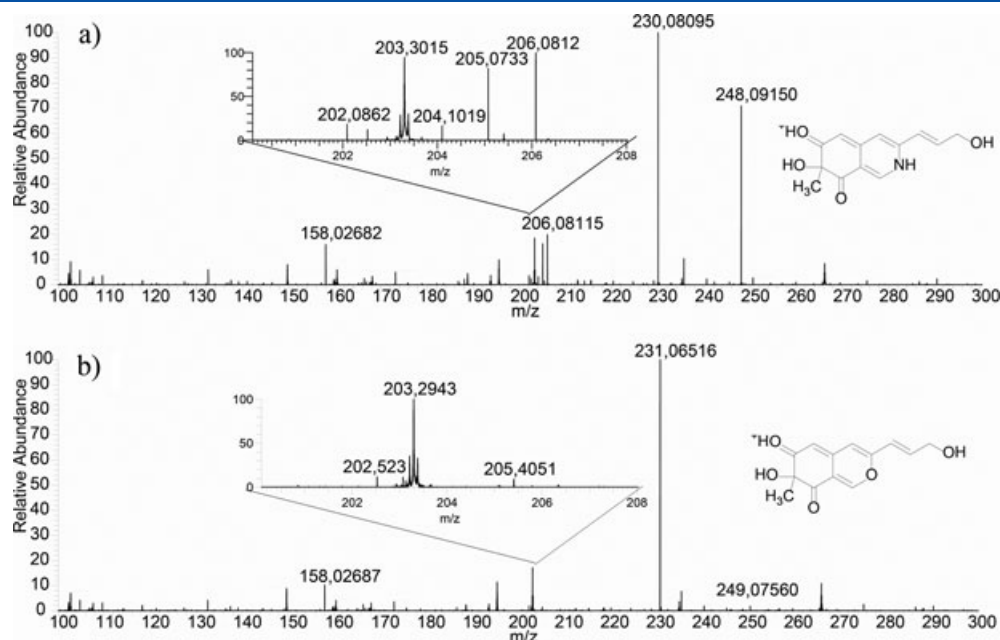
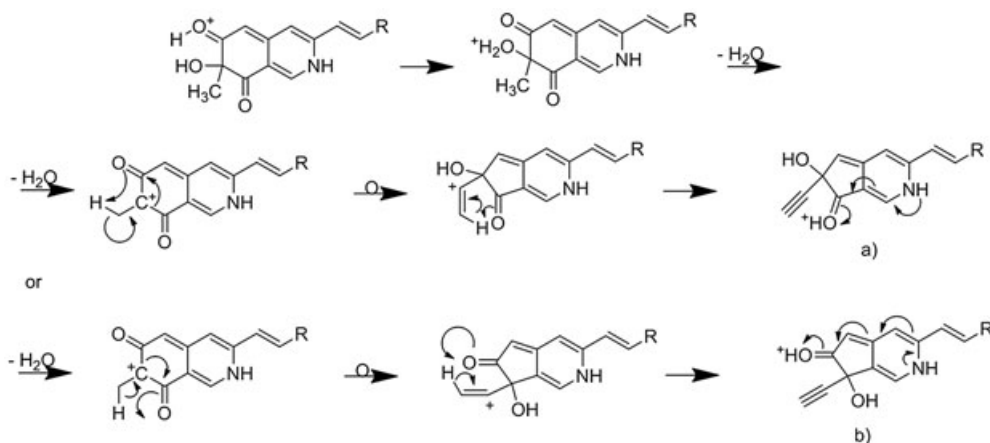


Figure 2. Sequential MS³ experiments of main product ions (a) *m/z* 248 and (b) *m/z* 249 (CID 17% normalized collision energy) that were previously observed in CID of mitorubraminol (*m/z* 398) and mitorubrinal (*m/z* 399) (22% (1.1 mV_{p-p}) normalized collision energy).



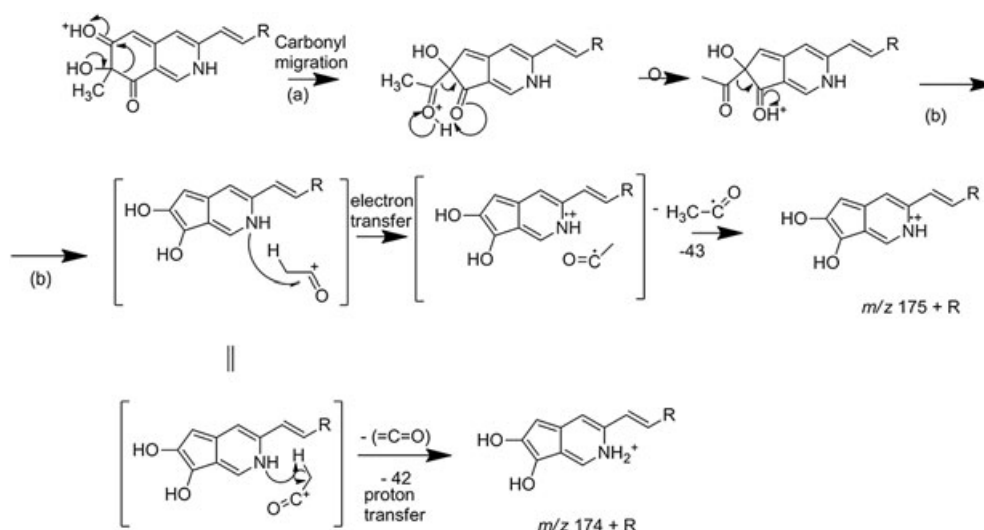
Scheme 2. Assumed mechanism of water loss from mitorubramines from product ions at *m/z* 217+*R*, obtained in sequential MS³ experiment.

geminal to the two carbonyl groups (Scheme 3(a)). The produced cyclopentenone system can isomerize into a protonated cyclopentenyl system, allowing formation of an ion-dipole complex (Scheme 3(b)). The ion-dipole complex thus formed comprises an alkyl cyclopenta-pyridine-6,7-diol and an acylium moiety. From this intermediate, two further competitive pathways occur. By direct internal proton transfer from the acylium moiety, ketene (42 Da) is released giving the alkyl cyclopenta-pyridine-6,7-diol ion. Competitively to this, electron transfer from the nitrogen of the tetraenic system to the acylium moiety can occur, giving CH₃CO[•] radical release (43 Da), and formation of the odd-electron alkyl cyclopenta-pyridine-6,7-diol.

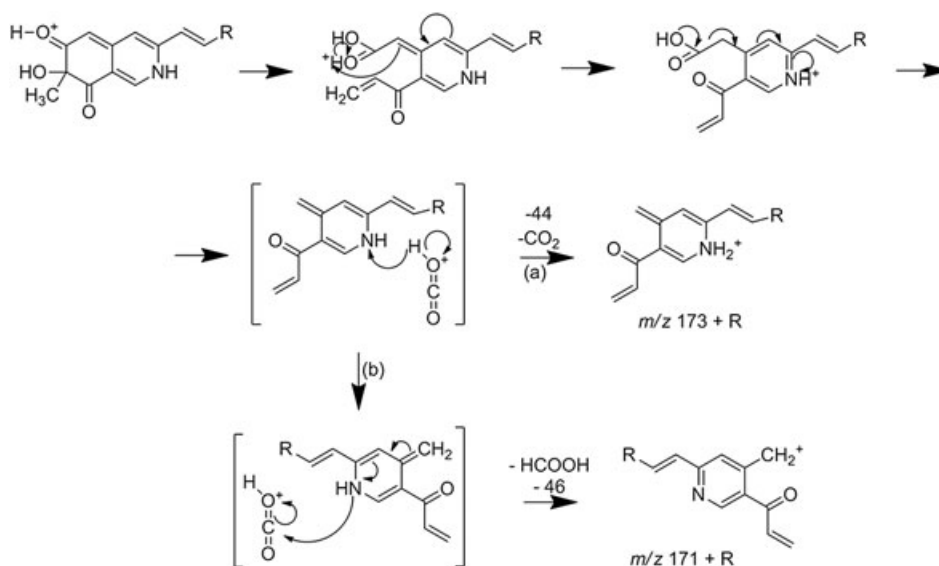
Losses of CO₂ and HCOOH are competitive processes independent of the CH₂CO and CH₃CO[•] radical losses, forming the [(217+*R*)-CO₂]⁺ and [(217+*R*)-HCOOH]⁺ ions. The assumed

mechanism of fragmentation and formation of these neutral species is presented in Scheme 4.

First, a 1,2-hydroxyl transfer concurrently with 1,2-hydride transfer from the methyl group takes place and yields ring opening and the protonated carboxylate.^[19,20] This process is followed by proton migration from the carboxylate site to its α position due to migration to the conjugated double bonds promoted by the migration of the electron lone-pair of nitrogen. Its formation results from the tri-substituted pyridinium species comprised in particular of the *p*-ethanoic acid group. Proton transfer from the hydroxyl group takes place by 1,2-proton migration. The benzylic bond geminal to the carboxylate moiety can be cleaved through charge migration to generate an ion-dipole complex. This ion-dipole complex is comprised of protonated CO₂ and the heterocyclic system. Internal proton transfer from CO₂H⁺ to



Scheme 3. Proposed fragmentation mechanism for MS³ experiment of mitorubramine family and loss of CH₃CO[•] radical and CH₂CO.



Scheme 4. Proposed fragmentation mechanisms for MS³ experiment of mitorubramine family and loss of CO₂ and HCOOH.

the amine of the heterocyclic system initiates neutral loss of CO₂ (44 Da) yielding the m/z [188+R]⁺ ion (Scheme 4(a)). On the other hand, assisted by double-bond migrations, hydride transfer from the NH site of the heterocyclic system to the protonated CO₂ results in the neutral loss of formic acid (46 Da) and detection of the m/z [171+R]⁺ ion (Scheme 4(b)).

Isomerization is possible for both the mitorubramines and the mitorubramines, but only in the latter proton transfer from the exocyclic carbon to the α -carbon can occur, owing to the presence of a labile lone-pair of electrons on the nitrogen. After electron delocalization the charged nitrogen is neutralized and it promotes allylic bond cleavage. An ion-dipole complex formed in this way can directly lose CO₂, a pathway which is not possible in mitorubramines.

Formation of an ion-dipole complex and proton transfer from the acylium to the heterocyclic nitrogen can give losses

of CH₂CO and CH₃CO[•] radical. However, this process cannot occur in mitorubramine azaphilones. In addition, electron transfer is known to take place specifically in heterocyclic systems with nitrogen, rather than with oxygen. The losses of CO₂, CH₃CO[•], CH₂O and HCOOH are possible due to the presence of the vinylic amino group, which stabilizes the product ion by its electron donor character. Such elimination does not take place in the mitorubramines. On the other hand, the presence of a nitrogen atom at other possible sites, e.g. an amide function instead of an ester, is ruled out because the loss of CONH would have been observed in that case. For all these reasons, the multi-decomposition pathways observed for mitorubramines cannot take place for mitorubramines. This gives us unambiguous evidence about the structures and presence of these molecules in the crude extract of *Hypoxylon fragiforme*. The diagnostic fragmentation pathways are of crucial

importance for the structural identification of vinylogous 4-pyridone derivatives, i.e., mitorubramines, and to establish the exact position of the nitrogen atom in the molecule, and also for their structural distinction from their oxygen-containing analogues.

CONCLUSIONS

A novel family of fungal secondary metabolites, mitorubramines, was found in the fungus *Hypoxylon fragiforme* by means of high-resolution mass spectrometry. Sequential CID experiments, along with information on the constitution of the known mitorubrams, provided unambiguous information on the chemical structures of the newly observed compound family. As information derived from MS-MS experiments often proved insufficient for structural elucidation, additional experiments, such as CID of product ions, were performed. The sequential CID of product ions gave the most important information about the structure of mitorubramines, and particularly about the position of the nitrogen atom in the molecule, based on complicate fragmentation pathways in which the nitrogen atom, and its lone-pair played the main role, enabling clear structural distinction between two very similar families of molecules, directly from the crude extract, applying just MS methods.

SUPPORTING INFORMATION

Additional supporting information may be found in the online version of this article.

Acknowledgements

The authors want to thank Ministry of Education and Science Republic of Serbia (Grant No. 172047), French Grant from Industry and SM3P Platform for financial support. Ljubica Svilar expresses her sincere gratitude to the French Government and Embassy of France in Serbia for the scholarship provided for her PhD program.

REFERENCES

- [1] M. Stadler, H. Wollweber, A. Muhlbauer, T. Henkel, H. Wollweber, Y. Asakawa, T. Hashimoto, J. Rogers, Y.-M. Ju, H.-G. Wetzstein, H.-V. Tichy. Secondary metabolite profiles, genetic fingerprints and taxonomy of *Daldinia* and allies. *Mycotaxon* **2001**, 77, 379.
- [2] W. Steglich, M. Klaar, W. Furtner. (+)-Mitorubrin derivatives from *Hypoxylon fragiforme*. *Phytochemistry* **1974**, 13, 2874.
- [3] M. Stadler, J. Fournier, A. Granmo, E. Beltran-Tejera. The 'red-Hypoxylons' of the temperate and subtropical northern hemisphere. *North American Fungi* **2008**, 3, 73.
- [4] V. Hellwig, Y.-M. Ju, J. D. Rogers, J. Fournier, M. Stadler. Hypomiltin, a novel azaphilone from *Hypoxylon hypomiltum*, and chemotypes in *Hypoxylon* sect. *Hypoxylon* as inferred from analytical HPLC profiling. *Mycolog. Prog.* **2005**, 4, 39.
- [5] A. Muhlbauer, D. Triebel, D. Persoh, H. Wollweber, S. Seip, M. Stadler. Macrocarpones, novel metabolites from stromata of *Hypoxylon macrocarpum*, and new evidence on the chemotaxonomy of *Hypoxylon* species. *Mycolog. Prog.* **2002**, 1, 235.
- [6] M. Stadler, D.-N. Quang, A. Tomita, T. Hashimoto, Y. Asakawa. Changes in secondary metabolism during stromatal ontogeny of *Hypoxylon fragiforme*. *Mycolog. Res.* **2006**, 110, 811.
- [7] N. Arai, K. Shiomi, H. Tomoda, N. Tabata, D.-J. Yang, R. Masuma, T. Kawakubo, S. Omura. Isochromophilones III–VI, inhibitors of acyl-CoA:cholesterolacyltransferase produced by *Penicillium multicolor* FO-3216. *J. Antibiot. (Tokyo)* **1995**, 48, 696.
- [8] T. Akihisa, H. Tokuda, K. Yasukawa, M. Ukiya, A. Kiyota, N. Sakamoto, T. Suzuki, N. Tanabe, H. Nishino. Azaphilones, furanoisophthalides, and amino acids from the extracts of *Monascus pilosus*-fermented rice (redmold rice) and their chemopreventive effects. *J. Agric. Food Chem.* **2005**, 53, 562.
- [9] H.-M. Ge, W.-Y. Zhang, G. Ding, P. Sarpapakorn, Y.-C. Song, S. Hannongbuac, R.-X. Tan. Chaetoglobins A and B, two unusual alkaloids from endophytic *Chaetomium globosum* culture. *Chem. Commun.* **2008**, 5978.
- [10] W.-G. Wei, Z.-J. Yao. Synthesis: studies toward chloroazaphilone and vinylogous γ -pyridones: two common natural product core structures. *J. Org. Chem.* **2005**, 70, 585.
- [11] G. Buchi, J.-D. White, G.-N. Wogan. The structures of mitorubrin and mitorubrinol. *J. Am. Chem. Soc.* **1965**, 5, 87.
- [12] J. Bitzer, B. Kopcke, M. Stadler, V. Hellwig, Y.-M. Ju, S. Seip, T. Henkel. Accelerated dereplication of natural products, supported by reference libraries. *Chimia* **2007**, 51, 332.
- [13] T. Larsen, J. Smedsgaard, K. Nielsen, M. Hansen, J. Frisvad. Phenotypic taxonomy and metabolite profiling in microbial drug discovery. *Nat. Prod. Rep.* **2005**, 22, 672.
- [14] Q. Hu, R. Noll, H. Li, A. Makarov, M. Hardman, G. Cooks. The Orbitrap: a new mass spectrometer. *J. Mass Spectrom.* **2005**, 40, 430.
- [15] J. Olsen, L. de Godoy, G. Li, B. Macek, P. Mortensen, R. Pesch, A. Makarov, O. Lange, S. Horning, M. Mann. Parts per million mass accuracy on an Orbitrap mass spectrometer via lock mass injection into a C-trap. *Mol. Cell. Biochem.* **2011**, 4, 12.
- [16] L. Lopez, P. Tiller, M. Senko, J. Schwartz. Automated strategies for obtaining standardized collisionally induced dissociation spectra on a benchtop ion trap mass spectrometer. *Rapid Commun. Mass Spectrom.* **1999**, 13, 663.
- [17] A. Tutara, M. Balci. Bromination of an N-carbethoxy-7-aza-2,3-benzonorbornadiene and synthesis of N-carbethoxy-7-aza-2,3-dibromo-5,6-benzonorbornadiene: high temperature bromination. Part 14. *Tetrahedron* **2002**, 58, 8979.
- [18] E. Nikitina, A. Safronova, A. Varlamov, F. Zubkov, G. Aleksandrov, K. Turchin. First synthesis of 6-spiro [5-aza-2-oxatricyclo[6.2.1.0^{3,9}]undec-3-ene-6,1'-cyclohexane]. *Chem. Heterocycl. Compd.* **2003**, 39, 130.
- [19] N. Morlender-Vais, A. Mandelbaum. The role of hydrogen migration in the mechanism of alcohol elimination from MH⁺ ions of ethers upon chemical ionization. *J. Mass Spectrom.* **1997**, 31, 1124.
- [20] I. Kuzmenkov, A. Etinger, A. Mandelbaum. Role of hydrogen migration in the mechanism of acetic acid elimination from MH⁺ ions of acetates on chemical ionization and collision-induced dissociation. *J. Mass Spectrom.* **1999**, 34, 797.